Context-Specific Causal Graph Discovery with Unobserved Contexts: Non-Stationarity, Regimes and Spatio-Temporal Patterns

Martin Rabel[a,b], Jakob Runge[a,b]

November 27, 2025

[a]University of Potsdam, Institute of Computer Science, An der Bahn 2, 14476 Potsdam, Germany
[b]Center for Scalable Data Analytics and Artificial Intelligence (ScaDS.AI) Dresden / Leipzig, Germany

Abstract

Real-world data, for example in climate applications, often consists of spatially gridded time series data or data with comparable structure. While the underlying system is often believed to behave similar at different points in space and time, those variations that do exist are twofold relevant: They often encode important information in and of themselves. And they may negatively affect the stability / convergence and reliability / validity of results of algorithms assuming stationarity or space-translation invariance. We study the information encoded in changes of the causal graph, with stability in mind. An analysis of this general task identifies two core challenges. We develop guiding principles to overcome these challenges, and provide a framework realizing these principles by modifying constraint-based causal discovery approaches on the level of independence testing. This leads to an extremely modular, easily extensible and widely applicable framework. It can leverage existing constraint-based causal discovery methods (demonstrated on IID-algorithms PC, PC-stable, FCI and time series algorithms PCMCI, PCMCI+, LPCMCI) with little to no modification. The built-in modularity allows to systematically understand and improve upon an entire array of subproblems. By design, it can be extended by leveraging insights from change-point-detection, clustering, independence-testing and other well-studied related problems. The division into more accessible sub-problems also simplifies the understanding of fundamental limitations, hyperparameters controlling trade-offs and the statistical interpretation of results. An open-source implementation will be available soon[1].

1 Introduction

In science and technology, the researcher often is interested in causal relationships [39; 43]. One reason being that causality is key to understanding actions and their consequences. Even without the intent to actually take an action, scientific reasoning and insight often revolve around the impact an action would have.

The flavor of causal reasoning we will focus on is the study from *observational* data: In practice, potential consequences may prohibit the experimental exploration of possible actions. In other cases an experiment may not be feasible; for example, because an action, like the release of greenhouse gases, may not be taken voluntarily or repeatable, yet the consequences, like climate change, may mandate scientific study. In such cases, causal knowledge must be extracted from observations alone.

Generally, the study of causal relationships, causal inference [39; 43; 61], encompasses many tasks, ranging from the estimation of effects (of actions / interventions) to the answering

---

[1]Placeholder for link to code-repository and documentation.

of counter-factual queries (what would have happened?). All these tasks build on the knowledge of basic cause-effect relationships; a knowledge often represented by a causal graph. This causal graph may not be known a priori, in which case it has to be discovered from data. This graph-discovery task is referred to as causal discovery (CD). Especially CD from observational data has recently garnered substantial attention from climate- and other applications [40; 50].

In real-world scenarios CD faces many challenges [52]. These challenges may stem, for example from the type and quality of data or the violation of simplifying assumptions required to make the CD task tractable. A particularly common assumption is that of IIDness or stationarity in the time series case: A single underlying model is postulated to describe all data-generation uniformly. Yet in the real world, almost any observed model is subject to some degree of variability. A local climate might experience qualitatively different dry and moist regimes over time in a single place, or in different places at the same time; many climate and weather parameters are subject to seasonality; a policy might affect public health in ways related to untracked parameters or a technological device may break or otherwise change its internal state for some time or some firmware-version.

Indeed these examples reveal another challenge, entirely separate from assumption violations and incurred stability issues: A mayor point of interest oftentimes is the occurrence and form of a change itself; it is the existence of and insight into changes in itself that is the subject of study. With the goal of understanding precisely these *variations* of the causal model, the challenge to CD studied in this paper, is, to extract additional information: Does a causal model – and in particular its causal graph – change within a data-set, and if so how? We will refer to this task as multi(-valued) causal discovery (MCD), see Fig. 1.1.
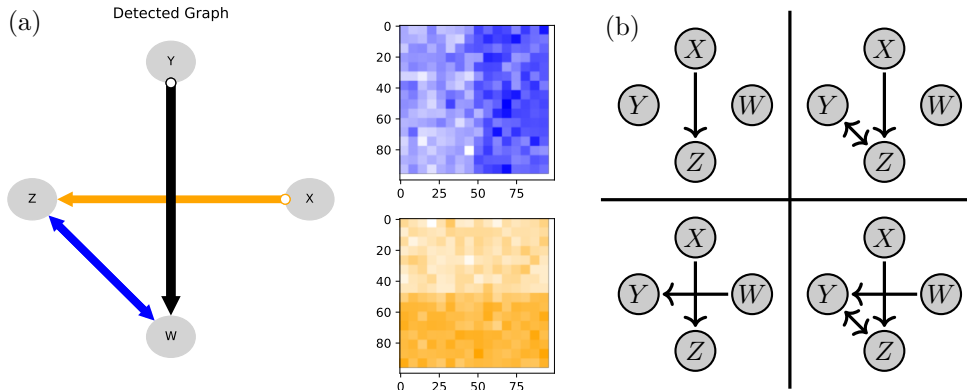

Figure 1.1: Simple toy-model to illustrate method-output (a; applied with FCI): Data is given on a spatial 100×100 grid (i.e. 10,000 data points in total), the link marked in orange is present in the southern half, the one marked in blue is present in the eastern half. This spatial distribution is unknown / hidden. Our focus is on how the graph on the left-hand side (including the designation of changing links) can be recovered. In this example, different graphs correspond to (spatial) quadrants (b). While this illustrates the interpretation of output (a), the association of changing links to spatial directions is a very special case, see Fig. 1.2.

Our focus is on the *extraction* of information about changes of the causal graph, and *robustness* against other kinds of non-stationarity. From the perspective that contexts are intervened instances of a shared model, this means we gain knowledge about a notion of soft intervention that modifies parent-sets. Such interventions seem to occur in the real world: From the closing of a window disrupting temperature exchange or the damaging of an electrical insulation enabling new currents, via phase-transitions qualitatively changing physical interactions or the day-night-cycle (or cloud-cover) controlling the effect of solar parameters, to climate-science phenomena like ENSO or soil-moisture feedbacks. We discuss acyclic (no contemporaneous cycles) models, with a primary, but not exclusive, focus on the

causally sufficient (no hidden confounders) case. This is not a fundamental limitation of our approach, but a choice to keep the presentation reasonably succinct.

Choice of Inductive Bias: We want to be more precise concerning the nature of such changing models. First, the principle of causal modularity suggests that causal mechanisms change independently of each other. From this perspective it appears reasonable to direct our focus to changes that occur *locally in the model*. To this end, we will expand around the limit where changes in different mechanisms (more precisely: different links) occur independently.

Second, variations of the generating model seem particularly relevant for large data-sets. By relevant we really mean two things: Changes in the generating model seem more likely to occur in large data-sets, but from a practical perspective this challenging problem may also not possess satisfying solutions on too small datasets. Thus we pay particular attention to the careful statistical description and scaling properties – both statistically and concerning compute-resources – with increasing sample-size.

Also the notion of large requires further comment: We specifically account for scaling of the sample-size N not necessarily being matched by typical (time-)scales ℓ of regime-changes; instead of a limit with N/ℓ fixed, an uninformative prior (for example uniformly distributed mechanism-typical length-scales of ℓ over scales from 1 to N) seems to capture finite sample properties better. This can also be phrased in terms of information contained in the regime-structure. Proportional scaling would assume that there is always an equal absolute amount of information in the regime-pattern independently of data-set size. We instead focus on limits where the regime-structure will typically contain more information on larger data-sets. For statistical reasons, this regime-information still has to be restricted to some degree however, for example by assuming temporal regimes to persist over a non-trivial period in time.

Challenges: For a better understanding of the challenges involved in the problem of MCD it also helps to briefly outline possible approaches to the problem considered in the literature. Particularly simple are sliding-window approaches that divide the data into smaller segments and apply a conventional CD-algorithm locally in time. Similarly, one may apply a change-point detection (CPD) method first and apply CD on detected segments. Besides finite-sample stability a difficulty in both cases is how to aggregate the resulting graphs. There is no simple way to leverage possibly reoccurring regimes, but for example one may cluster graphs. Indeed, one may also first cluster data, then apply CD per cluster. There are also more sophisticated methods that fit multiple models and optimize over regime-assignments by predictive quality with [4] or without [55] parametric assumptions about regime-structure. While evidently the MCD problem is connected to CD, clustering, CPD, optimality and more, this connection is as of now not well systematized making the combination of different solutions to the different aspects difficult.
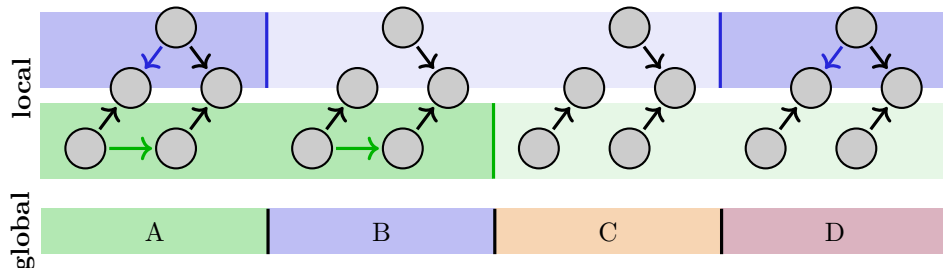

Figure 1.2: Illustration of complexity-scaling for local vs. global description of regimes over time. Locally there are two regimes (top panel), globally the number of regimes increases exponentially in the number of local changes (bottom panel). These global changes in the model can always be decomposed in terms of local changes, this does not require the existence of corresponding index-set / spatial directions as those used in Fig. 1.1b.

When comparing these quite diverse approaches to what we picked as an interesting inductive bias above, we note that they all share two deep conceptual challenges: First, they all are assigning regimes globally in the model / graph, while we came to belief that the model changes primarily locally. But given κ local (binary) changes one observes up to a total of 2^κ global combinations; thus global (in this sense) methods scale exponentially in the number of model-changes. This is illustrated in Fig. 1.2. Additionally, the local signal (independent of node-count) is obfuscated by the global noise (proportional to node-count); thus global (in this sense) methods suffer from large node-counts.

Second, less evident, but much more worrisome is an observation concerning the scaling to larger sample-size. All the above approaches (barring sliding windows) follow in some way the intuitive logic of reconstructing regimes, then running CD per-regime. However, the first step necessarily produces imperfect reconstructions, so we find ourselves in the difficult situation, where the second step (CD) *must not* converge fast enough to detect these imperfections. We are effectively racing our CD (or independence test) vs. our method of regime-assignment. Especially, if the information contained in the regime-structure is not artificially held constant by matching typical regime-scales to sample-size, the reconstruction of regimes will often converge slower than the independence tests used by CD. Indeed, this leads in numerical experiments §7 to a systematic and substantial degradation of results on large data-sets. This is illustrated in Fig. 1.3.
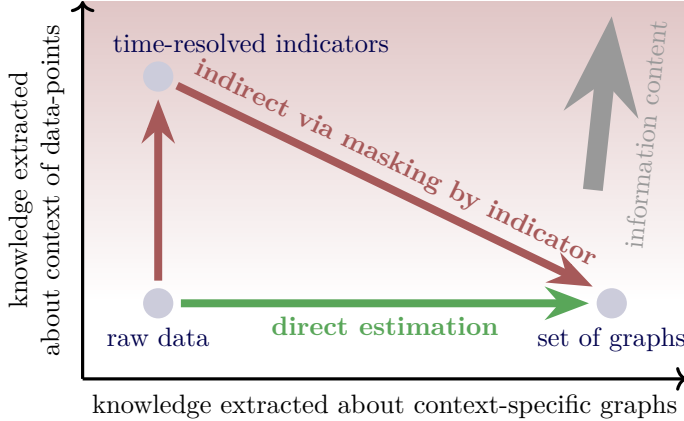

Figure 1.3: Illustration of direct vs. indirect graph-discovery. Green arrows require only the extraction of low-complexity knowledge, red arrows require the extraction of high-complexity knowledge. The information-content of time-resolved indicators will typically increase with larger sample-size (§C), while the information contained in causal graphs does not. So the gradient in information-content (gray arrow), for larger data-sets, points steeply upwards.

To approach these fundamental challenges, we seek to adapt two guiding principles: Work locally in the graph (gL) and test directly (D). By testing directly, we mean, avoid the intuitive but perilous detour through recovering the (plausibly large) information contained in the regime-indicator, but approach the eventually required result directly (this will become much clearer with the concrete approach in §5). In reference to these principles we will refer to our approach as a gLD-framework. Besides these statistical principles, there is also a practical one: We try to keep the framework modular, making the relation of its separate parts to conventional CD methods, independence-testing, CPD and clustering clearer. This modularity also applies to the assumptions about regime-structure: As the reader may have noted at the list of examples above, we emphasized how similar problems arise from patterns in time, in space or other parameters. Indeed, our framework allows for the precise kind of pattern to be specified and leveraged for detection almost entirely separate from other aspects of the setup.

Remark 1.1. Intuitively, one would first recover the regime-structure, then per-regime graphs. Testing for graphs directly also means, the recovery of regime-structure (now the second step) can employ the graphical results, for example to optimize signal-to-noise, for better results. Indeed there are multiple simplifications possible §B.9. The present paper focuses on the (direct) graph-discovery step of this scheme.
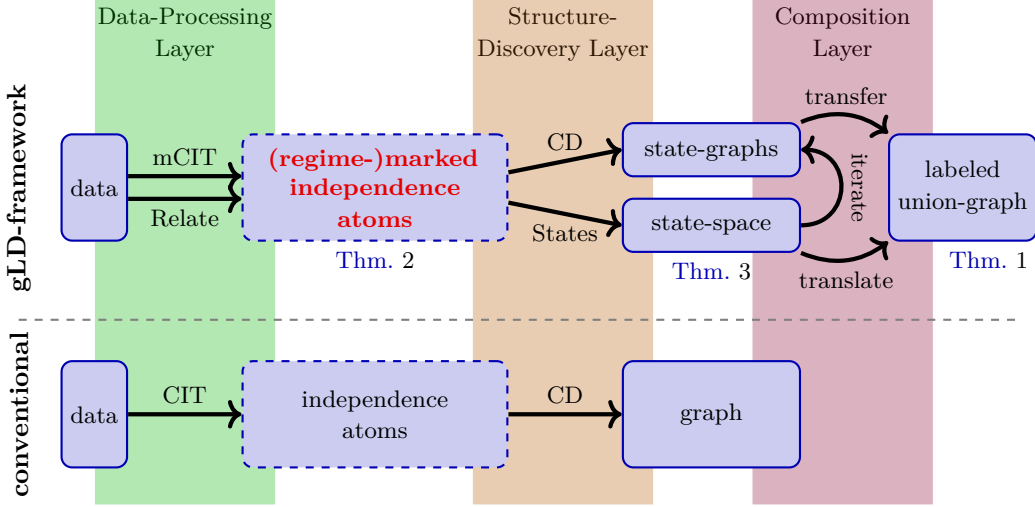
Figure 1.4: Framework Architecture. Blue boxes are abstract concepts encoding knowledge (dashed: lazily evaluated). Arrows represent algorithmic components converting such knowledge (see §4); these components are highly modular: Conventionally one may combine different CD-algorithms with different CITs; in our framework individual components enjoy similar independence. By independence "atoms" we refer to individual independencies (no relations like d-separations are implied at that stage). The core idea is the introduction of a new abstraction of independence atoms that additionally encode regime-information. Its careful choice enables our framework.

Realization of the guiding principles: Having laid out the problem, its challenges, and conceptual bounds for its realization, we can finally discuss how to actually approach the solution of the problem. Figure 1.4 illustrates the high-level architecture of our framework. First focus on the lower panel conceptualizing the dataflow in conventional CD: There are two abstract layers. A CD-logic, which operates not on data directly, but rather on independence-statements, and a conditional independence test (CIT) transforming data into independence-statements. The core idea of our framework is to modify the CIT to also bear the main burden of pattern-discovery. This means we can retain CD almost unchanged (both in theory and code-implementation; both IID and time series), and have produced a problem local in the graph already. The direct-testing principle has to be realized only by the data-processing layer if it produces sufficiently simple output; sufficiently simple meaning not scaling with information in the regime-structure.

Evidently the main difficulty is now in actually realizing such a modified CIT that checks for the existence of a pattern in independence rather than just independence vs. dependence. This test can avoid scaling with information in the regime-structure, because an output deciding between three alternatives – independence, dependence or existence of any regime-structure realizing both – turns out to be (almost; §6) enough information to complete MCD. This main difficulty of producing suitable modified CITs, can further be subdivided into sub-tasks (see §5). Among other advantages, this simplifies the identification of CPD, CIT and clustering related subtasks, and isolates the underlying problem sufficiently to make a direct testing approach not just feasible, but makes it manifest itself intuitively. Finally, this systematic analysis of the task also reveals two unavoidable limitations to what kinds of results are possible for MCD, irrespective of what methodology is employed. Knowing of these fundamental bounds, we can then understand theoretically and numerically the incurred trade-offs one has to consider, which also helps making informed hyperparameter decisions.

The ideas outlined in the previous paragraph modify what is labeled as "data-processing layer" in Fig. 1.4. However, we also have to systematically evaluate the additional information provided by this modified data-processing layer. In particular, we have to recover a space of

model-states (even the number of changes in the independence-structure need not be the same as the number of changes in the model; arrow labeled "States" in Fig. 1.4). Finally, other than for conventional CD, we have to compose a meaningful MCD output: We have to co-ordinate multiple applications of CD (there are evidently multiple graphs to produce). Further, observed changes in the independence-structure can be attributed non-trivially to model-properties. Additionally, some edge-orientation information can be transferred between states. At least in the (suitably) acyclic case, the result can then be represented as a labeled union-graph: a single graph where regime-specifically changing links are labeled (or marked in some other way, see Fig. 1.1).

We follow the nomenclatural convention that *regimes* refer regions of the index set (with oftentimes not explicitly modeled attached meaning: time, space, . . .) containing data points of similar, typically unobserved, system-states. Observations are then collected within the hidden *context* of the associated regime. By slight abuse of terminology, we refer to models featuring such non-trivial structure as *non-stationary*.

Contributions: The main contributions of this paper are to

- analyze the choice of useful inductive biases, improve the understanding of the problem and its challenges, and lay out guiding principles to avoid apparent difficulties on a conceptual level.

- devise a framework based around modifying the independence-testing procedure that can realize these principles in a highly modular way.

- analyze in detail the realization of the modified independence-testing (§5) theoretically and in (sub-system level) numerical experiments; the analysis includes the uncovering of fundamental limitations to the feasibility of MCD, practical resolutions via trade-offs and meaningful convergence statements, as well as potential paths forward.

- analyze in detail the specification and realization of the state-space recovery (§6). This includes a meaningful notion of identifiable states and theoretically sound, practically feasible algorithmic implementations. We also provide a proof-of-concept implementation of the required indicator-relation test (§D.4.7).

- analyze in detail the properties of the composition algorithm (§4). This includes a proof of its soundness given an oracle for the modified independence-tests and sound state-space recovery (previous two bullets).

The structure of our framework may, after the fact, appear evident and unsurprising, however, there are a great many plausible approaches to the problem, and it seems to be primarily the *correct structure* that decides, whether ultimately everything fits together and produces useful results on finite data.

To demonstrate the feasibility and validate our ideas about the inductive bias incurred, we further

- implement, for each module of our framework, a simple baseline version and combine them into a reference method.

- perform extensive numerical experiments and comparisons to other approaches to test our expectations concerning the behavior with a number of parameters.

- discuss the results of these experiments, and some weaknesses unveiled.

We focus on simple settings (continuous variables, linear models, no non-graphical non-stationarities), but we belief that our very modular approach should generalize well to more complex settings, and include discussions of potential future work, supporting this idea.

2 Related Literature

The notion of causality we use is the one developed by Pearl and others, see e.g. [39; 43; 21]; other approaches to formally capture causation, for example from temporal properties [23], are also employed by some references below. **Causal discovery** algorithms have been a subject of study for decades. Our work builds on constraint-based algorithms [61; 60; 59; 51; 49; 20], but also other approaches like score-based methods [36; 11] especially when using local scores may be compatible with many of the ideas presented. Besides the study of different data-setups like (discrete) time series [51; 23], also event-based models like [68] or, especially more recently, continuous-time models [35; 6] are studied in the literature. Below, we focus in particular on variants that take into account multi-context data (like multiple datasets or multiple regimes) from a mostly constraint based view-point. We study the case of observational data, interventional data from multiple contexts is studied for example by [42; 32].

Accounting for non-stationarity can mean many things, we try to give a systematic account to connected goals studied in literature: Non-stationarity affects test-quality, and thus it can be studied as a problem of robustness of testing [28; 37]. A related question is that of the *interpretation* of heterogeneous information in terms of shared model-information, for example a "union-graph" [54; 62]. Evidently multi-context data does contain additional information about the system. An often studied aspect of this is information about edge-orientations[2], for example "Constraint-based causal Discovery from heterogeneous/non-stationary Data" (CD-NOD) [28] (with a recent more time series focused variant [53]) uses kernel-tests to analyze which mechanisms vary (how strong); this information can under a causal modularity assumption be interpreted as orientation information. **Given knowledge about context-assignments**, such information can also more generally be exploited to get orientation information and locate changes in the graph [28; 37; 24], much of which was systematized by the "joint causal inference" (JCI) framework [37]. Context-assignment can be highly flexible, for example [8; 72; 68] employ a graphical structure also on context-information (reflecting for example a device-network-topology), with a formalization that ultimately draws on the theory of Hawkes-processes [14], while [16] uses periodic structures, but many methods specialize to persistent temporal regimes [55] or multiple data-sets [5; 41; 37; 24]. CD-NOD [28] can treat the second case and additionally the case of quantitative (effect strength) temporal variation, where it does not require prior information about precise regime-locations, see below. Further also knowledge about *context-specific* graphs (as opposed to union-models) can be exploited for example for down-stream tasks like effect-estimation [5; 41]. Indeed this problem has also been studied for example by [25] and from the perspective of specifically finding differences (for example in causal effects) between contexts by [3].

Not knowing the context-assignments in advance, some of the above ideas still indirectly apply, for example [24] is able to deconfound certain context-related (in the sense of [37]) situations. The full recovery of context-specific graphs and context-assignments (the main topic of the present paper) also has been studied before. A simple, but very practical, approach is to use some sort of sliding window-procedure. The work pursuing the most similar goals to ours is probably [55], who develop an algorithm called Regime-PCMCI to discover different regimes and associated graphs. The basic idea there is, to (starting from an initial guess) iteratively improve regime-assignments by fitting causal models per regime and optimizing assignments for optimal predictive quality. The requirement to fit a model puts some restrictions on possible models (no confounders and edges must be orientable, [55] study time series without contemporaneous links and without confounders), but it allows to discover also shifting (but stable within each regime) causal effects, beyond graphical changes (which we focus on). There are also comparable parametric approaches [33]. Albeit for very different types of data [4], propose a approach which also employs model (density) fitting plus a parametric (hidden Markov model-like) assumption on regime-assignments. A

---

[2]Additional edge-orientations can also be found for example by restricting function-classes of mechanism (e.g. assuming linearity) [58], multi-context information provides an additional pathway to such information.

final remark, especially compared to typical [37] settings, should be that we study a local and binary (dependent or independent) problem, so that it will for our purposes always suffice to study binary context-variables.

This binary (in particular categorical) nature of the context means we are looking for **qualitative changes**. It is of course also reasonable to investigate quantitative changes (drifts or more complex dependencies on a sample-index like time), see for example [34]; interestingly their approach seems to be local in the graph (for CD-NOD, see end of paragraph). Ultimately one is in such cases often interested in qualitative questions, like "is there an upward / downward trend", at which point the philosophy behind our framework might be helpful. Generally the idea of testing such properties directly is of course not new, see for example [64, §10.13], but we are not aware of this idea having been applied to independence-testing, CD (as studied in this paper) or even effect-estimation questions (as posed above).

For the temporal case **CD-NOD** [28] specializes precisely in finding quantitative changes. While this formally includes quantitative changes as a special case, no information about such a quantitative nature is extracted. Indeed this might also prove extraordinary challenging in a kernel-setting. CD-NOD and our approach in many ways supplement each other, it would be an interesting question for future work, if they actually synergize well in practice: CD-NOD can in particular extract orientation-information that would not be conventionally accessible by constraint-based causal discovery methods, and the kernel-based implementations it provides are well-suited for the analysis of quantitative smooth changes; our approach on the other hand focuses on extracting qualitative information and wraps CD methods in a way that could also incorporate CD-NOD's orientation information in principle. CD-NOD introduces new information to what we label the data-processing layer in Fig. 1.4; while not phrased as a modification of the independence-structure in [28], the orientation-information produced by in their test could probably be systematically included in such a way.

An important conceptual step in our framework is to modify the notion of **independence-structure**. Indeed there is a related class of concepts loosely referred to as "local independence" (local in the indexing, e. g. time, not in a causal graph) according to [27] "the concept of local (conditional) independence has been ascribed at least a dozen definitions in the testing literature". Typically, the assumption is that (in some formal sense) there is a latent L such that knowing L we have for example $X \perp\!\!\!\perp Y | L$ while $X \not\perp\!\!\!\perp Y$, where L contains little enough information (in some sense) for this problem to become testable. Compare this to our setup, which can instead be formulated as there being an L such that values of L split the data into subsets $X \perp\!\!\!\perp Y | L = 0$ while $X \not\perp\!\!\!\perp Y | L = 1$. Local independence ideas in this sense have played a role in causal methodology for example in [24]. [48] introduces a related idea of conditional stationarity for quantitative properties. There are also modifications of (graphical) independence-models to account for known context-assignments, especially (but not only) for categorical variables as "stratified graph" [38] and (closely related) "labeled DAG" (LDAG) [13; 29]. For context-specific knowledge, the translation of independence information into causal information can become quite non-trivial [25; 45]. On the practical testing of conditional independence, there is of course likewise a large corpus of literature; a comprehensive review is not possible within the scope of this work. However, we want to highlight two examples relevant to our discussion: Already [1] discuss the testing of independencies on mixtures. Further there are known impossibility-results [57] beyond the (pattern-detection related) ones we encounter in §5.

The questions we ask may also be seen as (and are certainly related to) aspects of **multi-scale** problems. Such problems are ubiquitous in nature (e. g. [31]) and have formal approaches ranging from multi-level statistics [19] to causal discovery in the Fourier-domain[3] [47]. Further, we detect patterns in all-variable samples (like regions in time), while there is also the orthogonal problem of finding structures grouping variables in-sample in the

---

[3]Also the "driving force estimation" of CD-NOD [28], quantifies context-influence via suitable eigenvectors. While not a Fourier / Laplace-transform, this also is a basis-change in function-space, with focus on an additional relevance-sorting to make projection to a low-dimensional subspace meaningful.

approaches called causal feature learning (CFL) [10; 9] and causal representation learning (CRL) [56].

Finally, we will naturally encounter questions from a wide range of **related fields**. These include change-point detection [63] (or more generally signal processing), also by causal principles [17] (which could be helpful for the second step of indicator-resolution, see also §B.9), clustering, hyperparameter choices have relations to over- / under-fitting questions and the problem is inherently related to missing-value problems, so unsurprisingly many approaches [55; 4] are implicitly or explicitly related to EM-algorithm [15] and it seems plausible that such approaches could improve our current implementation of §5.2.3. Also ideas from the shape / pattern recognition literature [2] are related, even though the typical problem-statements seem to involve a signal vs. size behavior (e. g. keeping the integral over the signal fixed) that is not applicable to independence-testing (there is no such thing as a "stronger" independence signal, as this is the null hypothesis). An important connection that perhaps should be investigated further in future work is that to Vapnik–Chervonenkis (VC) theory. Many of the properties we encounter in §5 seem to mirror our expectations from VC-theory, yet they are surprisingly difficult to make concrete. The fundamental limitation of Prop. 5.3 can be intuitively understood as a maximum amount of asymptotic pattern-information per sample, which seems closely related to VC-entropy [64, §7.A1].

3 Underlying Model

Causal properties are properties of the underlying generating model, not of the underlying distribution [39, §1.5 (p. 38)]. We want to study causal properties of non-IID (or non-stationary time series) systems and it is thus of great importance, to clearly specify what such a model may look like and which of its properties we are interested in. We start from structural causal models (SCMs) in the usual sense §3.1 and generalize them in a way that formally captures the properties relevant to changing causal graphs §3.2. If the graph associated to our model can change, then the underlying model must transition between different states §3.3 each described by a simpler model. Not all such model-states will occur in data, and not all of them can necessarily be distinguished by a CD-algorithm in practice; to make the second point clearer, we will first discuss CD in a standard sense in §3.4, before returning to model-states in §3.5. The discussion of CD in a standard sense §3.4 also gives a more abstract perspective on constraint-based CD as an abstract machinery transforming independence information into information about causal graphs, which will simplify arguments in §4. Finally we outline assumptions and goals for causal discovery in this setup §3.6. Throughout this section we focus on the case where the regime-structure is random, but fixed as part of the model; details on the modeling of randomness of the regime-structure itself in a meta-model are discussed in the appendix §C.

3.1 SCMs

We start from the standard formulation via structural causal models (SCM) [39; 43]:

Notation 3.1. For some finite I, fix a set of endogenous variables $\{X_i\}_{i \in I}$, taking values in $\mathcal{X}_i$, with $i \in \mathcal{O} \subset I$ observed (if $I = \mathcal{O}$ the model is called causally sufficient), and mutually independent exogenous noises (hidden) $\{\eta_i\}_{i \in I}$, taking values in $\mathcal{N}_i$. We write $V := \{X_i | i \in I\}$ for the set of all endogenous variables, $U := \{\eta_i | i \in I\}$ for the set of all exogenous noises. For $A \subset V$, denote $X_A = (x_j)_{j \in A} \in \mathcal{X}_A := \prod_{j \in A} \mathcal{X}_j$, and similarly for $B \subset U$, further $\mathcal{X} := \mathcal{X}_V$ and $\mathcal{N} := \mathcal{N}_U$.

For each $i \in I$ there is a set of parents $\mathrm{Pa}_i \subset I - \{i\}$ and a mechanism $f_i : \mathcal{X}_{\mathrm{Pa}_i} \times \mathcal{N}_i \to \mathcal{X}_i$ such that the endogenous variables satisfy the structural equations $X_i = f_i(X_{\mathrm{Pa}_i}, \eta_i)$ relative to its parents and noise-term. Parent-sets are assumed to satisfy a suitable minimality condition, e. g. [7, Def. 2.6]. The model is called additive if each f_i can be written as $f_i(X_{\mathrm{Pa}_i}, \eta_i) = \eta_i + \sum_{j \in \mathrm{Pa}_i} f_{ij}(X_j)$. It is called linear if each f_i is (affine-)linear.

In the causally sufficient case, the causal graph G is a graph on the vertex-set $\mathcal{O} = I$ with a directed edge from i to j iff $j \in \mathrm{Pa}_i$. In the presence of latent confounders $\mathcal{L} = I - \mathcal{O} \neq \emptyset$, bi-directed edges are added between i and j iff there is a latent $l \in \mathcal{L}$ and directed paths from X_l to X_i and X_j where only the respective endpoints (i and j) are observed.

3.2 Non-Stationary Models

Graphical changes are inherently qualitative: Each (directed) link in the graph may be present or not. In particular explicit time-dependence of the causal graph can always be described by a collection of "indicators" that indicate the presence (or absence) of any particular link. Links that never change have a trivial indicator:

Notation 3.2. To make the distinction to the variable-indices I clearer, we denote the sample-indices by T, where w. l. o. g. $T \subset \mathbb{Z}$. We refer to $t \in T$ as time for the same reason, but T can be any index set and may also encode spatial or other patterns (see §5.1.2).

Definition 3.3 (Indicators)**.** An indicator is a mapping $R : T \to \{0, 1\}$. An indicator R is trivial, if R is constant (as a mapping).

We will later put constraints on the form of indicators enforcing a kind of persistence, that is, limiting the frequency of change in a suitable sense §5.1.

3.2.1 Additive Models

For additive models, it is straightforward to define a non-stationary model with changes in the causal graph modeled by indicators:

Definition 3.4 (Non-Stationary Additive SCM)**.** Given variables $\{X_i\}_{i \in I}$, (possibly trivial) binary indicators $\{R_{ij}\}_{i,j \in I}$ and time-independent structural mappings $f_{ij} : \mathbb{R} \to \mathbb{R}$, the non-stationary additive SCM M is given on $\{X_i\}_{i \in I}$ by the modified structural equations $X_i^t = \eta_i^t + \sum_{j \in I} R_{ij}(t) \times f_{ij}(X_j^t)$.
  Remark: We formally sum over all $j \in I$ (we have not yet defined parent-sets). Because the R_{ij} are allowed to be trivially equal to zero, we will w. l. o. g. assume all f_{ij} are non-constant.

Parent-sets may then be defined by non-vanishing of indicators:

Definition 3.5 (Non-Stationary Parents)**.** The parents at time t of X_i in the non-stationary additive SCM M are the elements of the set

$$\mathrm{Pa}_i^t = \{j \in I | R_{ij}(t) \neq 0\}.$$

We define the non-stationary causal graph $G(t)$ relative to Pa_*^t as before (see notations 3.1).

Remark 3.6. If all R_{ij} are constant on an interval $[a, b] \subset T$, then for $t \in [a, b]$ the non-stationary graph $G(t)$ is the causal graph of the model obtained for the system restricted to $[a, b]$ in the standard sense.

3.2.2 Non-Additive Models

This subsection generalizes the previous construction to non-additive models; it is not required for the understanding of the remainder of the paper and may be safely skipped on first reading. In the general (non-additive) case, constness can be modeled by replacing a parent as input by an exogenous indicator as follows:

Definition 3.7 (Non-Stationary General SCM)**.** Given variables $\{X_i\}_{i \in I}$ with $|I| = K$, (possibly trivial) non-additive mappings $\{r_{ij}\}_{i,j \in I} : T \to \mathbb{R} \sqcup \{*\}$ (formally add a disjoint special point $*$), such that the r_{ij} are constant between $*$-values in the sense that $\forall t < t'$:

$r_{ij}(t) \neq r_{ij}(t') \Rightarrow \exists t_* \in [t, t']$ s.t. $r_{ij}(t_*) = *$; and time-independent structural mappings $f_{ij} : \mathbb{R}^{K+1} \to \mathbb{R}$. Define the shorthand

$$\tilde{X}_{ij}^t := \begin{cases} X_i^t & \text{if } r_{ij}(t) = * \\ r_{ij}(t) & \text{if } r_{ij}(t) \neq * \end{cases}$$

The non-stationary SCM M is given on $\{X_i\}_{i \in I}$ by

$$X_j^t = f_{ij}(\eta_j^t, \tilde{X}_{1j}^t, \dots, \tilde{X}_{Kj}^t).$$

Remark 3.8. The mappings r_{ij} taking values in $\mathbb{R} \cup \{*\}$ induce binary indicators R_{ij} by collapsing the $\mathbb{R}$-component to a point: Set $R_{ij}(t) = 1$ if $r_{ij}(t) = *$ and $R_{ij}(t) = 0$ otherwise. From these R_{ij} parents and graphs may be defined as in the additive case.

3.2.3 Limitations

This description does not capture other, potentially practically relevant, non-stationarities like parameter-drifts or other explicit time-dependence of mechanisms or noises. One might be inclined to start from a very general model-definition (like explicitly time-dependent mechanisms), however, one has to be very careful to avoid tautologies: To learn something from a model, it must make interesting properties explicit. A model with arbitrary time-dependence of mechanisms may implicitly capture the presence of edges, for example by (non-)constness in a particular parent at a fixed time t, but this property (which we are ultimately interested in) itself is not explicit from its structure. For this reason, we decided to give a minimal extension beyond standard SCMs that explicitly captures what we need; every state (see §3.3) then has fixed parent-sets, per state models may still be modified to capture other types of non-stationarity, but this approach separates graphical and non-graphical changes in a clear hierarchy. Indeed it may also be useful for the interpretation of results to further consider changes in noise-terms separately (extending to general probability-kernels as mechanisms in another step). Nevertheless the other view-point – to generalize first – is of course also useful, especially in cases where graphical changes are not of interest.

3.3 Model States

The above models become SCMs in the standard sense once we fix the values of the indicators. There is only a finite number of combinations of values of the non-trivial indicators, and many causal properties of the model may be understood from knowing the causal graph of each such "state".

Definition 3.9 (States)**.** The set of non-trivial indicators is

$$\mathcal{R} := \{ R_{ij} \mid i \neq j \text{ and } R_{ij} \not\equiv \text{const} \} \quad \text{with } \kappa = |\mathcal{R}| \text{ elements.}$$

Denoting the κ elements of $\mathcal{R}$ by $R_1, \dots, R_\kappa$ we may capture the state of the model by

$$\sigma : T \to \{0, 1\}^\kappa, t \mapsto (R_1(t), \dots, R_\kappa(t)).$$

We call the 2^κ elements of $S := \{0, 1\}^\kappa$ potential (as opposed to reached, Def. 3.21) system states and write $T_s := \sigma^{-1}(\{s\}) \subset T$ for the time-indices realizing state s.

States capture all qualitative (graphical) causal non-stationarity (proof in §C.6):

Lemma 3.10 (State-Factorization)**.** *The map $G : T \to \mathcal{G}, t \mapsto G(t)$ factors through $\sigma : T \to S$ ("G can be written as a function of $s \in S$"), i.e. there is a unique mapping $G_{(s)} : S \to \mathcal{G}$ such that $G(t) = (G_{(s)} \circ \sigma)(t) := G_{(s)}(\sigma(t))$. We will by slight abuse of notation write $G(s) = G_{(s)}(s)$.*

This means, all qualitative graphical changes are captured by the map $G(s)$ defined on the finite state-space S. We will focus on learning $G(s)$ soundly and approximating $\sigma(t)$, when of interest, in a post-processing step, see §3.6 and §B.9. This notion of states will be further refined in §3.5.

3.4 Constraint-Based Causal Discovery Revisited

Constraint-based causal discovery algorithms employ conditional independence-relations of an observed distribution to draw conclusions about the underlying causal graph. Indeed, this structure of independencies is the *only* information used; while this limits the results obtained, for example to Markov equivalence-classes (sets of possible graphs rather than individual graphs), it is important for the remainder of this paper to note that no other information is needed. Thus an abstract constraint-based causal discovery algorithm can be defined as a mapping from independence-structures to sets of graphs, with certain properties encoding soundness, completeness and others. In practice, it is of course of great relevance, how this mapping can be efficiently computed. Abstracting this aspect away will later allow us to employ standard algorithms and implementations to compute the abstract mapping; thereby we will not have to reinvent such efficient realizations but can instead leverage existing technology. For simplicity we only consider CD-algorithms that will (given independence-test results) execute deterministically. This includes to our knowledge most constraint-based causal-discovery algorithms used in practice.

We will start with a simple yet convenient abstraction of independence-structures[4], then continue with a description of what results are produced (e.g. Markov equivalence-classes), what algorithms formally compute, how their correctness may be defined, and how the sparsity of algorithms (small number of independencies actually evaluated) comes into play. For the remainder of this section we fix a K-element index-set I and variables $\{V_i\}_{i \in I}$ to avoid confusion with X, Y, Z denoting individual or sets of V_i used in independence statements.

Definition 3.11 (Independence Atoms)**.** We define multi-indices (corresponding to conditional independence-tests, see below) of the form[5] (with $A \sqcup B$ denoting the disjoint union)

$$\vec{i} = (i_x, i_y, (i_z^1, \ldots, i_z^m)) \quad \in \quad I^{2+*} := I \times I \times \left(I^0 \sqcup I^1 \sqcup \ldots \sqcup I^{K-2} \right).$$

An independence-structure is (for our purposes) a mapping

$$\mathrm{IS} : I^{2+*} \to \{0, 1\}.$$

The set of all independence-structures is denoted by $\mathcal{I}$.

Notation 3.12. Using the shorthands $X := V_{i_x}$, $Y := V_{i_y}$ and $Z_j := V_{i_z^j}$, we will denote

$$\mathrm{IS}(i_x, i_y, (i_z^1, \ldots i_z^m)) = 0 \ \text{ as } \ X \perp\!\!\!\perp_{\mathrm{IS}} Y | Z_1, \ldots, Z_m \ \text{ and}$$
$$\mathrm{IS}(i_x, i_y, (i_z^1, \ldots i_z^m)) = 1 \ \text{ as } \ X \not\perp\!\!\!\perp_{\mathrm{IS}} Y | Z_1, \ldots, Z_m.$$

Example 3.13 (Independence Oracle)**.** The independence oracle $\mathrm{IS}_{\mathrm{oracle}}(M)$ for an SCM M is the (unique) independence-structure with the property

$$X \perp\!\!\!\perp_{\mathrm{IS}_{\mathrm{oracle}}(M)} Y | Z_1, \ldots, Z_m \quad \Leftrightarrow \quad X \perp\!\!\!\perp_M Y | Z_1, \ldots, Z_m$$
$$\overset{\text{faithful, Markov}}{\Leftrightarrow} \quad X \perp\!\!\!\perp_G Y | Z_1, \ldots, Z_m$$

where $X \perp\!\!\!\perp_M Y | Z_1, \ldots, Z_m$ denotes independence in the distribution induced by M. In the faithful and Markov case (usually assumed), the right-hand-side (and thus the left-hand-side) is further equivalent to d-separation in the causal graph G of M (second line).

CD algorithms output sets of compatible graphs rather than individual graphs:

---

[4]Here denoting simple atomic conditional independence-statements, without reasoning about logical implications between these statements [13], which suffices for our purposes.

[5]We use the usual convention that for a set A, the set $A^0 = \{*\}$ is the one-element set. Below, we denote $\mathrm{IS}(i_x, i_y, (*)) = 0$ as $X \perp\!\!\!\perp_{\mathrm{IS}} Y$.

Definition 3.14 (Resolved Graphs)**.** Let $\mathcal{G}_{\text{gt}}$ be a set whose elements are the graphs describing the possible ground-truths, e.g. directed acyclic graphs (DAGs) or ancestral graphs (AGs). We call an equivalence-relation $\sim$ on $\mathcal{G}_{\text{gt}}$ (e.g. Markov-equivalence) a graphical kernel (it will capture which graphs end up in the same output class) and its equivalence-classes $\mathcal{G} = {}^{\mathcal{G}_{\text{gt}}}/\sim$ the resolved graphical structure (its elements will be distinguishable).

Example 3.15. Standard algorithms have resolved graphical structures in this sense:

(a) PC-Algorithm [59]: Let $\mathcal{G}_{\text{gt}}^{\text{DAG}}$ be the set of directed acyclic graphs (DAGs). Define $\sim_{\text{Markov}}$ as Markov equivalence and $\mathcal{G}_{\text{Markov}}$ as the set of Markov equivalence-classes of DAGs.

(b) FCI-Algorithm [61]: Let $\mathcal{G}_{\text{gt}}^{\text{AG}}$ be the set of ancestral graphs (AGs). Define $\mathcal{G}_{\text{PAG}}$ as the set of inducing-path (maximal, MAG) graphs with partial orientations in the sense of FCI (the equivalence relation here also takes the potential existence of inducing paths into account).

(c) PC-Skeleton: Let $\mathcal{G}_{\text{gt}}^{\text{skeleton}}$ be the set of undirected graphs. The Markov equivalence-classes are identical to $\mathcal{G}_{\text{skeleton}} = \mathcal{G}_{\text{gt}}^{\text{skeleton}}$ if orientations are ignored [65].

These together already allow for an abstraction of constraint-based causal discovery algorithms as follows:

Definition 3.16. An (abstract) constraint-based causal discovery algorithm is a mapping

$$\text{CD} : \mathcal{I} \to \mathcal{G}_{\text{CD}}$$

into an algorithm-dependent resolved graphical structure $\mathcal{G}_{\text{CD}}$, induced by $\sim_{\text{CD}}$.

Example 3.17. Standard algorithms are abstract algorithms in this sense:

(a) PC-Algorithm: Use $\mathcal{G} = \mathcal{G}_{\text{Markov}}$ (cf. example 3.15a) and define PC(IS) as the output of the PC-algorithm when given the independencies in IS.

(b) FCI-Algorithm: Use $\mathcal{G} = \mathcal{G}_{\text{PAG}}$ (cf. example 3.15b) and define FCI(IS) as the output of the FCI-algorithm when given the independencies in IS.

(c) PC-Skeleton: Use $\mathcal{G} = \mathcal{G}_{\text{skeleton}}$ (cf. example 3.15c) and define $\text{PC}_{\text{skeleton}}(\text{IS})$ as the output of the skeleton phase of the PC-algorithm given the independencies in IS.

We also need a notion of correctness. So far, we only captured what algorithms do, but not under which assumptions they are sound and complete. Up to finite-sample errors, this is the question about consistency in the oracle case:

Definition 3.18 (CD Correctness)**.** Given a class $\mathcal{M}$ of SCMs on the variables $\{X_i\}_{i \in I}$ indexed by I, where $M \in \mathcal{M}$ has the (true) causal graph $g(M) \in \mathcal{G}_{\text{gt}}$ (using g for individual graphs as opposed to equivalence-classes) a causal discovery-algorithm $(\text{CD}, \mathcal{G}_{\text{CD}})$ is $\mathcal{M}$-consistent, if given the independence oracle $\text{IS}_{\text{oracle}}(M)$ (example 3.13), it satisfies $\forall M \in \mathcal{M}$

$$g(M) \in \quad \text{CD}(\text{IS}_{\text{oracle}}(M)).$$

At this point, standard consistency proofs under assumptions restricting models to a specific $\mathcal{M}$ translate to:

Example 3.19. For the algorithms above, it holds that [61; 70]:

(a) PC-Algorithm: Let $\mathcal{M}_{\text{ff, cs}}^{\text{ac}}$ be the class of faithful, causally sufficient SCMs with acyclic graphs. Then $(\text{PC}, \mathcal{G}_{\text{PC}})$ is $\mathcal{M}_{\text{ff, cs}}^{\text{ac}}$-oracle-consistent.

(b) FCI-Algorithm: Define $\mathcal{M}_{\text{ff}}^{\text{aac}}$ as the class of faithful SCMs with almost acyclic graphs. Then $(\text{FCI}, \mathcal{G}_{\text{FCI}})$ is $\mathcal{M}_{\text{ff}}^{\text{aac}}$-oracle-consistent.

(c) PC-Skeleton: Let $\mathcal{M}^{\mathrm{ac}}_{\mathrm{ff,\,cs}}$ be the class of faithful, causally sufficient SCMs with acyclic graphs. Then $(\mathrm{PC}_{\mathrm{skeleton}}, \mathcal{G}_{\mathrm{skeleton}})$ is $\mathcal{M}^{\mathrm{ac}}_{\mathrm{ff,\,cs}}$-oracle-consistent.

Remark 3.20. The strength of a statement about consistency depends on *both* the size of the class $\mathcal{M}$ (larger is more general) *and* on the amount of information provided by knowledge of an element $G \in \mathcal{G}_{\mathrm{CD}}$ (smaller sets G contain more detail). So, for example, there is no strict hierarchy between PC and FCI: FCI applies more generally, but may provide less information in cases where PC does apply.

Finally, of particular practical relevance is the sparsity of lookups: There are a lot of statements in the independence-structure, but only few of them are actually "consumed" by most algorithms. This reduces runtime(-complexity) and helps to keep error-rates in check. While the general treatment is substantially simplified by abstracting these implementation-details away, knowledge of such properties *can* be helpful (and can be formalized), a simple example will be seen in §6, more details are provided in §B.8.

3.5 Identifiable State-Space

Identifiability considerations concerning the state-space will require a formal account to three similar but conceptually disparate problems: Deterministic relations between indicators may make states *unreachable*; for finite observation-time, it may simply happen that some state never occurs making them *not reached*; and states $s \neq s'$ with $g_s \sim_{\mathrm{CD}} g_{s'}$ are not CD-*distinguishable*.

Reached State-Space: A more formal definition requires some clarifications concerning the model-structure given in §C; the question whether a state is *sufficiently* reached to be detected in a finite-sample sense can be treated similarly. This is a very intuitive problem, and the following simple definition will suffice to read the remainder of this paper:

Definition 3.21 (Reached States). A state $s \in S$ (Def. 3.9) is T-reached, if $T_s = \sigma^{-1}(\{s\}) \neq \emptyset$. Denote by $S_T \subset S$ the set of T-reached states in S.

It should be evident that, given data for T, we will not be able to learn anything about specifics of non-T-reached states.

Resolved State-Space Our approach inspects the (multi-valued) independence-structure only, so states s, s' featuring the same independence-structure are indistinguishable. Consider the following example:

Example 3.22 (Non-Identifiable Regions of the State-Space). We are given a model with two states, A and B. In state A, the causal graph of the model is $X \leftarrow Z \rightarrow Y$, in state B the causal graph is $X \rightarrow Z \rightarrow Y$. In both states, the independence-structure is identical. *Remark:* This model is neither union-acyclic nor order 1 (Def. C.3).

Generally, which states are actually distinguishable could depend on the CD-algorithm used, so we specify which states are distinguishable as follows:

Definition 3.23 (Identifiable States). Given an abstract causal discovery algorithm (Def. 3.16) CD, we call two states CD-indistinguishable $s \sim_{\mathrm{CD}} s'$, if

$$s \sim_{\mathrm{CD}} s' :\Leftrightarrow g_s \sim_{\mathrm{CD}} g_{s'},$$

where g_s and $g_{s'}$ are the ground-truth graphs for s and s' and $\sim_{\mathrm{CD}}$ on the right-hand side (as a relation on graphs) denotes the equivalence-relation of Def. 3.14 (e.g. Markov-equivalence if $\mathrm{CD} = \mathrm{PC}$). This defines an equivalence-relation on the model states S. We call the equivalence-classes the (T-)identifiable (by CD) state-space

$$S^{\mathrm{CD}} := {}^S\!/_{\sim_{\mathrm{CD}}} \quad \text{and} \quad S^{\mathrm{CD}}_T := {}^{S_T}\!/_{\sim_{\mathrm{CD}}}.$$

Non-equivalent (in this sense) states are thus distinguishable in the oracle case, if the output of the used causal discovery algorithm is consistent (Def. 3.18). On the other hand, there is little hope to detect (by constraint-based causal discovery alone) a more fine-grained state-structure than S_T^{CD} on the system.

3.6 Assumptions and Goals

We focus on patterns in exogenous variables, for example persistence in *time*; possible extensions to patterns in endogenous variables are briefly discussed in §B.2. Our approach is tailored towards modular (independently changing) mechanisms (see §7; Def. C.3). Since, on each non-empty T_s, the associated graph $G(s)$ (lemma 3.10) is the causal graph in the standard sense of the model in state s, it makes sense to assume:

Assumption 3.24 (Statewise Faithfulness Property). Given $s \in S_T^{\mathrm{CD}}$, then independence $X \perp\!\!\!\perp_{P_s} Y | Z$ in the distribution $P_s(\ldots) := P(\ldots | t \in T_s)$ implies d-separation $X \perp\!\!\!\perp_{G(s)} Y | Z$ in $G(s)$.

And we also immediately obtain (cf. [43, Prop. 6.31 (p. 105)]):

Lemma 3.25 (Statewise Markov Property). *Given $s \in S_T^{\mathrm{CD}}$, assume $G(s)$ is acyclic, then d-separation $X \perp\!\!\!\perp_{G(s)} Y | Z$ in $G(s)$ implies the corresponding independence $X \perp\!\!\!\perp_{P_s} Y | Z$ in the distribution $P_s(\ldots) := P(\ldots | t \in T_s)$.*

The information we reconstruct from data concerns the following qualitative properties. Their complexity increases with model-complexity, but not with sample-size:

- Existence of states: Which model-states exist? Which states are reachable?

- Causal graphs of identifiable states: For each identifiable $s \in S_T^{\mathrm{CD}}$, what is $G(s)$?

- Attribution to model properties: Which indicators R_{ij} in the model are non-trivial?

These are supplemented with quantitative information about the form of non-trivial R_{ij}. Here complexity necessarily increases with sample-size, so only approximations are possible (even in asymptotic limits):

- Temporal location of states: When is the system in state s? I. e. approximate T_s. Or for all states together, approximate $\sigma(t)$.

- Uncertainty quantification: Estimate and represent expected errors.

Giving an estimate for the (temporal) location of regimes is a post-processing step in our framework (see also §B.9), we focus on the MCD problem. Especially giving good uncertainty statements on time-resolutions seems relevant. Due to the length of this paper, we leave a detailed study of this conceptually separate problem to future work.

4 Multiple Causal Discovery

We extend the standard notion of an independence-structure in two steps. This extension together with the viewpoint of abstract causal discovery algorithms will in §4.4 allow the direct application of both theoretical results for, and practical implementations of, standard CD-algorithms to non-stationary settings. We describe the IID-case, the stationary case works analogously.

4.1 Regime-Marked Independence Structure

Conventionally, a conditional independence takes one of two possible values: Independence $X \perp\!\!\!\perp Y|Z$, or dependence $X \not\perp\!\!\!\perp Y|Z$. Here, Z denotes a set of variables. We will add a third outcome: The presence of a (true) regime. We assume some ground-truth structure on the data which is related to a notion of persistence in §5.1, and automatically exists for example for the models discussed in §3. We fix a single test / multi-index (i. e. the variables X, Y and the set Z in $X \perp\!\!\!\perp Y|Z$), definitions below are to be understood to exist for any particular such choice.

Assumption 4.1 (Regime Structure)**.** We assume, the data indexed by T can be divided into regimes, that is n (possibly $n = 1$) disjoint ($i \neq j \Rightarrow T_i \cap T_j = \emptyset$), non-empty subsets $T_1, \ldots, T_n$ with $T = T_1 \cup \ldots \cup T_n$ and such that for each regime T_i the data points with $t \in T_i$ in that regime are IID distributed according to a (jointly for all variables X, Y and $W \in Z$) distribution P_i. We assume these subsets are maximal with this property, i. e. $i \neq j \Rightarrow P_i \neq P_j$. In the one-dimensional case (e. g. if T encodes time) we call (maximal) connected intervals within regimes segments (as is typically done in CPD literature). We call the random variable L measuring the number of data-points per segment the segment-length.

Example 4.2. A non-stationary model as described in §3 produces data which is globally (for all variables) structured by times T_s spend in state s. For any specific test $X \perp\!\!\!\perp Y|Z$, changes in mechanisms at non-ancestors of $Z \cup \{X, Y\}$ will not change P_i, thus regimes are unions of T_s over all $s \in S$ with relative changes only in such non-ancestors.

We are interested in three different ground-truth configurations:

Definition 4.3 (Regime Marked Dependence)**.** (See also Def. 5.9.)

0 : We call X globally independent of Y given Z, denoted $X \perp\!\!\!\perp Y|Z$, if $\forall i : X \perp\!\!\!\perp_{P_i} Y|Z$.

1 : We call X globally dependent on Y given Z, denoted $X \not\perp\!\!\!\perp Y|Z$, if $\forall i : X \not\perp\!\!\!\perp_{P_i} Y|Z$.

R : We say there is a true regime between X and Y given Z, denoted $X \perp\!\!\!\perp_R Y|Z$, if $\exists i_0 : X \perp\!\!\!\perp_{P_{i_0}} Y|Z$ and $\exists i_1 : X \not\perp\!\!\!\perp_{P_{i_1}} Y|Z$.

Definition 4.4 (Detected Indicator)**.** There is an associated indicator $R_{XY|Z}$, which we call the detected indicator, given by $R_{XY|Z}(t) = 0$ for $t \in T_i$ with $X \perp\!\!\!\perp_{P_i} Y|Z$ and $R_{XY|Z}(t) = 1$ otherwise. This indicator is trivially $\equiv 0$ in case 0, trivially $\equiv 1$ in case 1 and non-trivial if and only if we are in case R.

A regime-marked independence-structure is then (in analogy to Def. 3.11):

Definition 4.5 (Regime Marked Independence-Atoms)**.** A regime-marked independence-structure is a mapping (where R on the rhs is just some special value)

$$\text{IM} : I^{2+*} \to \{0, 1, R\}.$$

We denote the set of all regime-marked independence-structures by $\mathcal{I}_{\text{marked}}$ and

$$\text{IM}(i_x, i_y, (i_z)) = 0 \text{ by } X \perp\!\!\!\perp^{\text{IM}} Y|Z_1, \ldots, Z_m,$$
$$\text{IM}(i_x, i_y, (i_z)) = 1 \text{ by } X \not\perp\!\!\!\perp^{\text{IM}} Y|Z_1, \ldots, Z_m \text{ and}$$
$$\text{IM}(i_x, i_y, (i_z)) = R \text{ by } X \perp\!\!\!\perp_R^{\text{IM}} Y|Z_1, \ldots, Z_m.$$

The formal connection to the models of §3 is again (cf. example 3.13) made via an oracle structure:

Example 4.6 (Marked Independence Oracle). The regime-marked independence oracle $\text{IM}_{\text{oracle}}(M)$ for a non-stationary SCM M is the regime-marked independence-structure with the property

$$X \perp\!\!\!\perp^{\text{IM}_{\text{oracle}}(M)} Y | Z_1, \ldots, Z_m \quad \Leftrightarrow \quad X \perp\!\!\!\perp^M Y | Z_1, \ldots, Z_m$$

$$X \not\perp\!\!\!\perp^{\text{IM}_{\text{oracle}}(M)} Y | Z_1, \ldots, Z_m \quad \Leftrightarrow \quad X \not\perp\!\!\!\perp^M Y | Z_1, \ldots, Z_m$$

$$X \perp\!\!\!\perp_R^{\text{IM}_{\text{oracle}}(M)} Y | Z_1, \ldots, Z_m \quad \Leftrightarrow \quad X \perp\!\!\!\perp_R^M Y | Z_1, \ldots, Z_m$$

where $X \perp\!\!\!\perp_*^M Y | Z_1, \ldots, Z_m$ denotes the respective statement (Def. 4.3) for the distribution induced by M; regimes are fixed according to example 4.2.

It is of course of pivotal importance if and how this structure can be discovered from data in theory and in practice. In §5 we propose statistical testing strategies to approach this problem, and show that these have good theoretical and practical properties.

4.2 Multi-Valued Independence Structure

If there are multiple independence-statements with true regimes, then two questions remain (illustrated by example 4.8 below): Which combinations of values actually appear (see below)? And how are these related to model states (§3.3)? Both problems will be systematically addressed in §6.

Notation 4.7 (Indicator Naming). Given X and Y corresponding to variables V_{i_x}, V_{i_y} with indices $i_x, i_y \in I$, we denote the indicator $R_{i_x i_y}$ appearing in the definition of models 3.4 by $R_{XY}^{\text{model}}(t) := R_{i_x i_y}(t)$. Additional we use the detected indicators $R_{XY|Z}$ (possibly $R_{XY|\emptyset}$) of Def. 4.4 if there is a true regime between X and Y given Z.

Example 4.8 (Induced Indicators). Consider $X \leftarrow Y \rightarrow Z$ with only R_{XY}^{model} non-trivial. This will, besides $R_{XY|\emptyset}$ non-trivial, also lead to $R_{XZ|\emptyset}$ non-trivial, even though R_{XZ}^{model} is trivial. Further, while both are non-trivial, $R_{XZ|\emptyset} \equiv R_{XY|\emptyset}$; the underlying model only has two states (as opposed to the four potential values the pair $(R_{XY|\emptyset}, R_{XZ|\emptyset})$ could take): One with the link $X \leftarrow Y$ active, one with the link $X \leftarrow Y$ not active.

We capture what we need to know about co-occurrence of true regimes as follows:

Definition 4.9 (Multi-Valued Independence Structure). A multi-valued independence-structure IX is a set of independence structures. We call elements of IX detected states.

Remark 4.10. A multi-valued independence structure IX induces a regime-marked independence structure IM by mapping a multi-index $\vec{i} = (i_x, i_y, i_{\vec{z}})$ to 0 (or 1) if all $\text{IS} \in \text{IX}$ take the same value 0 (or 1) on the argument $\vec{i}$, and to R if there are $\text{IS}, \text{IS}' \in \text{IX}$ with $\text{IS}(\vec{i}) \neq \text{IS}'(\vec{i})$.

Example 4.11 (Multi-Valued Independence Oracle). The multi-valued independence oracle $\text{IX}_{\text{oracle}}(M)$ for a non-stationary SCM M is the multi-valued independence-structure

$$\text{IX}_{\text{oracle}}(M) := \left\{ \text{IS}_{\text{oracle}}(M_s) \big| s \in S(M) \right\}$$

where $S(M)$ is the set of states of M (Def. 3.9), and $\text{IS}_{\text{oracle}}(M_s)$ is the independence oracle (Example 3.13) of the model M in state s.

Example 4.12 (Implicit Marked Oracle). The multi-valued independence oracle $\text{IX}_{\text{oracle}}(M)$ induces by Rmk. 4.10 a regime-marked independence structure IM. This regime-marked independence structure is the regime-marked oracle $\text{IM} = \text{IM}_{\text{oracle}}(M)$ of example 4.6.

We will in practice divide the discovery of multi-valued independence-structures from data into three simpler sub-problems:

(i) Discover the regime-marked structure IM induced by IX. This is fully local in the graph and can be decided per independence-statement; see §5.

(ii) Discover simple binary relations between (small) sets of indicators. This requires only tests with binary results (see §6, §F.3, §D.4.7).

(iii) In §6 we will show in detail how these entail the full multi-valued structure from constraints arising in causal modeling.

In the schematic picture of our framework given in the introduction (Fig. 1.4) the first two points contribute the data-processing layer, and the box labeled "marked independence atoms". The third point realizes the arrow labeled "states" in the structural layer, the multi-valued independence structure as defined here combines the states (labeled "state space" in the figure) and the associated independence-structure(s).

4.3 Necessity

Knowledge of the (qualitative) multi-valued causal structure $\{G_s\}_{s \in S}$ of a model M is stronger than knowledge of its multi-valued independence-structure $\mathrm{IX}_{\mathrm{oracle}}(M)$. I. e. it is necessary to implicitly or explicitly discover the multi-valued independence-structure to solve the MCD problem:

Lemma 4.13 (Multi-Valued d-Connectivity)**.** *Given a non-stationary SCM M with states M_s faithful and Markov to their respective causal graphs G_s, then $\{G_s\}_{s \in S}$ determines* $\mathrm{IX}_{\mathrm{oracle}}(M)$.

Proof. By hypothesis, for each s d-connectivity is equivalent to independence, and G_s determines $\mathrm{IS}_{\mathrm{oracle}}(M_s)$ by d-connections. By definition, $\mathrm{IX}_{\mathrm{oracle}}(M) = \{\mathrm{IS}_{\mathrm{oracle}}(M_s)|s \in S\}$. $\square$

Remark 4.14. $\mathrm{IX}_{\mathrm{oracle}}(M)$ further determines $\mathrm{IM}_{\mathrm{oracle}}(M)$ by Rmk. 4.10 and all indicator implications by Rmk. F.14.

In the next section §4.4, we show that the reverse direction, discovering multi-valued causal structure $\{G_s\}_{s \in S}$ from the extended independence-structure, can be reduced to the problem of causal discovery in the IID or stationary case. For the IID / stationary case, there is of course a large range of algorithms available; these can easily be integrated with our approach.

4.4 The Core Algorithm

In this section, we explain the pseudo-code given in algorithms 1 and 2. Formal properties are then described in Thm. 1. The general outline is as follows: We are given a multi-valued independence structure whose discovery from data will be described in §5 and §6. More precisely, we are given two functions encoding multi-valued independence information by implementing

- the discovery of marked independence (Def. 4.3): Given a multi-index $\vec{j} = (i_x, i_y, i_{\vec{z}})$ corresponding to a conditional independence query $X \perp\!\!\!\perp Y|Z$, this algorithm called `marked_independence` returns one of three possible outcomes: 0 (global independence), 1 (global dependence) or R (true regime), cf. example 4.6. The implementation is described in §5.

- partial state-space construction: Let J be a (possibly incomplete) set of marked independencies (i. e. a set of multi-indices $\vec{j}$ with `marked_independence`$(\vec{j}) = R$). Then independence-statements in J, by definition, do *not* take a definite (global) value dependent or independent (or 1 and 0), but rather a state-dependent value. The possible combinations of values of elements in J are precisely the mappings from J to 0 or 1, denoted $\mathrm{Map}(J, \{0, 1\})$. As already the simple example 4.8 above shows not all elements of $\mathrm{Map}(J, \{0, 1\})$ are reachable. In §6 we will discuss in detail why this is

the case, and how it can be resolved; to understand the core algorithm, it suffices to know that §6 will produce an algorithm `construct_state_space`, which recovers the *reached* states $S^J \subset \mathrm{Map}(J, \{0, 1\})$. The implementation is described in §6.

From this information encoding the multi-valued independence structure, we want to find the set of identifiable states S_T^{CD} (Def. 3.23) and associated (equivalence-classes of) graphs $\{G_s\}_{s \in S_T^{\mathrm{CD}}}$. Indeed we will focus on producing the correct set of graphs $\{G_s | s \in S_T^{\mathrm{CD}}\}$, the association of model-states (translation into model properties) is discussed in §F.6.

Details on the formal description of the core algorithm 2 and a proof of the correctness (in the oracle case) of its output is given in §E. Indeed, there are some important aspects, like the completeness of the recovered set of graphs that require a careful analysis. Nevertheless the general behavior of algorithm 2 can be understood informally as follows:

Algorithm 1 `run_cd` (Run Causal Discovery with Pseudo Test)

1: **Input:** A J-state $s : J \to \{0, 1\}$ on a set J of marked dependencies $\vec{j}$.
2: **Output:** A graph G_s and a set J'_s of additional regime-dependent tests.
3: $J'_s := \emptyset$
4: **function** PSEUDO_CIT$(\vec{j})$ ▷ capture J'_s by reference
5:     **if** $\vec{j} \in J$ **then**   ▷ value depends on J-state
6:        **return** 'independent' **if** $s(\vec{j}) = 0$ **else** 'dependent'
7:     **else**   ▷ not (yet) known to feature a regime
8:        **if** `marked_independence`$(\vec{j}) = $ '0' (globally independent) **then**
9:           **return** 'independent'
10:       **else if** `marked_independence`$(\vec{j}) = $ '1' (globally dependent) **then**
11:          **return** 'dependent'
12:       **else**   ▷ only case left is 'R' (true regime)
13:          $J'_s := J'_s \cup \{\vec{j}\}$ ▷ we were not previously aware of this regime-dependence
14:          **return** 'dependent' ▷ continue in arbitrary choice of state, here: 'dependent'
15:       **end if**
16:     **end if**
17: **end function**
18: $G_s := $ `CD`(`pseudo_cit`)
19: **return** G_s, J'_s

Here 'CD' is treated as a function taking another function (the lazily evaluated independence-structure) as an input, cf. §3.4.

Algorithm 2 `run_mcd` (Multiple Causal Discovery)

1: **Input (implicitly):** Multi-valued independencies encoded as `marked_independence` (in `run_cd`) and `construct_state_space` functions.
2: **Output:** A set of graphs $\{G_s | s \in S\}$.
3: $J := \emptyset$ ▷ will record marked independencies $\vec{j}$ encountered so far
4: **repeat**
5:     $S := $ `construct_state_space`(J)
6:     **for** $s \in S$ **do**
7:        $G_s, J'_s := $ `run_cd`(s, J)
8:     **end for**
9:     $J' := \cup_s J'_s$
10:     $J = J \cup J'$
11: **until** $J' = \emptyset$
12: **return** $\{G_s\}_{s \in S}$

The function '`run_cd`' is specified in algorithm 1. See main text §4.4 for further explanation.

Initially we know of no state-dependent independence-statements $J_0 = \emptyset$, and using `construct_state_space` will in this case always return the one trivial map $\emptyset \to \{0, 1\}$, that is, $S_0 = \{*\}$ has a single element. We thus invoke `run_cd` once, with $J = \emptyset$. This executes a standard causal discovery-algorithm CD, for example CD = PC. Whenever a CIT would be executed by CD, it instead runs `pseudo_cit`, which for $J = \emptyset$ simply runs `marked_independence`. If the outcome is "true regime" we remember this test, by storing it in J', and continue as if the result had been dependence (in the initial iteration this convention yields the union-graph, Lemma F.18). We end up with a single graph G and a set of regime-specific independence-statements J', which we remember as J_1.

In the ith iteration, S_i, by specification of `construct_state_space`, contains those combinations of known state-dependent independence-statements in J_i that actually appear (the reached J_i-states, see above). For each such state s, we invoke `run_cd` once with this state s. This again executes a standard causal discovery-algorithm CD, and whenever a CIT would be executed, it instead runs `pseudo_cit`. For the state-dependent independence-statements in $\vec{j} \in J_i$, we fix values to $s(\vec{j})$. Effectively `run_cd` runs once for each actual state (combination of values taken by the state-dependent statements J_i fixed). Any previously unknown state-dependent statements (across all states) are recorded into J_i' and included additionally for the next iteration $J_{i+1} = J_i \cup J_i'$.

At some point, no new state-dependencies are found $J' = \emptyset$ and the algorithm terminates. It returns all graphs discovered in the last iteration. In the last iteration (since $J' = \emptyset$), for each state s, the result of `pseudo_cit` is always determined either by a "standard" independence result ('dependent' or 'independent') or by the state s. Thus `run_cd`, for each actual state s, produces the graph discovered by CD if state-dependent independencies take the values prescribed by the state, while non-state-dependent independencies take their global values.

Properties: The above algorithm potentially has to rerun the underlying (stationary) CD-algorithm often. This is surprisingly not a problem in practice: The limiting factor both in terms of runtime-requirements and in terms of statistical sample-efficiency is in the number of actually executed tests. But the output of `marked_independence` is deterministic (given data) and can be cached, so there is little increase in the required number of tests compared to the union-graph. In fact, the union-graph is denser (contains more edges) than any regime-specific graph, thus for example for CD = PC already the first iteration will run all tests required for (the skeleton-phase of) any of the reruns.

The output of Algo. 2 is sound and complete in the following oracle-case (for details and proofs, see §E):

Theorem 1 (Core Algorithm). *Given a non-stationary model M (Def. 3.4 / 3.7), a marked independence oracle* $\text{IM}_{\text{oracle}}(M)$ *(Def. 4.6; invoked as* `marked_independence` *in algorithm 1), an abstract CD-algorithm CD (Def. 3.16; invoked as* CD *in algorithm 1), which is consistent (Def. 3.18) on a set of models $\mathcal{M}$ including all reached states (Def. 3.21) $\forall s \in S_T : M_s \in \mathcal{M}$ and a sound and complete on a model-class containing M, state-space construction (Def. E.13; invoked as* `construct_state_space` *in algorithm 2).*

Then algorithm 2 terminates after a finite number of iterations and its output is a set (i. e. no ordering or characterization of states by model properties is implied) which consists of precisely one graph (a CD equivalence class, Def. 3.14) per CD-identifiable state $s \in S_T^{\text{CD}}$

$$\left\{ G_s \big| s \in S_T^{\text{CD}} \right\} \quad \text{such that} \quad \forall \tilde{s} \in s : g_{\tilde{s}} \in G_s,$$

where $g_{\tilde{s}}$ is the ground-truth graph in state $\tilde{s}$ (which is a representative of the CD-identifiable state s).

Example 4.15. If CD = PC, all states S are in different Markov-equivalence-classes, reached (occur in data) and the models M_s of the individual states are causally sufficient, faithful with acyclic true graph g_s and acyclic union-graph, then the identifiable state-space is $S_T^{\text{PC}} = S$

and in the oracle case algorithm 2 returns the set of Markov equivalence-classes $\{G_s | s \in S\}$ representing the true graphs g_s, i.e. $g_s \in G_s$ (by $S = S_T^{\text{PC}}$, each s has a single representative "$\tilde{s} = s$").

5   Marked Independence Tests

Our framework relies on knowledge of the multi-valued independence structure described in §4.2. Indeed, as shown in §4.3 *any* solution to the MCD problem has to (implicitly or explicitly) extract this knowledge. Thus there is a profound interest in understanding its recovery from data. However, this recovery from data turns out to be a quite challenging problem: We show two impossibility-results that put limits to what can be identified from data even in principle. These impossibilities are inherent to the problem, their occurrence is general not specific our approach.

A major strength of our approach is that it can make these limitations explicit and allows to understand and navigate them through hyperparameter controlled trade-offs. Indeed our main goal is to *understand* the problem and the behavior and implied inductive biases of different solutions. To this end, we divide the problem further into conceptually separate sub-tasks. This allows for the theoretical and numerical analysis of assumptions, null-distributions and power on different alternatives. Still with the primary goal of gaining insights, we focus on very simple and transparent solutions for the separate tasks. We do, however, outline how they are interconnected with well-known standard tasks and believe that leveraging more sophisticated state-of-the-art methodology on these tasks will allow for substantial improvements on finite sample performance in the future; these connections will be summarized in §5.5 at the end of this section. Both the subdivision into simpler tasks and the use of simple and transparent solutions also aids numerical verification of the theoretical findings: Benchmarking simple modular components at sub-millisecond runtimes allows for otherwise impossible exploration of the behavior with large numbers of model and algorithmic parameters.
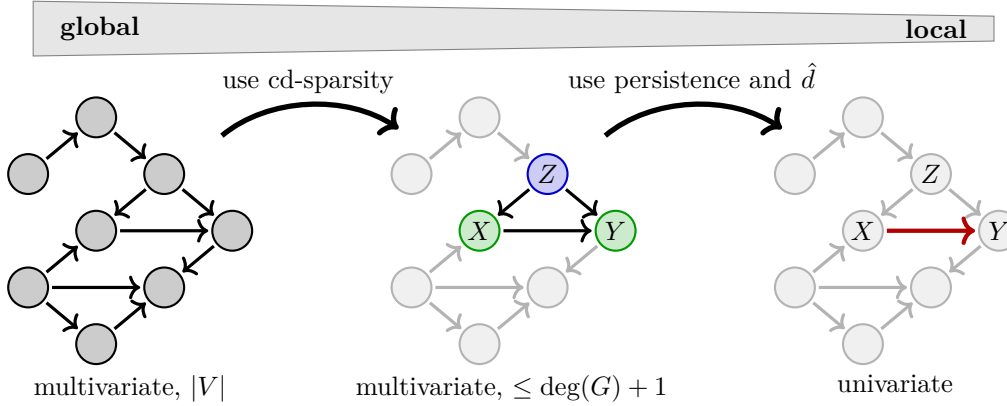

Figure 5.1: Our framework turns a (graph-)global clustering problem into (graph-)local ones.

As already outlined in the introduction §1 to this paper, our approach is guided by the principles of (graph-)locality and directness of testing; further our architecture (Fig. 1.4) confines the associated issues to the data-processing layer discussed here. Therefore we emphasize throughout this section the role and realization of these principles. Locality is achieved, as illustrated in Fig. 5.1, in two steps: The first one is to reduce the problem from a global question to a question about few variables involved in an independence test; this step is realized by design and factoring through the multi-valued independence structure. The second step focuses on the causal mechanism relating two variables. For optimal signal to noise, one should ask: How does one isolate, from the information contained in these few

variables $X, Y, Z_1, \ldots, Z_k$, precisely that information describing the (possible) dependence between the pair X and Y (given Z)? This question has of course a very standard answer: dependence scores (for example partial correlation), as used in conditional independence tests (CITs) are designed precisely to do so. Even more conveniently these scores are typically univariate, so that we obtain not only good signal to noise, but also a dramatically simplified problem. This simplified problem will be described and studied in §5.2, where it will also become apparent, why it can be efficiently tested in a "direct" way.

Remark 5.1. Going from one global problem with poor signal-to-noise to many local problems with good signal-to-noise, one should ask oneself: How many is "many", and is this better after accounting for multiple testing? Given a suitable, sparse testing strategy (in our case provided by the CD-algorithm), testing locally realizes an inductive bias favoring sparse graphs. It will typically perform better than global methods on sparse enough problems. Sparsity of the underlying graph is a pivotal assumption underlying constraint-based causal discovery in general, so that we require it here, should not lead to substantial *additional* restrictions.

Remark 5.2. Typically, there are multiple different conditioning sets Z tested for each pair X, Y. At this point, there is a subtle but very powerful conceptual advantage of performing graph-discovery before any other regime-detection: As long as we maintain the faithfulness assumption (not erroneously conclude independence or a true regime), the result of graph-discovery will be consistent if we can correctly accept independence or a true regime for a *valid separating set Z*. For CD our FPR-control only has to work correctly if Z is a valid separating set. In this sense graph-discovery can be *truly local* / occur on a single test without prior knowledge of the multiple causal graph(s).

This section starts with the introduction of persistence assumptions and their necessity due to a first impossibility-result §5.1. Then we discuss the details of combining persistence with dependence scores to reduce the problem to a univariate one §5.2. Next, we discuss the structure of this univariate problem, with particular focus on which inductive biases are meaningful and should be realized and how these considerations affect the precise formulation of sub-tasks and their order of execution §5.2.1. One scenario, which we will refer to as a "weak-regime" §5.2.3 turns out to be particularly challenging; this can be explained by a second impossibility-result concerning finite-sample error-control. We propose assumptions, trade-offs and potential future paths to handle this fundamental limitation. Afterwards, we briefly discuss details specific to conditional ($Z \neq \emptyset$) independence-tests §5.3. In §5.4 we show that our direct testing philosophy does lead to good asymptotic behavior in theory (and also in numerical experiments, §7). Finally we summarize our findings and discuss future work §5.5. Further details and proofs can be found in the appendix §D.

5.1 Persistence Assumptions

We analyze the existence of statistical tests for the multi-valued independence-structure, finding the necessity of assumptions. The underlying problem is closely related to randomness / IIDness testing [67; 66] (see also §5.2.2). We focus on the assumption of persistence in the following sense: Real world regimes often persist for an extended period of time, i.e. regime-switches occur on a time-scale larger than the primary dynamics under study. This kind of prior knowledge about patterns in the assignment of data points to regimes is not itself in any way specific to time series. Rather, for example spatially resolved data may be available where regimes are oftentimes likely to "persist" to neighboring (in space) sites. This kind of persistence assumption can be seen to allow for the resolution of the initial impossibility result. Persistence is formalized in §5.1.2 in a way suitable for the remainder of §5; there is not one objectively best way to leverage persistence, and we briefly explain the reasoning behind choices made.

5.1.1 Necessity

(possibly multimodal)
densities

different mixtures
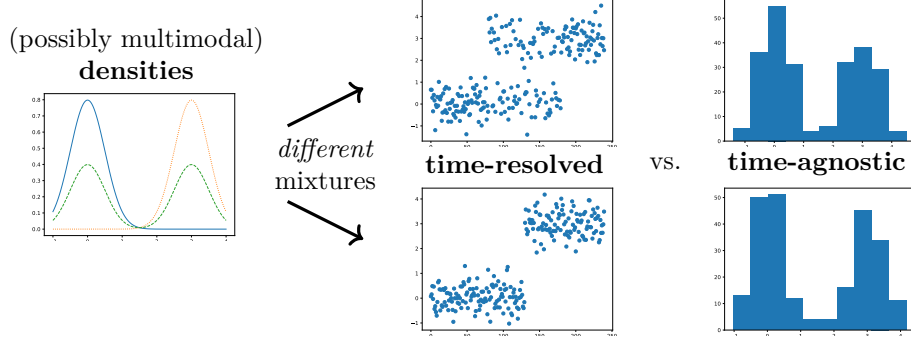
time-resolved   vs.   **time-agnostic**

Figure 5.2: Without strong parametric restrictions on the form of densities (lhs), mixtures cannot be uniquely decomposed (rhs). Persistence can help resolving this ambiguity (middle).

As show in Fig. 5.2, mixtures generally cannot be easily decomposed into contributing densities: The histograms on the right-hand-side differ for the two mixtures (top and bottom row) only by finite sample effects. On time-resolved data with persistent structure (middle panel) the difference is clearly visible. However, in the IID case only the information in the histograms (total density) is considered. While easy to illustrate on multi-modal densities, this problem is not specific to multi-modality. Indeed it occurs, if the density candidates (families from which to pick representatives) are *not* linearly independent in a very specific way [69; 4], and even in such cases, one would in the finite sample case certainly want to leverage persistence as well. There are many formal statements that capture this general behavior. In §D.1.1 we show the following result:

Proposition 5.3 (Impossibility Result A). *Given data as a set (without non-IID structure on the index-set), then the marked independence statement is not in general identifiable. By Lemma 4.13 (see also Rmk. 4.13) also the MCD-problem is not in general identifiable.*

While Fig. 5.2 may provide some intuition *that* persistence can help with this problem, we provide in §D.1.2 additionally some formal arguments to demonstrate *how* it helps.

5.1.2 Formulation

We start by two simple definitions that can be used to formalize a persistence requirement at great flexibility, making it applicable not only to persistent-in-time regimes but also to more general patterns in data. The general form of this pattern (for example persistent in time) must of course be known a priori.

Definition 5.4 (Patterns: Blocks, Alignment and Validity). Let I be a set indexing our data. Given an integer $B \geq 1$, we call a subdivision of I (and thus of the data) into disjoint subsets, containing B elements each, a subdivision into blocks of size B. We will assume that the number Θ of blocks is maximal, i.e. $\Theta = \lfloor N/B \rfloor$. Let $\mathcal{B}_I$ be the set of block subdivisions of I. A pattern is a fixed a priori structure that, given a block-size B, determines a subdivision of I into blocks of size B. Formally it is a mapping:

$$\text{Patt} : \mathbb{N} \to \mathcal{B}_I, B \mapsto T_B,$$

such that T_B is a subdivision into blocks of size B. We call a block b (Patt-)aligned if $b \in \text{Patt}(|b|)$. Given a regime structure (Ass. 4.1) we call a block b valid, if all indices $i \in b$ are in the same regime, otherwise we call b invalid.

Example 5.5 (Time-Aligned Blocks). The time-aligned pattern is the subdivision of $I = T = [0, N) \cap \mathbb{Z}$ into size B blocks of the form $b_\tau = [\tau B, (\tau+1)B) \subset T$ with $\tau \in [0, \Theta) \cap \mathbb{Z}$.

For more examples, see §B.1. To study convergence-behavior, a careful analysis of the asymptotic behavior of a persistence assumption is necessary and carried out in §C. For finite sample and practical considerations the following definition conveys the general idea.

Definition 5.6 (Persistence)**.** We say a random indicator (cf. §C) is (L, χ)-Patt-persistent, if a Patt-aligned block of size L is invalid with probability less than χ.

In practice, it is relevant to have (L, χ)-persistence with L large enough, yet χ small enough. This is one possible formulation of persistence (see §D.1.2). More creative formulations like requiring the applicability of a particular CPD method, leveraging prior knowledge about CP-candidates (for example a technological system may be known to transition its state only, but not always, at specific points) or parametric models for the indicator itself can also leverage the compatibility with a (known) pattern. In principle, our framework can be used with any such approach to persistence-based aggregation of data (§D.7.3). For further motivation of the choice employed here see §D.1.5.

5.2   The Univariate Problem

Here we discuss the emerging univariate problem, and thus the main practical challenges associated to testing marked independence. We start by clarifying the reduction to a univariate problem already indicated at the beginning of §5. Of the two steps shown in Fig. 5.1 we focus on the second one: turning data for X, Y and (multiple) Z_j into a local score associated to an edge via an *underlying* dependence-score $\hat{d}$. Our numerical experiments focus on partial correlation, but in principle the precise nature of $\hat{d}$ is not important, we need only properties typically satisfied by scores used for independence-testing (in a standard sense):

Assumption 5.7 (Underlying CIT)**.** The underlying dependence-score d is estimated by $\hat{d}$ in an unbiased and consistent (see §D.2) way and equals 0 on independent data. The α-confidence interval around zero for a given sample-count is known or can be estimated.

Remark 5.8. Conditional independence testing is a hard problem [57]. The additional information reported by a mCIT will certainly not make this problem easier. We do, however, want to focus on which *new* problems arise for mCITs compared to conventional CITs. These new problems can be studied in isolation by formally searching not for independent and dependent regimes, but rather for regimes with dependencies $d_0 \neq d_1$ and checking if $d_0 = 0$ while assuming reasonable convergence behavior (see §D.2). General CIT-testing related problems can then be accounted for either by assumptions on models (for example linearity) or by suitable interpretation of results (for example interpret "independent" regimes as uncorrelated instead).

Definition 5.9 (Marked Score-Independence Atoms)**.** In the light of Rmk. 5.8, we reformulate Def. 4.3 of marked independence relative to d. Denoting the dependence-score estimate for the test $X \perp\!\!\!\perp Y | Z$ by $d(X \perp\!\!\!\perp Y | Z)$ we distinguish the following hypotheses:

0 : We call X globally independent of Y given Z, denoted $X \perp\!\!\!\perp Y | Z$, if

$$\forall i : E_{P_i}[d(X \perp\!\!\!\perp Y | Z)] = 0.$$

1 : We call X globally dependent on Y given Z, denoted $X \not\perp\!\!\!\perp Y | Z$, if

$$\forall i : E_{P_i}[d(X \perp\!\!\!\perp Y | Z)] \neq 0.$$

R : We say there is a true regime between X and Y given Z, denoted $X \perp\!\!\!\perp_R Y | Z$, if

$$\exists i_0 : E_{P_{i_0}}[d(X \perp\!\!\!\perp Y | Z)] = 0 \text{ and } \exists i_1 : E_{P_{i_1}}[d(X \perp\!\!\!\perp Y | Z)] \neq 0.$$

For the sake of concreteness and simplicity, we restricted our numerical results and implementation to a partial-correlation test. An efficient (both in statistical and runtime terms) implementation of non-parametric scores can probably benefit substantially from more specific optimizations and is left to future work.

The estimate $\hat{d}$ is statistical in nature and requires a collection of data points to act upon. We take the simplest possible approach and apply $\hat{d}$ to the collections of data points obtained by exploiting a persistence assumption as described in §5.1. Concretely, this means for the approach by data-blocks §5.1.2 we apply $\hat{d}$ to each block of data individually. This defines our univariate problem: analyze the resulting collection of dependence-values to decide the marked independence query.

We focus on the question of marked independence, implication-testing (see §6) is discussed in §D.4.7 behaves very similarly. We distinguish three outcomes (dependence, global independence, existence of an independent regime) on four possible ground-truths, see Fig. 5.3. On the collection of dependence values this can be formulated as a clustering-like[6] problem: On valid blocks (those blocks contained entirely in a single regime) we could simply ask, "Is there more than one cluster?" and "Is one (possibly the only) cluster at $d = 0$?" to decide the problem. The presence of invalid blocks asks for a robust assessment of these questions, but does not fundamentally change the logic.
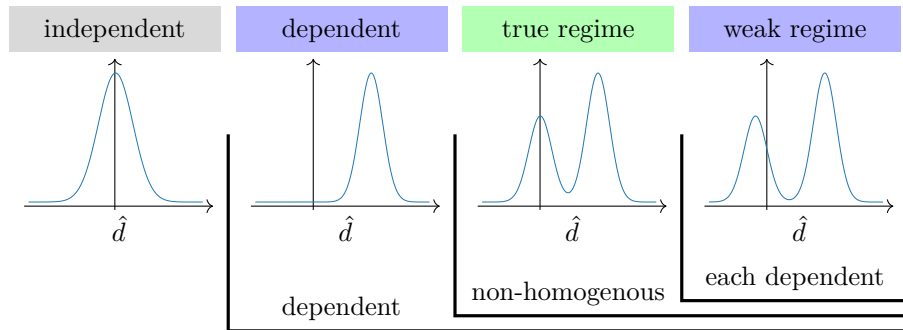

Figure 5.3: Different ground-truths for the univariate problem, expected outputs (color of headings), examples for density of per-block dependence-scores $\hat{d}$, and grouping by tests (braces below plots; reject independence, reject homogeneity, reject independence in low-dependence regime).

It is of great significance that this is a direct testing formulation: We do not insist on any knowledge concerning the assignment of blocks (or data points) to regimes. Rather if multiple peaks overlap, we only ask is one of them is centered at zero. We can thereby accept, that for points in such an overlap we do not have substantial information about their regime-assignments; we do not need such information to solve our task.

We formulated the problem above by asking two yes / no questions. Indeed statistical testing of binary hypotheses is more common and seems simpler in the present case. Deciding between four ground-truth scenarios (three potential results) will require at least two binary tests. It turned out that the second question ("is there a cluster at zero?") on homogeneous data is rather standard (it is an independence test), while in scenarios with multiple clusters it is very difficult. So we treat both cases separately, thus will discuss a total of three binary tests. This also leads to rather intuitive tests with simpler failure-modes: Is the data dependent? Is it non-homogeneous? Is the lowest-dependence cluster centered at $d \neq 0$? As shown in Fig. 5.3, these tests distinguish the four ground-truth scenarios.

Generally, in an oracle case (no finite sample errors), the order of execution of these tests is irrelevant. Nevertheless, there are at least two evident finite-sample effects to consider:

(a) Not all three problems are equally difficult, so unsurprisingly in practice the associated tests have different statistical properties. More concretely, the (global) dependence test

---

[6]We have specific prior knowledge, like the value $d = 0$ being special with known α-confidence region, and are interested in a weaker notion of solution as is typically discussed in clustering literature.

and the homogeneity (IIDness / randomness) test are more reliable than the distinction between weak and true regimes (deeper reasons will be discussed in §5.2.3 and §D.1.3). Using three binary tests implies a total of eight possible combinations of results, which is more than needed, so some will collapse to the same output. This has the convenient side-effect that one will not have to execute all three tests on all scenarios. Thus, we can e.g. on any homogeneous scenario entirely avoid the more difficult test.

(b) There is an inductive bias in the order of test execution that encodes our belief about the relative frequency of different ground-truth scenarios and the severity of different error-types (for example the weak regime and global dependence are assigned the same outcome, so errors confusing these two scenarios are much less harmful than others).

Next, we lay out the details of ordering the dependence and homogeneity tests (the weak-regime test will be executed last, see (a)). Afterwards we discuss the realization of the individual tests.

5.2.1 Testing Order

Inspecting Fig. 5.3, we could apply tests in order from left to right (dependence, homogeneity, weak regime), executing the next one whenever the previous one is positive. But since all inhomogeneous results are dependent, we could also test for homogeneity (as will be explained in §5.2.2) first, and depending on the outcome test either (global) dependence or weak regimes afterwards. In the oracle-case this does not change the outcome, but in the finite sample case it may (see points (a) and (b) in the introduction to the univariate problem above).

Applying an underlying score $\hat{d}$ (and associated independence-test) designed for IID data to a non-IID sample does *not* affect FPR-control: Inhomogeneity of d-values implies they are non-zero somewhere, thus true negatives (the null) are independent *and homogeneous*[7] (see also Fig. 5.3). Thus type I errors remain controlled. Concerning type II errors (statistical power) however, an estimator which is well-suited for rejecting IID alternatives, may no longer perform well on heterogeneous alternatives. Optimality in this case depends on the composition (rate of IID-alternatives vs. rate of non-IID alternatives and their form) of the model-prior; so there is typically no uniformly best estimator, rather we should seek to understand the inductive biases of different approaches.

We restrict our discussion of this power-optimization to the comparison of the two possible orders of independence- and homogeneity-test. We expect the following: Applying the independence test first ensures optimal power on IID data and will perform well if the typical alternative encountered is close to IID. Applying the homogeneity-test first avoids type II errors on certain types of inhomogeneous data. A simple example for a problem where IID-approaches may have low power for the case of correlation-based independence-testing is the case of two regimes with similar size and similar correlation but of different sign (which is also given as a motivating example in [55, 2.D]).

Testing homogeneity first, on (homogeneous) independent IID data produces a false positive, if *either* the homogeneity test produces a false positive or if – after a true negative from the homogeneity test – the dependence test produces a false positive. So if both control errors at a rate α, the total false positive rate is $\alpha + (1 - \alpha)\alpha \approx 2\alpha$. We are ultimately interested in the full marked independence result, and there is no objectively fair comparison; luckily this effect is small enough to not hinder the verification of our understanding of the associated inductive biases. We include in Fig. 5.4 the global dependence first approach twice with $\alpha = 2.5\%$ and with $\alpha = 5.0\%$ on its single stage (to illustrate the above mentioned effect) and the homogeneity first approach with $\alpha = 2.5\%$ on both of its stages.

Numerical experiments (see Fig. 5.4) support the qualitative understanding outlined above: Error control works in both cases; the homogeneity test used tends to overcontrol

---

[7]This is slightly oversimplified: Different models satisfying the null hypothesis need not produce the same variance of $\hat{d}$. For practical considerations focusing on expectations is not a substantial restriction.
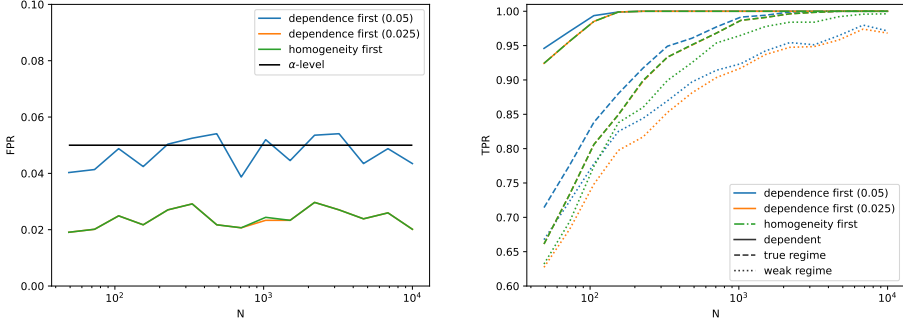
Figure 5.4: Global Dependence (dependence first vs. homogeneity first): FPR (lhs) targeting 5% (blue, green) and 2.5% (orange), and TPR (rhs) for different ground-truth scenarios (see main text). Details on the benchmarking setup are given in §C.

false-positives for larger N, this is discussed in the next section §5.2.2. Power against IID alternatives and against the true-regime case differs mostly due to the ambiguous choice of α (see above; in Fig. 5.4 for solid lines and dashed lines respectively, green is between orange and blue). The most evident difference is visible for the weak regime case (see §5.2.3, dotted lines): Here the homogeneity first approach substantially outperforms the global dependence first approach.

Our choice of inductive bias for subsequent numerical experiments and recommendation for application of our method is to use the homogeneity first approach. The reasons for this conclusion are:

- The loss in power against IID-alternatives by applying homogeneity first is small.

- There is a substantial gain on a particularly challenging case (weak regimes, §5.2.3); an approach that performs well on simple cases will eventually produce diminishing returns, a focus on challenging cases seems to make sense.

- We expect our framework and method to be applied in cases where there is substantial interest in, and a plausible presence of, non-IID effects; a focus primarily on the IID case seems like an inappropriate choice of inductive bias.

5.2.2 Homogeneity

We want to decide whether our data is IID (random) or not. This is a longtime and extensively studied problem [67; 66], so we again focus on simplicity and insights about the problem, rather than giving an extensive review of related literature. Future implementations of our framework can easily switch to more sophisticated approaches. Generally it is of course not possible to test if data is IID considering all possible alternatives (see also prop. 5.3). However, by the persistence-assumption, we already singled out a specific class of alternatives. So we study testing of IIDness vs. persistent alternatives. Our goal is to remain close to our intuition about persistence, while still providing a sound statistical test. This also includes a solid understanding of the relation of hyperparameter-choices to persistence assumptions.

Indeed this intuition is very simple: Under the null (no regime-structure) all blocks (aligned or not) are equal. Pretend for the moment that we knew the true value of d and the β-confidence intervals for $\hat{d}$ per block around this d. Then the number of blocks with $\hat{d}$ outside of the β-confidence region are binomially distributed; thus confidence bounds can be obtained. Under the alternative (persistent regime-structure) on the other hand, valid blocks are distributed as if drawn from either regime exclusively, say with ground-truth values $d_0 \neq d_1$. So the valid blocks lead to a multi-modal distribution spaced by $|d_1 - d_0|$. If each regime contains at least a ratio of β many valid blocks, and $|d_1 - d_0|$ is large compared

to the size of the β-confidence-region (which depends on block-size, cf. also Fig. 5.6 and discussion in §5.2.3), we can reject IIDness. More formally:

Lemma 5.10 (Binomial Test)**.** *Fix a hyperparameter $\beta \in (0,1)$. Given $\alpha \in (0,1)$ and a sound estimator $\hat{q}_{\bar{\beta}}^{\leq}$ of a lower bound of the β-quantile of the distribution in the d_1-regime (Def. D.17), then we can reject data-homogeneity with type I errors controlled at α as follows:*

Let $k := |\{\tau | d_\tau < q_\beta\}|$ be the number of blocks with d_τ less than q_β. Denote by $\phi_{\Theta,\beta}^{\mathrm{binom}}$ the cumulative distribution-function of the binomial distribution $\mathrm{Binom}(n = \Theta, p = \beta)$. Then $p_0 := 1 - \phi_{\Theta,\beta}^{\mathrm{binom}}(k)$ is a valid p-value under the null:

$$P_{\mathrm{homogenous}}(p_0 < \alpha) \leq \alpha.$$

In particular rejecting homogeneity iff $p_0 < \alpha$ leads to a valid test (Def. C.11).

Remark 5.11. Controlling via a binomial, thus via an *integer* count, will typically not control at α but rather below α (at the next larger count k such that the cdf at k is greater than $1 - \alpha$); this would be true even if all approximations were exact.

An appropriate definition of soundness for the estimator $\hat{q}_{\bar{\beta}}^{\leq}$ is discussed in §D.3.1. In §D.3.1 we also provide such sound estimators based on analytical results for partial correlation and based on bootstrapping / shuffling for general estimators and analyze them numerically. Our other numerical results employ the analytical estimate, primarily for low run-time at small loss of power; applications and specialized versions for time series (beyond MCI, cf. §B.6) may want to reconsider this choice. Proofs and a discussion of power-results can be found in §D.3.
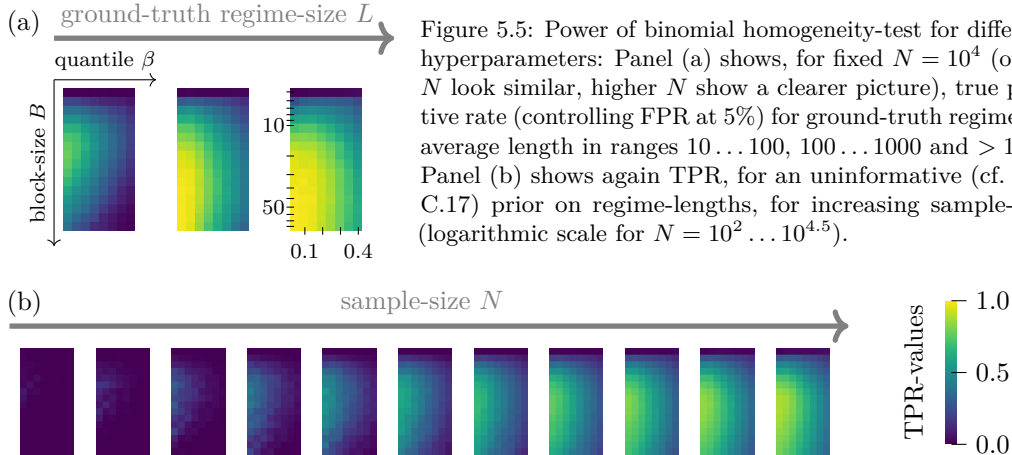

(a)

Figure 5.5: Power of binomial homogeneity-test for different hyperparameters: Panel (a) shows, for fixed $N = 10^4$ (other N look similar, higher N show a clearer picture), true positive rate (controlling FPR at 5%) for ground-truth regimes of average length in ranges $10 \ldots 100$, $100 \ldots 1000$ and > 1000. Panel (b) shows again TPR, for an uninformative (cf. Def. C.17) prior on regime-lengths, for increasing sample-size (logarithmic scale for $N = 10^2 \ldots 10^{4.5}$).

Choice of hyperparameters: Scans over the hyperparameters block-size B and quantile β on uninformative priors (see Fig. 5.5) can be used to pick reasonable hyperparameters. Unsurprisingly, on large (ground-truth) regimes, larger blocks perform better, thus we propose, additionally to the "uninformed" hyperparameters, a second set of parameters for the case where background-knowledge suggests large ($\gtrsim 100$ data points per segment) regimes. We pick hyperparameters based on sample-size N and size of the conditioning-set $|Z|$ based on a simple semi-heuristic form. A detailed analysis is given in §D.3.4. If substantial prior knowledge on ground-truth regime-sizes is available it may make sense to consult the figures in D.3.4 for better choices.

5.2.3 Weak Regimes

By the previous testing-stages, we have (almost, see §D.2.2 and §D.4.5) reduced the problem to the following situation: We are given data with precisely two different persistent regimes

of dependence d_1 and d_0 respectively, where $|d_1| > |d_0|$. The question we seek to answer is whether $d_0 = 0$. Unfortunately this cannot be tested statistically in a standard sense, a problem resulting essentially from the combination of the *rejection* of homogeneity with the *acceptance* of independence:

Proposition 5.12 (Impossibility Result B). *Assume the model-class considered has well-defined model-properties $d_0 \in \mathbb{R}_{\geq 0}$ and $\Delta d \in \mathbb{R}_{\geq 0}$ such that a model M has an independent regime iff $d_0(M) = 0$ and is homogeneous iff $\Delta d(M) = 0$. Further assume that we are given an mCIT $\hat{T} \in \{0, 1, R\}$ such that $\mathrm{Pr}(\hat{T} = R | d_0, \Delta d)$ is continuous in d_0 and Δd, and that there is no a priori known gap in realized parameters d_0 and Δd, that is $P(d_0, \Delta d) > 0$ near $d_0 = 0$, and there is no a priori known gap in Δd on weak regimes, that is $P(\Delta d | d_0 = 0) > 0$ near $\Delta d = 0$.*

Then, given $\alpha > 0$, no such mCIT can for any finite sample-size N

(a) on true regimes uniformly control FPR at $< \alpha$ and have non-trivial power $> \alpha$ on any global independence alternative or

(b) on global dependence or the union of global hypotheses control FPR at $< \alpha$ and have non-trivial power $> \alpha$ on any true regime alternative.

A more detailed discussion is provided in §D.1.3; this is an important conceptual reason why the weak-regime test is more difficult to realize, than the homogeneity test. One may of course ask about convergence of a specific decision-procedure (without finite-sample error control) in some appropriate limit. We do provide such an argument in §D.3.3. However, the above result shows that even if a procedure yields the correct decision asymptotically, given any finite sample-count N, there are always regime-structures on which it will not produce meaningful results. So the more urgent question is: *How* should a procedure look like to make it transparent *when* it will work and what are the *trade-offs* we necessarily have to make?

This section focuses on the concrete challenges arising for this problem. The viewpoint we take is a rather practical one, focusing on assumptions on model / regime structures that are intuitive, have a clear relation to the hyperparameters of the method we introduce and lead to reasonable finite-sample performance on uninformative model-priors, where they restore FPR-control in a Bayesian (averaging) sense. A potential path forward to a theoretically more satisfying solution is laid out in §D.7.2 based on the idea to first assess whether the model / regime structures satisfy given assumptions, and insist on a decision *only* then.

There are also some further subtleties that arise from the integration of the test with the other stages: If we understand testing d_0 as an independence-statement on a subset of data, than a (false) positive leads to a (false) rejection of the existence of a true regime. From the perspective of detecting regimes, it thus leads to a (false) negative. To avoid confusion, we show below the impact of hyperparameter choices on recall and precision *of regime-detection*, as this is more clearly interpretable in the greater context of our framework. This also affects some practical decisions, for example:

Remark 5.13. In cases where too few data points of low dependence are available for reliable testing, we do *not* interpret the result as a regime, which makes sense from the regime-detection perspective, but is unnatural from the independence-testing perspective.

By testing in the wake of the homogeneity test, the prior over parameters which the weak-regime test sees (even for an uninformative model-prior) is rather specific. For example it encounters up to α only (persistence-)non-homogeneous data, because the homogeneity test must have had power to reject.

We return to the concrete test-implementation. The weak-regime test could be approached by clustering the $\hat{d}$-scores obtained on blocks. For example for partial correlation the score (z-values) is approximately normal so that a multi-modal normal approach could yield good results. In practice there are at least two difficulties in making this work: One requires a

good uncertainty estimate on the cluster-means, and one requires robustness against invalid blocks. We belief that it is possible to substantially improve performance in this step by using an appropriate clustering method, but because of these difficulties, we opt for a modified independence-test instead. This also makes the applicability assumptions and trade-offs, which we laid out as our principle goals before, more accessible.

Concretely we study the statistical behavior of those blocks with $\hat{d}$-scores below a certain cutoff c; we will assume w. l. o. g. $d_1 > 0$. We face multiple challenges:

(i) There are impurities below the cutoff, coming from the dependent regime.

(ii) There are data points above the cutoff lost from the low-dependence-regime, this incurs a bias on those remaining.

(iii) Even in the persistent case, not *all* blocks are valid, and we have to account for the impact of invalid blocks.

Importantly, by our direct approach, we can treat these contributions statistically, without the need to reason about the identity of individual blocks: It is enough to assess the rate of impurities and their impact, but we do not need to know which particular blocks are impurities. The choices of the cutoff c and block-size B allow to navigate the trade-offs between these problems as illustrated in Fig. 5.6. Finally, the choice of cutoff also affects the available sample-size (below c).
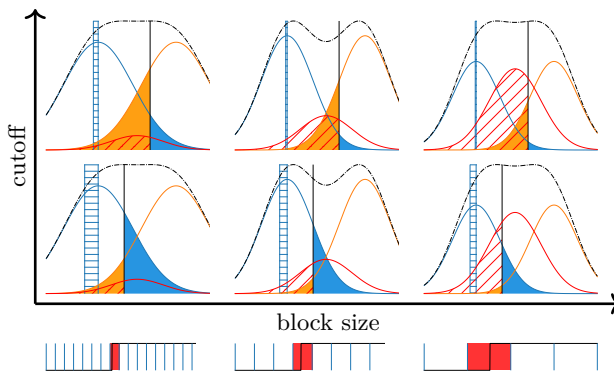

Figure 5.6: Trade-offs in hyperparameter choices. The two rows of density-plots have different cutoffs (vertical black line). Illustrated for both are densities for independent (blue) and dependent (orange) regime, as well as rates of: impurities (orange shaded); lost data points (blue shaded) and bias induced by not using them (distance between vertical blue lines, hatched blue); invalid blocks (hatched red). The bottom panel shows the increase in the amount of data in invalid blocks with larger block-size.

How can one account for these effects? The effect of the lost samples can be well approximated by considering a cutoff normal density; the incurred shift $\mu_c^B < 0$ of the mean-value is shown in Fig. 5.6 as blue-hatched region. For the effect of impurities one may give a simple upper-bound as long as there are less impurities, say k_I than lost data points, say k_L: Impurities individually contribute less than c to the mean, thus at most $\leq \frac{k_I}{\Theta} c$ in total, while lost data points loose at least c, thus at least $\geq \frac{k_L}{\Theta} c$, so that the mean changes by $\frac{k_I - k_L}{\Theta} c < |\mu_{0,\sigma_B}^c|$. This argument required less impurities than lost data points ($k_I \leq k_L$). Thus, as long as there are few invalid blocks, the mean-value of block-scores below c is in the range $[\mu_{0,\sigma_B}^c, 0]$ if $d_0 = 0$ up to the expected finite-sample confidence of $\hat{d}$. In summary we have just constructed the following method:

Assumption 5.14 (Acceptance Interval Applicability)**.** Require controlled impurities $c < q_a$ where $q_a(B)$ is the a-th quantile of $\hat{d}$ on all data, and few invalid blocks $\chi \approx 0$:

$$c < q_a \quad \text{and} \quad B \ll L$$

Lemma 5.15 (Acceptance Interval)**.** *Some additional but rather weak assumptions are required, these are discussed in §D.2, see also the more formal statement Lemma D.31 in the appendix.*

Choose a cutoff $c > 0$ and a minimal valid size $n_0^{\min}$, compute the mean $\hat{d}_{\text{weak}}$ of blocks of dependence $\hat{d}$ with $\hat{d} < c$ where the number of such blocks is n_c.

$$\hat{d}_{\text{weak}} = n_c^{-1} \sum_{\tau | \hat{d}_\tau \leq c} \hat{d}_\tau$$

We assume that the variance σ_B^2 of $\hat{d}$ estimated on B samples under the null is known.

Given an error-control target $\alpha > 0$, let $\sigma_{n_c}^\alpha = n_c^{-\frac{1}{2}} \sigma_B \phi(1 - \frac{\alpha}{2})$ be the (two-sided) α-interval around 0. Define an acceptance interval $I := [\mu_{0,\sigma_B}^c - \sigma_{n_c}^\alpha, \sigma_{n_c}^\alpha]$. Accept the null hypothesis (independence of the weak regime) if $n_c \geq n_0^{\min}$ and $\hat{d}_{\text{weak}} \in I$, otherwise reject it. Under Ass. 5.14, this test controls false positives.

For proofs, a more detailed discussion of assumptions and a formal interpretation of the assumption $\chi \approx 0$ see §D.4, where also a statistical power analysis is given. The assumption 5.14 and Fig. 5.6 inform us about the meaning of our hyperparameters:

$$B \leftrightarrow L \quad : \quad B \text{ has to be chosen small enough relative to } L$$
$$c \leftrightarrow d_1 \approx \Delta d \quad : \quad c \text{ has to be chosen small compared to}$$
$$\text{regime-separation } \Delta d = |d_1 - d_0| \text{ (measured by } d)$$
$$\alpha, |I| \leftrightarrow d_0 \quad : \quad \alpha \text{ controls the sensitivity for small } d_0,$$
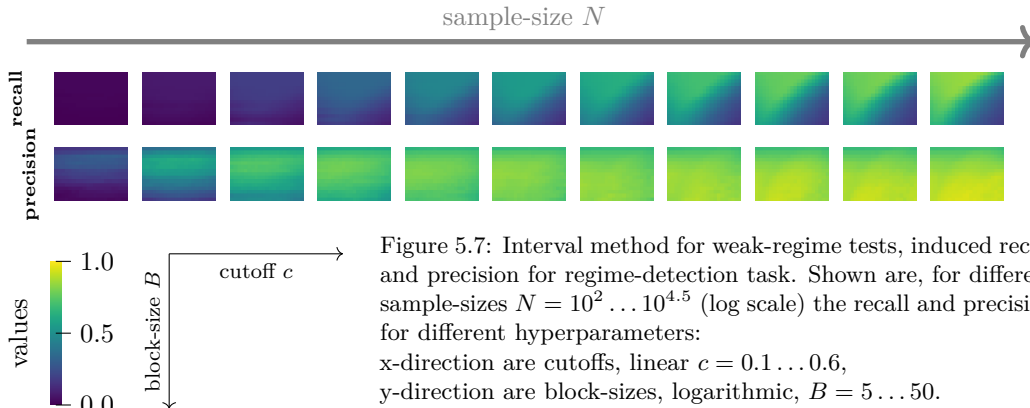$$\text{but also the size of the interval } I \text{ (thus } B, c) \text{ contributes.}$$

Figure 5.7: Interval method for weak-regime tests, induced recall and precision for regime-detection task. Shown are, for different sample-sizes $N = 10^2 \ldots 10^{4.5}$ (log scale) the recall and precision for different hyperparameters:
x-direction are cutoffs, linear $c = 0.1 \ldots 0.6$,
y-direction are block-sizes, logarithmic, $B = 5 \ldots 50$.

The average recall and precision resulting for regime-detection on the (uninformative prior) benchmark are shown in Fig. 5.7. The observed structure and the choice of hyperparameters is discussed in detail in §D.4.6. The main observation is that the resulting precision is comparatively insensitive to hyperparameter-choices, at least for larger $N \gtrsim 10^3$ samples, while the recall breaks down for poor choices. Other than that, similar remarks as for the homogeneity-test are in place. We again provide two simple recommendations for hyperparameters for generic cases and for cases for large ($L \gtrsim 100$) ground-truth regimes in §D.4.6.

5.3 Conditional Tests

Conditional independence tests are of great importance for constraint-based casual discovery. In principle the above discussion applies to arbitrary dependence-scores $\hat{d}$, in particular they can be conditional ones. Clearly, there are some optimizations possible. For example if conditional tests are evaluated by regressing out the conditions and testing on residuals (as it is the case for partial correlation), then the regressors, if associated to homogeneous

links themselves, could be shared between blocks. We find that such sharing for linear regressors (which converge comparatively fast) does not lead to tremendous improvements. Interestingly, not sharing them does make the conditional testing more robust against other types of non-IIDness, like drifting coefficients (cf. §D.6). From this perspective, one may want to choose a suitable middle-way using multivariate (additionally time-dependent) regressors. The appendices §D.3.4 and §D.4.6 study hyperparameter choices for conditional tests.

A noteworthy finite-sample effect encountered concerns mediators: Our method has difficulties with near-deterministic mediators (mediators that are very strongly correlated to the source-node). We consider this to be a known challenge to causal discovery in general, it seems to appear more generally for CITs not just our mCIT (see also §C.5.5).

5.4 Full Test and Asymptotics

We show in the appendix §D that our method has good asymptotic properties. While finite-sample guarantees, point-wise convergence and a convergence for limits where typical regime-sizes are constant (of order N^0), does not seem possible (Prop. 5.12), we can show that our method, under weak assumptions, satisfies the "next best statement" of convergence given any (arbitrarily slow) increase of typical regime-sizes. Typical regimes-size here takes into account how well the chosen pattern Patt matches the actual pattern in data.

Theorem 2 (mCIT Convergence). *For a formal statement, see §D.5. Given a pattern* Patt *(Def. 5.4), in an asymptotic limit such that the system is eventually* (L, χ)-Patt-*persistent for every* $L, \chi > 0$, *the mCIT described above is asymptotically correct in a Bayesian sense (on average, but not point-wise).*

The scaling assumption is extremely weak, for example it includes all "trivial" scaling results $\mathcal{R}_N(t) := \bar{\mathcal{R}}(t/\Lambda(N))$ with $\Lambda(N) \to \infty$ (Cor. D.45) and even meaningful uninformative priors for the case of persistent in time regimes (Cor. D.44). Numerical experiments (§7.2, paragraph "Scaling behavior with N") strongly support this claim.

5.5 Summary

Our approach to MCD reduces the data-processing layer within the pipeline Fig. 1.4 to comparatively simple "marked independence" statements (and indicator-relations §6). The testing of such statements was in this section further reduced to a series of what might be considered standard problems:

- The segmentation of data, for example by simple division into blocks, or CPD (§D.7.3).

- The focus on a single link's strength by dependence-scores.

- A univariate clustering problem, for which additional constraints are known, that allow for further substructure into:

  - Independence Testing.

  - IIDness / randomness testing.

  - Selection bias and independence testing on selected datasets.

A thorough review of the extensive literature on these topics is beyond the scope of this paper. Instead, we focused on a well-defined structure of the full problem, its reduction to these well-studied topics and a detailed analysis of the difficulties encountered. We provide a simple baseline method realizing the structure and principles of our framework. Its primary goal is to demonstrate feasibility and gain insight into finite-sample challenges.

While we expect that future work on these subproblems should be able to substantially improve finite-sample properties, our baseline already turns out to perform very competitive to state-of-the-art methods §7. We attribute this to the systematic addressing of the two

deep underlying challenges outlined in the introduction, by following the guiding principles of locality and direct testing. The qualitative trends observed in the numerical experiments §7 support this interpretation. In §D.7 more ideas concerning future work are outlined.

6 State-Space Construction

Induced indicators as encountered in example 4.8 make the extraction of the multi-valued independence-atoms IX from the knowledge of a marked independence-atoms IM a non-trivial task. This section describes, how, despite these difficulties, this goal can be achieved with few additional test. We provide an implementation of `construct_state_space` as required by the core-algorithm which under reasonable assumptions (see below) is theoretically sound and comparatively easy to implement; details and proofs can be found in §F. The approach requires an additional type of test (i. e. the data-processing layer requires slight extension), to inter-relate detected indicators. This test can be realized similar to weak-regime tests (see §D.4.7). While already the comparatively simple analysis provided in §F can substantially simplify the type of additional tests needed and reduce their number, we strongly suspect that considerable further improvement should be possible (see §F.10.1).

We employ assumptions (see §F.1 for technical details) about

(a) acyclicity to simplify the problem and representation of solutions. Our approach should be extensible to cyclic models, however, this will require a more complex state-space construction and an additional type of (data-processing layer) test (§F.10.2).

(b) modularity of changes and reachedness of states, to avoid the complexity of an additional post-processing phase §F.10.4. Again, our approach should be extensible.

(c) skeleton discovery in the used CD-algorithm. While our framework is almost entirely agnostic of the implementation details of the CD-algorithm employed, we use a simple assumption about the skeleton discovery (that seems to be satisfied for all algorithms used in practice) to simplify proofs.

Under these assumptions, the state-space construction can be realized in two phases. In the first phase (Algo. 3) model-indicators are identified as those links X–Y, for which a regime-dependence is found (the mCIT returns R), but no Z with $X \perp\!\!\!\perp Y | Z$ was encountered. Each model-indicator is then represented by a test of the form $X \perp\!\!\!\perp Y | Z$ such that $R_{XY|Z} \equiv R_{XY}^{\mathrm{model}}$. A suitable Z is found as a minimum under an ordering-relation on Z that corresponds to a subset-relation of regions of independence on detected indicators $R_{XY|Z}$. The evaluation of this ordering-relation is the first encounter of the new type of data-processing layer test. Under the assumption of modular changes, these model-indicators span the state-space.

In the second phase (Algo. 4), the value of detected indicators in each state is deduced. This will again require the new type of test. In general the space of detected indicators grows very fast in the number k of model-indicators (as 2^{2^k}), there are, however, some restrictions on the form of detected indicators that can be leveraged to obtain a much smaller search-space. A particular helpful observation is that the removal of a link (vanishing of a model-indicator) from one state to another can close a causal path (in the sense of d-connectivity), but never open a new one.

The results of both phases allow for the realization of the `construct_state_space` sub-algorithm required for the core-algorithm in §4.4. We show in §F:

Theorem 3 (State-Space Construction)**.** *A formal statement is given as Thm. 3F in §F.8. Pseudo-code for the two phases of the algorithm is provided in Algo. 3 and Algo. 4.*

Under the assumptions (a-c) outlined above, the described two-phase algorithm, in the oracle-case, implements a sound and complete state-space construction (Def. E.13), satisfying the requirements of Thm. 1 (soundness of the core algorithm).

Finally, the interpretation of the discovered state-space in terms of model-properties can also be non-trivial. For example in presence of hidden confounders two states may differ by one or more inducing paths being present in one of them. This is excluded by a suitable acyclicity assumption, but for the general case jeopardizes both the independence of model indicators (even in the case of modular changes) and their interpretation as changing causal mechanism at that location in the graph. While for the discovery of states there is a rather clear path forward, their interpretation in terms of model-properties appears to be non-identifiable in some cases (see §F.10.3); non-identifiable here refers to identifiability from the extended independence-structure in principle, not specifically to our proof-of-concept method. Such (possibly only partial) translations, together with knowledge-transfer results (§F.9) allow for an easy-to-read representation of the full results by a labeled (or colored) union-graph (Fig. 1.1a).

Our current approach does not take into account constraints on the potential representation of detected indicators that arise from (partial) knowledge of discovered graphs from previous iterations. We belief that in future work it should be possible to considerably improve the scaling to much larger models with many changing model-indicators by systematically exploiting such constraints (see §F.10.1).

7 Numerical Experiments

We evaluate the full method on randomly generated non-stationary SCMs (for details see §C). To allow for a comparison with [55], we focus on the case of time series data without contemporaneous links and without hidden confounders. Further numerical experiments, especially for non-time series data, are included in §A. We first briefly describe the methods we compare, then discuss results for different scenarios obtained via these methods, with details about evaluation metrics deferred to the end of this section.

7.1 Methods Applied

We compare multiple methods representing different classes of approaches. These representatives may not accurately capture, in terms of absolute numbers, what finite-sample performance *could* potentially be achieved by each respective class. We will focus on the trends observed for individual approaches when changing the model behavior in different ways / "scenarios" (see next subsection).

Regime-PCMCI [55] in simple terms can be described of as follows: Divide the data into regimes, run causal discovery (via PCMCI) and fit a model per regime, then find regime-assignments of data points that minimize the prediction-error from these models. Then iterate these (EM-)steps. Here persistence is leveraged by constraining the maximum number of regime-switches. The optimization-procedure may not always converge, we only took converged results into account. Fitting a model is not practically feasible with confounders or with unorientable links, which restricts the applicability of such a method to time series models without contemporaneous links and without confounders. Model fitting and regime-assignment is *global* in the causal graph, and causal discovery is run *indirectly* via the discovered indicators. Regime-PCMCI requires prior knowledge of the number of regimes and an upper bound for the number of switches; we provide it with ground-truth for both, as well as minimum and maximum time-lags. We further analyze three different hyperparameter-sets, two are recommended by the original paper [55] for simple / complex models, the third is the default parameter-set proposed by the implementation in the `tigramite`[8] python package. In the plots these are marked as: diamond (tigramite), plus (simple), X-symbol (complex).

---

[8]see `https://github.com/jakobrunge/tigramite`

Clustering: We compare to a simple clustering approach. This approach clusters data points *globally* (in the causal graph), then applies causal discovery (via PCMCI) *indirectly* per cluster. Here the absolute values are not of great significance, as the use of other clustering-algorithms could change it (we use a simple kmeans clustering), but the qualitative behavior should be sufficiently representative for such global clustering approaches. The method is provided with ground-truth information about the number of clusters, as well as minimum and maximum time-lags. To allow the approach to take advantage of persistence, the clustering is also applied to aggregations of data points over different window-sizes.

Sliding-Window: A sliding-window approach is easy to implement: Apply causal discovery (via PCMCI) to each "sliding window" *globally* (in the graph). For practical reasons our "sliding" windows do not slide, but rather the data is again divided into fixed size non-overlapping windows. It is, however, difficult to evaluate. We start by counting for each link the number of windows on which it is present in the specific window's causal graph. Then pick two cutoffs $a_\pm$ and consider links absent if they appear less often than a_-, changing (regime-dependent) if they appear at least a_- but less than a_+ often, (non-regime-dependent) present in the graph otherwise. The authors are not aware of any detailed investigations into the practical choice of $a_\pm$; generally this seems to be a difficult problem. The study of the practical choice of $a_\pm$ is beyond the scope of this paper. Instead, our evaluation fixes $a_\pm$ *a posteriori* to the values which *would have* provided the best evaluation metric. This is not a method applicable in practice, but it does provide an estimate of an *upper bound* on the possible performance of sliding-window methods; to emphasize this hypothetical nature, the corresponding results will be plotted as dashed (as opposed to solid) lines. Again, also ground-truth about minimum and maximum time-lags is provided. The approach takes advantage of persistence by the choice of time-aligned windows. We apply this approach with different window-sizes. In practice the union-graph should in this case be more reliably obtained from a standard (stationary) method applied to all data, and we do not include the union of regime-specific edge-sets for comparison in the union-graph results. See also §B.5.

gLD-PCMCI (ours): We will, of course, also include results for the baseline method as described above (using PCMCI as CD algorithm), realizing the *graph-local and direct* framework described in this paper in a simple but transparent way. We compare two sets of hyperparameters that were chosen respectively for an uninformative prior and with an inductive bias slightly favoring larger regimes in §5 for IID-data (see also §A.8 and §A.9 concerning relevance of and policy of choice of hyperparameters). Again, ground-truth about minimum and maximum time-lags is provided, *no* ground-truth about the number of regimes or number of transitions is needed. Since the other methods here use PCMCI, we show results for gLD-PCMCI in the main text. Applications may consider using gLD-PCMCI+ for time series, as this combination seems to often perform more robustly (§A.1.1, §B.6).

Stationary PCMCI: We additionally compare to the results one obtains by applying the PCMCI-algorithm (also underlying the other methods) without modifications to the data. This produces only a union-graph. Due to its special role as a reference, this line will be drawn in a dash-dot style in the plots below.

7.2 Scenarios for Numerical Experiments

The problem of non-stationary data-generation has by far too many degrees of freedom to define a universal benchmark. So we focus instead on a comparison of the qualitative behavior of different approaches given different variations of the benchmark data-set, for example the behavior with increasing sample-count N, with different model or regime-structure complexity or with different typical segment lengths. Thus, our primary goal of this numerical experiments section is to understand and verify our understanding of the

inductive biases of the compared classes of methods. To this end, we study a sequence of "scans" over model- (and data-)parameters and analyze the observed behavior.
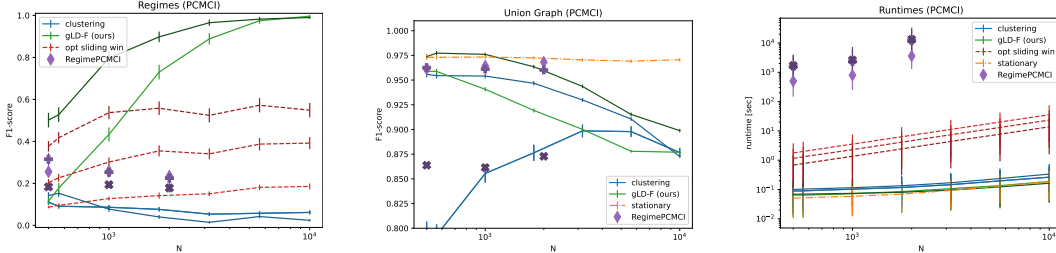

Figure 7.1: Scaling with N: Shown are F1-score of regime-detection, union-graph and runtime in seconds (log scale) vs. sample-size N. Darker lines represent larger window-sizes or the hyperparameter choice optimized for large regimes. All approaches used PCMCI as basic CD-algorithm.

Scaling behavior with N: An important aspect of any statistical analysis is convergence speed or more generally the behavior under the increase of the sample-size. With regimes in the data, a non-trivial choice with regard to the behavior of segment-sizes with increasing N has to be made. We decided for a plausible uninformative prior: For each indicator, a typical length-scale is picked first, then all segments of that indicator are drawn at random, but similar to this scale. An extensive discussion of the rational behind this choice is given in §C. Figure 7.1 show results for the detection of changing links (regimes) and the (summary-) union-graph skeleton (details on the precise evaluation-metrics are given below in §7.3). The most apparent feature is that both clustering and the Regime-PCMCI approach actually become *worse* for this choice of limit. This makes theoretical sense. Both methods are *indirect* and essentially race against themselves: There are abstractly two tasks performed. First the assignment of data to regimes, second the independence-testing (via causal discovery) on the imperfectly reconstructed per-regime data. Both tasks benefit from more data, however, for the second task, testing on imperfectly reconstructed per-regime data, this also means that the sensitivity for these imperfections in the reconstruction increases. For example, the reconstructed independent regime, erroneously containing some dependent data points, will have non-zero correlation of say $E_N[\hat{d}] = d_0(N) \neq 0$. With growing N, the sensitivity of a correlation-test typically improves with $N^{-1/2}$, so if the reconstruction does not converge fast enough to keep $d_0(N)$ dropping at a rate of at least $N^{-1/2}$, the correlation-test will eventually be able to detect the spurious dependence. In practice this rate of convergence would at most be plausible for limits where $L = \mathcal{O}(N^1)$. While the Regime-PCMCI and clustering fall off with larger sample-count, their performance on low sample-counts can be quite good. So especially for small sample-count, these approaches can be a good alternative; additionally they can detect non-graphical changes.

Our method is testing in a very simple, but direct way (cf. §5), therefore does not suffer from this convergence-race problem. The regime-sizes are bounded below to allow for a meaningful comparison, thus it is not surprising that the hyperparameter set for large regimes performs better. Also for clustering and sliding-windows, the larger window-sizes seem to perform better, probably for the same reason. For the sliding-window approach with optimal (a posteriori) cutoffs, there is also no indirection and therefore it improves with larger N in this limit. However, the convergence is slower than for our method, likely due to propagating errors in CD first, before aggregating across windows. Similarly the sliding-window variants seems to cap out at a lower value; given the fundamental limitations / impossibility results found in §5 such a non-trivial soft[9] cap is expected for any method (it becomes more evident for our method with more challenging setups).

---

[9]The cap is "soft", because under the used model-prior, low typical regime-sizes eventually do become less common, albeit only logarithmically fast, cf. Lemma C.28.

Another very apparent effect is a decrease in the quality of the recovered union-graph (for our method and clustering). This effect seems to be present only for time series models (see §A.3 for IID-results). This observation is clearly worrisome. A practical "fix" is to run a stationary algorithm separately and use its output to validate the union-graph. However, this means that it unfortunately is not easily possible to benefit from potential improvements for the union-graph discovery (in the time series case), that our method could provide (see below). There are at least two plausible explanations for this issue. Our homogeneity-first approach is designed for IID-data and may not work well as-is with the MCI idea, we belief this can be fixed and might also help improve independence-tests for MCI-approaches (see also §B.6). Using PCMCI+ and skipping the homogeneity-test in the PC_1-phase seems to improve the behavior of the union-graph supporting this idea, see §B.6, even though it is not entirely clear, why this would require the use of the PCMCI+ algorithm. The second explanation is particular intriguing, because it might simultaneously explain the fall-off observed for the clustering-method: Having k time series of length n is not the same as having a single time series of length $N = k \times n$. For multiple time series, the stationary distribution is sampled k times, as opposed to once, for initial states, injecting additional information into the system, so that one might expect the effective sample-count to be higher. While we do account for changes in sample-size and aggregation-methods, we do not account for this effect, and we are not aware of other methods accounting for this effect.

Finally, the problem might of course be due to a bug in our code. However, clustering and our method use different implementations of the partial correlation test and share very little to no code, so while we cannot exclude this possibility, we belief the issue is "real", due to a statistical effect, not an implementation issue.
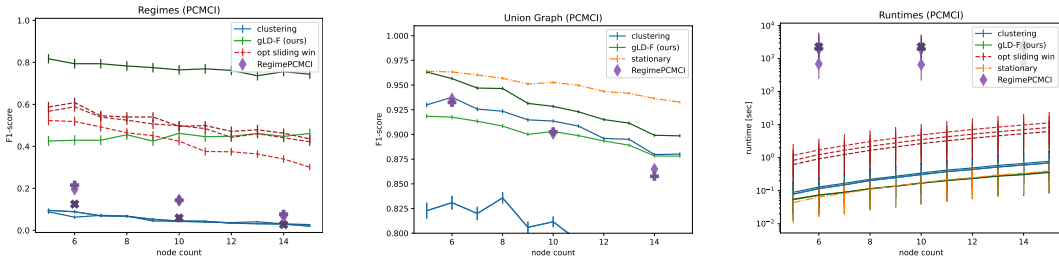

Figure 7.2: Scaling with node-count: The number of nodes in the system can serve as a proxy for model-complexity.

Model Complexity by Node-Count: We use the number of nodes (at fixed link-density per node) as a proxy for model complexity (for results on changing link-density, see §A.5). Figure 7.2 shows the results, again for regimes and union-graph. Concerning regimes, our method, being local in the graph, does not considerably suffer from an increase in model complexity (in the sense of node-count). All other methods show a downward-trend, as would be expected for global methods. The effect is comparatively weak however. The recovery of the (summary-)union-graph suffers for all methods from an increase in complexity, which is not surprising.

Regime-Structure Complexity by Indicator Count We use the number of changing links (at otherwise fixed graph-parameters) as a proxy for regime-structure complexity. We consider two cases: Independently changing links (which our method is optimized for) and synchronized changes in multiple links (which should favor global methods). Some care should be taken in the interpretation of F_1-scores because the increase in the number of changing indicators changes the actual (ground-truth) positive rates (see §A.1.2). See Fig. 7.3. At least for Regime-PCMCI, this understanding of biases can be confirmed (for independent-indicators, it has very severe convergence-issues, fully breaking down at around
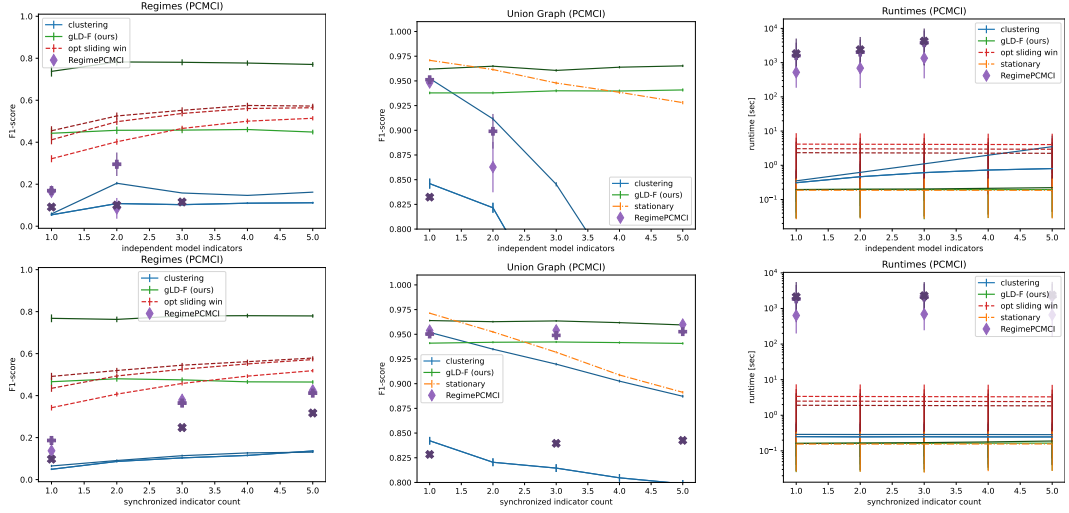
Figure 7.3: Scaling with indicator-count: The number of changing indicators can be used as a proxy for regime-structure complexity.

three indicators, precluding results for larger counts). Generally clustering would probably also benefit from synchronized changes more substantially, if these changes would for example change noise-offsets (mean-values of additive noise) at the same change-points. So one learning from this experiment is that the model-fitting and evaluation approach of Regime-PCMCI is better at finding (global) model changes in the fitted *effects* than for example clustering.

It is noteworthy that our approach, likely due to its built-in robustness towards non-stationarities (cf. §D.6), can almost maintain the quality of the recovered union-graph even under the addition of more non-stationarities. This also applies to Regime-PCMCI in the case of synchronized changes.
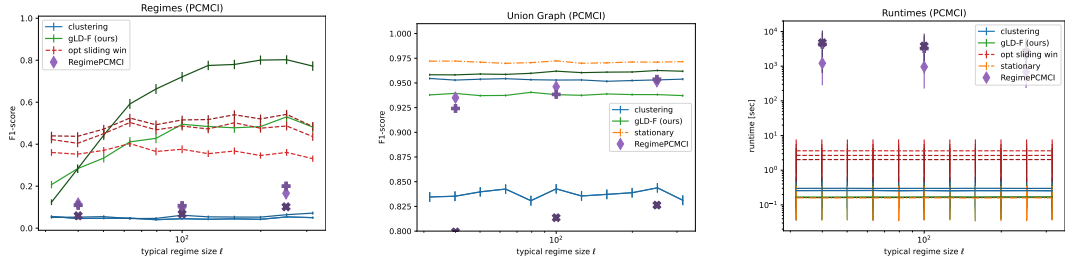

Figure 7.4: Scaling with regime-size: Ground-truth regime-sizes should affect relative effectiveness of hyperparameters.

Regime-Sizes We use different window-sizes and a hyperparameter-set for large regimes vs. one for the general case. One would expect that starting at small ground truth segment-lengths, then increasing them would demonstrate a clear hand-off / cross-over at some point in the middle. Interestingly, while there is some crossover-behavior, it is not very pronounced for time series models (see Fig. 7.4). The behavior is closer to this expectation in the IID-case (§A.6), so we belief that this is a time series effect (at least for our method). From this observation, we recommend to typically use the hyperparameter set for larger regimes in the time series case for now. It might make sense to investigate good hyperparameter choices for the time series case in future work.

7.3 Evaluation Metrics

We usually compare F_1 scores on two problems:

- Which links are found to change between regime? – Each method outputs (potentially among other information) a collection of per-context graphs G_s. We compare these, to see which links occur for only some G_s, thus *change* (for the sliding window case, see §7.1). Such a changing link is a 'positive', it is a 'true positive' if the model on this link has a non-trivial model indicator, and a 'false positive' if the associated true model-indicator is trivial. For computing F_1, a negative is any possible link which is not included in the set of changing links, but excluding auto-lags[10].

- How well is the summary-union-graph recovered? – The union-graph is the edge-union over the individual G_s returned by the method. Since we use PCMCI with $\tau_{\min} = 1$ all links are lagged and oriented forward in time, so there is no ambiguity on orientations at this point. The summary-graph is then the edge-union over all time-lags. A 'positive' is a link in this summary-union-graph, it is a 'true positive' if the true summary-union-graph also contains this edge, and a 'false positive' if the true summary-union-graph does not contain this edge.

We are particularly interested in the first question, which captures the actual detection of the presence of regimes in a way that can be compared for the different methods providing different output-information in a simple and fair way. Regime-PCMCI (see below) is based on the PCMCI causal discovery algorithm for time series; the other methods can be applied with other methods, we compare time series results for PCMCI [51], PCMCI+ [49], LPCMCI [20] (via implementations in the `tigramite`[8] python package) and IID-data results for PC [59], PC-stable [12] and FCI [61] (via implementations in the `causal learn` [71] python package) in more detail in the appendix §A.

F_1-score favors recall over precision; for example the best (w. r. t. F_1-score) purely random method is always the trivial-true algorithm (always return true). Our method particularly features a very high precision, so this puts it at a slight disadvantage; for the most part this is not a problem, only the results on increasing indicator count should be interpreted with particular care: Increasing the number of non-trivial model-indicators changes the number of true positives relative to the number of true negatives, which means the behavior across different counts, even the qualitative behavior, is only easily interpreted for methods with comparable precision and recall. For details see §A.1.2. F_1-score is, however, simple and in very wide-spread use which is the reason why we employ it here.

8 Conclusion

The ideas behind our framework allow to break the MCD problem down into much more attainable and well-defined sub-problems: A (stationary) CD task, a state-space reconstruction task, a marked independence testing task and the composition task implemented by the core-algorithm itself to combine solutions to these sub-tasks into a useful framework. This gives a structure to the problem which allows for a detailed an insightful study of the many challenges implicit in the original problem. These insights reach from limitations on identifiability and the construction of meaningful solutions and their interpretation to systematic improvements in the scaling behavior with sample-size (by directness of testing) and with complexity of model and regime-behavior (by locality).

Limitations: Our approach so far does *only* discover changes in the graph. It will neither inform about nor leverage changes in effect-strengths or noise-distributions. It can also not benefit from co-occurrence of multiple changes; it can only account for such synchronized or

---

[10]Our data-generation generates no non-trivial indicators on auto-lags, see §C. All methods can report changes on auto-lags, and those are counted as false positives; this seems to happen very rarely.

related changes in principle (§F.10.4). It seems that co-occurrence of graphical (and likely regime-form effect-strength) changes favors model-fitting approaches like Regime-PCMCI [55], while co-occurrence with changes of noise-distributions might favor clustering approaches. Finally, our approach requires comparatively large data-sets, its major benefits seem to show primarily if $\gtrsim 1000$ data points are available, but this number of course also depends on model-complexity and effect-sizes.

We currently focus on partial correlation tests, thus on linear models. It should be possible to support other independence tests, but doing so efficiently and at acceptable runtime will require further work. For indicator-relation tests as used in §6, we provide a proof of concept (§D.4.7), but we belief that a careful analysis, especially of the observations in §F.10.1, has the potential to provide additional insight and improved orientation-correctness.

On time series data our baseline implementation encounters unexpected difficulties in the quality of the recovered union-graph. The most likely cause of this problem is our simple MCI-based time series adaptation §B.6. This problem can likely be fixed a appropriate tests for the time series case, at least for the PC_1 phase. For the moment, we recommend the additional execution of the underlying stationary CD-algorithm directly on the data to obtain a reference union-graph to assess the stability of (regions of) the union-graph. Using PCMCI+ and skipping the homogeneity-test in the PC_1-phase seems to improve the behavior of the union-graph as well, see §B.6.

We did not include an application to real-world data. A thorough analysis of a result on real-world data would doubtless be interesting, but it would also require an extensive discussion which considering the length of this paper seems more adequate for a dedicated write-up. Our implementation in code and numerical experiments are currently limited to linear, acyclic models and we focus in the evaluation on causally sufficient (no hidden confounders) examples and (for the IID case) on graph skeletons.

Strengths: Our approach can benefit substantially from large data-sets; it demonstrates both in theory and numerical experiments good statistical convergence properties and maintains low run-times. Similarly it scales well to large systems and complex regime-structures with many non-trivial model-indicators, again at comparatively low run-times. It behaves, except for the union-graph issue on time series mentioned above, as expected from the inductive biases realized by a local and direct approach. This makes its strengths, weaknesses and applicability to a given problem comparatively easy to assess. Our implementation is also compatible with the presence of latent confounders and contemporaneous links (thus IID problems) if the underlying CD-algorithm is chosen accordingly. It can also not only be used for persistent-in-time regimes but also for other types of patterns in data. Finally, from a practical perspective, our method does not face numerical-convergence problems (like Regime-PCMCI does on some data-sets) and produces succinct and easy to interpret output (see also §F.9) at low run-time, making it an easy to use potential first extension beyond the stationary case for many applications.

A good framework should be extensible and be able to leverage existing technology. The use of standard CD-algorithms is already possible in our baseline implementation, while we only used partial correlation for our numerical experiments, our framework was designed to easily accommodate other independence test scores. Also the integration of existing CPD or clustering technology seems plausible (§D.7.3). Similar remarks apply to the combination with JCI-like [37] ideas (see §B.7). An extension to account additionally for changes in effects or noise-terms, and a combinations with methodology like CD-NOD [28] for other (non-regime-like) types of non-stationarities should be possible at multiple points of the framework, by its highly modular design.

Acknowledgments

References

[1] M. Aitkin and D. B. Rubin. Estimation and hypothesis testing in finite mixture models. *Journal of the royal statistical society series b-methodological*, 47:67–75, 1985.

[2] E. Arias-Castro, D. L. Donoho, and X. Huo. Near-optimal detection of geometric objects by fast multiscale methods. *IEEE Transactions on Information Theory*, 51(7): 2402–2425, 2005.

[3] C. K. Assaad. Causal reasoning in difference graphs. *arXiv preprint arXiv:2411.01292*, 2024.

[4] C. Balsells-Rodas, Y. Wang, and Y. Li. On the identifiability of markov switching models, 2023.

[5] E. Bareinboim and J. Pearl. Transportability of causal effects: Completeness results. In *Proceedings of the AAAI Conference on Artificial Intelligence*, volume 26, pages 698–704, 2012.

[6] P. Boeken and J. M. Mooij. Dynamic structural causal models. *arXiv preprint arXiv:2406.01161*, 2024.

[7] S. Bongers, P. Forré, J. Peters, and J. M. Mooij. Foundations of structural causal models with cycles and latent variables. *The Annals of Statistics*, 49(5):2885–2915, 2021.

[8] R. Cai, S. Wu, J. Qiao, Z. Hao, K. Zhang, and X. Zhang. Thps: Topological hawkes processes for learning causal structure on event sequences. *IEEE Transactions on Neural Networks and Learning Systems*, 35:479–493, 2021.

[9] K. Chalupka, T. Bischoff, P. Perona, and F. Eberhardt. Unsupervised discovery of el nino using causal feature learning on microlevel climate data. In *Proceedings of the Thirty-Second Conference on Uncertainty in Artificial Intelligence*, pages 72–81, 2016.

[10] K. Chalupka, F. Eberhardt, and P. Perona. Multi-level cause-effect systems. In *Artificial intelligence and statistics*, pages 361–369. PMLR, 2016.

[11] D. M. Chickering. Optimal structure identification with greedy search. *J. Mach. Learn. Res.*, 3:507–554, 2002.

[12] D. Colombo, M. H. Maathuis, et al. Order-independent constraint-based causal structure learning. *J. Mach. Learn. Res.*, 15(1):3741–3782, 2014.

[13] J. Corander, A. Hyttinen, J. Kontinen, J. Pensar, and J. Väänänen. A logical approach to context-specific independence. *Annals of Pure and Applied Logic*, 170(9):975–992, 2019.

[14] S. Delattre, N. Fournier, and M. Hoffmann. Hawkes processes on large networks. *Annals of Applied Probability*, 26:216–261, 2016.

[15] A. P. Dempster, N. M. Laird, and D. B. Rubin. Maximum likelihood from incomplete data via the em algorithm. *Journal of the royal statistical society: series B (methodological)*, 39(1):1–22, 1977.

[16] S. Gao, R. Addanki, T. Yu, R. Rossi, and M. Kocaoglu. Causal discovery in semi-stationary time series. *Advances in Neural Information Processing Systems*, 36:46624–46657, 2023.

[17] S. Gao, R. Addanki, T. Yu, R. A. Rossi, and M. Kocaoglu. Causal discovery-driven change point detection in time series. *arXiv preprint arXiv:2407.07290*, 2024.

[18] A. Gasull and F. Utzet. Approximating mills ratio. *Journal of Mathematical Analysis and Applications*, 420(2):1832–1853, 2014.

[19] A. Gelman and J. Hill. *Data analysis using regression and multilevel/hierarchical models.* Cambridge university press, 2006.

[20] A. Gerhardus and J. Runge. High-recall causal discovery for autocorrelated time series with latent confounders. *Advances in neural information processing systems*, 33: 12615–12625, 2020.

[21] M. Glymour, J. Pearl, and N. P. Jewell. *Causal inference in statistics: A primer.* John Wiley & Sons, 2016.

[22] N. Gnecco, N. Meinshausen, J. Peters, and S. Engelke. Causal discovery in heavy-tailed models, 2020. URL https://arxiv.org/abs/1908.05097.

[23] C. W. Granger. Investigating causal relations by econometric models and cross-spectral methods. *Econometrica: journal of the Econometric Society*, pages 424–438, 1969.

[24] W. Günther, U. Ninad, and J. Runge. Causal discovery for time series from multiple datasets with latent contexts. In *Uncertainty in Artificial Intelligence*, pages 766–776. PMLR, 2023.

[25] W. Günther, O.-I. Popescu, M. Rabel, U. Ninad, A. Gerhardus, and J. Runge. Causal discovery with endogenous context variables. *Advances in Neural Information Processing Systems*, 37:36243–36284, 2025. arXiv:2412.04981.

[26] D. Haughton. On the choice of a model to fit data from an exponential family. *Annals of Statistics*, 16:342–355, 1988. URL https://api.semanticscholar.org/CorpusID: 121859486.

[27] G. Henning. Meanings and implications of the principle of local independence. *Language testing*, 6(1):95–108, 1989.

[28] B. Huang, K. Zhang, J. Zhang, J. Ramsey, R. Sanchez-Romero, C. Glymour, and B. Schölkopf. Causal discovery from heterogeneous/nonstationary data. *The Journal of Machine Learning Research*, 21(1):3482–3534, 2020.

[29] A. Hyttinen, J. Pensar, J. Kontinen, and J. Corander. Structure learning for bayesian networks over labeled dags. In *International conference on probabilistic graphical models*, pages 133–144. PMLR, 2018.

[30] N. L. Johnson, S. Kotz, and N. Balakrishnan. *Continuous Univariate Distributions.* John Wiley & Sons, 1970.

[31] S. A. Kannenberg, K. A. Novick, M. R. Alexander, J. T. Maxwell, D. J. Moore, R. P. Phillips, and W. R. Anderegg. Linking drought legacy effects across scales: From leaves to tree rings to ecosystems. *Global Change Biology*, 25(9):2978–2992, 2019.

[32] A. Li, A. Jaber, and E. Bareinboim. Causal discovery from observational and interventional data across multiple environments. In *Neural Information Processing Systems*, 2023.

[33] D. Malinsky and P. Spirtes. Learning the structure of a nonstationary vector autoregression. In *The 22nd International Conference on Artificial Intelligence and Statistics*, pages 2986–2994. PMLR, 2019.

[34] S. Mameche, L. Cornanguer, U. Ninad, and J. Vreeken. Spacetime: Causal discovery from non-stationary time series. *arXiv preprint arXiv:2501.10235*, 2025.

[35] G. Manten, C. Casolo, E. Ferrucci, S. W. Mogensen, C. Salvi, and N. Kilbertus. Signature kernel conditional independence tests in causal discovery for stochastic processes. *arXiv preprint arXiv:2402.18477*, 2024.

[36] C. Meek. *Graphical models: selecting causal and statistical models*. PhD thesis, Carnegie Mellon University, 1997.

[37] J. M. Mooij, S. Magliacane, and T. Claassen. Joint causal inference from multiple contexts. *The Journal of Machine Learning Research*, 21(1):3919–4026, 2020.

[38] H. Nyman, J. Pensar, T. Koski, and J. Corander. Stratified graphical models : Context-specific independence in graphical models. *BAYESIAN ANAL*, 9(4):883–908, 2014. doi: 10.1214/14-BA882. QC 20150225.

[39] J. Pearl. *Causality: Models, reasoning and inference*. Cambride University Press, 2000.

[40] J. Pearl. Causal inference in statistics: An overview. *Statistics Surveys*, 3:96 – 146, 2009. doi: 10.1214/09-SS057. URL https://doi.org/10.1214/09-SS057.

[41] J. Pearl and E. Bareinboim. External validity: From do-calculus to transportability across populations. *Statistical Science*, 29(4):579–595, 2014.

[42] J. Peters, P. Bühlmann, and N. Meinshausen. Causal inference by using invariant prediction: identification and confidence intervals. *Journal of the Royal Statistical Society Series B: Statistical Methodology*, 78(5):947–1012, 2016.

[43] J. Peters, D. Janzing, and B. Schölkopf. *Elements of causal inference: foundations and learning algorithms*. The MIT Press, 2017.

[44] D. N. Politis and J. P. Romano. The stationary bootstrap. *Journal of the American Statistical association*, 89(428):1303–1313, 1994.

[45] M. Rabel, W. Günther, J. Runge, and A. Gerhardus. Causal modeling in multi-context systems: Distinguishing multiple context-specific causal graphs which account for observational support. *arXiv preprint arXiv:2410.20405*, 2025.

[46] J. Ramsey, J. Zhang, and P. L. Spirtes. Adjacency-faithfulness and conservative causal inference. *arXiv preprint arXiv:1206.6843*, 2012.

[47] N.-D. Reiter, A. Gerhardus, J. Wahl, and J. Runge. Causal inference on process graphs, part i: the structural equation process representation. *arXiv preprint arXiv:2305.11561*, 2023.

[48] C. B. Rodas, R. Tu, and H. Kjellstrom. Causal discovery from conditionally stationary time-series. *arXiv preprint arXiv:2110.06257*, 2021.

[49] J. Runge. Discovering contemporaneous and lagged causal relations in autocorrelated nonlinear time series datasets. In *Conference on Uncertainty in Artificial Intelligence*, pages 1388–1397. PMLR, 2020.

[50] J. Runge, S. Bathiany, E. Bollt, G. Camps-Valls, D. Coumou, E. Deyle, C. Glymour, M. Kretschmer, M. D. Mahecha, J. Muñoz-Marí, et al. Inferring causation from time series in earth system sciences. *Nature communications*, 10(1):2553, 2019.

[51] J. Runge, P. Nowack, M. Kretschmer, S. Flaxman, and D. Sejdinovic. Detecting and quantifying causal associations in large nonlinear time series datasets. *Science advances*, 5(11):eaau4996, 2019.

[52] J. Runge, A. Gerhardus, G. Varando, V. Eyring, and G. Camps-Valls. Causal inference for time series. *Nature Reviews Earth & Environment*, pages 1–19, 2023.

[53] A. Sadeghi, A. Gopal, and M. Fesanghary. Causal discovery from nonstationary time series. *International Journal of Data Science and Analytics*, 19(1):33–59, 2025.

[54] B. Saeed, S. Panigrahi, and C. Uhler. Causal structure discovery from distributions arising from mixtures of dags. In *International Conference on Machine Learning*, pages 8336–8345. PMLR, 2020.

[55] E. Saggioro, J. de Wiljes, M. Kretschmer, and J. Runge. Reconstructing regime-dependent causal relationships from observational time series. *Chaos: An Interdisciplinary Journal of Nonlinear Science*, 30(11), 2020.

[56] B. Schölkopf, F. Locatello, S. Bauer, N. R. Ke, N. Kalchbrenner, A. Goyal, and Y. Bengio. Toward causal representation learning. *Proceedings of the IEEE*, 109(5):612–634, 2021.

[57] R. D. Shah and J. Peters. The hardness of conditional independence testing and the generalised covariance measure. *The Annals of Statistics*, 48(3):1514, 2020.

[58] S. Shimizu, P. O. Hoyer, A. Hyvärinen, A. Kerminen, and M. Jordan. A linear non-gaussian acyclic model for causal discovery. *Journal of Machine Learning Research*, 7 (10), 2006.

[59] P. Spirtes and C. Glymour. An algorithm for fast recovery of sparse causal graphs. *Social Science Computer Review*, 9:62–72, 1991.

[60] P. Spirtes, C. Glymour, and R. Scheines. Causality from probability. In *Conference Proceedings: Advanced Computing for the Social Sciences*, 1990.

[61] P. Spirtes, C. Glymour, and R. Scheines. *Causation, prediction, and search*. MIT press, 2001.

[62] E. V. Strobl. Causal discovery with a mixture of dags. *Machine Learning*, 112(11): 4201–4225, 2023.

[63] C. Truong, L. Oudre, and N. Vayatis. Selective review of offline change point detection methods. *Signal Processing*, 167:107299, 2020.

[64] V. Vapnik. Estimation of dependences based on empirical data. In M. Jordan, J. Kleinberg, and B. Schölkopf, editors, *Vapnik: Estimation of Dependences Based on Empirical Data*, Information Science and Statistics, pages 1–399. Springer Science + Business Media, New York, second edition, 2006. Reprint of 1982 edition.

[65] T. Verma and J. Pearl. Equivalence and synthesis of causal models. In *Uncertainty in Artificial Intelligence*, volume 6, pages 220–227. Elsevier Science, 1991.

[66] V. Vovk. Testing randomness online. *Statistical Science*, 36(4):595–611, 2021.

[67] A. Wald and J. Wolfowitz. An exact test for randomness in the non-parametric case based on serial correlation. *The Annals of Mathematical Statistics*, 14(4):378–388, 1943. ISSN 00034851. URL http://www.jstor.org/stable/2235925.

[68] H. Xu, M. Farajtabar, and H. Zha. Learning granger causality for hawkes processes. *ArXiv*, abs/1602.04511, 2016.

[69] S. J. Yakowitz and J. D. Spragins. On the identifiability of finite mixtures. *The Annals of Mathematical Statistics*, 39(1):209–214, 1968.

[70] J. Zhang. On the completeness of orientation rules for causal discovery in the presence of latent confounders and selection bias. *Artificial Intelligence*, 172(16):1873–1896, 2008. ISSN 0004-3702. doi: https://doi.org/10.1016/j.artint.2008.08.001. URL https://www.sciencedirect.com/science/article/pii/S0004370208001008.

[71] Y. Zheng, B. Huang, W. Chen, J. Ramsey, M. Gong, R. Cai, S. Shimizu, P. Spirtes, and K. Zhang. Causal-learn: Causal discovery in python. *Journal of Machine Learning Research*, 25(60):1–8, 2024.

[72] K. Zhou, H. Zha, and L. Song. Learning social infectivity in sparse low-rank networks using multi-dimensional hawkes processes. In *International Conference on Artificial Intelligence and Statistics*, 2013.

A   Further Numerical Experiments

The experiments in the main text §7 focused on the time series case. The rational behind this decision was, to include comparisons to existing methods into the main-text; with Regime-PCMCI being applicable to the time series case only, this lead to the corresponding restriction in §7. More precisely, in order to have only (time-lag-)orientable links for fitting models, Regime-PCMCI requires time series without contemporaneous links, which means it does *not include* the IID-case as a special case.

Since our framework is not limited to time series, it makes sense to demonstrate its capabilities with IID-data algorithms as well. We study the PC [59], PC-stable [12] and FCI [61] algorithms via implementations provided by the `causal learn` [71] python package. These are among the best understood and most studied choices for constraint-based causal discovery. Beyond demonstrating the capability of application to IID-data and flexibly exchanging underlying CD-algorithms, there are at least three more questions that this section can answer:

- In §7, we encountered an issue with union-graph discovery becoming worse given more data. We will find below that this problem does not occur for IID-data, so it is likely a time series effect.

- In §7, we noticed that of our two hyperparameter-sets, the one for larger regimes seems to almost always perform better, even for small regimes. For IID-data we will find that this effect becomes much weaker, but still seems to be present. We take this as an indication that both the way multiple independence-tests are combined in CD and time series effects should play a role for hyperparameter choices.

- For time series, different parameters like maximum time-lag and node-count are interdependent. Also, stability considerations make it difficult to systematically explore the behavior under different effect-to-noise ratios. So we study some additional parameters and the dependence on type and quantitative scale of noise-distributions on IID-algorithms instead.

Methods and evaluation metrics are the same as in the main text.

A.1 Details on Time Series

Results for time series are already discussed in the main text §7. Here we provide some additional information about the impact of the choice of underlying CD-method (PCMCI [51], PCMCI+ [49], LPCMCI [20]; using implementations of the `tigramite`[11] python package) and a more detailed discussion about the evaluation of the behavior with changing numbers of ground-truth model-indicators.
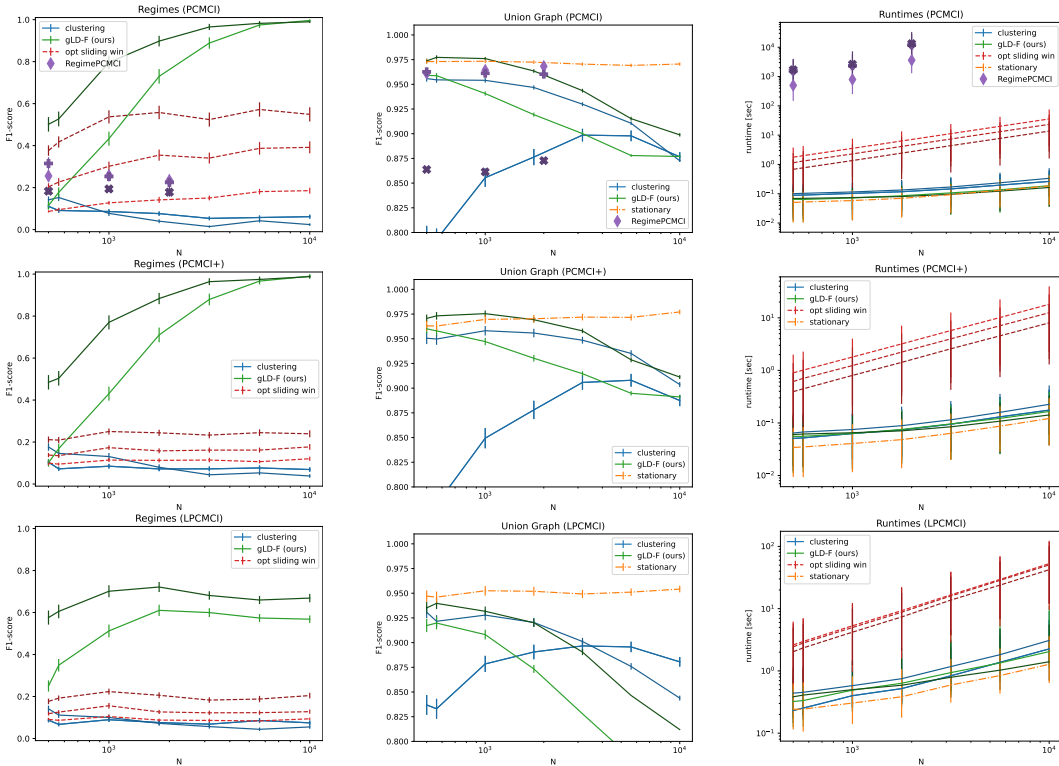
A.1.1 Comparison of Methods

Figure A.1: Comparison of results for PCMCI [51] (also shown as Fig. 7.1), PCMCI+ [49] and LPCMCI [20] (rows), for regimes, union-graph and runtime (columns) for different baseline-methods (colors) and different window-sizes / hyperparameter sets (where applicable; shades, darker is larger).

In figure A.1, we compare results for different underlying (time series) CD-algorithms. The details of the MCI-implementation vary (see §B.6). For our method, PCMCI and PCMCI+ perform very similar, this behavior can vary for other configurations of the PC_1-phase, see §B.6. For LPCMCI, the results for the union-graph seem to suffer stronger than for the other methods (see main text); also the results for regime-detection seem to plateau, this is to some degree expected, as the current MCI-logic (§B.6) for LPCMCI may not execute enough tests as mCITs (consider too many tests "PC_1-like") to detect all model-indicators.

While the adaptation in the implementation of the MCI-philosophy for different time series methods makes the application of our framework with different methods in this case more complicated than for the IID-case, it is still possible with reasonable effort. Our results show that for complex settings like for LPCMCI (time series with contemporaneous effects and latent confounders) there is room for improvement by more specialized adaptation,

---

[11]see `https://github.com/jakobrunge/tigramite`

but nevertheless they also demonstrate the modularity and flexibility in choosing different underlying CD-algorithms.
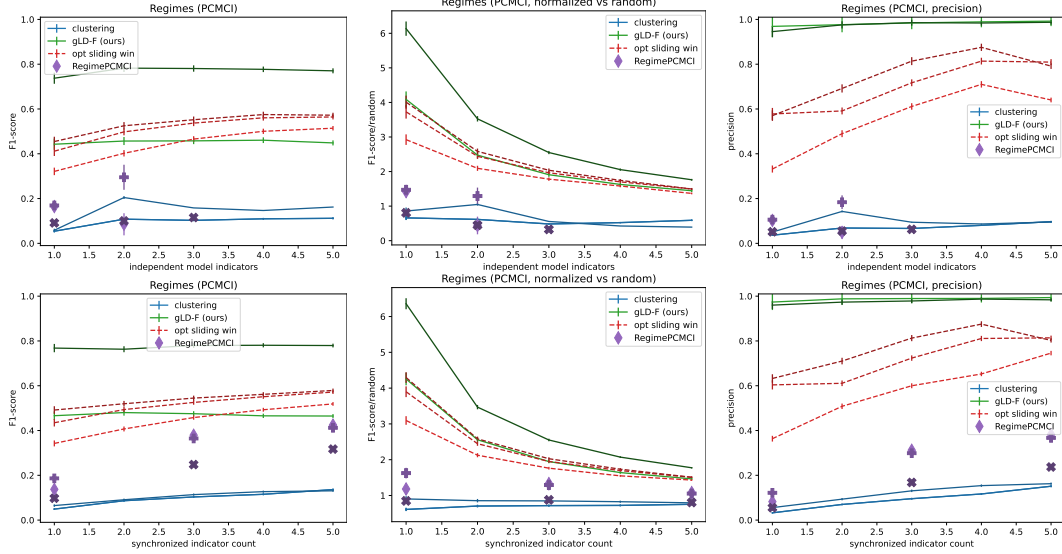
A.1.2 Behavior with Indicator Count Revisited

Figure A.2: Results for the quality of regime-detection with increasing indicator count. Left-most is F_1-score, also shown in Fig. 7.3, center is F_1-score normalized by F_1-score of a random algorithm with the same recall, right-most is precision. In the upper row, indicators vary independently (see Def. C.3), in the bottom row, they are synchronized (change simultaneously).

In the main text (§7.2) we already indicated that F_1-score may not be well-suited to discuss the results on behavior with different indicator counts. To compare the effects of non-trivial indicator count in isolation, node-count, link-count and sample-size are kept constant. But for a fixed link-count, increasing the number of non-trivial model-indicators increases the actual (ground-truth) number of and *rate of* positives.

A higher rate of actual positives means random guessing at fixed recall gets better. So some insight can be gained, by normalizing the F_1-score by the F_1-score that would be obtained by random guessing at the same recall. This is shown in the middle panel of Fig. A.2. From this representation it becomes clear that compared to random performance, clustering and Regime-PCMCI do *not* get better with larger numbers of independent non-trivial indicators, as the F_1-score might suggest. This score is not well-suited to compare different methods (with different recall vs. precision), but (for low precision, see next paragraph) methods it can likely capture the behavior with increasing indicator-count well.

For a guess to be accidentally correct – and more likely so for higher rates of actual positives – one has to guess. As the last panel in Fig. A.2 shows, our approach has very high precision, thus it rarely "guesses" positives, so that the effect discussed above only has a small impact. Standard F_1-score may be more appropriate in this case to study the behavior with larger non-trivial model-indicator counts. The slight up-wards trend in the left panel of Fig. A.2 is probably due to the effects mentioned above, but the strong downward trend in the middle-panel may not accurately represent the behavior.

A.2 IID Methods

The difference between different underlying CD-methods (we used PC [59], PC-stable [12] and FCI [61]; using implementations in the `causal learn` [71] python package) is small,
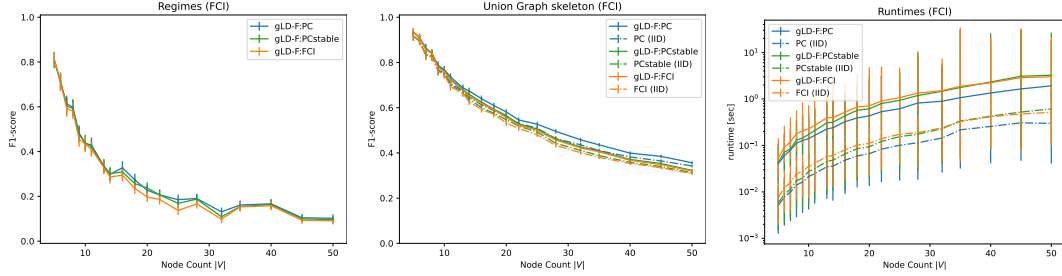
Figure A.3: Comparison of the combination with different underlying CD-algorithms for the IID-case: PC [59], PC-stable [12] and FCI [61].

likely because for the sample-sizes where regime-detection works adequately the union-graph discovery is mostly stable and these methods to a large degree end up executing the same tests. We did not include systematic experiments with latent confounders, so FCI tends to perform slightly worse than PC and PC-stable (which leverage causal sufficiency).

The most pronounced difference seems to occur in the analysis of node-counts (for details on this problem itself, see §A.4 below). Results for different methods in this case are shown in Fig. A.3. This comparison may not be particularly interesting, but it demonstrates the simple adaptation of our method to different underlying CD-algorithms. The more relevant consequence of this adaptability is in the applicability for example with latent confounding via FCI.
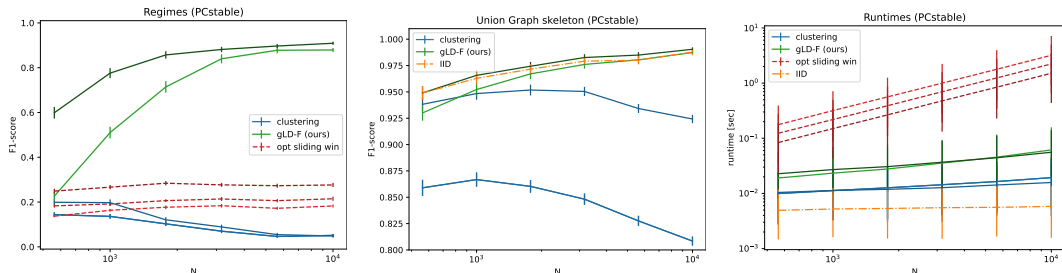
A.3   Sample Size

Figure A.4: Behavior if IID-Methods with sample-size for the PC-stable algorithm.

The behavior with increasing sample-size, see Fig. A.4, with regard to the detection of regime-changes is similar to the time series case. However, the union-graph-skeleton no longer shows a fall-off for larger data-sets. This does not strictly imply that said falloff is a time series effect only – it could still exist and negatively effect convergence-speed, while not changing the sign – but it is at least an indication that a time series effect is a plausible explanation. For our method, the next subsection (§A.4) shows some additional N-dependence across different node-counts.

Here, and for other results in this section, our approach has higher runtime (Fig. A.4, right-most plot; shown are median and error-bars from 10%–90% quantiles) than standard (union-graph only) causal discovery or clustering plus CD (at least for the simple k-means clustering used here), while it has lower runtime than sliding-window approaches (which likely suffer from very slow iteration and additional overhead from multiple CD-executions in python). The differences are much less pronounced than for example in comparison to more complex methods like Regime-PCMCI (see §7). For stability of runtimes, see also §A.4 below.
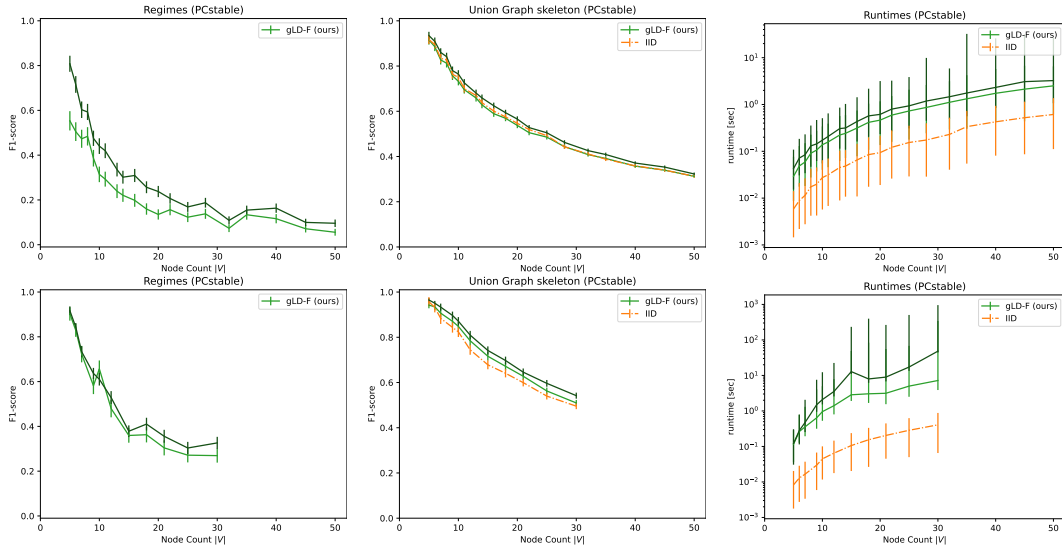
48

A.4 Node Count / Model Complexity

Figure A.5: Behavior if IID-Methods with node-count for the PC-stable algorithm. First row is for $N = 1000$, second row for $N = 5000$.

Both the union-graph and especially the regime-recovery do suffer substantially from large node-counts, see Fig. A.5. It should be remarked that at up to 50 nodes and three independently changing indicators the setup is quite challenging for recovery from only $N = 1000$ data points. Increasing to $N = 5000$ seems to improve the situation somewhat, but leads to runtime-problems (see below). We target a link-density of 2 parents per node. This density cannot be achieved for very small node-counts, correspondingly the density ramps up to 2 initially. We belief that the strong falloff in the recovery of regime-changes is primarily driven by the difficulties in detecting the union-graph correctly and the more frequent occurrence of larger conditioning sets. With the sparser setup used for time series (Fig. 7.2) the recovery of regime-changes could maintain a good quality better, which supports this interpretation. See also next subsection.

When increasing the sample size N, we find quite unstable runtimes. Note that, in Fig. A.5 (lower row, $N = 5000$) the y-axis scale of the runtime-plot (right hand side) is very different from the upper row ($N = 1000$). Further the error-bars around the median values (10%–90% quantiles, see §C.5.6) become quite large; note, that the y-axis is log scale, so the 90% quantile is almost two orders of magnitude (a factor of 10^2) above the median. Both the large increase in median runtime and the encountered instabilities when going to $N = 5000$ may arise from lower false negative-rates: Nodes that are separated by multiple "hops" (subsequent edges) in the graph are technically dependent. However, after how many hops this dependence is actually detected in the finite-sample case depends on N. False negatives (more likely for smaller N) in this case may *not* substantially worsen CD results (at least for the skeleton), rather they make the graphs sparser more quickly, thus make CD much faster (and more stable).

Due to these stability issues, we included for $N = 5000$ data points only up to 30 nodes. For a comparison with other approaches (like sliding-window or clustering), see the time series case §7.

A.5 Link Count / Graph Density

The link count at a fixed node-count also provides a reasonable measure of "model complexity". Results are shown in Fig. A.6.
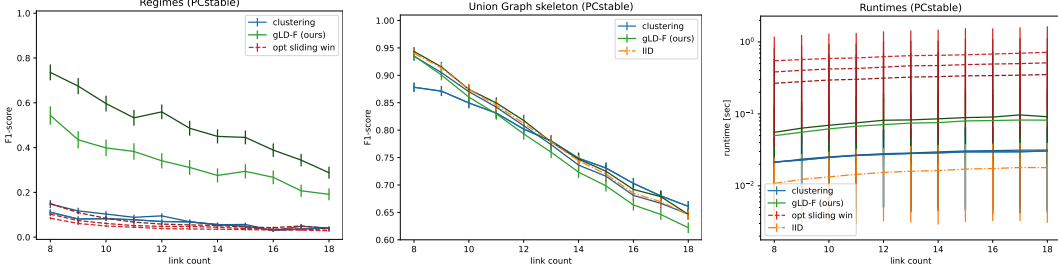
Figure A.6: Behavior of IID-Methods with link-count for the PC-stable algorithm.
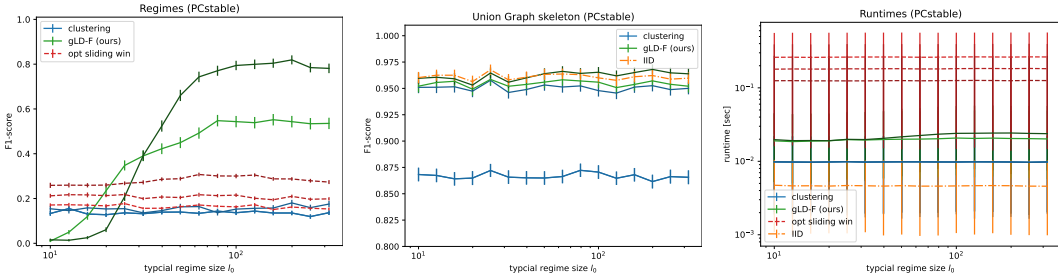
A.6 Regime Sizes

Figure A.7: Behavior if IID-Methods with ground-truth typical regime-size for the PC-stable algorithm.

Generally we expect our regime-detection to be sensitive down to a certain ground-truth typical regime-size. A inductive bias towards larger regimes should cap out at a higher score eventually, but at the cost of falling off earlier when going to smaller regime-sizes. While this effect is not very strongly visible in Fig. A.7 (compare dark green and light green lines), it is visible much more clearly than for the time series results (Fig. 7.4). Nevertheless the hyperparameter set for larger regimes seems to work surprisingly well again. This is likely due to the way multiple tests are combined in CD, where false negatives and false positives effectively have unequal severity for overall score.

A.7 Noise Types

We use tests based on z-scores. In general z-scores approach a normal distribution rather quickly, however, we are computing them on potentially small (a few tens of data points) blocks. The resulting distribution will thus depend at least weakly on the true noise-distributions. This effect seems to be typically rather small, but for more heavy-tailed distribution seem to negatively affect the overall quality of regime detection. Among the examples analyzed below, this is particularly visible for Cauchy-distributions.

We analyzed different noise-distributions across different parameters shared across all nodes, and also included a mixed setup, where each node is assigned one of the above distributions at random (with equal probability). Our analysis is structured to study more specifically:

- Distributions that are relevant for modeling errors under different *practical considerations*. Following the logic of [64, 4.4 (p. 87–91)] normal, Laplace and uniform distributions provide reasonable corner-cases to study.

- The effect of heavy-tails and more generally challenging moment-(convergence-)properties. We include a Cauchy-distribution as practically relevant example.

- The effect of noise-scale, which can be parameterized well for the examples given above.

- The effect of asymmetry. As a concrete example we use β-distributions with suitable parameters to study this question.

- The effect of multi-modality, for simplicity studied on a multi-modal normal, with different distances between modes.
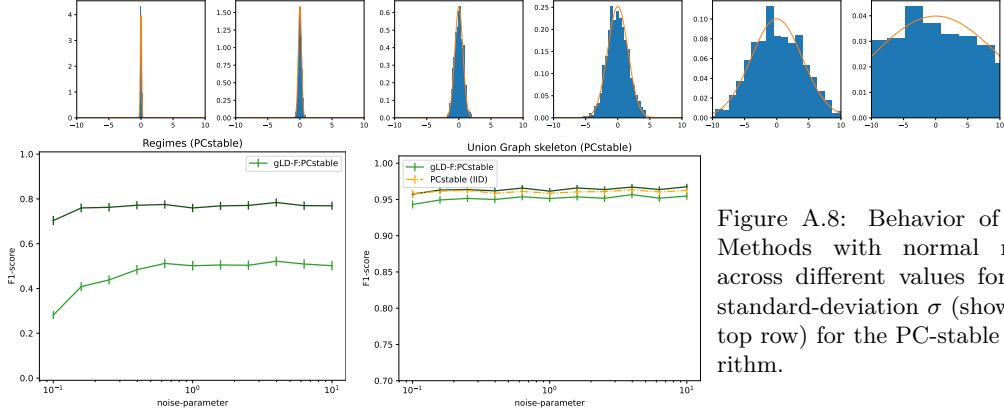
A.7.1 Normal Distributions

Figure A.8: Behavior of IID-Methods with normal noise across different values for the standard-deviation σ (shown in top row) for the PC-stable algorithm.

Normal distributions are often employed as a plausible model for noise terms. There are many arguments justifying this choice. For example, as Vapnik [64, 4.4 (p. 87–91)] points out, the normal distribution, having maximal entropy given a fixed variance, models a minimum knowledge (pure noise) distribution under fixed experimental conditions ('fixed' here means the variance itself remains fixed across repetitions of a measurement, see also the next point §A.7.2 about Laplace distributions).

The width of the noise is picked uniformly for all nodes in the graph. The resulting signal seen by the independence-test depends on the variation of the source (which is composed of the source's noise and its ancestors' noises) and the (model-)effect-strength (the multiplier). Thus signal-to-noise should not be affected by the (shared among nodes) width of the noise-distributions, as this width contributes equally to signal and noise (within the limits of numerical floating-point precision, but we should be far from these limits for the experiments presented here). This does not make for terribly interesting plots, but the primary purpose of this subsection on the behavior with varying noise-types is the *validation* of approaches and implementations; for this purpose the plots presented to provide useful information.

For normal distributions, results in Fig. A.8, this behavior is mostly generated as expected. The only non-trivial feature is a slight fall-off of the lower-regime-length hyperparameter set results for regime detection.

A.7.2 Laplace

Laplace distributions are often employed as a plausible model for noise terms if experimental conditions are believed to change between repeated measurements [64, 4.4 (p. 87–91)]. This is in contrast to normal distributions being well-suited to model noise under fixed conditions; considering that we are interested in non-stationary / non-IID data, this seems like a relevant distribution to study. The above notion is made more precise for example by Vapnik [64, 4.4 (p. 87–91)], based on an argument of maximizing the entropy of the distribution of σ, and then further of the mixture with varying (according to this distribution of σ) variance.

Both our expectations and our observations do not differ substantially from the case of normal noise §A.7.1, see Fig. A.9. An interesting feature of Laplace-distributions is
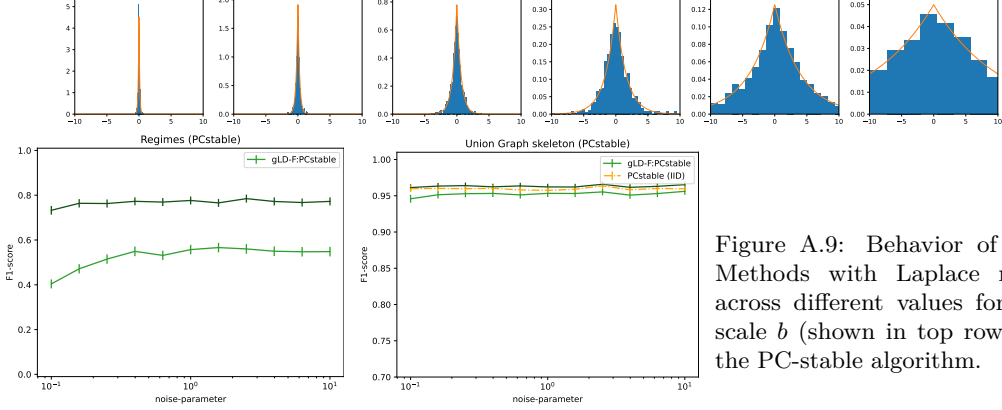
Figure A.9: Behavior of IID-Methods with Laplace noise across different values for the scale b (shown in top row) for the PC-stable algorithm.

the "singularity" (discontinuity of its derivative) of the density at zero (or rather, at its location-parameter, here 0). However, we do not use density-estimation or smoothing-kernels, so this does not seem to considerably affect our method.

A.7.3 Uniform
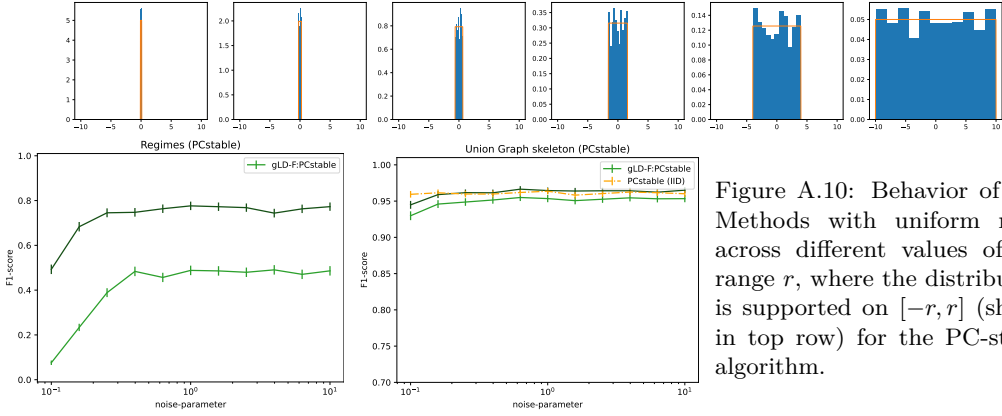
Figure A.10: Behavior of IID-Methods with uniform noise across different values of the range r, where the distribution is supported on $[-r, r]$ (shown in top row) for the PC-stable algorithm.

Vapnik [64, 4.4 (p. 87–91)] gives a simple and convincing argument for the relevance of uniform distributions: With limited resolution or encoding precision, real-world measurements are often quantized (in the literal sense, not necessarily in the sense of quantum theory). To make them easier to process, it is often reasonable to de-quantize them. Given the absence of any knowledge on the distribution within such quanta, the logical choice for de-quantization is a uniform distribution.

Generally, the observations we make are similar to those in the normal §A.7.1 and Laplace §A.7.2 case. The fall-off of the regime-detection quality for small noise-values is stronger however, see discussion A.7.8.

A.7.4 Cauchy

Cauchy-distributions are an often employed example of distributions with challenging formal properties, like the non-existence of (any) moments. This makes it *interesting* to study, but it is also *relevant* as it naturally appears in statistical physics, for example in (Doppler-free) spectroscopy applications.

While innocent-looking at first Fig. A.11, this density seems to have the by far most dramatic impact on our method, and also on union-graph discovery. We belief that this is due to outliers from the tails shaping the derived statistics in a way that prevents fast
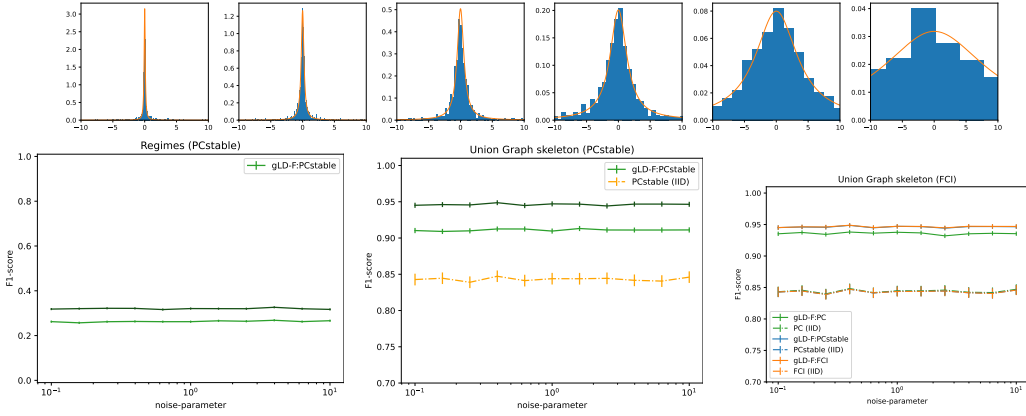
Figure A.11: Behavior of IID-Methods with Cauchy noise across different values for the scale γ (shown in top row) for the PC-stable algorithm. Third plot shows difference between CD-methods.

convergence to normality, and thereby jeopardizes our null-distribution estimates. We do not fully understand why our method seems to outperform the standard IID-method on union-graphs, but the observed signal is rather strong. Even more confusing, while for the other noise-experiments PC, PC-stable and FCI perform extremely similar (on skeletons) for the case of Cauchy-distributions, the vanilla PC algorithm seems to fall off compared to PC-stable and FCI in terms of recovery of the union-graph through our method.

A possible explanation for the difference on the union-graphs might be that our method, being built to be (at least to some degree) robust against non-stationarities (see §D.6), may also be able to compensate for rare (thus local in "time", confined to a single block) outliers better, or to find dependence observed on rare outliers indirectly through the homogeneity-test.

There has been a substantial recent interest in causal discovery on heavy-tailed data [22], and our framework is in principle flexible enough to supplement independence-tests with, for example, tail-coefficients, so this might be a topic of interest for future work.

A.7.5   Beta
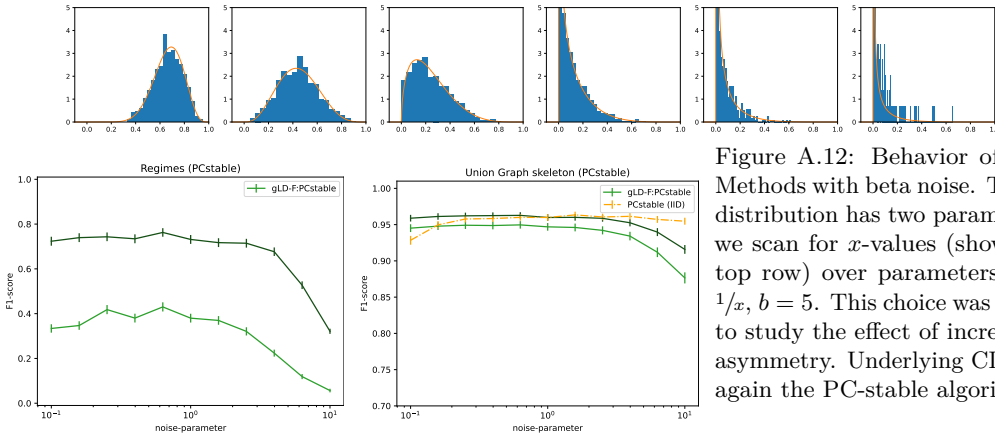
Figure A.12: Behavior of IID-Methods with beta noise. The β-distribution has two parameters, we scan for x-values (shown in top row) over parameters $a = 1/x$, $b = 5$. This choice was made to study the effect of increasing asymmetry. Underlying CD was again the PC-stable algorithm.

Beta-distributions are of great relevance for the modeling of random variables of compact support. A systematic account for the behavior under arbitrary configurations of the (two parameter) family would be out of scope for this appendix, however, we can employ a specific choice of parameters to study the effect of asymmetry in the noise-density, see Fig. A.12.

We observe some falloff with high asymmetries, but in this case the distribution also becomes very narrow, so that this observation may be due to the same effects observed for example for normal distributions §A.7.1. In the parameter-regime in the middle of the plot, where the distribution is not yet narrow, but already very asymmetric, there is nothing new observed, so that asymmetry in itself is likely not a substantial problem to our method.

A.7.6 Multi-Modal Normal
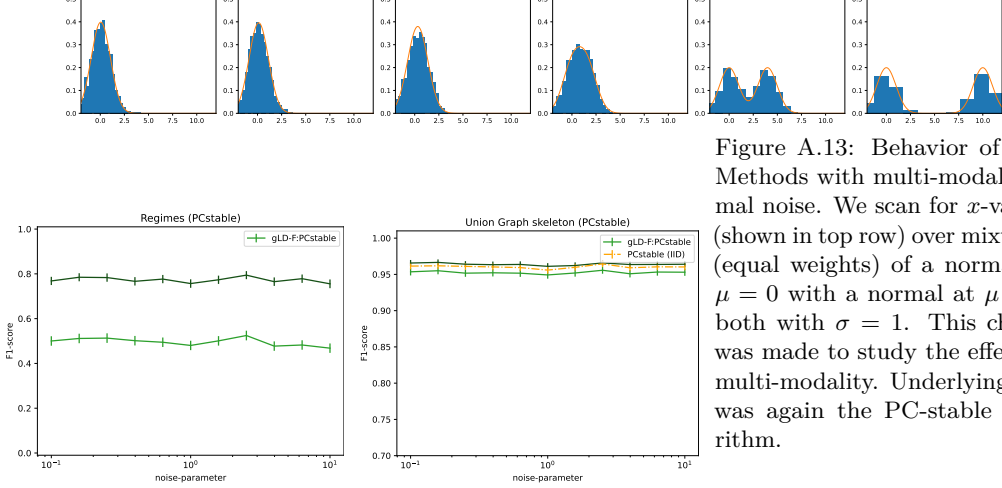
Figure A.13: Behavior of IID-Methods with multi-modal normal noise. We scan for x-values (shown in top row) over mixtures (equal weights) of a normal at $\mu = 0$ with a normal at $\mu = x$, both with $\sigma = 1$. This choice was made to study the effect of multi-modality. Underlying CD was again the PC-stable algorithm.

Much in our method revolves around the question of the presence of multiple peaks in dependence-distributions (see Fig. 5.3), so one should naturally be somewhat worried about the effect of multi-modal noise-distributions.

In practice, we do not observe any problems from the presence of multi-modal noises.

A.7.7 Combinations
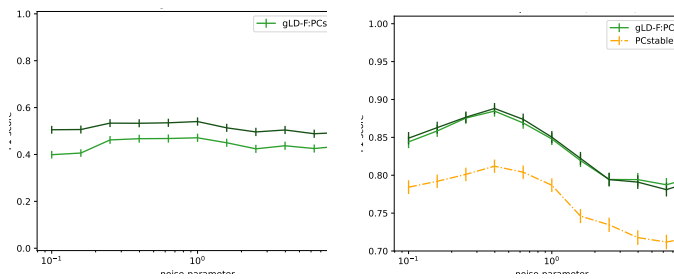
Figure A.14: Behavior of IID-Methods with combinations of different noises. Here each node is randomly assigned one of the noise-types discussed above. This choice was made to study the effect of combining different noise-types within the same model. Underlying CD was again the PC-stable algorithm.

Finally, one should wonder what happens, if different nodes follow different distributions. As the results in Fig. A.13 show, the detection-quality, in particular for the hyperparameter set for large regimes does suffer, as does the union-graph. Note, that while we keep the noise-parameter the same for all nodes in the system, this parameter does not have a meaningful interpretation as a scale for all of the noise-types, so in practice this setup is also expected to be more challenging as it combines different *noise-scales*, not just noise-types.

The union-graph results for the two hyperparameter sets for our method appear curiously close together. While we of course cannot exclude a bug, since all noise-types (including the combinations one) where generated, run and evaluated with precisely the same code,

this seems, however, unlikely. Again, our approach seems to provide better union-graphs, than the vanilla algorithm; the only plausible explanation we have at the moment is as for the Cauchy case (see §A.7.4): robustness against non-stationarity might help to cope with outliers.

A.7.8 Discussion

We find two main challenges in our quick study of different noise-types. The first arises for Cauchy distributions, where the quality of regime-detection decreases substantially compared to for example normal-distributions. Cauchy distributions are formally challenging. We do not currently know what precisely causes the difficulties encountered, but we belief it could plausibly be an issue with outliers. These outliers will slow down the approach to normality of z-scores, especially on small datasets (or small blocks). However, the hyperparameter set for larger regimes (with larger blocks) seems to suffer more than the smaller regimes one, which seems to contradict this interpretation. Further also the standard (on all data / without blocks) union-graph discovery seems to suffer particularly strongly, which poses a similar difficulty to this explanation. Generally correlation-based test-approaches provide little control over the weighting of outliers compared to other samples. It might be interesting to study the effect of up- or down weighing outliers. Indeed causal discovery in the presence of heavy-tailed distributions is an active area of research, and also combinations of our framework with for example tail-coefficient techniques [22] may be interesting.

The second challenge arises for very small value-scales, for example very small σ-values for normal distributions. The effect seems to be present for all distributions where we scanned across a parameter (barring Cauchy-distributions, where other effects are more formative, see above) which can be interpreted as a proxy for scale: normal, Laplace and uniform distributions. We do not belief this is a problem of floating-point precision, but we cannot exclude this at the moment either. There may in practice be some virtue in normalizing data.

A.8 Preliminary Experiments

Before studying the hyperparameter dependence of the individual sub-modules of the mCIT implementation discussed in §D, we ran some initial benchmarks to assess the viability of our approach with preliminary hyperparameters (educated guess based on expected typical regime-lengths in the benchmark data-set). We include these results in tables A.1 and A.2, for completeness and transparency, but also because of an interesting observation: Especially when used with PCMCI+, even with extremely crude hyperparameters (fixed across all Z, and N [thus both experiments], picked without any kind of sophisticated procedure), our approach seems to be able to maintain good precision, even though recall does suffer, especially for larger / more complex models.

With our method being competitive in run-time to union-graph (standard) CD, and the main effect of miss-specification of hyperparameters apparently being found in low recall, our approach can likely be useful already as a "low noise" (rare false positives) extension beyond union-graphs.

The runtimes listed in the tables are not immediately comparable – Regime-PCMCI instances were run on a cluster on 16 CPU-cores per instance (summed into the CPU-seconds given, i. e. CPUs are total core-seconds), while the preliminary runs with our method were done on a laptop (with substantially different hardware). Results in the main text show more comparable times (all on the same cluster) and show a very similar picture. For some hyperparameter choices for Regime-PCMCI, the rate of convergence (where at least one of the re-runs produced a result) is low, it is unclear if chance of convergence and error-probability are independent, thus the performance on converged runs only may not accurately represent the true error-rates in these cases (assuming that convergence is more likely on "easy" examples, the shown numbers may be favoring configurations with *low* convergence-rate,

which might explain the lower F_1 score of the hyperparameters recommended by [55] for complex systems on the complex system).

Method	hyperparams	F_1-score	precision	recall	convergence	av. runtime
Regime Dependent Edges (trivial-true F_1 would be ~ 0.10):						
Regime-PCMCI	tigramite	0.48	0.35	0.77	57.1%	569.2 CPUs
Regime-PCMCI	[55], simple	0.58	0.46	0.78	80.7%	1682.7 CPUs
Regime-PCMCI	[55], complex	0.33	0.22	0.72	94.0%	1877.2 CPUs
gLD-F PCMCI	preliminary	0.78	0.83	0.73	100%	0.044 CPUs
gLD-F PCMCI+	preliminary	0.80	0.92	0.71	100%	0.040 CPUs

Table A.1: Preliminary results on a very simple time series setup: 5 nodes, 5 links plus 50% of nodes with auto-correlation, acyclic summary-graph, max (and thus only) lag 1, one changing link in ground-truth. (233 runs)

Method	hyperparams	F_1-score	precision	recall	convergence	av. runtime
Regime Dependent Edges (trivial-true F_1 would be ~ 0.07):						
Regime-PCMCI	tigramite	0.14	0.08	0.98	21.6%	2 485 CPUs
Regime-PCMCI	[55], simple	0.14	0.07	0.94	27.6%	6 111 CPUs
Regime-PCMCI	[55], complex	0.05	0.03	0.80	99.5%	11 267 CPUs
gLD-F PCMCI	preliminary	0.52	0.54	0.51	100%	0.979 CPUs
gLD-F PCMCI+	preliminary	0.64	0.90	0.50	100%	0.686 CPUs

Table A.2: Preliminary results on a more challenging time series setup: 10 nodes, 9 links plus 50% of nodes with auto-correlation, acyclic summary-graph, max lag 4, two changing links in ground-truth. (199 runs)

A.9 Hyperparameter Policy

After initial validation (see §A.8) with hand-picked fixed hyperparameters, we studied the different stages of the mCIT on IID data (see §D.3.4, §D.4.6), with the goal of picking hyperparameters in a robust way: An evaluation of numerical results on a mostly uninformative prior is combined with theoretical considerations to pick hyperparameters in a "minimax-like" spirit to provide good performance across a large range of plausibly encountered model-priors. These choices are made for IID-data, but conceptually they should be useful for time series data as we adopt the MCI [51] idea (see §B.6); they may, however, not apply for the PC_1-phase (also discussed in §B.6), see also the discussion of the quality of union-graph discovery in §7.

These hyperparameter sets were than frozen for all numerical experiments on causal discovery in §7 and §A. The only exception to this rule is that we fixed a bug that prevented data-blocks from being centered correctly for computations of correlation-scores and re-ran all CD-experiments with the fixed CIT-implementation. This code-fix did not lead to perceptible changes in any of the results outside of the study of different noise-types (§A.7).

B Further Topics

There are a few closely related topics, whose inclusion can shed light on certain aspects of our framework. We include a few short discussions on such topics here.

B.1 Examples for Patterns

Our definition of patterns (Def. 5.4) is quite general: It only requires prior knowledge of "neighborhoods" (blocks) of a given size of points, which define a tiling of the index set I

(assuming data is given in the form $(X_i, Y_i, Z_i, \ldots)_{i \in I}$). Indeed this tiling need not even be without gaps, as long as enough blocks are available for a statistical analysis.

Patterns of this form include temporal regimes, where blocks are intervals (example 5.5), spatially persistent regimes, where blocks are for example rectangles or hexagons tiling the plane. Generally any exogenous quantity (for the endogenous case, see §B.2), like height above sea-surface for spatial locations, or terrain slope for river-catchments can for example be rank-transformed and then employ example 5.5. But also sufficiently regular networks (undirected graphs) – for example computer-networks, electricity-grids etc. – where sufficiently regular may mean for example "similar number of neighbors for all nodes", can plausibly be approximately tiled.

These patterns can also be combined, in at least two meaningful ways:

(i) Assume each indicator follows at least one of the two patterns, for example for all times the same spatial pattern-realization, or everywhere (in space) the same temporal pattern-realization. In this case, homogeneity and weak-regime tests can be considered independently for both patterns. State-space construction §6 could then additionally exploit this product-structure on the state-space, with assignment to factors in this case being implicit in mCIT results.

(ii) Assume each indicator follows both patterns locally, for example varies slowly in space for all times and varies slowly in time everywhere in space. In this case blocks can be formed as suitable products (with potentially different weights for different patterns). The two-dimensional spatial patterns described above are a product of one-dimensional patterns as in example 5.5 in this sense.

Further, patterns can be combined with exact knowledge, i.e. observed contexts C: For example, for climate dynamics, a difference between sea-surface vs. land-surface may be plausible. In such cases, it is in principle possible to find an (approximate) tiling of either context (sea and land) individually to assess (marked) conditional independencies of the form $X \perp\!\!\!\perp Y | C$ better. As another such example, assume we are given time series data for multiple (but not many) spatial locations, which are believed to feature similar temporal regime structure-realizations [24]. We then may use intervals (as in example 5.5), but make them shorter (improving our resolution) by considering all spatial locations for each interval as part of the block.

B.2   Endogenous Indicators

So far our indicators are functions of sample-indices, which in practice will typically mean they are functions of time or space or similar extraneous constructs. This makes them exogenous to the system-variables. Many real-world problems are changing in response to endogenous – system-driven – variables, this includes both natural and technical (state-machine like) systems. Such endogenous-indicator systems have been studied for causal discovery [25; 45], but only for the case where indicators are known or well-approximated by known deterministic functions of observed variables.

So, how can our framework be extended to endogenous indicators? The first clue is that a "pattern" as we detect it on space or time etc., can in principle just as well be detected *in the values of a system-variable.*

Example B.1 (Endogenous Pattern). Consider the particular simple case of a system with only three variables, X, Y, C, and causal graph $X \to Y \leftarrow C$ and mechanism at Y of the form $Y = \alpha \mathbb{1}(C \geq t)X + \eta_Y$, i.e. Y depends on X, but only if $C \geq t$ for an unknown threshold t. Since C is not a descendant of either X or Y, it behaves essentially as if it where exogenous to the problem, therefore we could try to find a pattern in C, by building blocks by similarity of values in C. Finding t is a particularly simple (much simpler than the rather general case discussed in §5) case of pattern-detection. The pattern in this case is known a priori to be described by a single parameter. Our framework could exploit this

knowledge through a suitable mCIT implementation. Even with only the knowledge that the system is likely to behave similar for similar values of C, the material in §5 – and therefore our framework – is applicable.

Remark B.2. In practice, such effect often are additionally persistent. If the endogenous variable C in the example above is auto-correlated, it may cross the threshold only rarely, effectively leading to persistent regimes. Our current implementation *can* thus indirectly find these endogenous effects, but it cannot yet attribute them to C (even though resolved detected indicators could of course be compared to C, see §B.7) and further including prior knowledge about the dependence on C could substantially improve finite-sample properties.

Generally, there are some challenges involved in using endogenous variables to find patterns. For example selection bias could create the illusion of regime-specific links between ancestors of C, if C is the descendant of a collider on a path that is open / closed depending on the state of other model-indicators. More surprisingly selection-bias, through shifts in observational support, can effectively even make links between ancestors vanish [25], see also §B.3.

A potential remedy could be the inspection of the union-graph and subsequent restriction to testing between definitive non-ancestors of C or an adaptation of the testing-scheme of [25].

Further, an endogenous indicator can, at least in principle, act as a mediator. In particular, for the example above, also the link $C \to Y$ may appear to be changing, but the interpretation is different: Here a simplified latent (the binary indicator) suffices to explain the relation-ship (the dependence factors through $c \mapsto (c \geq t)$). This is similar to the problem studied in [24], but not a regime-dependence in the sense one might expect. In practice, adherence to a pattern (with large blocks) together with the binary value-space of indicators, means the information-flow through them is very limited. So in the finite sample case, it may not be possible to effectively detect these effects anyway; even though the interpretation of change-points in indicators as events and application of tests designed for point-processes might allow to sufficiently boost power.

B.3 Interpretation under Limited Observational Support

As analyzed by [25], different contexts can render certain causal mechanisms (thus their corresponding links in the graph) effectively invisible by concentrating the observational support in regions of low or vanishing derivative of the mechanism, rather than by physically deactivating them. These changes are dubbed *descriptive* by [25] as opposed to *physical* changes for which multivariate mechanisms are constant in one (or more) parents for specific values of a context-parent.

To tackle the problem in practice, [25] introduces assumptions that ensure contexts are chosen sufficiently expressive (dubbed context-sufficiency, in analogy to causal sufficiency), so that all changes are physical when expressed relative to this context. Such "sufficient" contexts always exist: If a mechanism is constant in one parent (say X) for certain values of X, then formally one can always define a binary context variable that takes on one value if X is in the constant region and the other value for other values of X. This is essentially the scheme proposed in §B.2 for the treatment of endogenous variables.

Indeed for endogenous variables our approach can thus be interpreted as finding this (deterministic) endogenous indicator that suffices to describe the change as physical. While in the endogenous case the change of context is effectively a detection of structure in the functional form of a mechanism, our method for exogenous patterns (e. g. in time) as described in the main text of this paper finds non-IID (or non-stationary) changes in mechanisms. Here the multivariate mechanism whose form varies qualitatively is of the form $f_Y(X, t)$ with dependence on t being subject to persistence (or any other pattern) and leading to qualitative changes in the dependence on X in a "physical" sense.

B.4   Relation to Clustering and CPD

The problem of MCD studied in this paper is closely related with a clustering problem. In principle one could solve the multivariate clustering-problem to find all ($\approx 2^k$) states of the system, then perform causal discovery on each cluster individually. Our approach can be understood as an automated translation of this multivariate clustering problem with a large number of clusters into a sequence of simple univariate clustering tasks, by exploiting non-trivial structure of the problem:

(1) *Exploit causal structure* through a CD algorithm and §6 to obtain a problem-statement in terms of marked independencies (and implication tests).

(2) *Exploit persistence* by applying a dependence score to blocks of data, to obtain a well-behaved univariate data-set.

(3) *Exploit the binary nature* of the result of a hypothesis test (independence) and

(4) *exploit the known value $d = 0$* in the independent regime to simplify a problem with many clusters into: Is more than one cluster, and is one cluster centered at zero?

Leveraging change-point-detection (CPD) or clustering methodology while also retaining the ability to exploit these special properties can be difficult in practice. Our framework enables this combination: A plausible approach would be and an application of the dependence-score on CPD-assigned segments rather than blocks. See §D.7.3 for more information about how to leverage CPD and clustering *within* our framework and §D.1.5 which summarizes why we currently use the simple block-based approach. In our framework CPD – when used as a drop-in for the block-based approach – can be applied locally for example to gradients of scores or changes in the target (often, albeit not always, a changing link will change the variance and entropy of its target) or on dependence-scores on (smaller) blocks of data, avoiding the much more difficult global / multivariate problem.

The assumption of causal modularity (Def. C.3) we make, also leads to a signal-to-noise ratio problem for global algorithms. One may intuitively think that the removal of a link leaves traces in the values of many variables (which it does), but these changes[12] are strongly correlated and including more variables does not actually improve signal. It does of course increase noise however. So, given causal modularity (Def. C.3), local approaches should typically have a substantially better signal to noise than global ones, especially on data-sets with many variables.

The problem of having a potentially very large number of clusters (see Fig. 1.2) on complex datasets leads to yet another problem for global approaches: Performing causal discovery per cluster dramatically reduces the amount of available data per cluster. A local method can always use all data for each local decision, and only for weak-testing (§4.4 has to split the data-set; edge-orientations in the present baseline implementation of our framework rely on the currently only partially local §6, see §F.10.1 however). With clustering, error-propagation through the CD algorithm happens per cluster (per global regime, cf. Fig. 1.2), leading to potentially much less stable results.

See also §B.9, where we return to the discussion of CPD as a post-processing step *after* graph-discovery.

B.5   Relation to Sliding Windows

Sliding window approaches in principle apply quite generally: As long as the used CD-algorithm applies per window (or the number of windows with actual change points in them is at least low for practical purposes), there are little restrictions. Time series, IID-data, latent variables etc. can be handled if the used CD-algorithms is suitable for this kind of

---

[12]Assuming there is no substantial measurement noise.

data. Other than our present version of §6, sliding window approaches can also handle cyclic union-graphs.

In many way, the details of our mCIT §D implementation are reminiscent of sliding window approaches. There are, however, important differences because . . .

(a) . . . our approach is local:

- The "validity" of windows (absence of change-points) relies only on *local* change-points, avoiding exponential decay in available valid lengths with increasing indicator-count.

- The actual causal discovery-logic (the underlying CD-algorithm), is executed on mCIT results using *all* data, while for standard sliding windows CD first propagates finite-sample errors, then composes the obtained graphs (including propagated errors).

(b) . . . our approach is direct:

- The choice of hyperparameters can be guided by trade-offs from the statistical analysis of the mixture-dataset (see Fig. 5.6), while for standard sliding-window approaches the practical choice (especially of the cutoffs $a_\pm$, see §7.2) is extremely difficult.

In §7.2 we compare to a posteriori optimal hyperparameters for the sliding-windows. This removes the effect of (b) from the comparison. The convergence-speed for increasing N even so is lower than for our approach, demonstrating the relevance of (a). For any practical application, point (b) is of course similarly of great relevance, as the a posteriori choice of hyperparameters is not possible in practice (it requires perfect knowledge of the ground truth).

B.6 Time Series

For the treatment of time series, we adopt the "MCI-idea" [51]: The PCMCI-family algorithms first systematically search for super-sets of time-lagged parents (the "PC_1-phase"), then test *momentary* independence. Momentary here means that $X \perp\!\!\!\perp Y$ is always tested conditional at least on all lagged parents; in the case of a regression based CIT like partial correlation, this means lagged parents are regressed out. The result is a data-set of approximately IID residuals; the application of IID tests (and confidence-intervals) in the momentary sense has been systematically studied and proven a very useful practical approach [51]. In the same spirit we integrate PCMCI by running regime-detection (marked independence tests) only (or only to the full extend, see below) in the MCI phase.

For other algorithms like PCMCIplus [49] and LPCMCI [20] we use a similar idea, but with slightly different implementation. For PCMCIplus, a ad hoc reinterpretation of different parts of the algorithm as (non-)MCI works surprisingly well (indeed it outperforms PCMCI in our numerical experiments, even though PCMCI's stronger assumptions *are* satisfied). More generally, the first iteration of Algo. 2 in the acyclic case produces a union-graph (its acyclification [7] in the cyclic case), which can also be used to provide supersets of (lagged) parents for subsequent iterations. Indeed this is how we integrate regime detection into LPCMCI: After the first iteration, we consider a test MCI if its conditioning set contains the lagged parents form the graph found in the initial iteration, and apply full regime-detection only in these cases. We do not actively enlarge conditioning-sets (to ensure the occurrence of sufficiently many MCI-like tests), and we do not ensure that lagged effects through contemporaneous parents are blocked. So this is a heuristic approach with potentially low expected (and numerically observed) recall on regimes even asymptotically. Considering the complexity of the task (time series, with contemporaneous links and latent confounding *plus regime detection*), that this integration with LPCMCI aims to solve, it performs rather well,
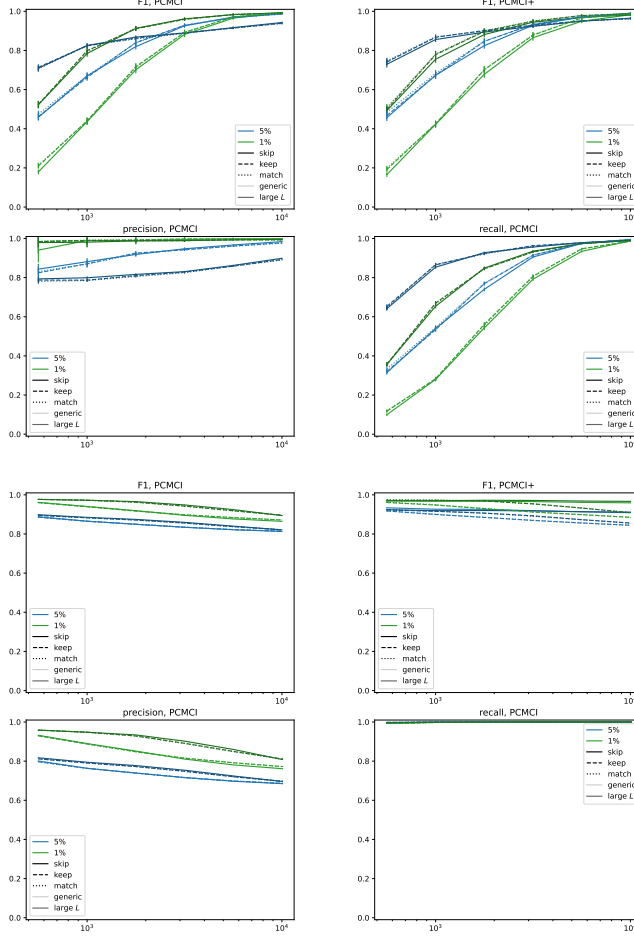
Figure B.1: Results for regime-detection quality (see §7.3). Shown are F_1-score for PCMCI and PCMCI+ (plots in top row), as well as precision and recall for PCMCI (bottom row). Line-colors correspond to different α-values, line-styles corresponds to different realizations of the PC_1-phase, see main text.

Figure B.2: Results for union-graph-recovery (see §7.3). Shown are F_1-score for PCMCI and PCMCIplus (plots in top row), as well as precision and recall for PCMCI (bottom row). Line-colors correspond to different α-values, line-styles corresponds to different realizations of the PC_1-phase, see main text. Error-bar based on counting-statistics only are negligibly small.

especially considering the extreme simplicity of the current integration. Nevertheless, there is certainly room for future improvement on the combination of our framework with LPCMCI.

In figures B.1 and B.2, we show some numerical results for regime-detection and union-graph recovering comparing different configurations for the PC_1-phase: Here the "skip" configuration (solid line) skips the homogeneity test in the PC_1-phase. This means instead of the homogeneity-first approach §5.2.1 the independence-test (with conservative α) is considered more robust to auto-lags. In the "keep" configuration (dashed line), both PC_1- and MCI-phase use the same α-value for homogeneity-testing, while in the "match" configuration the ratio of α-values in the PC_1- vs. in the MCI-phase is the same as for independence-testing (here 5% and 20%, blue line; 1% and 10%, green line). For the other numerical experiments (in particular those in §7), the "keep" configuration was used; for PCMCI this seems to be a reasonable choice (there is little difference, thus little reason to deviate from the logic of §5.2.1). For PCMCI+, skipping the homogeneity-test in the PC_1-phase seems to offset (some of) the convergence problems for the union-graph. The convergence problem further seems to originate from a loss of precision (see lower row of plots in §B.2) on edge detection.

Currently in cases where the homogeneity test is used in the PC_1-phase, it is used as is (potentially with a modified α-value). A more sophisticated approach using a homogeneity-test that is properly adapted to the time series case for the PC_1-phase could probably considerably improve finite-sample performance. We leave the detailed study of such modifications to future work.

B.7 JCI Ideas

Studying regimes with different graphs is very closely related to the study of multi-context data as for example in [41; 37; 28; 25]. Usually these treatments assume prior knowledge of the assignments to data-sets / contexts (for a detailed discussion of the relation between CD-NOD and our approach, see the related literature section, §2).

There are some such joint causal inference (JCI; [37]) ideas that apply almost immediately in the present context.

Example B.3. Let $X \to Y$ be a changing link, if we call the (hidden) indicator C and include it into the graph, we obtain $X \to Y \leftarrow C$, which has a (detectable given knowledge of C) unshielded collider at Y (this is the viewpoint taken by [37]). Even if C is initially hidden, its sufficient (potentially implicit) recovery from data can be used to orient the link $X \to Y$ [28]. In our case, this requires a stochastic time-resolution of the indicator (stochastic in the sense that other than for independence-testing, there is no deeper problem from the assignment being only approximate), which can be easily obtained for example by thresh-holding. Then the target of the changing link should depend on this approximate indicator, while the source should not (again in precisely the same spirit as in the JCI and CD-NOD cases).

There are, however, some difficulties. The JCI idea assumes that conditional independencies involving both arbitrary context- and system-variables can be tested. For context-variables that are not "sufficiently independent" (sufficiently independent in this sense are for example different spatial directions or space and time directions), this is not typically true (not even in principle). Even if context-variables are exogenous, tests may not satisfy this assumption, i.e. they may *not* be testable, even in principle.

Example B.4 (Limits of JCI like Ideas)**.**

(a) Consider two exogenous indicators C and C', such that both switch their value only once, i.e. there is a unique t with $C_{t+1} \neq C_t$ and a unique t' with $C'_{t+1} \neq C'_t$. How could we test $C \perp\!\!\!\perp C'$? We could compare the distance $|t - t'|$ to the total number N of data points. If switches of C and C' are independent and uniform ($t \sim \text{Unif}(\{0, \dots, N-1\})$) and always occur precisely once, then we can control errors at α if we reject independence whenever $|t - t'| < \alpha N$. However, this requires a lot of assumptions, and depending on the alternative it may gain power slowly or never with increasing N.

(b) If we assume (as for JCI) that contexts are exogenous (thus pairwise independent), we never need to test $C \perp\!\!\!\perp C'|Z$ for any Z for causal discovery. Consider the following simple model: $X \to Y \to Z$ with both R_{XY}^{model} and R_{YZ}^{model} non-trivial (corresponding to C_{XY} and C_{YZ}). The argument of the previous example B.3 works for the link $X \to Y$, because both indicators are independent of X. But to orient the link $Y \to Z$, we have to figure out that $C_{YZ} \perp\!\!\!\perp Y$. However, this pairwise test may be difficult: We know that $C_{XY} \not\perp\!\!\!\perp Y$, if dependence were transitive, then the combination of both tests would show $C_{YZ} \perp\!\!\!\perp C_{XY}$ (which is not testable by (a)). Now, dependence is *not* transitive, but in our case indicators are binary and contain very little information, so for most models in practice (like $Y = X \times C_{XY} + \eta_Y$ and $Z = Y \times C_{YZ} + \eta_Z$) this conclusion would hold.

(c) The problem from (b) actually *can* be reasonably resolved: While $C_{YZ} \not\perp\!\!\!\perp Y$ may not be testable, $C_{YZ} \not\perp\!\!\!\perp Y|C_{XY}$ (which would also be ok for CD), seems to be testable: For example assume (for simplicity) that there are few invalid blocks $\chi \approx 0$, then on blocks that are *above* a certain cutoff for the independence $X \perp\!\!\!\perp Y$ (associated to C_{XY}) and below a p-value of say α we will have about a fraction α of impurities (from $X \perp\!\!\!\perp Y$). Next, test the dependence between Y and C_{YZ}, discard the α highest values, and check if on the remaining blocks independence can still be rejected. Discarding

$\alpha + \chi_0$ values could even maintain error-control in a conventional sense up to $\chi \approx \chi_0$. This may not be a sample-efficient procedure, but it demonstrates that the problem is surprisingly accessible.

While part (c) indicates that some JCI-like conclusions can still be drawn, it may not always be obvious which tests have to be done. The problem in the example arises, because true independence with one indicator may be erroneously rejected due to the dependence on another indicator. This leads to a false positive, which in turn affects our interpretation of links out of contexts (which seems fine) but also the ability to orient links, because the collider at Z no longer is unshielded. For the simple example above, the next iteration(s) of most CD-algorithms would find the valid adjustment set C_{XY} (or any parents of Y blocking the influence of other contexts) to delete the link $C_{YZ} \to Y$ which then allows for subsequent orientation of $Y \to Z$. It is, however, not entirely clear if a suitable adjustment set always exists and is always found by a classical CD-algorithm. In any case, a suitable test (comparable to part (c) of the previous example) is required. Hence the details on a systematic study of JCI-like techniques for orienting links based on detected indicators is left to future work. This is also related to §F.10.1 and §F.10.4.

B.8   Lookup Regions

Sometimes, we need to be able to abstractly reason about the "sparsity of lookups" involved in the efficient algorithmic computation of a CD mapping from independence-structures to graphs (see §3.4). The following simple formalized version will often suffice for this purpose; note that we will never need to actually compute $\mathrm{L_{CD}}$.

Definition B.5 (Lookup Region)**.** The lookup region $\mathrm{L_{CD}}$ of an (abstract) constraint-based causal discovery algorithm CD is an algorithm-specific mapping of independence-structures IS to sets of multi-indices $I_{\mathrm{IS}} = \{\vec{i}_0, \dots, \vec{i}_M\} \subset I^{2+*}$

$$\mathrm{L_{CD}} : \mathcal{I} \to \mathrm{Subsets}(I^{2+*}), \mathrm{IS} \mapsto I_{\mathrm{IS}},$$

with the property

$$\mathrm{IS}\,|_{\mathrm{L_{CD}(IS)}} = \mathrm{IS'}\,|_{\mathrm{L_{CD}(IS)}} \quad \Rightarrow \quad \mathrm{CD(IS)} = \mathrm{CD(IS')}.$$

Remark B.6 (Lookup-Region Always Exists for Deterministic Algorithms)**.** Think for example of PC which will execute tests $\vec{i}_0$, then $\vec{i}_1$ etc. with the choice of later tests to execute depending on the results obtained on previous ones. These results on previous ones are formally encoded / supplied by a fixed independence-structure IS. After a finite number $M+1$ of tests the algorithm terminates. It will "look up" precisely the tests $I_{\mathrm{IS}} = \{\vec{i}_0, \dots, \vec{i}_M\}$ from IS. Since subsequent tests are chosen depending on results of previous tests, I_{IS} depends on IS. Finally, the algorithm of course decides its output based only on the tests it actually inspects, i.e. based on the restricted mapping $\mathrm{IS}\,|_{I_{\mathrm{IS}}}$.

The property $\mathrm{IS}\,|_{\mathrm{L_{CD}(IS)}} = \mathrm{IS'}\,|_{\mathrm{L_{CD}(IS)}} \quad \Rightarrow \quad \mathrm{CD(IS)} = \mathrm{CD(IS')}$ is an assumption on the formal mapping, but automatically satisfied if there is a deterministic algorithm implementing the mapping: This follows by induction. We assume the algorithm executes identically for IS and IS' with $\mathrm{IS}\,|_{\mathrm{L_{CD}(IS)}} = \mathrm{IS'}\,|_{\mathrm{L_{CD}(IS)}}$ up to step k (with $k = -1$ for the start of induction). The (deterministic) algorithm chooses a test $\vec{i}_{k+1}$ based on results obtained for tests $I_{\mathrm{IS}}^k = \{\vec{i}_0, \dots, \vec{i}_k\}$. For $k = -1$ (inductive start) $I_{\mathrm{IS}}^{-1} = \emptyset$ independently of IS, otherwise $I_{\mathrm{IS}}^k = I_{\mathrm{IS'}}^k$ by inductive hypothesis. Thus the (deterministic) choice $\vec{i}_{k+1}$ agrees for IS and IS'. In particular $\vec{i}_{k+1} \in I_{\mathrm{IS}}$, thus (by hypothesis) $\mathrm{IS}(\vec{i}_{k+1}) = \mathrm{IS'}(\vec{i}_{k+1})$ and the algorithm executes identically in step $k + 1$.

So any deterministic algorithm which terminates after a finite number of steps (this includes to our knowledge all constraint-based causal-discovery algorithms used in practice) always has a well-defined lookup-region in this sense.

Example B.7. In the skeleton-phase, the PC-algorithm checks first all pairwise independencies. Then (in the "stable" variant) it checks $X \perp\!\!\!\perp Y | Z$ if (and only if) Y is pairwise dependent to both X and Z. And so forth for increasing conditioning sets. In the oracle-case, given G, pairwise dependence occurs if and only if there is no d-separation given the empty-set. So for example for the graph $X \to Z \leftarrow Y$, in the oracle $X \perp\!\!\!\perp Y$, so that the only triples tested are $X \not\perp\!\!\!\perp Z | Y$ and $Y \not\perp\!\!\!\perp Z | X$. Thus $I_{\mathrm{IS_{oracle}}} = \{(X,Y), (X,Z), (Y,Z), (X,Z,(Y)), (Y,Z,(X))\}$ is the lookup-region for $\mathrm{PC_{skeleton}}$ and in particular $(X,Y,(Z)) \notin I_{\mathrm{IS_{oracle}}}$.

B.9   Indicator Resolution

One of the important novel conceptual ideas behind our approach was, to switch the order of (time-)resolution of indicators and graph-discovery. Albeit initially counter-intuitive, finding the causal graphs based on direct testing turns out to be both in theory and in numerical experiments better, than to first resolve indicators, then learn graphs per regime. This does of course not mean that we consider the resolution of indicators as functions of time (or any other parameter) not important, it simply becomes the second, rather than the first step. Indeed, also indicator resolution can benefit from this reordering: Having already discovered the causal graphs in the first step, we can now use this knowledge to guide our indicator-resolution.

Resolving (discrete in the global case, but not necessarily binary) indicators in a global approach has to solve a global (multi-variate) change-point detection (CPD) problem, then assign segments to regimes. Multi-variate change-point detection on finite data is a challenging task, mostly for the usual problems incurred by high-dimensional data. In our framework, we already know where to look for changes: In the general case, given a set of graphs, we need to find for example causal effects that are particularly well-suited to find the differences between any pair of graphs, then run CPD on these univariate problems. In the modular case (cf. §6), the results for different model-indicators are even mostly independent of each other (so it is enough to pick causal effects distinguishing the presence or absence of a model-indicator, for example the representor of §6).

While this means we have to solve multiple univariate CPD problems instead of a single multivariate one, the total number of change-points remains the same (see Fig. 1.2). If we imagine the concatenation of the time series for all univariate problems, then this is essentially a super-sampled (and thus easier) version of a single univariate problem with the original sample-count N and the same total number of change-points. So what we got in the end is arguably even (considerably, if there are many model-indicators) simpler than a single univariate CPD problem replacing the multivariate one!

Further, especially in the modular case, we also do not need a separate assignment of segments to regimes. Indeed the modular case can here also be efficiently represented, as there is simply one resolution per indicator (see Fig. 1.1). A simple representation (both formally and graphically) makes the result of our framework particularly easy to interpret. The tendency to produce high precision (and loosing primarily in recall for too small data-sets) on regime-detection (§7) further contributes to a comparatively easy-to-read output.

A very important, yet so far understudied, challenge to the resolution of regimes is the quantification of errors. The systematic simplification to binary indicators and univariate problems may make this problem more accessible for future work. Note, that in our case, there may be multiple, possibly to a sufficient degree independent, causal effects (or dependence-scores) associated to the same model-indicator. This could also provide information for consistency checks and error-estimation.

So while we do not, in this paper, study the problem of indicator resolution, our framework does in principle simplify this problem considerably.

B.10 Causal Models and Predictive Quality

Score-based methods like [4; 34] use a score (based on predictive quality of a model) directly while also constraint-based approaches like [55] usually revert to such a score for assigning data points to regimes. This requires fitting a model to data, which in the case of contemporaneous effects or IID-models, and especially in the presence of latent confounders can limit applicability in practice.

Model-fitting, but also our mCIT-testing approach are considerably more difficult to realize for non-linear models. There is an additional problem one has to consider: When is the causal model the best predictive (or best scoring) model? This is usually referred to as consistency of the score [11], and difficult to ensure beyond linear models with reasonable (e. g. curved exponential) noises [26]. Considering this, the question arises, to what degree regime-assignment by score is viable for non-linear models. A conclusive answer does not seem to be known, but a potential difficulty is illustrated by the following example:

Example B.8. We consider three nodes $X \to Y \to Z$, in regime (A), in regime (B) we add a link $X \to Z$. Let the dependence of Y on X be by some (potentially complicated) function f, and of Z on Y by some (potentially complicated) $g \approx \alpha f^{-1}$, such that $g \circ f(x) \approx \alpha x$. Further, for the direct dependence in regime (B) of Z on X also choose a simple (for example linear) function $h(x) = \beta x$. If we fit models to both regimes respectively, we have to be aware that non-parametric regressors will not converge uniformly on the function-space, thus the approximation of f and g may be much worse than the approximation of h. If $\alpha \approx \beta$ and both are considerably smaller than the (large) variance of $\hat{f}$ and $\hat{g}$, then there seems to be a rather high risk that the model from regime (B) has better predictive quality on segments or neighborhoods of change points of regime (A) than the correct model, which could lead to considerable instability, for example in sliding change-points during an optimization-step.

B.11 Score-Based Methods

Our framework is formulated specifically for constraint-based methods and via a modification of the independence structure. In practice, most score-based causal discovery approaches use a local notion of consistency for (typically also local) scores. For example in the very influential [11, Def. 6] defines local consistency in a way that asymptotically is equivalent to conditional independence-testing. Indeed the notion of correctness in our Thm. 2 should be suitable as a "marked" local consistency statement. Thus it should be possible to employ score-based technology with our framework as well. We have not studied this possibility in detail.

C Details on Models and Data-Generation

Statistical modeling and data-generation for numerical experiments usually consists of two stages: A prior distribution describes the probability for the occurrence of a particular set of true parameters (for example linear coefficients) defining a stochastic model. This stochastic model then describes the probability of obtaining a specific data-set. Data-generation for numerical experiments or benchmarking follows the same pattern; for this reason we incorporate many details of our data-generation into this section as examples for the more abstract probability theoretical and statistical ideas they seek to emulate.

The second step, the generation of a data-set from a model, typically has to employ assumptions about the reuse of model aspects to ultimately allow a meaningful statistical analysis. For example, it is often assumed that the data-generation is IID, in which case the distribution of a size N data-set is a N-fold product, where the model describes a factor and is reused for all samples. Similarly in the stationary case (for Markov-sequences), one usually assumes the existence of a model of the next time-step relative to few previous steps in the past, which is reused to successively generate the time series.

In the non-IID or non-stationary case, this symmetry is explicitly broken. Formally, this was approached in §3 as follows: All symmetry-broken information is by construction contained into (binary[13]) indicators, the remainder of the model can be reused across data points; this is also the reason why the parameters of this shared model can be subject to statistical treatment in a standard way.

For real world phenomena we seek to model, R itself is also random; at least it *should be modeled as random*, because it is not known a priori. Fixing the mapping $R(t)$ as part of the model in the second – data-generating – stage, puts the full burden of describing this *randomness* as part of the prior distribution over models. Conceptually this is fine, but we need a more fine-grained description of what this means for several reasons:

(1) The point-wise recovery of $R(t)$ is typically not possible from a single data-set, as this part of the model is not shared by multiple data points (see also §5.1). Instead we plan to recover in §5 information of the form: Is $R(t) \equiv$ const? In practice, we observe a finite number N data points, starting at some *arbitrary* point t_0 in time. It is possible that this might select a range of time-points where the restriction $R|_{[t_0,t_0+N)}$ is constant, while R is not (see reachable and reached states §3.5).

(2) Real-life phenomena often happen at some typical time-scale depending on the phenomenon. Indeed persistent non-stationarity is inherently a multi-scale problem. This should be modeled by a suitable model-prior. It is, however, not typically meaningful to try and reason on N (consecutive) discrete time-steps separated by Δt, about phenomena happening at time-scales τ with $\tau \ll \Delta t$ or $\tau \gg N\Delta t$, a restriction that is formally captured by the Nyquist–Shannon sampling theorem.

We find the following additional structure helpful to study these problems: We assume the prior distribution describes, *for each fixed N*, an "indicator meta-model" $\mathcal{R}_N$. This means, other than for example in the prior over linear coefficients, we explicitly allow for N-dependence of some aspects of the indicators; this seems to be necessary to accurately capture point (2), and provides interesting insights into convergence behavior. These indicator meta-models are formally binary random sequences, i.e. random-elements taking values in $\text{Map}(\mathbb{Z}, \{0,1\})$. We will call realizations $R \in \text{Map}(\mathbb{Z}, \{0,1\})$ unrestricted indicators. In the next step, given a random[14] starting time t_0, the restricted indicator $R|_{[t_0,t_0+N)}$ is simply a restriction of the mapping R. This restricted indicator can be used as indicator in a non-stationary SCM as described in §3.

Formally, this only factorizes what we previously called the first, or model-prior, stage: For a fixed N, instead of taking a single model from the prior, to than sample a single data-set of size N, the prior now describes probabilities of N-independent model information like linear coefficients and N-specific indicator meta-models $\mathcal{R}_N^{ij}$ for each pair of variables i, j and for this N. From each indicator meta-model we sample a single unrestricted indicator R_{ij} (for each i, j). Then we pick a single random t_0 and obtain a single restricted indicator $R|_{[t_0,t_0+N)}$. Finally we combine the N-independent model information like linear coefficients with the restricted indicators into a non-stationary SCM as described in §3. That is, the task and end-product remain the same, but we have subdivided the process in intermediate steps that (formally) record additional information, like the unrestricted indicators R_{ij}.

At this point, our description is already detailed enough that reachable and reached states are a simple and well-defined concept:

Definition C.1 (Formal Reachability)**.** For a model obtained by the procedure described above, we call the image $\text{img}(R_{ij}) \subset \{0,1\}$ reachable model-indicator values and the image $\text{img}(R_{ij}|_{[t_0,t_0+N)}) \subset \{0,1\}$ reached model-indicator values. We call a state $s \in S$ (Def. 3.9)

---

[13]The non-additive case Def. 3.7 can be treated more generally when including non-binary indicators, we focus on the binary case, however, for this treatment.

[14]The choice of prior over t_0 will not matter much, as we focus on stationary sequences $\mathcal{R}$, the core idea is that in principle multiple starting-points could be picked for the same unrestricted indicator R.

reachable, if its model-indicator values are reachable, and reached, if its model-indicator values are reached.

Further, the explicit N-dependence of $\mathcal{R}_N^{ij}$ leaves us with plenty of freedom to describe meaningful models and study interesting asymptotic behaviors.

The formulation above can easily be generalized from contiguous (uninterrupted) time series to more general data-sets, by replacing $t \in \mathbb{Z}$ by suitable indices $i \in I$ and restricting indicators to suitable random subsets of fixed size N rather than to intervals of size N. Nevertheless many of the relevant aspects can be most easily illustrated on the time series case with persistent over time regimes. For this reason, we will also discuss this special case in more detail, to than return to the general case with the time series results as examples to illustrate the more abstract description.

Notation C.2. In this section we will usually loosely state constructions of the form "sample XYZ from P_{XYZ}, then . . . ", where XYZ is some random element. This can of course be written down formally as plugging an element $\omega \in \Omega$ of the sample-space into the mapping XYZ to obtain an instance, then do subsequent constructions as compositions of mappings to obtain a suitable random-element in the end. This should not lead to confusion, but dramatically simplifies notation and makes it much easier to clearly lay out the underlying ideas.

C.1 Properties of Priors and Meta-Models

In principle, a model could have only few reachable states with potentially complicated transition patterns. Our priority at the moment is not the study of complicated state-machines but of the reconstruction of changing aspects of causal models. For causal models, it is believed that mechanisms typically change independently (cf. e. g. [43; 28]), a principle known as causal modularity. As laid out in the introduction §1, we want to prioritize such locally changing models. Formally this idea can be captured as follows.

Definition C.3 (Causal Modularity of Changes)**.** We say a prior describes models changing in a modular way (changing of order ≤ 1, see below), if the indicator meta-models $\mathcal{R}_{ij}$ are independent[15]. If the non-trivial (see Rmk. C.9) indicator meta-models can be assigned into sets with at most k elements each, such that any two such sets are (jointly) independent of each other, we say the prior describes models changing of order $\leq k$; of order k if k is minimal with this property. In particular a prior of stationary models (all indicators are trivial) is changing of order 0; a prior describes models that are changing, but in a modular way (see above) is changing of order 1.

Lemma C.4 (Modular Reachability)**.** *If a prior describes models changing in a modular way, then the states defined by Def. 3.9 are precisely the reachable (but not necessarily reached) states.*

Proof. This follows directly from Def. C.3, Def. C.1 and Def. 3.9. $\qquad\square$

Example C.5 (Data-Generation)**.** Most of our numerical experiments focus on the modular case. However, we do include some experiments specifically to study the effect of higher order changes (see Fig. 7.3). In these experiments all indicators are "synchronized" (i. e. the order is the total number of non-trivial indicators; indicators are not just dependent but deterministically related / agree up to "sign"). Together with experiments on the effect of the total number of (independent) indicators, this provides good insight into the effect of the order of changes.

For a fixed N, drawing a single data-set produces a single indicator (per link), so properties like the ratio χ of valid blocks for a given pattern (Def. 5.4), are well-defined *numbers*. But when we study the statistical power of our tests later on, we will be interested in the behavior under limits, thus for different N entailing different $\mathcal{R}_N$.

---

[15]While such independence is difficult to test (§B.7), there is no problem in formally assuming it.

Remark C.6. If the indicator meta-models are of the form $\mathcal{R}_N(t) = \bar{\mathcal{R}}(t/\Lambda(N))$, i.e. if the behavior for large N changes only by modifying the time-scale by a factor $\Lambda(N)$, this description can be retained, by using the same $\bar{\mathcal{R}}$ for all N. However, such a scaling behavior does not seem to be sufficiently expressive to capture realistic or interesting examples; it also comes with an entire host of new problems: For example $\bar{\mathcal{R}}$ should now be defined on the real numbers $\mathbb{R}$ for this notation to make sense. But going to large Λ effectively zooms into this the real axis, in particular it could reveal completely new behavior of the mapping $\bar{\mathcal{R}}$ on small scales. An exception is the case where $\Lambda(N) = \mathrm{const}$ (see "infinite duration limit", Def. C.22), but this limit turns out to be too challenging: By Prop. 5.12, it is typically not possible to achieve such convergence for weak-regime (and thus mCIT) tests. On the other hand, one can introduce a lower bound $\Delta t_{\min}$ on smallest structures in $\bar{\mathcal{R}}$, but this does not seem to lead to interesting insights (see Rmk. C.12).

Instead it seems to be easier to treat properties like χ_N as sequences of random variables.

Definition C.7 (Indicator Properties)**.** Recall the definition of a pattern in the sense of Def. 5.4: A pattern Patt is a mapping $\mathrm{Patt} : \mathbb{N} \to \mathcal{B}_I$ to collections $\mathrm{Patt}(b)$ of disjoint subsets $T_i \in \mathrm{Patt}(b)$ of T with individual size $|T_i| = b$.

Given an indicator $R : T \to \{0, 1\}$, a pattern Patt and a block-size b, there is a well-defined invalid-block-ratio χ (with R-validity of a block T_i defined in Def. 5.4 as $R|_{T_i} \equiv \mathrm{const}$)

$$\chi(R, \mathrm{Patt}, b) := \frac{|\{T_i \in \mathrm{Patt}(b) | T_i \text{ is not } R\text{-valid }\}|}{|\,\mathrm{Patt}(b)|}.$$

This property of individual indicators induces a random variable on indicator meta-models (technically we assume the following mapping is measurable, similar below)

$$\chi_N(\mathcal{R}, \mathrm{Patt}, b) : \Omega \to [0, 1], \omega \mapsto \chi(\mathcal{R}_N(\omega), \mathrm{Patt}, b).$$

Analogously we can define a fraction A of valid independent blocks (with corresponding induced random variables)

$$A(R, \mathrm{Patt}, b) := \frac{|\{T_i \in \mathrm{Patt}(b) | R|_{T_i} \equiv 0\}|}{|\,\mathrm{Patt}(b)|},$$

$$A_N(\mathcal{R}, \mathrm{Patt}, b) : \Omega \to [0, 1], \omega \mapsto A(\mathcal{R}_N(\omega), \mathrm{Patt}, b).$$

We will sometimes allow $b = b(N)$ to depend on N, which similarly induces random variables χ_N and A_N.

We will later often consider limits where $\chi \to 0$, so the following property is useful:

Lemma C.8 (Relating A to χ)**.** *Given the (true) regime-fraction a,*

$$a - \chi \leq A \leq a$$

Proof. $A \leq a$ is clear from its definition. There are at most $\chi|\,\mathrm{Patt}(b)|$ invalid blocks, thus at most $\chi|\,\mathrm{Patt}(b)|b = \chi N$ data points contained within any invalid block. There are aN data points in the independent regime in total, thus at least $(a - \chi)N$ data points in valid blocks. These are $(a - \chi)|\,\mathrm{Patt}(b)|$ many, such that indeed $A \geq a - \chi$. $\qquad\square$

We will treat the regime-fraction a as a regular model-parameter (i.e. the same way we treat for example linear coefficients). It would of course be possible to treat a (or any other parameters) as N-dependent as well, however, in practice this does not seem to lead to substantial insights. Hence we restrict the N-dependent treatment to the aspects (in particular χ) of the indicator-modeling that seem to be required (see introduction to this §C) to keep things as simple as reasonable.

Notation C.9. We will also consider the triviality-property (constness) of model-indicators as logically N-independent. This is formally not a problem: Even if $\mathcal{R}_N$ may produce a non-trivial unrestricted or restricted indicator R only with a certain probability $p_{ij} \neq 0, 1$, we can always rewrite it as a "structural" prior (describing the causal graph and non-triviality of model-indicators) with a an additional parameter p_{ij} for each link and a logically decoupled description of a non-trivial indicator meta-model (for example the original meta-model conditioned on this property being true) only to be invoked in case a *non-trivial* indicator would be encountered based on the roll on p_{ij}. This is the same as factoring

$$P(\mathcal{R}) = P(\mathcal{R}|R \text{ non-trivial})P(R \text{ trivial} = \text{false}) + P(\mathcal{R}|R \text{ trivial})P(R \text{ trivial} = \text{true}),$$

where $P(\mathcal{R}|R \text{ trivial})$ is binary (it only decides if R is trivially dependent or independent) and $P(R \text{ trivial})$ is binary, so all the interesting structure is in $P(\mathcal{R}|R \text{ non-trivial})$. Triviality can refer to both the restricted or unrestricted indicator, we will for simplicity focus on the non-triviality of the restricted indicator. For the remainder of this section we consider only non-trivial indicator meta-models in isolation.

Example C.10 (Data-Generation). Our data-generation includes a sanity-check for non-triviality of generated indicators. This does not guarantee reachedness of all *states*, but together with reasonable maximal regime-lengths and modular changes, it provides sufficiently reached states for statistical analysis of our (and other) method(s).

C.2   Statistical Testing

Conventionally, statistical tests are considered consistent if they control false-positive rate and gain power asymptotically point-wise on the support of the prior. Here, point-wise, means for example when testing independence, for any model satisfying the null hypothesis the error-rate is controlled and that for every $\epsilon > 0$ and for every individual model satisfying the alternative hypothesis (with true dependence value $d_1 \neq 0$; a point in the space of possible alternative hypotheses), there is a N_0 such that $\forall N \geq N_0$ the test will have power at least $1 - \epsilon$ on samples of size N on this alternative.

As already noted before (see Rmk. C.6), a definition of point-wise that is both meaningful and achievable in terms of controlling false-positives point-wise is difficult to achieve (for details see §D). At the same time, note that gaining power point-wise can be too weak for our use-case for the following subtle reason: From a practical viewpoint, we want our test to gain power in a Bayesian sense on an unknown (thus optimally on any "reasonable") prior, that is drawing an alternative at random from this prior and using the point-wise power as likelihood of a correct detection, we want the posterior probability of a correct detection to approach 1. If the model-prior is independent of N, than this follows from the point-wise property for example under reasonable continuity assumptions. However, generally, the pointwise existence of $N(\epsilon)$ may not be sufficiently uniform, the Bayesian criterion would require that the prior-weighted integral of pointwise values of $N(\epsilon)$ (i.e. the expectation value $E[N(\epsilon)]$) does not diverge, which may not be the case.

In our case, the prior changes with N. Indeed, it changes *critically* with N: By Prop. 5.12, it is not possible to achieve convergence in an infinite duration limit (for the weak-regime test), yet we will show that under plausible assumptions on the prior, convergence in a Bayesian sense *is possible*. Why this is the case, will become much clearer on the example of persistent-in-time regimes §C.3 below (see Rmk. C.27). In the end, what we show is that our mCIT implementation is asymptotically correct in the following "weak[16] Bayesian" sense:

Definition C.11 (Asymptotic Correctness). Let $\{\hat{T}_N\}_{N \in \mathbb{N}}$ be a family statistical tests of hypothesis T. We formally allow T to take a finite number (possibly ≥ 2, e.g. the mCIT has

---

[16]We call this notion of correctness 'weak', because it does not provide finite-sample error-guarantees, which would require a point-wise guarantee.

$T \in \{0, 1, R\}$) of values. We say $\hat{T}_N$ is weakly asymptotically correct under the indicator meta-model $\mathcal{R}_N$, if for any (fixed) parameters $\theta = (d_0, d_1, a, \dots)$

$$\lim_{N \to \infty} P_\theta\big(\hat{T}_N(D_N) = T(R|_N, \theta)\big) = 1,$$

where $R|_N$ is the restricted indicator of length N and D_N the corresponding data-set of size N. Thus N-independent parameters θ are fixed (point-wise), but convergence over the N-dependent indicator meta-model $\mathcal{R}_N$ is in a Bayesian sense. The hypothesis T depends on the non-stationary SCM (Def. 3.4 / 3.7), thus on $R|_N$ and θ; for example it can be a marked independence (Def. 5.9; Is $R|_N$ trivial, and is $d_0 = 0$?).

Remark C.12. One of the reasons, why we do not restrict ourselves to much simpler meta-models of the form $\mathcal{R}_N(t) = \bar{\mathcal{R}}(t/\Lambda(N))$ (see Rmk. C.6) is that it does not seem to be informative here. For example in the CPD literature, assuming an infinite sampling limit (define R on an interval, for example $[0,1]$ with some smallest structure for example $\Delta t_{\min}$, then subdivide into N equal steps) is quite common. This is often reasonable to achieve a goal like the correct discovery of *all* change-points, where in practice the number of change-points cannot arbitrarily increase with N in order to be achievable. Our goal ("Is the indicator constant?") also gets more difficult to achieve if the number of change-points increases, but is much more tolerant to errors on individuals ones. In practice this means that an infinite-sampling limit is not informative: Writing down any plausible method, we find convergence in this limit for arbitrary plausible hyperparameters. Thus this notion of convergence does not inform us about which method or hyperparameters are a *good* choice. Note, that our results *do* also hold in this simpler case, cf. Example. C.23 and Cor. D.45.

C.3   Persistent-In-Time Regimes

We start with an exemplary treatment of persistent-in-time regimes. This will shed light both on the potential form of indicator meta-models, and on the intuition behind what makes the test-specification Def. C.11 accessible. For our present purposes, we take persistent-in-time regimes to mean the applicability of the time-aligned pattern of the main text, recall:

Example 5.5 (Time-Aligned Blocks)**.** The time-aligned pattern is the subdivision of $I = T = [0, N) \cap \mathbb{Z}$ into size B blocks of the form $b_\tau = [\tau B, (\tau + 1)B) \subset T$ with $\tau \in [0, \Theta) \cap \mathbb{Z}$.

Persistent non-stationarity as discussed here is inherently a multi-scale problem. There is some process driving regimes that happens at larger time-scales than the primarily modeled problem. For most realistic scenarios such a regime-driving process will itself have its typical time-scale. For example daily climate data may feature regimes driven by weather phenomena happening at a weekly scale, by El Niño like effects happening over months or years, by climate change happening over decades etc. For each phenomenon individually the assumption of IID segment-lengths may be plausible and useful. But with typical segment-lengths substantially different for different regime-driving phenomena, we get a more concrete version of the point (2) at the beginning of §C: We have to distinguish between a "random" indicator *before* fixing a phenomenon (thus length-scale), in our formalism $\mathcal{R}_N$, compared to a "random" indicator *after* fixing a phenomenon (thus length-scale), in our formalism the choice of t_0 and were to restrict R.

Remark C.13 (Exchangeability)**.** Formally this means, we replace the basic idea of IID segment-lengths by exchangeable segment lengths. If "choosing a typical length-scale" is modeled in a sufficiently expressive way (as a random measure describing the length distribution for this phenomenon), then randomizing first length-scale, then IID segment lengths per scale is by de Finetti's theorem precisely the same as allowing exchangeable segment lengths in the indicator meta-model.

Notation C.14. In the exchangeable case (Rmk. C.13), the distribution over the lengths of segments (intervals with R taking the same value, and maximal with this property) do

not depend on the absolute value of t, so there are random variables $L_\pm$ with these laws (dependent '+' for dependent, '−' for independent). We will for the persistent-in-time case focus on such exchangeable models and switch between the encoding as $\mathcal{R}$ and $\mathcal{L}$. We denote the exchangeable meta-model as $\mathcal{L}$ and the IID (see Rmk. C.13) "instance model" (after drawing a length-scale) as L.

C.3.1 Indicator Meta-Model for Temporal Regimes

There are many plausible models for the indicator meta-model. One typically attempts to rely on few simple properties of the prior (here: the indicator meta-model), such that conclusions are likely to apply to actual (unknown) priors. Further we want to understand how to formulate an "uninformative" prior, a model, for the case where we do not know anything special about the regime-length distributions, i.e. a prior to express our lack of knowledge; this is relevant especially for numerical experiments. We focus on structures similar to the following one:

Example C.15 (Data-Generation)**.** Let the scale $S \sim \mathcal{N}(\log(\ell), \gamma)$, then we call

$$L = \exp(S)$$

the scale-normal length-distribution at ℓ of width γ. Note, that S has median $\log(\ell)$ and exp is a strictly monotonic function, thus L has median ℓ.

We define a meta-model – a model providing a model for length-distributions in form of a random variable L – with parameters A, B and γ as follows: Let $\log(\ell) \sim \mathrm{Unif}(\log(A), \log(B))$ and the resulting model (random length-scale L) is the scale-normal length-distribution at ℓ of width γ. In principle, it may make sense to have separate length-scales ℓ_+ and ℓ_- for segments in the dependent and independent regime respectively. In practice, a large discrepancy, e.g. $\ell_+ \gg \ell_-$, leads to very imbalanced data-sets ($a \approx 0$ or $a \approx 1$), a challenge which we leave to future work.

In our numerical experiments we typically use this meta-model together with $A = 5$, $B = {}^N\!/2$ and a fixed value $\gamma \approx 0.3$. Instead of separate scales ℓ_+ and ℓ_-, we use a single scale and a uniform at random imbalance (approximately, $a \sim \mathrm{Unif}(0.15, 0.85)$) to slightly modify ℓ_+ vs. ℓ_-.

For the numerical experiments of the full (causal discovery) method (§7), the lower bound was increased to $A = 200$ to make the baselines used for comparison more applicable. Our method seems to be comparatively stable also for lower regime-sizes, see Fig. 7.4 and Fig. A.7.

The most important aspect here is that the meta-model first fixes a typical time-scale ℓ for each indicator. Each indicator individually will then contain segments of similar scale. We will consider an indicator meta-model "uninformative" if ℓ is distributed uniformly across scales. For true multi-scale problems this seems to be a plausible choice. We first need a formal convention for what "typical scale" will mean on arbitrary priors:

Definition C.16 (Typical Regime-Length)**.** For a random (segment-length) variable L we define the typical regime-length ℓ as the median $\ell = \mathrm{median}(L)$.

Then we can already formalize what we mean by an uninformative prior:

Definition C.17 (Uninformative Prior)**.** We call a meta-model for L (inducing $\mathcal{R}$) an uninformative prior if the typical segment-size $\ell_N := \mathrm{median}(L_N)$ is distributed uniformly across *scales* between a single sample and the sample size N, i.e. if $\log(\ell_N) \sim \mathrm{Unif}(0, \log(N))$.

Example C.18 (Data-Generation)**.** The data-generation as described above (example C.15) is not in a strict sense uninformative in this sense (because it disregards length-scales that are too small or too large for stable numerical experiments), but especially for large N it is a very good approximation of an uninformative prior in this sense.

This does not imply any specific model for L, and indeed no such specific model will be needed for theoretical results; this is due to the median entailing a lower bound on valid blocks with increasing certainty for increasing block-size, see also (proof of) Lemma C.26.

Lemma C.19 (Median-Limited Switch-Frequency)**.** *Given $N = b\Theta$ data points, and $\mathcal{R}$ with regime segment lengths L and median $\ell = \text{median}(L)$, such that the law of L is non-singular at ℓ. For $\epsilon > 0$, there is Θ_0 such that $\forall \Theta \geq \Theta_0$, the regime changes at most $\frac{2N}{\ell - \epsilon}$ times (i. e. there are at most $\frac{2N}{\ell - \epsilon}$ values $t \in T$ with $R(t+1) \neq R(t)$) with probability at least $1 - \epsilon$.*

Proof. This is a simple application of Markov's inequality which states that for any non-negative random variable X and any $t > 0$, the inequality $P(X \geq t) \leq \frac{E[X]}{t}$ is satisfied. $X = L$ is clearly non-negative, thus for $t = \ell$ the (true) median, the left-hand-side $P(L \geq \ell) = \frac{1}{2}$ (by non-singularity at this point). The right-hand-side is $\frac{E[L]}{\ell}$ and thus $E[L]$ is at least

$$E[L] \geq \frac{\ell}{2}.$$

In particular the mean $\bar{L}$ eventually (beyond some Θ_0) is larger $\frac{\ell - \epsilon}{2}$ with probability at least $1 - \epsilon$ by CLT. Note that the number of switches s (the number of values $t \in T$ with $R(t+1) \neq R(t)$) is

$$s = \frac{N}{\bar{L}} - 1 \leq \frac{2N}{\ell - \epsilon} \text{ with probability at least } 1 - \epsilon.$$

$\square$

C.3.2 Asymptotic Limits

As the total sample-size N grows, asymptotic properties strongly depend on the behavior of "typical" segment-sizes ℓ relative to N. We will classify limits by their relative growth rates. We fix an indicator meta-model $\mathcal{R}$. First recall the following standard definition:

Definition C.20 (Stochastic Ordering)**.** Given two real-valued random variables A and B, then A is stochastically less than B, denoted $A \preceq B$, if the cdf is pointwise less

$$A \preceq B \quad :\Leftrightarrow \quad \forall x \in \mathbb{R} : \Pr(A > x) \leq \Pr(B > x),$$

and similar for strict versions (replace $\preceq$ and $\leq$ by $\prec$ and $<$).

Example C.21. If $X \sim \mathcal{N}(\mu_X, \sigma^2)$ and $Y \sim \mathcal{N}(\mu_Y, \sigma^2)$ with the same variance parameter σ^2, then $X \preceq Y \Leftrightarrow \mu_X \leq \mu_Y$.

For persistent-in-time regimes specifically we use the following preliminary (for the general case, see §C.4) notion

Definition C.22 (Asymptotic Limits, Temporal Case)**.** We say regimes grow at least Λ-uniformly for a length-scale $\Lambda : \mathbb{N} \to \mathbb{R}$ if ℓ is bounded and Λ-decreasing in the sense that there are $N_0 \in \mathbb{N}$, C with $\Pr(\frac{\ell_{\pm}(N_0)}{\Lambda(N_0)} < C) > 1 - \epsilon$ and

$$N < N' \quad \Rightarrow \quad \frac{\ell_{\pm}(N)}{\Lambda(N)} \preceq \frac{\ell_{\pm}(N')}{\Lambda(N')}.$$

We will additionally require that any length-scale Λ is monotonically growing and such that $\Lambda(N) \leq N$. We say regimes grow at least Λ-uniformly eventually, if there is N_0' such that the implication above holds for $N, N' \geq N_0'$.

Example C.23 (Trivial Scaling)**.** If $\mathcal{R}_N(t) = \bar{\mathcal{R}}(t/\Lambda(N))$ for $\bar{\mathcal{R}} : \mathbb{R} \to \{0, 1\}$ with lower bound $\Delta t_{\min}$ on smallest structures, then regimes grow at least Λ-uniformly, because $\frac{L_{\pm}(N)}{\Lambda(N)} = \frac{L_{\pm}(N')}{\Lambda(N')}$, thus $\frac{\ell_{\pm}(N)}{\Lambda(N)} = \frac{\ell_{\pm}(N')}{\Lambda(N')}$.

Example C.24. Some intuitive examples are:

(a) $\Lambda_\gamma(N) = N^\gamma$ is a simple but often useful choice.

(b) $\Lambda(N) = N$ (or $\gamma = 1$): This is an "infinite sampling limit", where the regime-structure is (essentially) fixed on a finite interval (say $[0, 1]$), and for increasing N the time-steps are chosen as $\Delta t = 1/N - 1$. This limit is often considered for CPD consistency.

(c) $\Lambda(N) = \text{const}$ (or $\gamma = 0$): This is an "infinite duration limit", where the same system for increasing N runs for a time proportional N effectively appending new samples with the same regime-structure. This limit captures most finite sample properties.

This scaling information can be employed as sufficient condition to ensure validity of most blocks, in the sense of $\chi \to 0$:

Lemma C.25 (Relative Asymptotic Block-Size). *If regimes grow at least Λ-uniformly eventually for a length-scale $\Lambda : \mathbb{N} \to \mathbb{R}$ and $\frac{B(N)}{\Lambda(N)} \to 0$ then, in probability*

$$\frac{B(N)}{\ell(N)} \xrightarrow{\text{P}} 0.$$

Proof. Let $\epsilon > 0$ be arbitrary. By definition (Def. C.22), there are $N_0 \in \mathbb{N}$, C with $\Pr(\frac{\ell_\pm(N_0)}{\Lambda(N_0)} < C) > 1 - \epsilon$. With $N < N' \Rightarrow \frac{\ell_\pm(N)}{\Lambda(N)} \preceq \frac{\ell_\pm(N')}{\Lambda(N')}$ (again by Def. C.22), this remains true for all $N \geq N_0$.

By $\frac{B(N)}{\Lambda(N)} \to 0$, there is N_1 such that $\forall N \geq N_1$, $\frac{B(N)}{\Lambda(N)} < \frac{\epsilon}{C}$, thus for $N \geq \max(N_0, N_1)$, with probability at least $1 - \epsilon$,

$$\frac{B(N)}{\ell(N)} = \frac{B(N)}{\Lambda(N)} \times \frac{\Lambda(N)}{\ell(N)} < \frac{\epsilon}{C} \times C = \epsilon.$$

$\square$

Lemma C.26 (Sufficient Growth Implies Asymptotic Validity). *If regimes grow at least Λ-uniformly for a length-scale $\Lambda : \mathbb{N} \to \mathbb{R}$ and $\frac{B(N)}{\Lambda(N)} \to 0$ then*

$$\chi(B(N)) \xrightarrow{\text{P}} 0.$$

Proof. Let $\epsilon > 0$ be arbitrary. There are at most as many invalid blocks as regime-switches s, that is $\chi(N) \leq \frac{s(N) \times B(N)}{N}$. Thus it is enough to show $s \frac{B(N)}{N} \xrightarrow{\text{P}} 0$. With $\frac{B(N)}{\Lambda(N)} \to 0$ by hypothesis and $\Lambda(N) \leq N$ by definition (Def. C.22), the relative size of blocks $\frac{B(N)}{N} \to 0$ and the number of blocks $\Theta(N) = \lfloor \frac{N}{B(N)} \rfloor \to \infty$ approaches infinity. With $\Theta(N) \to \infty$, we eventually have $s \leq \frac{2N}{\ell} + \epsilon N$ with probability at least $1 - 1/2\epsilon$ by Lemma C.19. We get $\chi(B(N)) \leq (\frac{2N}{\ell} + \epsilon N)\frac{B(N)}{N}$ with probability at least $1 - \frac{\epsilon}{2}$. Applying Lemma C.25, we get $\frac{B(N)}{\ell} < \frac{\epsilon}{4}$ with probability at least $1 - \frac{\epsilon}{4}$ eventually. Thus eventually with probability greater $1 - \epsilon$

$$\chi(B(N)) \leq \frac{\epsilon}{2} + \epsilon \frac{B(N)}{N},$$

and by $\frac{B(N)}{N} \to 0$ (see above) eventually $\chi(B(N)) < \epsilon$ with probability greater $1 - \epsilon$. $\square$

Remark C.27. Essentially these arguments work, because error-rates ϵ can be split such that with probability $1 - \frac{\epsilon}{2}$ the setup is "benign" in the sense that regimes are at least of typical size $\propto \Lambda$, while giving up on the remaining setups (occurring with prior probability $\leq \frac{\epsilon}{2}$). Then on these benign setups error-rates are uniformly reduced below $\frac{\epsilon}{2}$. Combining both error-types leads to an error-rate of less than ϵ in a Bayesian sense, but without uniform pointwise guarantees.

Uninformative priors in the previous sense have scales growing logarithmically.

Lemma C.28 (Logarithmic Growth of Uninformative Temporal Regimes)**.** *Let* $\mathcal{R}_N$ *be an uninformative prior (Def. C.17), and* $\Lambda(N)$ *such that* $\frac{\Lambda(N)}{\log(N)} \to 0$, *then segments of* $\mathcal{R}_N$ *grow at least* Λ-*uniformly eventually.*

Proof. By Def. C.17, $\log(\ell_N) \sim \mathrm{Unif}(0, \log(N))$, in particular Def. C.22 is satisfied for Λ satisfying the hypothesis. □

C.4 General Pattern Applicability

For more general patterns, like multi-dimensional spatio-temporal ones, manifolds beyond the $\mathbb{R}^n$, periodicity or neighborhoods in graphs / networks the "applicability" of a pattern is hard to capture geometrically (cf. typical lengths ℓ above). However, the previous subsection showed, how temporal persistence as a simple type of pattern is compatible with certain limits and uninformative model-priors in the sense of ensuring useful behaviors of invalid block rates χ in the asymptotic limit (and similarly for valid independent blocks $A \to a$ by Lemma C.8). This information will turn out to be sufficient to assess the applicability of mCIT tests (§D). It therefore makes sense to elevate these properties to the status of a definition for the general case.

Definition C.29 (Pattern Compatibility)**.** Let $\Lambda : \mathbb{N} \to \mathbb{R}$ be a scale (see Def. C.22). A pattern Patt is asymptotically Λ compatible with an indicator meta-model $\mathcal{R}$ if for all $B(N)$ with $\frac{B(N)}{\Lambda(N)} \to 0$, for $N \to \infty$

$$\chi_{\mathcal{R}}(\mathrm{Patt}, B(N)) \xrightarrow{\mathrm{P}} 0.$$

Example C.30. A time-aligned pattern (example 5.5) is asymptotically Λ compatible with any meta-model whose regimes grow at least Λ-uniformly in the sense of Def. C.22. This result was formally shown as Lemma C.26.

A persistent-in-time pattern is asymptotically Λ compatible with the uninformative prior of Def. C.17, if $\frac{\Lambda(N)}{\log(N)} \to 0$. This follows from Lemma C.28 via Lemma C.26.

C.5 Data Generation for Numerical Experiments

Here we summarize how our data-generation integrates the indicator meta-models discussed above with random graphs and mechanism / noises into non-stationary SCMs in the sense of Def. 3.4.

C.5.1 Causal Graph

In our numerical experiments, we usually first generate a DAG. In the IID case this DAG will become the union-graph. In the time series case it will become the the union-summary-graph (see §C.5.3).

We generate the DAG with causal-order equal to index-order (i. e. ancestors are always lower index, descendants always higher index), a random causal order is generated in the very end to permute the resulting data. This is equivalent to generating a random causal order in the beginning but, easier to implement and thus less error-prone.

For each node, up to `max_parents_per_node` parents are drawn (uniformly, see below) from the possible ancestors (nodes of lower index) for each node. Depending on the requirements of the setup, for example the density of links `target_density` (number of actual links relative to number of possible links in a DAG of equal node-count, disregarding `max_parents_per_node`) or an average number of links per node `average_links_per_node` is fixed in advance; this fixes a number of requested links. We then analyze how many links *could* at most be included while still satisfying the requirement of at most `max_parents_per_node` parents per node (nodes of low index have less than `max_parents_per_node` possible

ancestors). From the set of these "legal slots" for parents we then draw a random subset of size equal to the number of requested links (see above). Finally we fill these selected "legal slots" with respectively valid parents (valid here means "of lower index", ensuring a consistent causal total ordering, thus a DAG).

This allows to draw DAGs with available slots for parents populated uniformly (in a reasonable sense), while also providing direct control over high-level parameters like `max_parents_per_node` and `target_density` or `average_links_per_node`.

C.5.2 Changing Links

All our experiments use a fixed in advance number of changing links. This number is known to the clustering and Regime-PCMCI algorithms (which need this information), but hidden from our method (which does not need this information, and in its current form also cannot exploit this information if known). In the sliding window case, the number of changing links is hidden from the method at runtime, but with hyperparameters chosen a posteriori (see §7.1), it is effectively known (at least in part).

This fixed number of links is picked uniform at random among all (non-autolag in the time series case §C.5.3) edges, see also §C.5.1. To these randomly chosen links, a non-trivial indicator is assigned. Non-trivial indicators are generated as described in detail in example C.15: For each changing link individually, a typical length-scale ℓ between the fixed parameters $\ell_{\min}$ and $\ell_{\max}$ is sampled log-uniformly. Then the random-segment-lengths for this indicator are drawn at random but on this scale ℓ (see example C.15). The initial (starting at $t = 0$) segment-length is multiplied by a uniform at random number $\sim \mathrm{Unif}(0,1)$ (as this segment may have started in the past). Indicators on different links are drawn independently. We employ a sanity-check that tests if the drawn indicator happens to be constant by coincidence. If this (or any other sanity-check) fails, data-generation is restarted (this happens extremely rarely; so while this happens more often for very large ℓ, it does not measurably affect the distribution of ℓ). We modify resulting segment-lengths according to a regime-fraction target a, by multiplying lengths of independent segments by $2a$, dependent segments by $2(1-a)$ (for example if $a = \frac{1}{2}$, all segment lengths remain unchanged). The true regime-fraction A may not be the same as the target a by randomness of segment-lengths. a itself is randomized per indicator, typically (approximately) $a \sim \mathrm{Unif}(0.2, 0.8)$ for the sub-system experiments in §D and $a \sim \mathrm{Unif}(0.3, 0.7)$ for integrated experiments in §7 and §A.

Changing links are taken into account by the actual data-generating SCM as specified by Def. 3.4. Currently our data-generation starts all regimes in the dependent states, but other conventions do not seem to change the observed behavior.

To ensure stable applicability of all methods, the minimum typical **regime-length is picked large** $\ell_{\min} = 200$ for time series experiments. The exception to this rule is Fig. 7.4 where on the x-axis different typical regime-sizes are shown. To make results immediately comparable, this convention also applies to the IID-case, again a detailed analysis of smaller typical regime-sizes is given in §A.6.

C.5.3 Time Series

We use a DAG as union-summary-graph. Generally the summary graph would not have to be acyclic. Even with the current implementation of the state-space construction §6, which requires an acyclic union-graph, only the *window*-union-graph as to be acyclic. We opted to run time series experiments with DAGs for summary-graphs, because otherwise (in the presence of time-resolved feedback-loops) the models tend to become less stable. This is in principle an interesting problem in itself, but not the primary subject of study here. Using union-summary-DAGs avoids the mingling of regime-dependent behavior (the primary interest of this paper) and such stability problems.

The union-summary-graph is supplemented by additional auto-lag edges: In the shown experiments, each variable has a (lag 1) auto-dependence with probability 0.5.

Our time series experiments use $\tau_{\min} = \tau_{\max} = 1$. The value $\tau_{\min} \geq 1$ is required for comparison with Regime-PCMCI [55]. The value of $\tau_{\max}$ could be varied, the resulting effect is very similar to increasing the number of nodes (in steps of the number of variables) while simultaneously changing link-densities and (effective) noise distributions. We instead included a detailed study of the dependence on node-counts (§A.4, in steps of 1), noises (§A.7) and link-densities(§A.5) individually, which allows us to analyze the individual behaviors in a decoupled and transparent way.

Time series data is generated with a burn-in period of 150 time-steps with the model residing (for these 150 time-steps) in the initial state (where data-generation proper will begin). The used models do not feature feed-back loops (see above) or very large auto-lags, thus they approach the stationary distributions (of the current regime) comparatively quickly. After 150 time-steps the initial time-step is effective sampled from the stationary distribution of the initial regime. All typical time-scales ℓ (see §C.5.2) should similarly be large compared to the typical approach to stationarity within each regime, so the choice of picking the initial data point (via burn-in) from a stationary distribution is reasonable.

C.5.4 Noises

Most of our experiments use standard-normal noises for simplicity. The effect of different noises is studied in detail in §A.7.

C.5.5 Mechanisms

We focus on linear models. Coefficients are drawn log-uniform, typically between 0.2 and 5.0 for the sub-system experiments in §D, between 0.5 and 1.0 for integrated experiments in §7 on time series (to avoid instabilities; auto-lags are drawn as all other effects) and for §A (even though in §A.7 the scale of noises is varied, which for IID-models effectively also explores different effect-scales). The sign of each effect is drawn by a fair coin-flip.

For evaluating mCITs on weak regimes in §D, the independent regime is replaced by a weak regime with effect-strength $\sim \mathrm{Unif}(0.1, 0.9)$ times the effect strength in the dependent regime, with independently randomized sign. Conditional test setups in this case inject a random number of mediators and confounders summing up to a fixed total number $|Z|$. Noise on the confounders and mediators is normal with σ log-uniform between 0.1 and 5.0. Effects involved with these mediators and confounders are drawn as described above with one exception: For mediators, the correlation with the source X is bounded to 0.75 (if it is higher than this value, the variance of the noise on the mediator is increased to reduce the correlation to 0.75). The reason for doing so is that if the mediator M is too good a proxy for the value of X the independence-testing becomes extremely noisy (this is not just a problem of our mCIT, it happens for CITs in general). This happens reasonably rarely, and our setup still seems to be very challenging and informative.

C.5.6 Integrated Scenarios

With the different numerical experiments presented in §7 and §A, we seek to explore across various data-generation parameters explicitly while keeping the other ones fixed. The used system configurations are summarized in Tab. C.1.

We did not enforce a target run count for experiments, instead we allocated a fixed total runtime for each experiment, potentially appending runtime if error-bars or noise-levels were unsatisfactory. This is easier to implement and much more effective to parallelize in practice. It also avoids the suggestion of a controlled error level and (potentially wrong) expectations that a fixed run count may induce. All our results are presented either as one or multiple curves with error-bars or as one or multiple 2D images. This allows for an assessment of the stability of results by comparison to neighboring points and pixels. Such inspection of noisiness of shown results seems a much more informative and reliable means

	Discussion	Sample-Size N	Node Count	Indicator Count	Link-Density	Run Count	Runs (R-PCMCI)
PC_1	§B.6	. . .	5	1	0.5	2066	–
Sample Size	Fig. 7.1	. . .	5	1	0.5	543	233, 294, 122
Node Count	Fig. 7.2	1000	. . .	1	0.3	1059	240
Indicator Count	Fig. 7.3	1000	8	. . .	0.4	976 / 1687	198 / 237
Regime Sizes	Fig. 7.4	1000	8	1	0.4	1118	159
Sample Size (IID)	§A.3	. . .	5	1	0.5	958	–
Node Count (IID)	§A.4	1000 5000	. . .	3	average: $\lvert \mathrm{Pa} \rvert = 2$	120 60	–
Link Count (IID)	§A.5	1000	8	1	. . .	394	–
Regime Sizes (IID)	§A.6	1000	5	1	0.5	1019	–
Noises (IID)	§A.7	1000	5	1	0.5	1424	–

Table C.1: Individual parameters for integrated CD-experiments. Shared parameters are listed in the text proper; sub-system level experiments use only shared parameters (with the exception of implication test demonstrators, which use larger typical regime-sizes, cf. Fig. D.12 and D.13.). Parameters that are actively varied in each experiment (shown as x-axis in corresponding plots) are indicated by "..." in the respective column. Run counts for Regime-PCMCI are total runs not successful (converged) runs, convergence rate ranges from few percent (multiple indicators) to 80–90% depending also on the hyperparameter sets, see error-bars. For sample-sizes, run-counts of Regime-PCMCI depend on N, for indicator-count, the run-counts are given as independent indicators / synchronized indicators.

of assessing results than an overemphasis of run-counts; nevertheless run-counts provide additional information and are summarized in Tab. C.1, C.2.

Error-bars were generated by starting from binomial counting-statistics (based on observed rates), then using normal approximations and Gaussian error-propagation. The approximations involved seem to be reasonably accurate for these purposes. For run-times, error-bars indicate 10%–90% quantiles. Run-times (curves) are median values for CD, and mean-values for mCITs; for mCITs, there is little difference between mean and median, for CD – see also §A.4 – mean-values may not reasonably represent runtimes.

C.6 Proofs of Claims in the Main Text

In §3.3 we stated that the assignment of time-indices to graphs $G : T \to \mathcal{G}$ factors through the space of states S.

Proof of Lemma 3.10. The graph $G(t)$ by definition depends only on the values of the indicators $R_{ij}(t)$ at t. By definition 3.9 a state s is a value taken by $s := \sigma(t) = (R_1(t), \ldots, R_\kappa(t))$, where $R_1, \ldots, R_\kappa$ are precisely the (re-indexed) non-trivial indicators. Thus the value of s fixes all non-trivial indicator-values. All trivial indicator-values are fixed in the (meta-) model, so given the model M and $s = \sigma(t)$ all $R_{ij}(t)$ and thus $G(t)$ are fixed. □

	Test Order	Homogeneity Null	Homogeneity Hyper	Homogeneity Cond.	Homogeneity Vali.	Weak Hyper	Weak Conditional	Indicator Relat.	mCIT	mCIT Cond.
Discussion	F. 5.4	F. D.1	D.3.4	D.3.4	D.3.4	D.4.6	D.4.6	D.4.7	D.5	D.5
Run Count	1405	4801	2876	726	3997	2742	778	4470	16496	1233

Table C.2: Actual number of runs executed for the generation of individual benchmark databases, see text. These are runs per pixel and per scenario.

D   Details on the Data Processing Layer

In this section, we study in detail the methods realizing the individual steps of mCIT-testing as outlined in the main text §5 up to and including in their combination into an mCIT. We put particular emphasis on the existence and understanding of fundamental limitations to the realization of mCITs and potential ideas and interpretations that allow to retain a meaningful method of testing, as already in part laid out in §C.2.

An important role in maintaining a meaningful test-interpretation is played by assumptions and the interplay of trade-offs and hyperparameters. Since the choice of reasonable hyperparameters is also very much of practical concern, we also use detailed numerical experiments to validate our theoretical understanding of behaviors under different hyperparameters and to inform semi-heuristic schemes to choose them in robust ways.

We start by discussing persistence (or pattern-compatibility more generally) and its relevance to the identifiability of the mCIT result. Then we discuss some simplifying assumptions needed in particular for keeping results on statistical power of our tests accessible. Next, details on the homogeneity test and the weak-regime test are given, and both are combined into a full mCIT. Finally, we give an overview of some relevant directions for future work.

As explained in Rmk. 5.8, it makes sense to study the mCIT problem as formulated by Def. 5.9: This means, we consider for example the interpretations of dependent but uncorrelated regimes for the use of correlation-based tests to be an independence testing (not mCIT-specific) problem. We focus on the mCIT-specific problems.

D.1   Persistence

Persistence, or more generally compatibility with patterns, is of core importance to our approach. We first give a brief illustration of the limits of identifiability that make additional assumptions necessary. We also demonstrate how and why persistence can serve as such an assumption. This further helps to shed light on the relative difficulty of individual sub-tasks, in particular it aids in understanding why the weak-regime test becomes the bottle-neck for finite-sample performance in numerical experiments – this is not (only) the result of a rather primitive method, but actually deeply rooted in a second impossibility-result. Finally, we briefly explain which considerations lead us to the use of blocks of data, rather than a more sophisticated subdivision of data, for example via CPD.

D.1.1   Formal Necessity

As we demonstrate in this subsection, there are fundamental limitations to the identifiability of regime-structures; there are cases, where gaining power (even asymptotically) is not possible. This problem is closely related to limitations known on randomness / IIDness tests [67; 66]. It necessitates the incorporation of additional assumptions like persistence of regimes into the formal approach.

Remark D.1. The necessity of an assumption does of course not imply that this assumption has to be about a non-IID structure (like persistence). Indeed if one insists on remaining in the IID case, the existence of a mixture is identifiable if and only if a suitable linear independence of the involved distribution-families is satisfied [69]. See also [4] of an application of such parametric assumptions to a MCD-like problem.

To demonstrate the problem, we start from a (potential) mixture $P = \lambda P_0 + (1 - \lambda)P_1$ of two distributions P_0 and P_1, where one (say P_0) is known. We want to decide, if $\lambda = 0$; we show that this question is not identifiable in general. For simplicity we assume that densities p_0 and p (of the potential mixture) exist. Then the following holds:

Lemma D.2 (Representation by Mixture)**.** *Define:*

$$\Xi_0(p, p_0) := \sup\{\beta \in [0, 1) | \forall \vec{x} : \beta p_0(\vec{x}) \le p(\vec{x})\}$$

Given P, P_0 with densities p, p_0, then there exists a density p_1 and a $\lambda \ge \Xi_0(p, p_0)$ with $p = \lambda p_0 + (1 - \lambda)p_1$.

Proof. Since we do not know p_1, we can always write $p = \Xi p_0 + (p - \Xi p_0)$. From $\int p = 1$ and $\int \Xi p_0 = \Xi$ together with $p > \Xi p_0$ we have $\mathcal{N} := \int (p - \Xi p_0) = 1 - \Xi$. So after normalizing $p_1' := \mathcal{N}^{-1}(p - \Xi p_0)$ is a probability density (again by $p - \Xi p_0 \ge 0$). We can, using $\lambda = \Xi$, write $p = \lambda p_0 + (1 - \lambda)p_1'$ as a mixture of p_0 and p_1' with $\lambda = \Xi$. ☐

This is bad: We had not yet assumed p *is* a mixture, rather this always works, irrespective of whether or not p was in any sense generated by a "true mixture". For the case of relevance here, we do not know P_0, only its factorization-property (as an independence null-distribution); knowing less will of course not improve identifiability:

Lemma D.3 (Representation by Mixture with Independent Component)**.** *Given a joint distribution $P(X, Y)$ with density p and*

$$\Xi = \sup_{p_0(X,Y)=p_0^X(X)\times p_0^Y(Y)} \sup\{\beta \in [0, 1) | \forall x, y : \beta p_0(x, y) \le p(x, y)\}$$

then $\forall \epsilon > 0$ there exist densities $p_0^X(x), p_0^Y(y), p_1(x, y)$ and a $\lambda \ge (1 - \epsilon)\Xi$ with $p(x, y) = \lambda p_0^X(x) \times p_0^Y(y) + (1 - \lambda)p_1(x, y)$.

Proof. Let $\epsilon > 0$ be arbitrary, w. l. o. g. $\epsilon < 1$. There are (by definition the Ξ) $p_{0,\epsilon}^X(x), p_{0,\epsilon}^Y(y)$ with $(1 - \epsilon)\Xi(p_{0,\epsilon}^X(x) \times p_{0,\epsilon}^Y(y)) \le p(x, y)$.

Thus the Ξ_0 of the previous lemma satisfies, using $p_{0,\epsilon} := p_0^X(x) \times p_0^Y(y)$, that $\Xi_0(p, p_{0,\epsilon}) \ge (1 - \epsilon)\Xi$. If we apply the previous lemma to p and $p_{0,\epsilon} = p_0^X(x) \times p_0^Y(y)$, we therefore find a $p_{1,\epsilon}$ with $p = \lambda_\epsilon p_{0,\epsilon} + (1 - \lambda_\epsilon)p_{1,\epsilon}$ for $\lambda \ge \Xi_0(p, p_{0,\epsilon}) \ge (1 - \epsilon)\Xi$. ☐

The value of Ξ can be large (close to 1) even for seemingly harmless examples, in particular counter-examples *do exist*:

Example D.4. Let P be a bivariate normal distribution with means μ_X and μ_Y and variances σ_X^2, σ_Y^2 and correlation coefficient ρ. Pick σ_-^2 as the smaller eigenvalue of the covariance-matrix Σ (for example $1 - |\rho|$ if $\sigma_X = \sigma_Y = 1$). Then by construction $\vec{x}^T \Sigma^{-1} \vec{x} \le \frac{\|\vec{x}\|^2}{\sigma_-^2}$. Define $p_0(x, y)$ as the product of normal distributions with means μ_X and μ_Y and standard-deviations $\sigma_X' = \sigma_Y' = \sigma_-$. Then this p_0 is such that the exponential term in the density contains $\frac{\|\vec{x}\|^2}{\sigma_-^2}$ where p contains $\vec{x}^T \Sigma^{-1} \vec{x}$ so that it falls off faster when moving away from the mean values; thus $\beta p_0 \le p$ iff $\beta p_0(\mu_X, \mu_Y) \le p(\mu_X, \mu_Y)$ and we find from the normalizations of these densities that this inequality is satisfied for $\beta = \frac{\sigma_-^2}{\sigma_X \sigma_Y \sqrt{1-\rho^2}}$. E. g. if $\sigma_X = \sigma_Y = 1$ this is $\beta = \sqrt{\frac{1-|\rho|}{1+|\rho|}}$ (by writing $1 - \rho^2 = (1 - \rho)(1 + \rho)$ in the denominator and case-distinction

for $\rho \leq 0$). Finally $\Xi \geq \beta$, because Ξ was defined as the supremum of all values satisfying this inequality. For example, if $\sigma_X = \sigma_Y = 1$, then $\Xi \geq \sqrt{\frac{1-|\rho|}{1+|\rho|}}$; it should be noted in particular that this approaches 1 for $|\rho| \to 0$.

Proposition 5.3 (Impossibility Result A)**.** *Given data as a set (without non-IID structure on the index-set), then the marked independence statement is not in general identifiable. By Lemma 4.13 (see also Rmk. 4.13) also the MCD-problem is not in general identifiable.*

Proof. By Lemma D.3 the same (law of) the *set* of data obtained as a random element can be obtained from a mixture and a non-mixture for $a < \Xi$. In particular the distinction is not identifiable from knowledge of the (law of) the random set alone in such cases. By example D.4, cases with $0 < a < \Xi$ exist. $\qquad\square$

Corollary D.5 (Non-Testability A)**.** *Given a joint distribution $P(X,Y)$ with density p and*

$$\Xi = \sup_{p_0(X,Y)=p_0^X(X)\times p_0^Y(Y)} \sup\{\beta \in [0,1)|\forall x,y : \beta p_0(x,y) \leq p(x,y)\}$$

then there is no hypothesis-test that assumes the data to be IID (considers only sets of data points without non-IID structure) distinguishing between true regimes and global dependence that, for regime-fractions λ with $\lambda < \Xi$, controls either error-rate (FPR / FNR) at $\leq \alpha$ and has asymptotically non-trivial power (i. e. which would have TPR / TNR $> \alpha$ for any sample-size N).

Proof. Let $\hat{T}$ be an arbitrary test that given N data points $D = \{(x_1, y_1), \ldots, (x_N, y_N)\}$ outputs a value $\hat{T}(D) \in \{0,1\}$ where e. g. 0 means true regime and 1 means global dependence (the choice of 0 vs. 1 is arbitrary). Let $p(x,y)$ be given, and consider N data points $(x_1, y_1), \ldots, (x_N, y_N)$ drawn IID from $p(x,y)$. This is a value of the random element D_p^N. Then $\hat{T}(D_p^N)$ is a random variable taking values in $\{0,1\}$, in particular (as any random binary variable) it is described by a single value $q_p^N \in [0,1]$, by $P(\hat{T}(D_p^N) = 1) = q_p^N$ and $P(\hat{T}(D_p^N) = 0) = 1 - q_p^N$.

Controlling FPR: Let $\lambda > 0$ with $\lambda < \Xi$ be arbitrary. Set $\epsilon = \frac{\Xi - \lambda}{2} > 0$. By the previous lemma, we can write p as $p = p_{\mathrm{mix}} = \lambda p_{0,\epsilon} + (1-\lambda)p_{1,\epsilon}$. To control the rate of false positives, i. e. outcomes where $\hat{T}(D_p^N) = 1$ (where T claims there is no regime) on the ground-truth scenario described by the mixture p_{mix}, necessarily $P(\hat{T}(D_{p_{\mathrm{mix}}}^N) = 1) \leq \alpha$. But without further knowledge about λ (like a persistence assumption on λ) – it is important here that by hypothesis $\hat{T}(D)$ depends *only* on the set D without employing any additional non-IID-structure – the *random set* D only depends on the density, i. e. $D_{p_{\mathrm{mix}}}^N = D_p^N$) and thus $q_p^N = P(\hat{T}(D_p^N) = 1) = P(\hat{T}(D_{p_{\mathrm{mix}}}^N) = 1) \leq \alpha$. Similar remarks on the factorization through D apply to all other paragraphs below.

On the other hand consider the (non-mixture) $p_{\mathrm{homog}} = 0 + 1 * p$ ground-truth scenario. Here the power to correctly reject the true regime is $P(\hat{T}(D_{p_{\mathrm{homog}}}^N) = 1) = P(\hat{T}(D_p^N) = 1) = q_p^N \leq \alpha$. That is $\hat{T}$ does not have non-trivial power if controlling FPR on mixtures with $\lambda < \Xi$ for any N.

Controlling FNR: Let $\lambda > 0$ with $\lambda < \Xi$ be arbitrary. Consider the (non-mixture) $p_{\mathrm{homog}} = 0 + 1 * p$ ground-truth scenario. To control the rate of false negatives (where T claims there is a regime) necessarily $P(\hat{T}(D_{p_{\mathrm{homog}}}^N) = 0) = P(\hat{T}(D_p^N) = 0) = 1 - q_p^N \leq \alpha$.

Set $\epsilon = \frac{\Xi - \lambda}{2} > 0$. By the previous lemma, we can write p as $p = p_{\mathrm{mix}} = \lambda p_{0,\epsilon} + (1-\lambda)p_{1,\epsilon}$. The power to correctly classify p_{mix}, i. e. outcomes where $\hat{T}(D_p^N) = 0$ (where T correctly claims there is a regime) on the ground-truth scenario described by the mixture p_{mix}, is given by $P(\hat{T}(D_{p_{\mathrm{mix}}}^N) = 0) = P(\hat{T}(D_p^N) = 0) = 1 - q_p^N \leq \alpha$. That is $\hat{T}$ does not have non-trivial power if controlling FNR on mixtures with $\lambda < \Xi$ for any N. $\qquad\square$

D.1.2 How Persistence Helps

To see the effect a persistence-assumption will have, we again look at the initial Lemma D.3, in particular at the definition

$$\Xi_0(p, p_0) := \sup\{\beta \in [0,1) | \forall \vec{x} : \beta p_0(\vec{x}) \le p(\vec{x})\}.$$

Next we divide the data into blocks of k data points each. Those blocks are sampled according to p^k if the data is IID. Note that (by monotonicity of the root / exponentiation by $1/k$)

$$\begin{aligned}
\Xi_0(p^k, p_0^k) :&= \sup\{\beta' \in [0,1) | \forall \vec{x} : \beta' p_0^k(\vec{x}) \le p^k(\vec{x})\} \\
&= \sup\{\beta \in [0,1) | \forall \vec{x} : \beta^{1/k} p_0(\vec{x}) \le p(\vec{x})\}.
\end{aligned}$$

Thus $\Xi' = \Xi_0(p^k, p_0^k) = \Xi_0(p, p_0)^k$, and with $\Xi_0(p, p_0) < 1$ further $\Xi_0(p^k, p_0^k) \xrightarrow{k \to \infty} 0$. So have we magically resolved the problem? Of course the answer is no – we are now comparing those blocks whose k data points *all* came from p_0 to the rest of the data. For IID data, the fraction of such blocks (by binomial statistics) is simply $\lambda' = \lambda^k$. Our impossibility-result really is about the comparison $\lambda \ge \Xi$ which is equivalent to $\lambda' \ge \Xi'$, so we have gained nothing, *so far*.

The simplest type of persistence here would be to assume that we know that regime-switches occur only every k data points, so that blocks containing only data points from p_0 occur as the total fraction of data points in p_0 which is λ (as opposed to λ^k for random / IID blocks). Thus in this case $\lambda' = \lambda$, so that with $\Xi' \to 0$ for $k \to \infty$ indeed $\lambda' \ge \Xi'$ is always satisfied for k large enough.

In practice regime-switches occur not exclusively at multiples of k like this. However, if regime-switches occur rarely (compared to k), $\lambda \approx \lambda'$ is still a good approximation (see Lemma C.8). So a persistence-requirement should be understood in the following sense: To resolve small (true) regime-fractions λ, we need a small enough Ξ – which depends also on the "distance" between the mixed distributions (cf. example D.4, where the correlation ρ is a suitable distance-measure) – and therefore a large enough ground-truth persistence length $L \gg k_\Xi$ such that $\lambda \approx \lambda'$ still holds.

Finally, inspecting Fig. 5.2 (middle panel in particular), the use of blocks (for say $k = 2$) can make precise the intuitive idea why this pair of examples can be distinguished using time-resolution. For any block (of $k = 2$ subsequent data points), one can assess how often both data points are in the same regime, which given many blocks provides useful information about which of the densities on the left-hand side were active.

The above argument only takes into account "fully valid" (all data points in the same context) blocks. However, the case where all blocks are valid should be easiest, thus limitations to the identifiability in this case should also apply to all other cases. More subtle, we only consider a single choice of L_0 at once, but for the case where all blocks are valid the joint distribution over L_0 data points contains all information about the joint over $L_0 - 1$ etc. data points by marginalization. So up to a suitable persistent length L_0 (where still reasonably many blocks are valid) the additional use of shorter (than L_0) blocks should not gain substantial information either ("substantial" in the sense of affecting the impossibility result or general trade-off; finite sample performance may very plausibly improve by a suitable combination of multiple block-sizes, see §D.7.4).

D.1.3 Relative Difficulty of Subtasks

The arguments in §D.1.1 and §D.1.2 concern the "full" problem of testing for the existence of true regimes. Meanwhile our arguments below and in the main text further divide the problem into subtasks (testing homogeneity and testing for weak regimes). Thus it is clear that the difficulties do *not* arise from this reformulation into sub-problems, rather they exist independently of this approach. However, it mandates the question, where precisely the difficulties come from in terms of these subtasks. The main insight discussed in this

subsection is that testing homogeneity is (relatively speaking) easy, while testing for weak regimes is particularly hard.

An easy way to understand why homogeneity / IIDness-testing is comparatively easy is that given *any* (non-zero) persistence in the data, that is if $\lambda_t \not\perp\!\!\!\perp \lambda_{t+1}$, then subsequent data points are not independent $(X_t, Y_t) \not\perp\!\!\!\perp (X_{t+1}, Y_{t+1})$ either (under mild assumptions). In principle any (non-parametric) independence-test can thus distinguish between homogeneous and persistent-heterogeneous models.

Remark D.6. Using an independence test directly may not be a good idea. Not only is the non-parametric testing-problem challenging on finite data (and in principle [57]), but even more the *type* of heterogeneity we are interested in for subsequent weak-regime / true-regime testing is *not* (auto-)lag behavior of the underlying model, but larger persistent data-regions (cf. §D.1.2). It thus seems to make more sense to allocate statistical power to finding such heterogeneity, hence our choice of inductive bias in §5.2.2 is tailored primarily to this alternative.

If the fundamental difficulty encountered in §D.1.1 does not appear to its full extend in homogeneity-testing, then it must appear when testing weak-regimes. This problem becomes more apparent if one considers not just (infinite sample) identifiability, but also finite-sample questions §D.1.4. The relative difficulty of the weak-regime test is heuristically supported for example by the results presented in Fig. D.14 and in theory by the statistical power-results in §D.3.3 and §D.4.4.

D.1.4   Conceptual Finite Sample Challenges

In hypothesis-testing, one is often interested in the ability to control finite-sample errors in one direction at a finite (and known) rate. This has many advantages, in particular for the interpretability of results. Considering the true regime case, in the formulation via a homogeneity and a weak-regime step, we note the following apparent problem: Homogeneity can be accepted or rejected (with finite sample control on false positives), and independence of the weak regime can be accepted or rejected (with finite sample control on false positives), but the true regime case is the combination *reject* homogeneity, then *accept* independence. This combination does not naturally allow for the control of any error-rate in the finite sample case.

Again, we want to see if this is a problem of our reformulation into sub-tasks or a genuine issue. The intuition behind our argument is that usually (for most model-classes) there are meaningful model-properties d_0 measuring dependence (in the weak or only regime) and Δd measuring non-homogeneity. With finite-sample error control being achieved through p-value bounds on the uncertainty of some test-statistic. This test-statistic may not involve an intermediate estimate of d_0 and Δd, but if these properties are well-defined and in a suitable sense "sufficiently continuous", then confidence regions will have non-trivial extension (for example containing the true value in its topological interior) in the d_0–Δd-plane. In this case error-control for standard hypotheses works, because the alternatives (to homogeneity / independence) are open (in the sense of topology), or equivalently because the null hypotheses are closed. In this intuition, the true regime case corresponds to $d_0 = 0$ and $\Delta d \neq 0$, which is neither open nor closed, thus is neither suitable as null hypothesis nor as alternative in the usual sense.

Capturing the above argument more formally requires two types of formal assumptions. First, there is a statistical aspect related to non-triviality of the problem. If by our prior knowledge, we already know that one or more of the hypotheses never occur, e.g. if $P(d_0 = 0, \Delta d = 0) = 0$, then the testing problem will become solvable for trivial reasons. This also means that we have to consider priors on d_0 and Δd which are *not* continuous in the d_0–Δd plane (the point $(0, 0)$ corresponding to global independence must have singular weight and also the axis $\Delta d = 0$ of global / non-regime models must have non-zero weight despite being a Lebesgue zero-set). We also have to account for a different problem with similar

consequences which arises if there are a priori known "gaps" in parameters, for example if we knew that $|d_0| \notin (0, d_{\min})$, i.e. if there is a lower bound for non-zero values taken by d_0, then it might suddenly be possible to control errors (for independence-testing in this case) in both directions. We are interested in the generic case and want to exclude this special case.

Second, there is a topological aspect, for example the measure of proximity in the sense of finite-sample bounds on estimates $\hat{d}_0$ and $\hat{\Delta d}$ (possibly implicit in $\hat{T}$) must be compatible with the topology of $\mathbb{R}^2_{\geq 0}$. There are many ways to formalize this, we opt for requiring $\Pr(\hat{T} = R | d_0, \Delta d)$ to be continuous. It is difficult to judge how plausible this assumption is. While it may appear somewhat ad hoc at first, this is also *because* it is chosen rather weakly: For example, one might also ask for data-sets $\vec{X} = (\vec{x}_1, \ldots, \vec{x}_N) \in \mathbb{R}^{2N}$ to arise from a continuous (in $\vec{X}$, d_0, Δd) conditional density $p(\vec{X} | d_0, \Delta d)$ and an mCIT $\hat{T}$ deciding based on a continuous (in $\vec{X}$) p-value estimate $p_R(\vec{X})$. This implies (is stronger than) the above assumption about their "composition". However, this continuous factorization might for example not apply to our binomial homogeneity test (where p-values are based on discrete block-counts), while the composition (averaging over realizations) should, for most constructions of this kind, smooth this problem away, so that the hypothesis as given in the proposition should still apply. The main point here is not maximal generality of the given formulation, but a formal illustration of the problem.

Proposition 5.12 (Impossibility Result B). *Assume the model-class considered has well-defined model-properties $d_0 \in \mathbb{R}_{\geq 0}$ and $\Delta d \in \mathbb{R}_{\geq 0}$ such that a model M has an independent regime iff $d_0(M) = 0$ and is homogeneous iff $\Delta d(M) = 0$. Further assume that we are given an mCIT $\hat{T} \in \{0, 1, R\}$ such that $\Pr(\hat{T} = R | d_0, \Delta d)$ is continuous in d_0 and Δd, and that there is no a priori known gap in realized parameters d_0 and Δd, that is $P(d_0, \Delta d) > 0$ near[17] $d_0 = 0$, and there is no a priori known gap in Δd on weak regimes, that is $P(\Delta d | d_0 = 0) > 0$ near $\Delta d = 0$.*

Then, given $\alpha > 0$, no such mCIT can for any finite sample-size N

(a) on true regimes uniformly control FPR at $< \alpha$ and have non-trivial power $> \alpha$ on any global independence alternative or

(b) on global dependence or the union of global hypotheses control FPR at $< \alpha$ and have non-trivial power $> \alpha$ on any true regime alternative.

Proof. First note, that uniform error-control over models implies uniform error-control over well-defined model-properties (where supported, cf. gap-hypotheses).

Part (a): Let M be an arbitrary global independence alternative (to a true regime), that is $d_0(M) = 0$ and $\Delta d(M) = 0$ by hypothesis. By absence of a gap in Δd on weak regimes $P(\Delta d | d_0 = 0) > 0$ near $\Delta d = 0$, uniform (over $d_0, \Delta d$, see initial comment of this proof) α-error control requires $\Pr(\hat{T} = R | d_0 = 0, \Delta d) \geq 1 - \alpha$ for all $\Delta d > 0$ near $\Delta d = 0$. By continuity of $\Pr(\hat{T} = R | d_0, \Delta d)$ (and for example the sequence criterion), thus $\Pr(\hat{T} = R | d_0 = 0, \Delta d = 0) \geq 1 - \alpha$. This implies $\Pr(\hat{T} = 0 | d_0 = 0, \Delta d = 0) \leq \alpha$ and by $d_0(M) = 0$ and $\Delta d(M) = 0$ and uniformity of error-control (over models) $\Pr(\hat{T} = 0 | M) \leq \alpha$. That is $\hat{T}$ does not have non-trivial power on M. Since the model M was arbitrary (among global independence alternatives), this shows part (a).

Part (b): Uniform error control over the union of global hypotheses in particular implies uniform error control over the (subset of) global dependence models, so it suffices to proof the claim for global dependence models. Let M be an arbitrary true regime alternative (to a globally dependent scenario), that is $d_0(M) = 0$ and $\Delta d(M) \neq 0$ by hypothesis. By absence of a gap in parameters $P(\Delta d, d_0) > 0$ near $\Delta d = 0$, uniform (over $d_0, \Delta d$, see initial comment of this proof) α-error control requires $\Pr(\hat{T} = 1 | d_0, \Delta d) \geq 1 - \alpha$ for all $\Delta d, d_0$ near $\Delta d = 0$. This implies $\Pr(\hat{T} = R | d_0, \Delta d) \leq \alpha$ for all $\Delta d, d_0$ near $\Delta d = 0$. By continuity of $\Pr(\hat{T} = R | d_0, \Delta d)$ (and for example the sequence criterion), thus $\Pr(\hat{T} = R | d_0 = 0, \Delta d = \Delta d(M)) \leq \alpha$. By $d_0(M) = 0$ and uniformity of error-control (over models) $\Pr(\hat{T} = R | M) \leq \alpha$. That is $\hat{T}$ does

---

[17]"Near ..." in this case means on an open neighborhood of ..., as this is a topological requirement.

not have non-trivial power on M. Since the model M was arbitrary (among true regime alternatives), this shows part (b). □

D.1.5   Rationale Behind the Use of Blocks

There are multiple reasons why we subsequently specialize to the simple block-based approach: It is very simple to analyze theoretically and very fast in practice. However, it is also surprisingly effective for the type of applications we have in mind. These applications are larger data-sets, with at least a few thousand data points, as we believe that in practice regime-structure – as any multi-scale structure – typically is interesting in particular for larger datasets.

In this case, the effectiveness of the simple block-based approach can be understood as follows. As illustrated in §5.2, the aggregation of data from the full index-set I to the final result about marked independence is itself performed in two steps: Use persistence to aggregate similar data (e. g. in blocks), then use the statistical distribution over blocks to "directly" (without explicit time-resolution of indicators) reason about marked independence. Especially for larger datasets, it turns out that this second step is decisive for finite sample performance; essentially increasing block-sizes leads to diminishing returns, so increasing the number of blocks becomes more reasonable. The simple subdivision into blocks provides blocks independently of the data (the mapping on indices is fixed a priori), while e. g. CPD-segments are inherently dependent on the underlying data, with biases the aggregation-procedure itself. Also blocks are of equal size and thus later on produce the same distribution after applying a dependence-score $\hat{d}$, again this is not the case for CPD-segments. These two properties make the statistical analysis of distributions over blocks comparatively easy and effective. One may thus think of the block-based approach compared to CPD as trading block-size (thus variance of $\hat{d}$) at a given rate of valid blocks for a more well-defined and accessible direct testing problem in the second step. This tends to be a particularly favorable trade on *large* datasets. It was also relevant to this decision that we currently specialize to the case of partial correlation, which initially converges much faster than non-parametric dependence-scores, thus suffers less from small block-sizes.

Finally, our pattern approach via blocks works quite generally, also for multi-dimensional (for example spatial) and even more exotic patterns like neighborhoods in graph-networks or periodic structures. While there is a vast array of one-dimensional CPD literature, the availability of established methods for more complicated setups is limited.

This does not mean that CPD could not be used at this point, rather that it does not help to tackle the core problem. For this reason we focus on the direct testing problem and leave the additional possibility to leverage CPD to future work, see §D.7.3.

D.2   Simplifying Assumptions

Here, we provide notation and assumptions for the subsequent theoretical study of the statistical tests proposed for homogeneity and weak-regime testing. Especially for the power results, some simplifying assumptions are made.

D.2.1   Underlying Dependence-Score and Estimator

At the beginning of §5.2, we fixed a notion of an underlying dependence-measure d with an estimator $\hat{d}$ (Ass. 5.7). The choice of underlying dependence-measure d (as opposed to its estimator) can be important here, as our ground-truth scenarios are formulated relative to d (see Rmk. 5.8 and Def. 5.9). For example for the case of correlations (or z-values) this means, to maintain a standard interpretation in terms of dependence (rather than correlation) statements, we implicitly assume that models are such that both cases coincide.

Assumption D.7 (Underlying CIT Convergence)**.** When we say "$\hat{d}$ consistently approximates d" in Ass. 5.7, more precisely, this will mean that when estimating $\hat{d}_N$ on N data points

and $\hat{d}_{N'}$ for $N' > N$ data points from the same generating process (with true value d), then (using the notation $\preceq$ for stochastic ordering, cf. Def. C.20)

$$|d - \hat{d}_{N'}|\sqrt{N'} \preceq |d - \hat{d}_N|\sqrt{N}$$

Note that for parametric tests, this is primarily an implementation assumption (Rmk. D.8).

Remark D.8. Given any parametric estimator $\hat{d}$ and $N' = k \times N$ (for simplicity assume $k \in \mathbb{N}$), dividing the set of N' data points into k disjoint subsets of N data points each, computing $\hat{d}_N$ on these k subsets and $\hat{d}_{N'}$ as the mean-value satisfies the above equation (by applying central limit theorem, then Chebyshev's inequality; assuming second moments exist). This does not violate the Cramér–Rao bound, rather it states that for larger N we get closer to the Cramér–Rao bound (or put differently, the smaller N, the harder it is to get close to this bound). *However*, non-parametric tests, to extend the region of applicability and / or non-trivial power, effectively increase the number of parameters progressively. Our hyperparameter choices for power-results (see also examples D.23 and D.35) use the asymptotic $\sim \sqrt{N}$ scaling for concreteness, but the specific form of scaling is not critical. But, as [57] show, even convergence (at any rate) is in full generality not possible. In this sense, the use of a convergence-assumption like Ass. D.7 (or possibly slower than square-root rates) for $\hat{d}$ separates these problems, which are typical for CITs in general (cf. Rmk. 5.8), from those specific to mCITs, which we are primarily interested here.

Example D.9. For z-transformed partial correlation with conditioning-set dimension $|Z|$, in good approximation $\hat{d}_N \sim \mathcal{N}\left(d, \sigma_N^2 = (N - 3 - |Z|)^{-1}\right)$. In particular $\sqrt{N}\sigma_N > 1$ and monotonically decreasing with limit 1. Thus Ass. D.7 is satisfied.

Further we will (primarily to make statements and proofs less intricate) assume that estimates of $\hat{d}$ are stochastically monotonic.

Assumption D.10 (Stochastic Monotonicity of Dependence-Estimators)**.** We assume that given N data points from generating processes with true values $d_0 < d_1$, then the distributions of the estimator $\hat{d}$ applied to such datasets $\hat{d_0^N}$, $\hat{d_1^N}$ are stochastically ordered:

$$d_0 < d_1 \quad \Rightarrow \quad \hat{d_0^N} \preceq \hat{d_1^N}$$

We will assume this ordering to be strict on the support (i. e. where cdfs are not 0 or 1).

Example D.11. Let $\hat{d}$ be an approximately normal, unbiased, variance-stabilized estimator, then (see example C.21) Ass. D.10 is satisfied. In particular for z-transformed partial correlation Ass. D.10 is satisfied.

Sometimes we need a slightly stronger variant:

Assumption D.12 (Dependence-Estimators on Mixed Data)**.** We assume that given $N = n_0 + n_1$ data points from generating processes with true values $d_0 < d_1$, then the distributions of the estimator $\hat{d}_{\mathrm{mix}}$ applied to the mixed data-set are stochastically ordered relative to application of $\hat{d}_0, \hat{d}_1$ to size-N data-sets drawn exclusively from either generating process:

$$d_0 < d_1 \text{ and } n_0, n_1 \neq 0 \quad \Rightarrow \quad \hat{d}_0 \preceq \hat{d}_{\mathrm{mix}} \preceq \hat{d}_1$$

We will assume this ordering to be strict on the support (i. e. where cdfs are not 0 or 1). Additionally we assume that for $N \to \infty$ this ordering also holds for $\hat{d}_{\mathrm{mix}}$ evaluated on invalid blocks (we never assumed "independence"[18] of switches and block-boundaries, in principle every switch could happen after the first data point of the respective invalid block, so that for example $n_0 = 1$, $n_1 \to \infty$ as $N \to \infty$; we exclude such singular mixing behavior by assumption).

---

[18]Blocks are chosen a priori, but switches could occur periodically, so block-boundaries and switches may appear dependent.

For simplicity, we in places (see Rmk. D.14) assume that the dependence measure $\hat{d}$ (on homogeneous datasets) is normally distributed, this is the case at least approximately for most estimators given sufficiently large blocks:

Assumption D.13 (Dependence-Estimator Normality). Given a (homogeneous) dataset with expectation-value $d = E[\hat{d}]$, the estimator $\hat{d} \sim \mathcal{N}(d, \sigma)$ is unbiased and normal distributed.

Remark D.14. Beyond Lemma D.30 this is primarily an assumption to simplify notation. In Lemma D.30, it is only really required for the distribution around d_0, and Lemma D.30 in turn is used in Lemma D.31 to ensure error-control. Thus it is used only under the null, which means for $d_0 = 0$. So this assumption is needed primarily for $d = 0$.

Normal estimators are compatible with stochastic monotonicity (Ass. D.10) only if the variances agree $\sigma_0 = \sigma_1$. The assumption $\sigma_0 = \sigma_1$ is reasonable for parametric models, where often variance-stabilized estimators (like z-transformed correlation) are used in practice. For non-parametric estimators this equality may not hold. In practice normality is here a good approximation for the "bulk" of the data, but breaks down on tails; indeed stochastic monotonicity seems a plausible assumption in these cases nevertheless (it would have to be violated in the tails, so this does not contradict the claim about normal approximations before). At the same time, we use normality primarily for truncated-normal approximations (see proof of Lemma D.30), so as long as the cutoffs are reasonably small (in terms of quantiles), this approximation still makes sense. A reasonable size of the quantiles is effectively ensured by the $n_c \geq n_0^{\min}$ in Lemma D.31.

D.2.2 Regime-Structure

For the theoretical analysis, especially of statistical power, it is often helpful to restrict possible models to the case of precisely two different regimes with individually constant (ground-truth) dependence values $d_0 \neq d_1$. For real-world data-sets, there may of course be both more than two regimes, and regimes of varying (for example smoothly drifting) dependence-values. Since the independent regime satisfies $d_0 = 0$, these variations are naturally limited to the dependent regime. Most of our arguments do not inherently depend on d_1 being constant, even though this can improve statistical power (compare also §D.3.1 below), this assumption is primarily made to simplify theoretical arguments. One notable exception is that of multiple regimes with different sign (or drifts reaching both signs), where a one-sided cut-off may be inappropriate (see §D.4.5); this of course only happens for *signed* dependence-scores $\hat{d}$ like (signed) correlation. It is also interesting to note that, for the application in causal discovery, the regime-structure for valid adjustment sets (those where the regime actually becomes conditionally independent) may be systematically *simpler* than for general (weak) regimes. This is, because the conditional independence usually is achieved by conditioning on (for example) a parent-set, which effectively removes regime-structure other than from the particular link under investigation from the problem.

Assumption D.15 (Exactly Two Regimes). We assume there are (locally, on the CIT) precisely two regimes, with $\hat{d}$ applied to valid blocks on either regime having expectation-values $d_0 \neq d_1$.

Notation D.16 (Standardize Signs and Order). W. l. o. g. $d_1 > 0$ and $|d_1| > |d_0|$ (otherwise flip signs or switch the indexing); d_0 may be negative.

D.3 Homogeneity

We provide details on the homogeneity-test proposed in §5.2.2.

D.3.1 Quantile Estimation

Estimating lower bounds on quantiles for the d_1 regime is surprisingly easy, but the formulation of requirements on "consistent" estimators is rather subtle. This subtlety is related to

the existence of results of the form of Lemma D.24 (see discussion in §D.3.3).

Definition D.17 (Quantile Estimator)**.** We call $\hat{q}_{\bar{\beta}}^{\leq}$ a sound estimator of a lower bound of the β-quantile of the distribution in the d_1-regime if on the null-distribution of homogeneity (only one regime) with dependence d_1 estimated on blocks by $\hat{d}_1$ it satisfies

$$\Pr(\hat{d}_1 \leq \hat{q}_{\bar{\beta}}^{\leq}) \leq \beta.$$

We further call $\hat{q}_{\bar{\beta}}^{\leq}$ consistent if additionally there is a (fixed) mapping $\beta(B)$ – we will formally consider the pair $(\hat{q}_{\bar{\beta}}^{\leq}, \beta(B))$ as defining information of the estimator – such that on any alternative satisfying Ass. D.15 (precisely two regimes with $d_0 < d_1$) with d_0 estimated on valid blocks of size B of the independent regime by $\hat{d}_0$ the following conditions are fulfilled:

(a) $\beta(B) \to 0$ for $B \to \infty$.

(b) $\Pr(\hat{d}_0 \leq \hat{q}_{\bar{\beta}(B)}^{\leq}) \to 1$ for $B \to \infty$.

Example D.18 (Analytic Quantile Estimation for Partial Correlation)**.** Consider $\hat{d}$ given as the z-value of partial correlation. Define first (using $\Theta = \lfloor \frac{N}{B} \rfloor$ the number of blocks)

$$\hat{d}_{\bar{1}}^{\leq} := \Theta^{-1} \sum_b \hat{d}(b)$$

given by the mean-value over estimates on blocks. We start by inspecting its properties on the null-distribution (only one regime) of dependence d_1. If B is the block-size and $d_z := |Z|$ the size of the conditioning set, then $\hat{d}$ evaluated on blocks is (approximately, we assume B is large enough) normal distributed with mean d_1 and variance $\sigma_B^2 = (B - 3 - d_z)^{-1}$. Thus $\hat{d}_{\bar{1}}^{\leq} \sim \mathcal{N}(d_1, \Theta^{-1}\sigma_B^2)$. For simplicity assume Θ is large, such that $\Theta^{-1}\sigma_B \ll \sigma_B$ and $d_1 \approx \hat{d}_{\bar{1}}^{\leq}$ (otherwise replace the p-value estimate at the end based on σ_B by a combinations of estimates based on σ_B and $\Theta^{-1}\sigma_B$ respectively). Then $\hat{d}$ evaluated on blocks is normal distributed with known mean $\hat{d}_{\bar{1}}^{\leq}$ and variance σ_B^2. We define (with ϕ denoting the standard-normal cdf)

$$\hat{q}_{\bar{\beta}}^{\leq} := \hat{d}_{\bar{1}}^{\leq} + \phi^{-1}(\beta)\sigma_B.$$

By construction, this estimate is sound on the null distribution.

This estimator is also consistent in the sense of Def. D.17 under Ass. D.12 (monotonicity of $\hat{d}$): Define $\beta(B) := 1 - \phi(B^{\frac{1}{4}})$. By $\phi(t) \to 1$ for $t \to \infty$ and $B^{\frac{1}{4}} \to \infty$ for $B \to \infty$, also $\beta \to 0$ for $B \to \infty$ showing property (a). Using $\sigma_B \sim B^{-\frac{1}{2}}$ in the defining equation of $\hat{q}_{\bar{\beta}}^{\leq} := \hat{d}_{\bar{1}}^{\leq} + \phi^{-1}(\beta)\sigma_B$ the second term $\phi^{-1}(\beta(B))\sigma_B \sim -B^{\frac{1}{4}}B^{-\frac{1}{2}} = -B^{-\frac{1}{4}} \to 0$ for $B \to \infty$, thus $\hat{q}_{\bar{\beta}}^{\leq} \to \hat{d}_{\bar{1}}^{\leq}$. By Ass. D.12 (and $a \neq 0$ when in the alternative), the mean $\hat{d}_{\bar{1}}^{\leq} \to d(a) > d_0$. Finally for $B \to \infty$ (and thus $\sigma_B \to 0$), we have $\hat{d}_0^B \xrightarrow{\mathrm{P}} d_0 < d(a)$, which also implies $P(\hat{d}_0^B < d(a) - \epsilon) \to 1$. By the above argument $\hat{q}_{\bar{\beta}}^{\leq} \to d(a)$ eventually becomes larger $d(a) - \epsilon$, thus also $P(\hat{d}_0^B < \hat{q}_{\bar{\beta}}^{\leq}) \to 1$ and property (b) is satisfied.

Finally note, that the "effective sample count" approximation of the distribution per block can be replaced by other analytical estimates, for example a large N expansion.

Remark D.19 (Meaning of hyperparameters)**.** The choice of β used in the example above may not be practically useful, it illustrates an important principle however: Eventually, β needs to become smaller than a (see proof of Lemma D.22) to gain power on small (ground-truth) regime-fractions, but at the same time β should be chosen large enough, such that $|q_\beta - d_1|$ is small compared to $\frac{\Delta d}{\sigma_B}$. Thus β parameterizes the trade-off between gaining power faster on regimes with small fraction a (prefers smaller β) and gaining power faster on regimes with low separation $\Delta d = |d_1 - d_0|$ (prefers larger β).

The second hyperparameter B is easier to interpret: Larger B improves effective separation $\frac{\Delta d}{\sigma_B}$ (because σ_B becomes smaller), but it also increases χ (as each switch of regimes invalidates approximately one block, thus B data points).

Example D.20 (Bootstrapped Quantile Estimation)**.** If the estimator $\hat{d}$ is more complex, a simple analytical estimate may not be possible. However, one seemingly (see below) can bootstrap quantiles simply as follows: Draw B samples from all data at random, and compute $\hat{d}$ on these samples, repeat. Estimate $q(\beta)$ as the β-th quantile of the resulting distribution. While this may seem trivial, it is crucial to note that this leads to "unaligned" (with the time-axis) blocks and typically produces the same distribution as evaluating $\hat{d}$ on time-aligned blocks if the data are IID (in particular this estimator is sound in terms of Def. D.17) but not if there are persistent regimes. By Ass. D.12 (estimating $\hat{d}$ on invalid blocks is ordered relative to valid blocks), and Ass. D.7 (square-root consistent convergence of $\hat{d}$), the choice $\beta(B) := 1 - \phi(B^{\frac{1}{4}})$ again makes this a consistent estimator (in the sense of Def. D.17).

There is also another catch: The naive bootstrap idea above actually over-controls false-positives, thus looses some power. This can be understood as follows:

Clearly the bootstrap has to break the time-alignment of the data to work. Interestingly this is also true under the null. Consider the following oversimplified example: If we bootstrapped random blocks *from the time-aligned blocks b_τ*, pick a quantile $q(\beta)$, and compare the values on the original b_τ to this q, we will find about $k \approx \beta\Theta$ blocks below q. However, while this agrees with the expectation of the binomial distribution $\mathrm{Binom}(n = \Theta, p = \beta)$, the result for k is *not* binomially distributed! Actually for $\Theta \to \infty$ we have $q \to q_{\mathrm{sample}}$, with q_{sample} the quantile of the original sample. The bootstrap introduces some randomness around this mean, but by the law of large numbers, it approaches the mean for large bootstrap-count, in particular $\mathrm{Var}(k) \to 0$. Meanwhile for the binomial $\mathrm{Var}(k) = \Theta\beta(1 - \beta) \to \infty$. For large bootstrap-count the approximation obtained for k in lemma 5.10 via this "aligned" bootstrap is thus extremely close to $k \approx b\tau$ and very rarely (with probability $\ll \alpha$) exceeds the upper α percentile of the much wider binomial.

We do not bootstrap from aligned blocks, but there is of course some non-trivial overlap and thus $q \not\perp q_{\mathrm{sample}}$. Indeed this effect is visible in benchmarking (see for example Fig. D.1). It can be avoided by cross-fitting (bootstrapping on two halves of the sample for the respective other half), up to the analytically tractable problem from rounding to integer cutoffs for k (see Rmk. 5.11). While the discrepancy in statistical power is not high, so that in most cases the simple / fast bootstrap is sufficient for practical purposes, it seems important to understand *why* it overcontrols false positives. Also the above argument shows that the bootstrap-count should, somewhat counter-intuitively *not be chosen too large*, to avoid loss of power. Since for the unaligned bootstrap, the random alignment is small, it makes still sense to have a large bootstrap-count in practice.

Remark D.21. As will be seen in the results concerning statistical power (§D.3.3) below, the difference between estimating q_β in an unbiased way and the consistency-requirement given by Def. D.17 does substantially affect scaling behavior of the test. Since heuristically it seems to still converge much faster than the weak regime test, this does likely not substantially affect our ability to implement an mCIT. Nevertheless, it should be noted that there are a few rather simple steps that may be taken to improve the estimation of q_β.

(i) Instead of through a mean, d_1 in the partial correlation approach (example D.18) could be estimated via a quantile β'. If $\beta' > a$, then this provides for $B \to \infty$ an unbiased estimate of d_1, and thus of q_β.

(ii) For homogeneity testing, other than for weak-regime testing, the value $d = 0$ is not special and the problem is essentially symmetric under exchange of d_0 and d_1. Instead of estimating a lower quantile of d_1 and comparing to $\hat{d}_0$, we could as well estimate an upper quantile of d_0 and compare to $\hat{d}_1$. In particular we could test in both directions, individually – and thus after correcting for multiple testing combined – control FPR and reject if either one has power.

(iii) In the light of (ii), we can assume w. l. o. g. $a \leq {}^1/_2$. Then the requirement $\beta' > a$ in (i) is effectively always satisfied (for at least one of the two tests) if $\beta' > {}^1/_2$. Thus for

partial correlation and for example picking $\beta' = {}^3\!/\!_4$ at least one of the two tests ends up with an unbiased estimate of q_β as $B \to \infty$.

Note, however, that while this may help keeping bias controlled better for finite B, it still becomes unbiased only for $B \to \infty$ (not for $N \to \infty$). Indeed by the impossibility of general IIDness / randomness tests (and Lemma D.24), clearly an unbiased estimate of q_β requires at least $B \geq 2$.
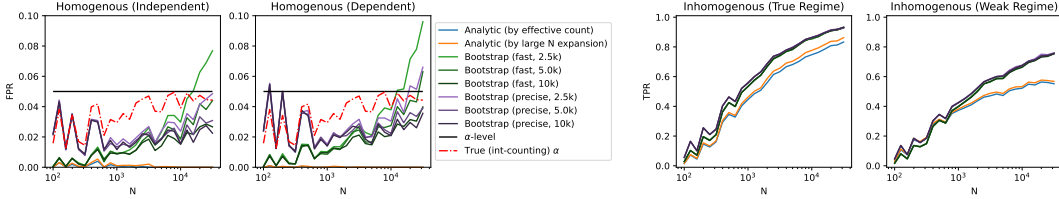

Figure D.1: Overview of results for homogeneity tests at $\alpha = 5\%$. Shown are FPR (type I errors) and TPR (power) for different estimates of the quantile q. Used $\alpha = 0.05$, $\beta = 0.1$ and block size $B = 15$, see §D.3.4. The red dash–dot line (lhs plot of FPRs) is slightly below α from rounding to an integer cutoff, cf. Rmk. 5.11.

Figure D.1 shows results (FPR and TPR) of numerical experiments for the homogeneity test combined with different quantile estimators. These numerical results support the functioning of this test at large, with the restriction that bootstrap approaches in particular seem to struggle with error-control on very large data-sets and require a sufficiently high number of bootstrap-samples to control errors on larger data-sets. Slightly more surprising, the analytical estimates are able to almost match bootstrap power despite over-controlling FPR on true-regime ground-truth scenarios. The main difference materializes for weak-regime cases. However, errors confusing homogeneous dependent and weak regime do not affect the marked independence tests immediately (they lead to the same output). This could affect the power of the homogeneity-first approach, discussed in §5.2.1. Intriguingly it does not: The fall-off in Fig. D.1 on weak regimes is primarily due to regimes with the same sign (of correlation) which reduces the separation, the need for homogeneity-first arises if the dependence-test does not perform well due to opposite sign (of correlation) in the different regimes (indeed for Fig. 5.4 an analytic estimate was used). This is also discussed in the paragraph "Validation and Weak Regimes" of §D.3.4.

Based on these considerations, we henceforth use the analytical estimates in our numerical experiments. For our general analysis, the potential performance gain by using a bootstrapped estimate does not seem to justify the runtime-cost. In applications and for extensions to time series (beyond MCI, cf. §B.6), the use of (suitable) bootstrapping strategies should be given further consideration.

D.3.2 Error Control

Using the quantile-estimates as described in the previous section, error-control is rather quick to show.

Lemma 5.10. *Fix a hyperparameter $\beta \in (0,1)$. Given $\alpha \in (0,1)$ and a sound estimator $\hat{q}_\beta^{\leq}$ of a lower bound of the β-quantile of the distribution in the d_1-regime (Def. D.17), then we can reject data-homogeneity with type I errors controlled at α as follows:*

Let $k := |\{\tau | d_\tau < q_\beta\}|$ be the number of blocks with d_τ less than q_β. Denote by $\phi_{\Theta,\beta}^{\mathrm{binom}}$ the cumulative distribution-function of the binomial distribution $\mathrm{Binom}(n = \Theta, p = \beta)$. Then $p_0 := 1 - \phi_{\Theta,\beta}^{\mathrm{binom}}(k)$ is a valid p-value under the null:

$$P_{\mathrm{homogenous}}(p_0 < \alpha) \leq \alpha.$$

In particular rejecting homogeneity iff $p_0 < \alpha$ leads to a valid test (Def. C.11).

Proof. By soundness of the quantile-estimator $p = \Pr(\hat{d} < \hat{q}_{\bar{\beta}}^{\leq}) \leq \beta$. The total number k of blocks with $\hat{d} < q$ under the null is binomially distributed as $\text{Binom}(n = \Theta, p)$. With $p \leq \beta$, we have $\phi_{\Theta,p}^{\text{binom}} \leq \phi_{\Theta,\beta}^{\text{binom}}$. Validity of p_0 then follows directly from the definition of the cumulative distribution function. $\qquad\square$

D.3.3   Power and Scaling Behavior

Error-control (Lemma 5.10) alone does not make for a meaningful statistical test. Even more so, since testing IIDness in general is not possible (cf. Prop. 5.3), the question arises, under which circumstances, our test will gain power asymptotically, and how the choice of hyperparameters will affect its convergence-speed. We discuss the asymptotic behavior theoretically and hyperparameter-choices semi-heuristically with the help of numerical experiments in §D.3.4.

Lemma D.22 (Binomial Test, Power)**.** *Let $\Lambda : \mathbb{N} \to \mathbb{R}$ be a scale (see Def. C.22), and assume we are given a pattern* Patt *(Def. 5.4) which is asymptotically Λ-compatible (Def. C.29) with the indicator meta-model $\mathcal{R}$ (see intro to §C) generating our data. Further we restrict to alternatives with exactly two regimes (Ass. D.15).*

Let $B(N) \to \infty$, such that $\frac{B(N)}{\Lambda(N)} \to 0$ and w. l. o. g.[19] $\Theta(N) = \lfloor \frac{N}{B(N)} \rfloor \to \infty$. We are given a consistent estimator $(\hat{q}_{\bar{\beta}}^{\leq}, \beta(B))$ of a lower bound of the β-quantile of the distribution in the d_1-regime (Def. D.17). Fix $\alpha(N) \to 0$ such that $\frac{\phi^{-1}(1-\alpha(N))}{\sqrt{\Theta(N)}} \to 0$, where ϕ is the standard-normal cdf. Such $\alpha(N)$ exist (cf. example D.23).

Then the test described in Lemma 5.10 with hyperparameters $B(N)$ and $\beta(B(N))$ is weakly asymptotically correct (Def. C.11).

Proof. In this case (homogeneity as opposed to weak-regime, see §D.4), there is uniform finite-sample error-control at $\alpha(N)$ by Lemma 5.10, thus by $\alpha(N) \to 0$ the probability of a correct results on models satisfying the null hypothesis (homogeneity) approaches 1, and we can focus on establishing the power-result, which by Ass. D.15 has exactly two regimes with $d_0 \neq d_1$ (see hypothesis).

Define
$$\beta_0(N) := P\Big(\hat{d}_{B(N)}^0 < \hat{q}_{\bar{\beta}(B(N))}^{\leq}\Big),$$

where $\hat{d}_B^0$ has the distribution of $\hat{d}$ applied to a valid block of size B in regime 0 with true value d_0. By definition D.17 of consistency of $\hat{q}_{\bar{\beta}}^{\leq}$, $\beta_0 \to 1$. The count k in Lemma 5.10 can be split as follows, where $\tau \in V$ are the valid blocks from the d_0-regime

$$k := |\{\tau | d_\tau < q_\beta\}| = |\{\tau | d_\tau < q_\beta, \tau \in V\}| + |\{\tau | d_\tau < q_\beta, \tau \notin V\}| =: k_0 + k_1.$$

In particular $k \geq k_0$ and $\frac{k_0}{\Theta} \to \beta_0 A \to A \to a > 0$ by asymptotic Λ-consistency and Lemma C.8. Let $\epsilon > 0$ be arbitrary. By $\frac{k_0}{\Theta} \to a > 0$, eventually $k_0 > \frac{\delta}{2}\Theta(N)$ with probability greater $1 - \epsilon$.

The null used by Lemma 5.10 is $k_{\text{null}} \sim \text{Binom}(\Theta, \beta(N))$, with $\beta \to 0$ thus eventually $\beta < \frac{\delta}{4}$. In particular, eventually $k_{\text{null}} \preceq \text{Binom}(\Theta, \frac{\delta}{4})$, and the cdf satisfies $\phi_{\Theta,\beta(N)}^{\text{binom}}(k) \geq \phi_{\Theta,\frac{\delta}{4}}^{\text{binom}}(k)$. Further, $\text{Binom}(\Theta, \frac{\delta}{4})$ approaches (for $\Theta \to \infty$), the normal distribution $\mathcal{N}(\mu = \Theta\frac{\delta}{4}, \sigma^2 = \frac{\delta}{4}(1 - \frac{\delta}{4})\Theta)$. Thus eventually

$$\phi_{\Theta,\beta(N)}^{\text{binom}}(k) \geq \phi_{\Theta,\frac{\delta}{4}}^{\text{binom}}(k) \approx \phi_{\mu=\Theta\frac{\delta}{4},\sigma^2=\frac{\delta}{4}(1-\frac{\delta}{4})\Theta}^{\text{normal}}(t).$$

---

[19]As long as $B(N) \to \infty$ is maintained, we may choose a smaller $B(N)$. In particular, it is always possible to ensure $\Theta(N) \to \infty$.

We reject for k above

$$k_{\text{null}}^{\alpha(N)} = \left(\phi_{\Theta,\beta(N)}^{\text{binom}}\right)^{-1}(1-\alpha) \leq \left(\phi_{\mu=\Theta\frac{\delta}{4},\sigma^2=\frac{\delta}{4}(1-\frac{\delta}{4})\Theta}^{\text{normal}}\right)^{-1}(1-\alpha)$$

$$= \Theta\frac{\delta}{4} + \phi^{-1}(1-\alpha)\sqrt{\frac{\delta}{4}(1-\frac{\delta}{4})\Theta}$$

$$= \Theta\left(\frac{\delta}{4} + \sqrt{\frac{\delta}{4}(1-\frac{\delta}{4})} \times \frac{\phi^{-1}(1-\alpha)}{\sqrt{\Theta}}\right),$$

where ϕ is the standard normal cdf. By hypothesis $\frac{\phi^{-1}(1-\alpha)}{\sqrt{\Theta}} \to 0$, thus eventually $k_{\text{null}}^{\alpha(N)} < \frac{\delta}{2}\Theta(N)$. Since $k \geq k_0 > \frac{\delta}{2}\Theta(N)$ with probability greater $1-\epsilon$, we eventually reject the null with probability greater $1-\epsilon$. The claimed power-result follows because $\epsilon > 0$ was arbitrary. $\qquad \square$

Example D.23 (Existence of hyperparameters). We show that choices for α with $\alpha(N) \to 0$ such that $\frac{\phi(1-\alpha(N))}{\sqrt{\Theta(N)}} \to 0$ exist. An example is $\alpha(N) = 1 - \phi(\Theta(N)^{\frac{1}{4}})$: By $\Theta \to \infty$ we get $\phi(\Theta(N)^{\frac{1}{4}}) \to 1$ and thus $\alpha \to 0$. Further $\frac{\phi^{-1}(1-\alpha)}{\sqrt{\Theta}} = \frac{\Theta(N)^{\frac{1}{4}}}{\Theta(N)^{\frac{1}{2}}} = \Theta(N)^{-\frac{1}{4}} \to 0$.

In Rmk. D.21, we have seen that obtaining an *unbiased* estimator of the β-quantile $\hat{q}_\beta$ is difficult. Indeed this subtlety is not by accident. Rather *knowing an unbiased estimator* would be extremely powerful, as the following *infinite duration limit* (see example C.24) result shows:

Lemma D.24 (Binomial Test, Power with Unbiased Quantile). *Modify the hypothesis of the previous Lemma D.22, by replacing $B \to \infty$ by $B = \text{const}$, and the pattern-applicability assumption by knowledge of an unbiased estimator $\hat{q}_\beta$ of the β-quantile of the distribution in the d_1-regime (Def. D.17). Finally additionally assume Ass. D.12 (invalid blocks are stochastically ordered relative to valid blocks). Then the conclusion that the test gains power asymptotically still holds.*

Proof. Define, as before,

$$\beta_0 := P\left(\hat{d}_B^0 < \hat{q}_\beta\right),$$

where $\hat{d}_B^0$ has the distribution of $\hat{d}$ applied to a valid block of size B in regime 0 with true value d_0. By Ass. D.10 (implied by the stronger Ass. D.12 given by hypothesis) $\beta_0 > \beta$. Still as before, the count k in Lemma 5.10 can be split, where $\tau \in V$ are the valid blocks from the d_0-regime

$$k := |\{\tau|d_\tau < q_\beta\}| = |\{\tau|d_\tau < q_\beta, \tau \in V\}| + |\{\tau|d_\tau < q_\beta, \tau \notin V\}| =: k_0 + k_1.$$

By Ass. D.12 (invalid blocks are stochastically ordered relative to valid blocks) $\hat{d}$ applied to an invalid block has $P(\hat{d} < \hat{q}_\beta) \geq \beta$, thus $k_1 \succeq \text{Binom}((1-A)\Theta, \beta)$ (where $\Theta = \lfloor\frac{N}{B}\rfloor$). Further $k_0 \sim \text{Binom}(A\Theta, \beta_0)$. For $\Theta \to \infty$ thus $\frac{k_0}{\Theta} \xrightarrow{P} A\beta_0$ and with probability approaching unity $\frac{k_1}{\Theta} \geq (1-A)\beta - \epsilon$, for any $\epsilon > 0$ in particular for $\epsilon = \frac{A}{2}(\beta_0 - \beta) > 0$. Therefore

$$\frac{k}{\Theta} = \frac{k_0 + k_1}{\Theta} \geq A\beta_0 + (1-A)\beta - \epsilon = \beta(A + (1-A)) + A(\beta_0 - \beta) - \epsilon$$

$$= \beta + \frac{A}{2}(\beta_0 - \beta) > \beta.$$

with probability approaching unity. The null used by Lemma 5.10 is $k_{\text{null}} \sim \text{Binom}(\Theta, \beta)$, thus $\frac{k_{\text{null}}}{\Theta} \xrightarrow{P} \beta$ and is rejected with probability approaching one (for details on the values of k, see the proof of Lemma D.22). $\qquad \square$

The reason why this argument could not be made in Lemma D.22 is that for a lower bound $q_{\bar{\beta}}^{\leq}$, the rate at which valid blocks in the d_1-regime have dependence below $q_{\bar{\beta}}^{\leq}$ does not approach β (as for an unbiased estimator). Instead, if $q_{\bar{\beta}}^{\leq} < d_1$ is strictly less, it will approach 0 (because $\hat{d}_1 \xrightarrow{\mathrm{P}} d_1$ in Lemma D.22). Thus $\frac{k_1}{\Theta}$ may get arbitrarily close to zero, and all contributions to k have to come from k_0 alone. Evidently, this is only possible if $a > \beta$, thus a consistent choice with $\beta \to 0$ is needed. This also further clarifies the choice of hyperparameters (see Rmk. D.19). These problems necessarily require that $B \to \infty$ if no unbiased estimator is available.

D.3.4 Semi-Heuristic Hyperparameter Choices

While the previous subsections provide a reasonable theoretical understanding of the meaning of the hyperparameters β (quantile) and B (block-size), the question for their practical numerical choice so far was not addressed. We do so by numerical experiments and a semi-heuristic interpretation. Given the systematic reduction of the MCD problem to simple stages within a local mCIT (see §5), typical runtimes of modular components (here: the homogeneity-test) are usually less than a millisecond per execution. Together with a comparatively simple specification of the individual subproblems solved by each stage, this allows for a rather comprehensive study of the behavior with different hyperparameters, ground-truth scenarios and data-set sizes. The present analysis also serves as a demonstrator for this advanced introspective capability.

Generally, the more prior information a user can supply, the better a choice of hyperparameters can be made. However, few applicants have infinite amounts of time to allocate to this task and to grind out every last bit of optimization here will often not be the best distribution of effort. To address real-world applications, we provide semi-heuristic hyperparameter-sets, where the user only has to specify one simple binary prior information: Are segments expected to be very large (hundreds of data points)? In this case, statistical power can be allocated to finding such very large structures substantially more efficiently than if one wants to search for smaller structures as well.

Convention D.25. We provide two hyperparameter sets: one for generic regime-sizes, one for large regime-sizes. Variation with sample-size N and conditioning-set size $|Z|$ will be handled semi-heuristically as explained below.

For this reason, most subsequent figures come in pairs (for example Fig. D.2 and Fig. D.3), once for data-generation with generic regimes (§C.3) and once with this same data-set filtered to include only typical lengths in the range $\ell = 100 \ldots 1000$ to better understand behavior of different hyperparameters on large regimes (see also Fig. 5.5a in the main text).

Pairwise Tests: We start by investigating the behavior of different hyperparameters for pairwise (unconditional, $Z = \emptyset$) tests under the four ground-truth scenarios of the univariate problem, see Fig. 5.3 in the main text; that is for global independence, global dependence, true regimes and weak regimes. Both global hypotheses are homogeneous (ground-truth negatives, null), while the true and weak regime cases are heterogeneous (ground-truth positives, alternatives) for the homogeneity test. In Fig. D.2, we thus study false positive rates (FPR) for the global hypotheses (on a color-scale that makes it easy to compare to $\alpha = 0.05$), and true positive rates (TPR) for the regime hypotheses. The underlying data-generation is for generic regimes as described in §C.3, Fig. D.3 shows the same information, but for larger ground-truth regimes.

We note first that FPR-control seems to work, but errors are over-controlled. This is expected (we use the analytic estimate, which really only bounds the error); for the shown results, $\alpha = 5\%$. Concerning statistical power (TPR), the most evident observation is that larger N improves power; this is a reasonable consistency-check, but of course expected – even though the scaling here is by an uninformative prior (see §C, in particular example C.15),
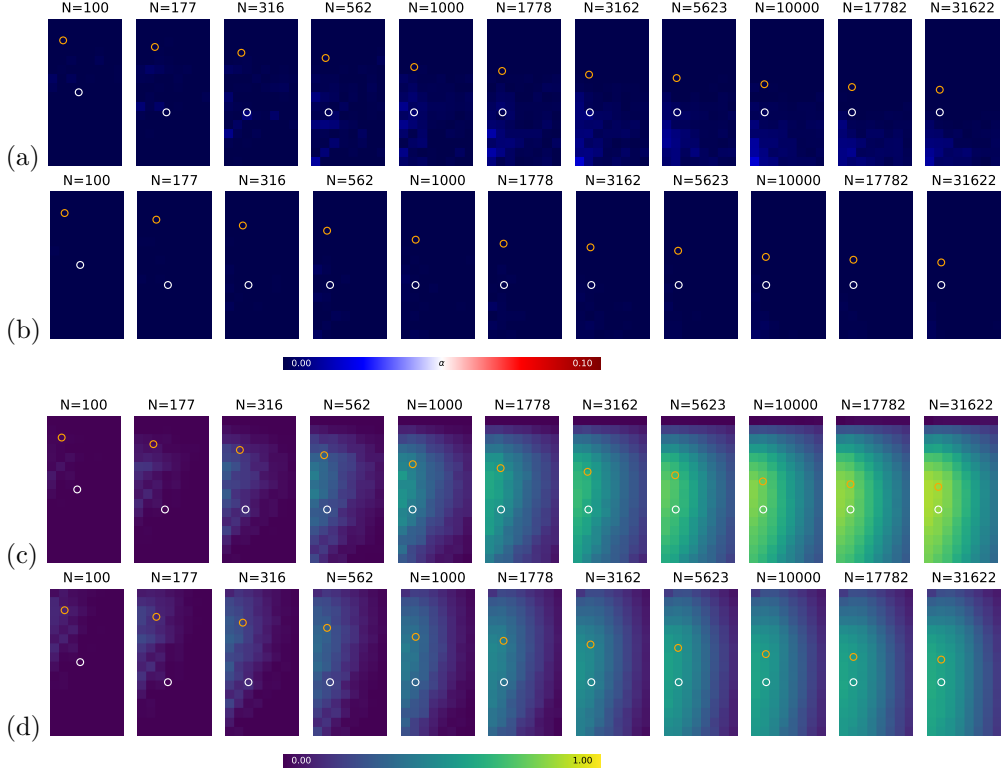
Figure D.2: *Pairwise Tests (generic L):* Behavior of false positives ((a) globally independent, (b) globally dependent) and true positives ((c) true regime, (d) weak regime) for generic prior of regime-lengths across hyperparameters (per image: x-direction is quantile $\beta = 0.05\ldots0.4$ linear, left-to-right, and y-direction is block-size $B = 5\ldots80$ logarithmic, top-to-bottom). Images within each row are for different sample-sizes $N = 10^2\ldots10^{4.5}$, logarithmic left-to-right. Indicated by circles are heuristic hyperparameter choices (orange: generic, white: optimized for large regimes).

that is typical segment-sizes only scale like $\log(N)$, which is a comparatively challenging benchmark.

Next, the left hand side region of the plots (small β) typically seem to perform favorable, even though Fig. D.3 suggests that at least for large ground-truth regimes, at smaller sample-sizes N a slightly higher choice of β can be favorable. Further a choice of β that is too small (especially for small N) seems to negatively affect stability and FPR-control; the panels (a) and (b) in the figures show only the average FPR (per pixel = hyperparameter choice), while FPR-control should work uniformly (not just across the the two global hypotheses (a) and (b), but also across regime-sizes, regime-fractions etc.). This is not really surprising, as small β, for small N (thus small number of blocks Θ) means the counting statistic $\text{Binom}(A\Theta, \beta)$ has to decide on the basis of typically very small counts. The choice of a decreasing β is also consistent with our theoretical considerations, even though the motivation there was in part different (see Rmk. D.19).

At least for the generic regime-lengths Fig. D.2, there is a trend discernible that for larger N larger B are more favorable. This does make sense, as for our data-set, the relative frequency of smaller regimes *does* at some point decay (see §C.3.2), even though only logarithmically fast (Lemma C.28). For already initially large regime-lengths this effect is much weaker, this could be simply because the logarithmic increase no longer matters at that point (relative to other factors). It could also be special to the (partial-)correlation setting, where dependence-estimates converge fast and increasing block-size has quickly diminishing return (increasing block-size decreases block-count, one would expect to operate
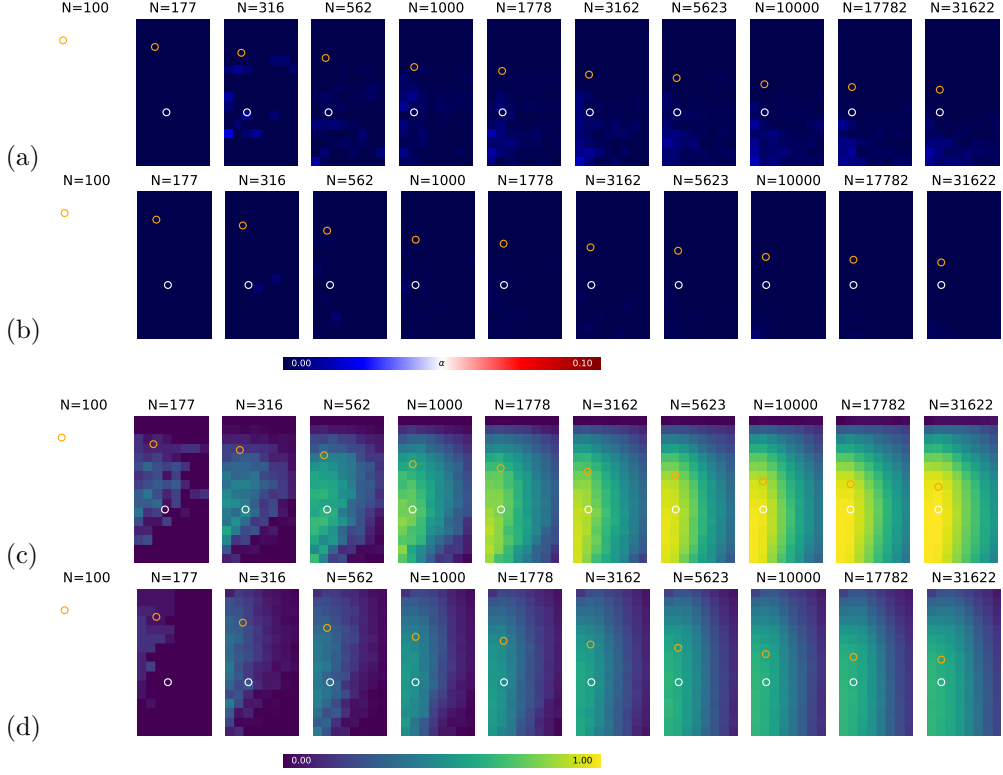
Figure D.3: *Pairwise Tests (large L):* Same as Fig. D.2, but for ground truth regime-length in the range $\ell = 100 \ldots 1000$, i.e. comparatively large.

on an effective sample-count $N\frac{B-3}{B}$ for correlation, which for large B no longer substantially depends on B).

We make our hyperparameter choices – indicated in Fig. D.2 and Fig. D.3 by orange (generic lengths) and white (large lengths) circles – for pairwise tests based on these observations: For large regimes, we pick a constant $B = 30$ (but with a minimum block-count of 5 for stability, which is why in the first column $N = 100$ and thus $B = \lfloor\frac{100}{5}\rfloor = 20 < 30$, moving the white circle up a notch in the first image). For the smaller regime-length case, we use the idea outlined in the explanation above, of logarithmically increasing typical lengths, to motivate a form $B = a\log_{10}(N) + b$, where a heuristic guess based on the numerical experiments for a and b is made as $a = 5$ and $b = -3$.

For β, we first have to discuss another issue: As already noted in Rmk. 5.11, the count k of below-q_β blocks used in the binomial test is discrete, so error-control will *not* happen at precisely α if we simply fix a value for β, then reject if $k \geq k_\beta$. Rather this controls somewhere below α (which is a valid test, but certainly not an optimal hyperparameter; as noted before, with the current parcorr-specific analytic estimate for q_β, we still overcontrol errors. Nevertheless we do not want to over-control more than we have to. Further, for other choices of quantile-estimators, see §D.3.1, this may become more relevant). The approach we employ instead is to start from an initial β_0, compute for the present values of N and B (thus of Θ), the value k_β^0 at which we could first reject with FPR less than α. Then we pick β as the largest value, for which rejecting above k_β^0 still controls FPR at α. Since this does not change the acceptance-threshold on k, only the estimate q_β, this can in practice only increase power. This procedure tends to produce $\beta \approx \beta_0$ for large Θ, while typically $\beta > \beta_0$ for small Θ (i.e. in particular for the combination of small N and large B, thus mostly for the large-regime hyperparameters and for small data-sets). Indeed starting from a reasonable

initial value $\beta_0 = 0.1$ typically seems to lead to acceptable results (the circles / parameters shown in the figures); thus there does not seem to be much reason for a more complicated choice of β_0 (given prior knowledge, or particular interest in small regime-fractions a may, however, motivate a deviation from this argument). Finally, this choice of β does not appear special in the figures. This is, because of the figures' finite resolution, providing pixels on nearby β only, which does not seem to resolve this rounding-optimization (on k_β).
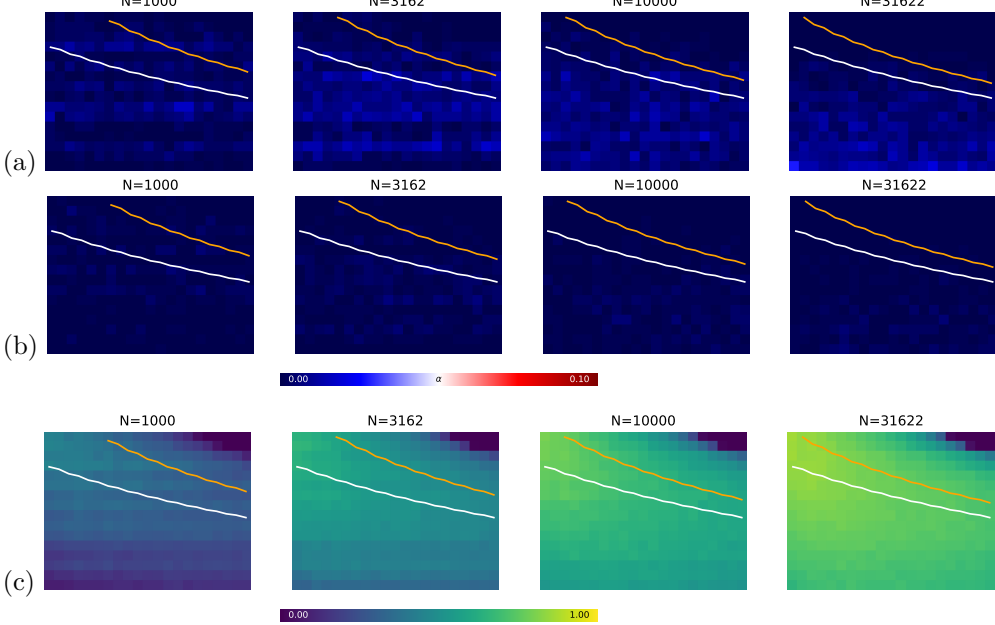
Figure D.4: *Conditional Tests (generic L):* Behavior of false positives ((a) globally independent, (b) globally dependent) and true positives ((c) true regime) for generic prior of regime-lengths for different conditioning-set sizes $|Z| = 0 \ldots 20$ (per image: x-direction; linear, left-to-right) across different block-sizes $B = 20 \ldots 150$ (larger than before; logarithmic, top-to-bottom; per image: y-direction) and for different sample-sizes. Indicated by plotted lines are heuristic hyperparameter choices (orange: generic, white: optimized for large regimes).

Conditional Tests: So far, we have only considered pairwise tests. We now move on to conditional tests (see §C.5 for details about the underlying model / data-generation). As discussed above, the choice of β (or rather $\beta_0 = 0.1$) can be kept simple. To avoid too high-dimensional data-sets, we thus only analyze different choices of B for different conditioning-set sizes $|Z|$. Figures D.4 and D.5 again show results for generic and filtered to large regimes respectively. The x-axes of the plots now show conditioning-set sizes from 0 to 20.

First, we note that again FPR-control seems to work. For statistical power, we initially focus on the true-regime case in these figures (see below for results on weak regimes).

We inspect panels (c) in both figures more closely. Focusing on a single row of pixels for any of the images shows a decrease of power with increasing $|Z|$. This does of course make sense, as larger conditioning-sets correspond to a more complex problem to solve. There is further an evident "dark corner" in the top right, corresponding to large $|Z|$ and small B. Note that for partial correlation, the effective sample count per block is $B - 3 - |Z|$ and if this number becomes non-positive, no rejection of the homogeneity-hypothesis is possible. For example the top-most row corresponds to $B = 20$, so $B - 3 - |Z| \leq 0$ for all $|Z| \geq 17$, i.e. for the top row, the last four pixels to the right will never have non-trivial power.

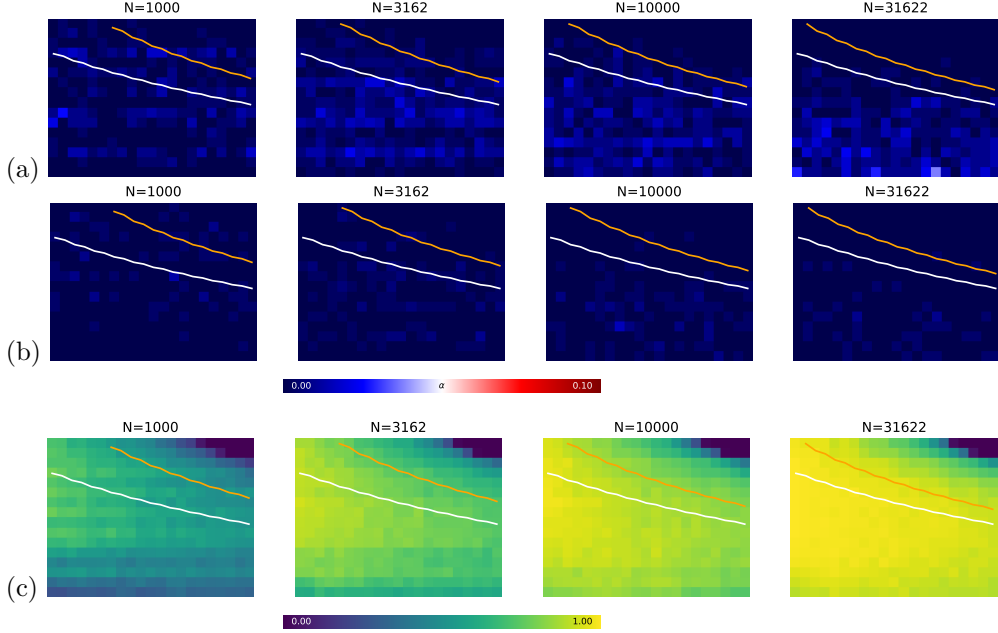A closer look at individual columns per image to check for optimal (per $|Z|$) values of

Figure D.5: *Conditional Tests (large L):* Same as Fig. D.4, but for ground truth regime-length in the range $\ell = 100 \ldots 1000$, i.e. comparatively large.

B suggests the use of larger B for larger $|Z|$, which makes sense, as we trade effective (per block) sample-size $B - 3 - |Z|$ vs. rate of invalid blocks χ; a trade-off which is affected by $|Z|$. This effective-sample count also suggests a linear behavior with $|Z|$, i.e. $B = B_0 + c|Z|$. Heuristically, we find $c = \frac{3}{2}$ as a reasonable choice (the y-axis in the images displayed in the figure is logarithmic).

Validation and Weak Regimes Finally, we validate our semi-heuristic hyperparameter choices for different N and $|Z|$ in figures D.6 and D.7 (for generic and large regimes respectively). Of particular note is the behavior on ground-truth weak-regimes (panel (d)).

The power on weak regimes is less relevant for the full mCIT. The mCIT only requires the homogeneity test *or* the global dependence test to have power on weak regimes. Global dependence primarily suffers a loss of power from cancellations between regimes. These occur for regimes with different signs (of correlation). Different signs tend to lead to large separation $\Delta d = |d_1 - d_0|$. Homogeneity tends to suffer from *low* separation Δd. Thus both tests are complementary in a very fortunate way. The homogeneity test, for example in Fig. D.6d, seems to approach TPR of around 0.5 rather quickly (different lines / colors), while it afterwards improves only much slower. To our understanding, this reflects the coin-flip in data-generation on relative sign of d_0 and d_1. Since (see above) the global dependence test works well for same-sign scenarios, it is in practice (for the mCIT) sufficient that the homogeneity-test gains power fast on the different-sign scenarios. This is reflected by the fast approach to around 0.5 in the figure.

The choice of α (not shown in included figures), does not seem to substantially affect the choice of other hyperparameters and produces very similar output.
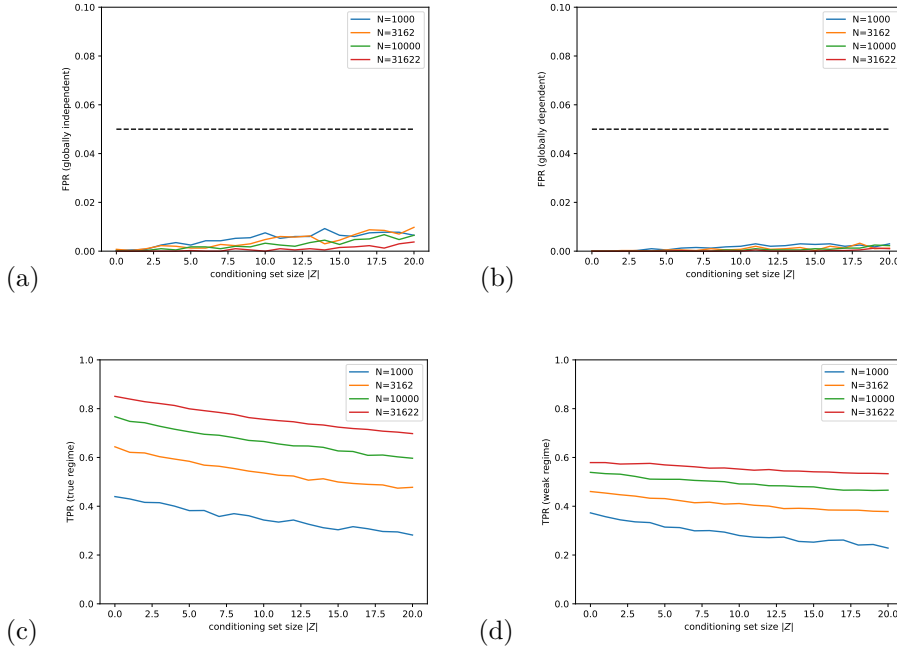
Figure D.6: Behavior of false positives ((a) globally independent, (b) globally dependent) and true positives ((c) true regime, (d) weak regime) for generic prior of regime-lengths validating heuristic hyperparameter sets for different sample-sizes.
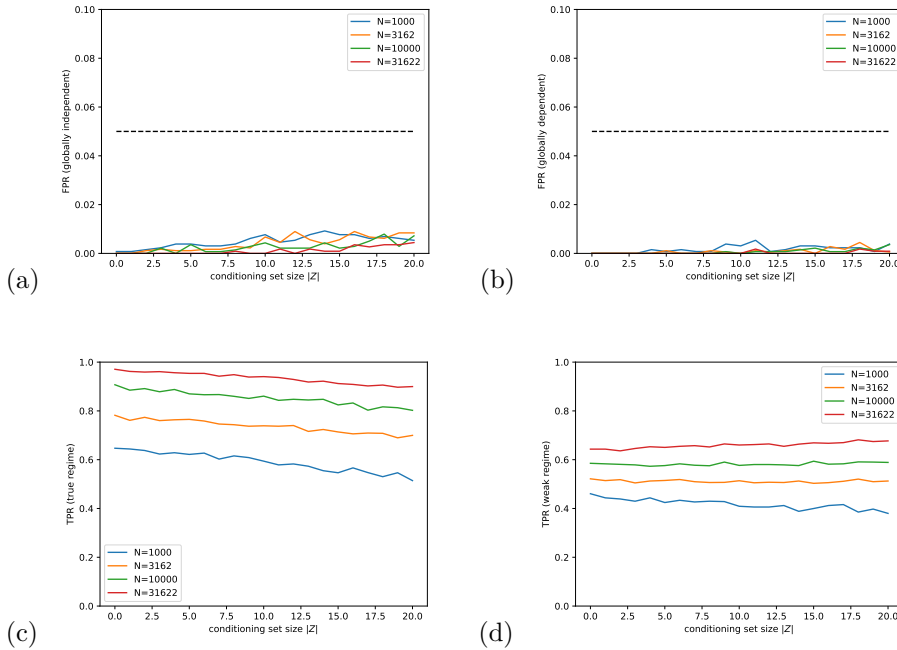

Figure D.7: Same as Fig. D.6, but for ground truth regime-length in the range $\ell = 100 \dots 1000$, i.e. comparatively large.

D.4 Weak Regimes

We analyze the weak regime problem (there are two regimes with dependencies d_0 and d_1, but both are non-zero) and the proposed acceptance-interval method (§5.2.3) in more detail. To do so, we will have to introduce some more notation and a few basic results concerning truncated normal distributions and mixtures. This makes a subsequent discussion of FPR-control, the interpretation of the $\chi \approx 0$ assumption of the main text (cf. Ass. 5.14) and finally of statistical power analysis more concise. We again conclude with semi-heuristic choices of hyperparameters.

D.4.1 Truncated Normal Distributions

We need to fix notation and collect some standard results on truncated normal distributions. This is a rather standard topic, for a textbook treatment see for example [30, §13]. Most computations can be reduced to statements about mills-ratios for which a vast array of approximations are known, see for example [18].

Definition D.26 (Truncated Normal Distribution). Let $X \sim \mathcal{N}(\mu, \sigma^2)$ and $a < b$, then $P(X|a \leq X \leq b)$ is the truncated at a and b normal distribution. If $a = -\infty$, $b = c$, we call $P_{\leq c} := P(X|X \leq c)$ truncated above the cutoff c.

Notation D.27. We use the following notations (usually these will be recalled or be clear from context where used):

$$\beta = \frac{c - \mu}{\sigma} \text{ (for a truncated above } c \text{ normal with parameters } \mu, \sigma)$$

$$\varphi(t) \text{ is the standard-normal pdf at } t$$

$$\phi(t) \text{ is the standard-normal cdf at } t$$

$$\phi^{-1}(p) \text{ is the standard-normal ppf (inverse cdf) at } p$$

$$\mu_{m,s}^c = E_{\mu=m,\sigma=s}[X|X \leq c]$$

$$m_{\mu,\sigma}^c(n) = n^{-1} \sum_{i=1}^{n} X \text{ for } X \sim \mathcal{N}(\mu, \sigma)_{\leq c} \text{ is the random variable describing}$$

$$\text{the sample-mean of a truncated normal distribution.}$$

$$\sigma_\alpha = \sigma \phi^{-1} \left(1 - \frac{\alpha}{2}\right) \text{ is the two-sided } \alpha \text{ confidence.}$$

Further, given n IID data points $D = \{x_1, \ldots, x_n\}$, then:

$$D_c = \{x_i \in D | x_i \leq c\} \text{ is the cut-off data-set with}$$

$$n_c = |D_c| \text{ data points.}$$

Lemma D.28 (Properties of Truncated Normal Distributions). *For a normal distributed $X \sim \mathcal{N}(\mu, \sigma)$ the truncation below c has the following properties:*

$$E[X|X \leq c] = \mu - \sigma \frac{\varphi(\beta)}{\phi(\beta)}$$

$$\text{Var}[X|X \leq c] = \sigma^2 \left(1 - \beta \frac{\varphi(\beta)}{\phi(\beta)} - \left(\frac{\varphi(\beta)}{\phi(\beta)}\right)^2\right) < \sigma^2.$$

Proof. These are standard results, see for example [30, §13, Eq. 13.134, Eq. 13.135]. A simple computation can already give good insight however: If $X \sim \mathcal{N}(0, 1)$ is standard normal, then the density of $P(X|\alpha \leq X \leq \beta)$ is $p(x) = \frac{\varphi(x)}{\phi(\beta) - \phi(\alpha)}$, thus

$$E[X|\alpha \leq X \leq \beta] = \frac{1}{\phi(\beta) - \phi(\alpha)} \int_\alpha^\beta x \varphi(x) \, dx.$$

A change of variables to $y := \frac{x^2}{2}$ (and splitting the integral at 0, if α, β have different signs) plugged into the explicit form of $\varphi(x)$, leads to an integral of the form $\int e^{-y}$ which can of course be solved. By reinstating x the result of the integration is again of the form $\varphi(\beta) - \varphi(\alpha)$. With the normalization of $p(x)$ and setting $\alpha = -\infty$ we get the result for $\mu = 0$ and $\sigma = 1$. The general case follows by suitable change of variables.

The variance result can be obtained for example by using $s := \sigma^{-2}$ and $\frac{d}{ds}\varphi\left(\frac{x-\mu}{\sigma}\right) = -\frac{1}{2}(x-\mu)^2\varphi\left(\frac{x-\mu}{\sigma}\right)$ to solve the quadratic integral (by exchanging order of integration with differentiation).

For the inequality for the variance, we have to show $\beta + \frac{\varphi(\beta)}{\phi(\beta)} \geq 0$. If $\beta \geq 0$, this is evident. If $\beta < 0$, use $\tilde{\beta} = -\beta > 0$, then the above inequality becomes $-\tilde{\beta} + \frac{\varphi(\tilde{\beta})}{1-\phi(\tilde{\beta})} \geq 0$. Since $\tilde{\beta} \geq 0$, the mills-ratio $m(\tilde{\beta}) = \frac{1-\phi(\tilde{\beta})}{\varphi(\tilde{\beta})}$ is known to satisfy $m(\tilde{\beta}) < \tilde{\beta}^{-1}$ (see e. g. [18, Eq. 32, p. 1844]), which gives a slightly stronger statement). Thus $\frac{\varphi(\tilde{\beta})}{1-\phi(\tilde{\beta})} > \tilde{\beta}$ and therefore indeed $-\tilde{\beta} + \frac{\varphi(\tilde{\beta})}{1-\phi(\tilde{\beta})} \geq 0$. $\qquad\square$

D.4.2 Mixtures

The direct testing problem naturally is formulated on mixtures (see also the illustration in Fig. 5.3). Formally we define mixtures follows:

Definition D.29 (Mixture). Given two random variables X and Y, then for $\lambda \in [0,1]$, the λ-mixture (Z,C) consists of an observed random variable $Z = CY + (1-C)X$ and an unobserved binary random variable $C \in \{0,1\}$ with $P(C=0) = \lambda$.

Given two random variables X and Y, then a (n^X, n^Y)-mixed data-set of size $n = n^X + n^Y$ is is a set $D = \{z_1, \ldots, z_n\}$ drawn from (an n-fold product of) a λ-mixture (see above) conditioned on $\sum_i c_i = n^Y$; the choice of λ is arbitrary (by the conditioning), as long as $\lambda \in (0,1)$ so that the conditioned distribution is defined.

Lemma D.30 (Means of Cutoff Mixtures). *Let $X \sim \mathcal{N}(\mu, \sigma)$, and $Y \sim Q$ independent stochastically ordered $X \preceq Y$ (Def. C.20) random variables. Given is a (n^X, n^Y) mixed data-set $z_1, \ldots, z_n$ of size n (cf. Def. D.29), set $\lambda := {}^{n^X}/n$. Further define q_λ as the λ-quantile of this mixture. Then $\forall c \leq q_\lambda$, on the cut-off dataset $D_c = \{z_i | z_i < c\}$ with n_c elements and mean*

$$m := n_c^{-1} \sum_{i|z_i < c} z_i$$

the following inequalities are satisfied for large n_c:

$$\Pr\left(m > \mu + \frac{\sigma_\alpha}{\sqrt{n_c}}\right) \leq \frac{\alpha}{2}$$

$$\Pr\left(m < \mu_{\mu,\sigma}^c - \frac{\sigma_\alpha}{\sqrt{n_c}}\right) \leq \frac{\alpha}{2}$$

Proof. From our definition of mixtures (Def. D.29), it is clear that we can formally (using the unobserved but well-defined values C_i) count data points in the cut-off mixture by their origin (X or Y) by defining $n_c^X := \sum_{i|z_i < c} c_i$ and $n_c^Y := n_c - n_c^X$ (in analogy to the non-cutoff n^X and n^Y). We introduce the notation (cf. Fig. 5.6) $n_{\text{lost}} := n^X - n_c^X$ the number of data points "lost" by cutting of at c and call data points n_c^Y from Y included into the cut-off data-set impurities.

From $c \leq q_\lambda$ and $\lambda = {}^{n^X}/n$ it is immediately evident that $n_c \leq n^X$, which implies a bound on impurities n_c^Y by lost data points n_{lost}

$$n_c^Y = n_c - n_c^X \leq n^X - n_c^X = n_{\text{lost}}.$$

Using this we readily obtain

$$m = n_c^{-1} \sum_{i|z_i<c} z_i = n_c^{-1}\Big(\sum_{i|z_i<c,c_i=0} z_i + \sum_{i|z_i<c,c_i=1} z_i \Big)$$

$$< n_c^{-1}\Big(\sum_{i|z_i<c,c_i=0} z_i + n_c^Y \times c \Big)$$

$$\le n_c^{-1}\Big(\sum_{i|z_i<c,c_i=0} z_i + \sum_{i|c\le z_i\le q^X,c_i=0} z_i \Big) =: m',$$

where q^X in the last term is the $n_c/n^X \le 1$ quantile such that the two sums in the last line contain precisely n_c terms (the first one contains n_c^X terms, thus the second contains n_c^Y terms each of magnitude $\ge c$, so the last inequality holds), actually the $n_c \le n^X$ (see above) lowest values drawn from X. The right-hand side is a mean $m_{\mu,\sigma}^{q^X}(n_c)$ over n_c values drawn from a cut-off at q^X normal-distribution, thus by

$$\Pr\Big(m > \mu + \frac{\sigma_\alpha}{\sqrt{n_c}}\Big) \overset{m\le m'}{\le} \Pr\Big(m' = m_{\mu,\sigma}^{q^X}(n_c) > \mu + \frac{\sigma_\alpha}{\sqrt{n_c}}\Big)$$

$$\le \Pr\Big(m_{\mu,\sigma}^\infty(n_c) > \mu + \frac{\sigma_\alpha}{\sqrt{n_c}}\Big) = \frac{\alpha}{2}.$$

This is the first inequality we have to show.

For the second inequality we first use the stochastic ordering hypothesis to employ the cut-off at c distribution of X as a (stochastic) lower bound for the mixture (by $X \preceq Y$, any λ-mixture Z of X and Y is such that $X \preceq Z$). so we have to show that taking a mean over n_c data points drawn from a cut-off above c normal $\mathcal{N}(\mu,\sigma)$ satisfies this inequality. Note that for n_c large enough, by CLT the distribution of this mean-value approaches a normal distribution with mean $\mu_{\mu,\sigma}^c$ and variance $n_c^{-1}\sigma_c^2$. By Lemma D.28 $\sigma_c^2 \le \sigma^2$, and thus the second inequality holds for large n_c. □

D.4.3   The Approximation of 'Few' Invalid Blocks

The main text, in Ass. 5.14, assumes $\chi \approx 0$, i.e. there are "few" invalid blocks. In the finite-sample case (and in practice) this can be understood as an approximation: As long as χ is small, the formal results provided yield a reasonable estimate. In the case of an asymptotic limit, a little bit more care should be taken in defining what "$\chi \approx 0$" is supposed to mean formally, and in validating that this approximation is meaningful (can be satisfied, hopefully plausibly so) even in a limit.

To this end, we first proof a slight modification of the soundness of the interval test (Lemma 5.15), the version in the main text follows as described in Rmk. D.33 below:

Lemma D.31 (Acceptance Interval). *Choose a cutoff $c > 0$ and a minimal valid size $n_0^{\min}$, compute the mean $\hat{d}_{\mathrm{weak}}$ of blocks of dependence $\hat{d}$ with $\hat{d} < c$ where the number of such blocks is n_c.*

$$\hat{d}_{\mathrm{weak}} = n_c^{-1} \sum_{\tau|\hat{d}_\tau\le c} \hat{d}_\tau$$

We assume Ass. 5.7/D.7 (there is an underlying $\hat{d}$ with known or estimated null-distribution, for its variance on block-size B write σ_B^2) additionally satisfying Ass. D.10 and Ass. D.12 (estimates by $\hat{d}$ are stochastically ordered, and on invalid blocks are stochastically ordered relative to valid blocks), Ass. D.13 ($\hat{d}$ is approximately normal; for valid blocks with $d_0 = 0$) and Ass. D.15 (there are exactly two regimes).

Given an error-control target $\alpha > 0$, and a hyperparameter $\sigma_\chi(\Theta, A_c) \ge 0$ (for A_c see below), let $\sigma_{n_c}^\alpha = n_c^{-\frac{1}{2}}\sigma_B\phi(1-\frac{\alpha}{2})$ be the (two-sided) α-interval around 0. Define an acceptance

interval $I := [\mu^c_{0,\sigma_B} - \sigma^\alpha_{n_c}, \sigma^\alpha_{n_c} + \sigma^\chi_{n_c}]$. Accept the null hypothesis (independence of the weak regime) if $n_c \geq n^{\min}_0$ and $\hat{d}_{\text{weak}} \in I$, otherwise reject it.

For any N, defining $A_c := \frac{n_c}{\Theta}$ (recall that A was the fraction of data points in valid d_0-blocks, and that $A \in [a - \chi, a]$, Lemma C.8), this method controls false positives if

(i) $\left(1 - \frac{A}{A_c}\right)c \leq \sigma_\chi(\Theta, A_c)$ *and*

(ii) $A \geq a^{\min}(n^{\min}_0)$, *see Rmk. D.32 below for $a^{\min}(n^{\min}_0)$.*

Proof. By construction of $a^{\min}(n^{\min}_0)$ (see Rmk. D.32), if (ii) is satisfied $n_c \geq n^{\min}_0$ (this may be true only up to $\tilde{\alpha} < \alpha$, in which case α below is to be replaced by $\alpha - \tilde{\alpha}$ to account for multiple testing) and we only have to check the rejection-criterion $\hat{d}_{\text{weak}} \in I$.

We want to apply Lemma D.30 with $X = \hat{d}_0$ on valid blocks from regime 0 and $Y = \hat{d}_1$ a mixture of valid blocks from regime 1 and invalid blocks. By the mixing assumption (Ass. D.12; applying $\hat{d}$ to invalid blocks is stochastically ordered relative to valid blocks) these satisfy $X \preceq Y$. By definition of A there are $n^X = A\Theta$ valid blocks in regime 0 (using the naming conventions of Lemma D.30) and $n = n^X + n^Y = \Theta$. To apply Lemma D.30, we need that for $\lambda = \frac{n^X}{n} = A$, the λ-quantile q_λ (on all considered blocks) satisfies $c \leq q_\lambda = q_A$.

If $c \leq q_A$, we can thus apply Lemma D.30 as is. If $c > q_A$, we proceed as follows: Define $\tilde{c} := q_A < c$, then apply Lemma D.30 with $\tilde{c}$, yielding (under the null, i.e. for $d_0 = 0$) a mean-value $\tilde{m} \in [\mu^c_{0,\sigma_B} - \frac{\sigma_\alpha}{\sqrt{\tilde{n}_c}}, \frac{\sigma_\alpha}{\sqrt{\tilde{n}_c}}]$ with probability $> 1 - \alpha$, where $\tilde{n}_c = A\Theta$ (by choice of $\tilde{c}$). Note that (using $\tilde{c} < c$, see above)

$$\hat{d}_{\text{weak}} = n_c^{-1} \sum_{\tau | \hat{d}_\tau \leq c} \hat{d}_\tau$$

$$= n_c^{-1} \left(\sum_{\tau | \hat{d}_\tau \leq \tilde{c}} \hat{d}_\tau + \sum_{\tau | \tilde{c} < \hat{d}_\tau \leq c} \hat{d}_\tau \right)$$

$$\leq \left(\frac{\tilde{n}_c}{n_c} \tilde{n}_c^{-1} \sum_{\tau | \hat{d}_\tau \leq \tilde{c}} \hat{d}_\tau \right) + \left(n_c^{-1}(n_c - \tilde{n}_c)c \right)$$

$$= \frac{\tilde{n}_c}{n_c} \tilde{m} + \left(1 - \frac{A}{A_c} \right)c,$$

where the inequality holds because the second sum has $n_c - \tilde{n}_c$ terms in the range $\tilde{c}$ to c. This provides an upper bound. By $\tilde{c} > 0$ (already the valid blocks from d_0 are distributed around zero, thus q_A should always be positive, at least if $n_c \gg 1$, which we may assume by suitable choice $n^{\min}_0$) the second sum can be approximated *below* by zero to yield $\hat{d}_{\text{weak}} \geq \frac{\tilde{n}_c}{n_c} \tilde{m}$. From the α-bounds on $\tilde{m}$ and $\tilde{n}_c < n_c$, thus $\sqrt{\frac{\tilde{n}_c}{n_c}} < 1$, we have $m \in [\mu^c_{0,\sigma_B} - \frac{\sigma_\alpha}{\sqrt{n_c}}, \frac{\sigma_\alpha}{\sqrt{n_c}} + \left(1 - \frac{A}{A_c}\right)c]$ up to probability α. In particular, if $\left(1 - \frac{A}{A_c}\right)c \leq \sigma_\chi(\Theta, A_c)$ the acceptance-interval I contains an α-confidence region. □

Remark D.32 (Choice of $n^{\min}_0$). Instead of choosing $n^{\min}_0$, it is also possible to choose a minimum regime-size $a^{\min}$, or to express a given $n^{\min}_0$ as $a^{\min}(n^{\min}_0, \chi)$ as follows. We are given precisely $n^0 = A\Theta$ valid blocks from the d_0-regime, each of these has a $\hat{d}$ score below the cutoff c with probability $\Pr(\hat{d}^B_0 \leq c)$. Let n^0_c be the number of valid d_0 blocks with $\hat{d} \leq c$. Clearly $n_c \geq n^0_c$ and n^0_c is distributed as $\text{Binom}(n^0, \Pr(\hat{d}^B_0 \leq c))$. Let ϕ_{n_c} be the cdf of this distribution, and define $n^{\min}_0 := \phi^{-1}_{n_c}(\alpha)$. If $A \geq a^{\min}$ (as assumed by the lemma) then $\Pr(n_c < n^{\min}_0) < \alpha$ by construction. Choosing appropriate α values here and for σ_α to account for multiple testing provides a valid test.

In practice, neither a nor χ are known, and a heuristic choice of $n^{\min}_0$ is employed with the understanding that α error control accounts for uncertainty in the dependence-estimate only, not for the uncertainty in the relation of $n^{\min}_0$ to $a^{\min}$.

Here $\sigma_{n_0}^\chi$ is an additional hyperparameter. This hyperparameter in many ways exists merely in a formal sense: It is not independent of α and can formally also be absorbed (in a suitable sense, see below) into c as long as $c < q_a$ is strictly smaller q_a. This is also the reason, why Lemma 5.15 as stated in the main text is correct with the interpretation of $\chi \approx 0$ as meaning $\chi \leq a - A_c$:

Remark D.33. For the formulation in the main text (Lemma 5.15), where $c < q_a$ (thus $A_c < a$), we can then interpret $\chi \approx 0$ formally as $\chi \leq a - A_c$, because then $A \geq a - \chi \geq A_c$ and Lemma D.31 applies with $\sigma_\chi = 0$.

Similarly, for $c \leq q_A$ (that is replacing the independent regime-fraction a by the fraction of valid independent blocks A on the quantile: $q_a \mapsto q_A$), we have $A_c \leq A$, thus $\left(1 - \frac{A}{A_c}\right)c \leq 0$ and Lemma D.31 again applies with $\sigma_\chi = 0$.

D.4.4 Power and Scaling Behavior

We start by a result for a (fixed) choice $c(N)$ in Lemma D.34. It appears to be the case that also the choice of a quantile[20] $\bar{c}$ entailing $c = \max(0, q_{\bar{c}})$ leads to a similar result. We focus on the fixed $c(N)$ case, at it seemed to produce more stable results in practice. The asymptotic behavior in that case is insightful only in part as the reliance in particular of step 2b on rejection by $n_0^{\min}$ seems to confound the finite-sample behavior rather than explain it.

Indeed a more insightful behavior is encountered when studying infinite-duration limits, see Lemma D.36. In this case, I will (and can, Prop. 5.12) no longer collapse to a single point. However, it becomes clearer which phenomena on finite sample sizes are actually relevant for gaining power fast. This second result as stated is not used elsewhere in this paper, but its proof provides substantial insight into the problem.

Lemma D.34 (Interval-Test, Power for fixed $c(N)$). *Let $\Lambda : \mathbb{N} \to \mathbb{R}$ be a scale (see Def. C.22), and assume we are given a pattern* Patt *(Def. 5.4) which is asymptotically Λ-compatible (Def. C.29) with the indicator meta-model $\mathcal{R}$ (see intro to §C) generating our data. Further we assume Ass. 5.7/D.7 (there is an underlying $\hat{d}$ with known or estimated null-distribution, for its variance on block-size B write σ_B^2) additionally satisfying Ass. D.10 and Ass. D.12 (estimates by $\hat{d}$ are stochastically ordered, and on invalid blocks are stochastically ordered relative to valid blocks), Ass. D.13 ($\hat{d}$ is approximately normal) and Ass. D.15 (there are exactly two regimes).*

Fix the hyperparameters according to the following (satisfiable, see example D.35) requirements:

(i) $B(N) \to \infty$, *while* $\frac{B(N)}{\Lambda(N)} \to 0$ *and* $\Theta(N) = \lfloor \frac{N}{B(N)} \rfloor \to \infty$

(ii) $c(N) \to 0$ *while* $c(N)\sqrt{B(N)} \to \infty$,

(iii) $\frac{n_0^{\min}(N)}{\Theta(N)} \to 0$, *while* $\frac{n_0^{\min}}{\Theta(N)} \exp(B(N)) \to \infty$ *and* $n_0^{\min} \to \infty$,

(iv) $\alpha(N) \to 0$ *while* $B(N)^{-\frac{1}{2}} n_0^{\min}(N)^{-\frac{1}{2}} \phi^{-1}(1 - \frac{\alpha}{2}) \to 0$,

(v) $\sigma_\chi(N) \to 0$ *while* $\sigma_\chi(N) \geq \varepsilon c(N)$ *for some* $\varepsilon > 0$.

The test described in Lemma D.31 with hyperparameters satisfying the above requirements is weakly asymptotically correct (Def. C.11).

Proof. We show first that the test gains power (steps 1 and 2), then that it controls false positives in a suitable sense (steps 3 and 4).

The test gains power: We show that we always reject either for the $n_c < n_0^{\min}$ criterion, or because $I \to \{0\}$ (step 1) and eventually the estimate $\hat{d}_0 \neq 0$ (step 2).

---

[20]The quantile $q_{\bar{c}}$ on the full dataset is of course known from data, given $\bar{c}$.

Step 1 (size of acceptance region approaches 0*):* We first show that $I \to \{0\}$. If $n_c < n_0^{\min}$, we reject for the $n_c < n_0^{\min}$ criterion. Otherwise $n_c \geq n_0^{\min}$ and thus $\sigma_{n_c}^{\alpha} \leq \sigma_{B(N)} n_0^{\min}(N)^{-\frac{1}{2}} \phi^{-1}(1 - \frac{\alpha}{2}) \sim B(N)^{-\frac{1}{2}} n_0^{\min}(N)^{-\frac{1}{2}} \phi^{-1}(1 - \frac{\alpha}{2}) \to 0$ (by Ass. D.7 and hypothesis iv). The acceptance interval I uses μ_{0,σ_B}^c, i.e. it truncates a normal with true parameter $\mu = 0$, calling the corresponding β (cf. notations D.27) $\beta_0 := \frac{c-\mu}{\sigma_B}$, we thus have $\beta_0(N) = \frac{c(N)}{\sigma_{B(N)}} \to \infty$ by $c(N)\sqrt{B(N)} \to \infty$ (hypothesis ii) and $\sigma_B^{-2} \sim B$ by Ass. 5.7, thus $\varphi(\beta_0(N)) \to 0$ and $\phi(\beta_0(N)) \to 1$ such that by Lemma D.28

$$\mu_{0,\sigma_B}^c = -\sigma_B \frac{\varphi(\beta_0(N))}{\phi(\beta_0(N)))} \to 0.$$

Finally $\sigma_\chi(N) \to 0$ (by hypothesis v).

Step 2 (rejection outside acceptance region): Since we are showing that the weak-regime test gains power, we study a model satisfying the alternative hypothesis, thus $d_0 \neq 0$. We distinguish sub-cases by the sign of d_0 (relative to d_1, notation D.16).

Case a $(d_0 < 0)$: By $d_1 > 0$ and $\sigma_B \to 0$ (by hypothesis i and Ass. D.7) we have $P(\hat{d}_1^B \leq c) \to 0$ via $c \to 0$ (hypothesis ii) and $d_1 > 0$ (notation D.16). With $a > 0$ thus $m \to \mu_{d_0,\sigma_B}^c < d_0 < 0$. Thus eventually $m \notin I$ by step 1.

Case b $(d_0 > 0)$: By $c \to 0$ (hypothesis ii) and $\sigma_B \to 0$ (by hypothesis i and Ass. D.7) the value $d_0 > 0$ eventually becomes large compared to c relative to the scale set by σ_B; with $d_1 > d_0$ this is also true for d_1, so eventually n_c becomes small. We have to show that $n_c \to 0$ faster than $n_0^{\min} \to 0$. Formally $P(\hat{d}_0^B \leq c) \to \phi(d_0/\sigma_B) < \text{const}(d_0) \times \exp(-\sigma_B^{-2})$. And by $d_1 > d_0$ (by Ass. D.12) also on invalid or dependent blocks $P(\hat{d}_1^B \leq c) \leq P(\hat{d}_0^B \leq c) < \text{const}(d_0) \times \exp(-\sigma_B^{-2})$ is bounded by this term. This thus covers *all* blocks in the data-set such that $n_c = P(\hat{d}^B \leq c) \times \Theta(N) < \text{const}(d_0) \times \exp(-\sigma_B^{-2}) \times \Theta(N)$. Thus $\frac{n_c}{\Theta} \exp(B(N)) \to \text{const}$ (where potentially $\text{const} = 0$, the previous term was an upper *bound*; using again $\sigma_B^{-2} \sim B$). Meanwhile (by hypothesis iii) for $n_0^{\min}$ we have $\frac{n_0^{\min}}{\Theta(N)} \exp(B(N)) \to \infty$. Therefore, eventually $n_c < n_0^{\min}$, which leads to rejection of the null hypothesis.

The test controls false positives: Whenever Lemma D.31 applies, i.e. if $\left(1 - \frac{A}{A_c}\right) c \leq \sigma_\chi(\Theta, A_c)$ and $A \geq a^{\min}(n_0^{\min}, \chi)$, false positives are controlled up to $\alpha(N) \to 0$ and the claim will follow. Thus we show that the asymptotic behaviors of $\left(1 - \frac{A}{A_c}\right) c \leq \sigma_\chi(\Theta, A_c)$ (step 3) and $A \geq a^{\min}(n_0^{\min}, \chi)$ (step 4) are such that the Lemma applies with probability approaching 1. Further, for false-positive control, we are considering the null, that is $d_0 = 0$.

Step 3: Again by $c(N)\sqrt{B(N)} \to \infty$ (hypothesis ii) and $\sigma_B^{-2} \sim B$ (by Ass. 5.7) we find $\frac{c(N)}{\sigma_B(N)} \to \infty$. This mean, eventually (up to any ϵ) all independent valid blocks are in the cut-off data-set thus $n_c \geq A\Theta$. With $\sigma_B \to 0$ and $d_1 > 0$ eventually valid dependent blocks are not in the cut-off data-set thus $n_c \leq (A + \chi)\Theta$. By $\chi \to 0$ (by hypothesis on pattern compatibility), thus $n_c \to A\Theta$ and therefore $A_c \to A$. So for any $\varepsilon > 0$ (in particular for the one in hypothesis v) eventually $1 - \frac{A}{A_c} < \varepsilon$. Therefore eventually $\left(1 - \frac{A}{A_c}\right) c \leq \varepsilon c \leq \sigma_\chi$ (the last inequality holds by hypothesis v).

Step 4: For $A \geq a^{\min}(n_0^{\min}, \chi)$, note that by asymptotic Λ-compatibility of the pattern (Def. C.29) $A \to a > 0$ (using Lemma C.8). Because $\frac{n_0^{\min}(N)}{\Theta(N)} \to 0$ (by hypothesis iii), $a^{\min}(n_0^{\min}, \chi) \to 0$ (see Rmk. D.32). In particular eventually $A \geq a^{\min}(n_0^{\min}, \chi)$ is satisfied with probability approaching one. $\qquad\square$

Example D.35 (Existence of hyperparameters)**.** First fix a $B(N)$ with property (i), which clearly exists if $\Lambda \to \infty$. Choices for the other hyperparameters with the required scaling-

properties exist for any such $B(N)$. For example:

$$c(N) = B(N)^{-\frac{1}{4}}$$
$$n_0^{\min}(N) = \Theta(N) \times \max\left(\Theta(N)^{-\frac{1}{2}}, B(N)^{-1}\right)$$
$$\sigma_\chi(N) = \varepsilon c(N)$$
$$\alpha(N) = 2 - 2\phi\left(B(N)^{\frac{1}{2}}\right)$$

The increasing scale Λ is required to ensure that the acceptance-region asymptotically does excludes any alternative and achieves false-positive control by ensuring applicability of Lemma D.31. The study of power under a finite acceptance region (conceding the possibility of gaining power on some alternatives) unveils interesting formal properties of the problem (cf. proof, case 2).

Lemma D.36 (Interval-Test, Power for constant B and c)**.** *We assume Ass. 5.7/D.7 (there is an underlying $\hat{d}$ with known or estimated null-distribution, for its variance on block-size B write σ_B^2) additionally satisfying Ass. D.10 and Ass. D.12 (estimates by $\hat{d}$ are stochastically ordered, and on invalid blocks are stochastically ordered relative to valid blocks), Ass. D.13 ($\hat{d}$ is approximately normal; for valid blocks with $d_0 = 0$) and Ass. D.15 (there are exactly two regimes).*

Fix $\alpha > 0$, $B \in \mathbb{N}$ and $c > \sigma_B$, assuming Ass. 5.14 (acceptance interval applicability). If $d_0 \notin [\mu_{0,\sigma_B}^c, \sigma_B]$, then the interval method asymptotically approaches unity power, i.e. for ground-truth weak regimes with $d_0 \notin [\mu_{0,\sigma_B}^c, \sigma_B]$ the probability p_{test} of correctly classifying this scenario as weak regime satisfies $p_{\text{test}} \to 1$ for $N \to \infty$.

Remark D.37. We will assume for the proof that $\frac{\varphi(\beta)}{\phi(\beta)}$ is monotonically decreasing, and that $\frac{\varphi(\beta)}{\phi(\beta)} + \beta$ is monotonically increasing. Numerical approximation very strongly suggests that this is true. It should follow from the results of [18], but unfortunately the authors were unable to find an elegant argument proofing this claim. We do not use this lemma elsewhere, it is only presented here to elucidate the behavior of the test further.

Proof. Let $\epsilon > 0$ be arbitrary. Since $d_0 \notin [\mu_{0,\sigma_B}^c, \sigma_B]$ we are in one of two cases:

Case 1 ($d_0 < \mu_{0,\sigma_B}^c$): Let $\delta := \frac{\mu_{0,\sigma_B}^c - d_0}{2} > 0$. For $N \geq N_0$, the mean m estimated on blocks of $\hat{d} < c$ satisfies $m \leq d_0 + \delta < \mu_{0,\sigma_B}^c$ with probability $P > 1 - \epsilon$.

Case 2 ($d_0 > \sigma_B$): We will use two further sub-cases approximated around two limits: The first limit has $c \to \infty$, where the cutoff becomes irrelevant and $\mu_{0,\sigma_B}^c \approx d_0$. The other limit has $\mu \to \infty$, where the mean within the tail $\mu_{0,\sigma_B}^c \approx c$ approaches the cutoff[21]. Most of the actual work to be done is to show that always at least one of these approximations is precise up to at most σ_B such that together with $c > \sigma_B$ (by hypothesis of the Lemma) and $d_0 > \sigma_B$ (by hypothesis of the case) the result $\mu_{0,\sigma_B}^c > 0$ can be established. We make heavy use of the Notations D.27.

Case 2a ($d_0 > \sigma_B$ and $c \geq d_0$): Let $\delta := \frac{d_0 - \sigma_B}{2} > 0$. For $N \geq N_0$, the mean m estimated on blocks of $\hat{d} < c$ satisfies $m \geq \mu_{d_0,\sigma_B}^c - \delta$ with probability $P > 1 - \epsilon$. In this case $\beta \geq 0$, using that $\frac{\varphi(\beta)}{\phi(\beta)}$ is monotonically decreasing in β (Rmk. D.37) and $\frac{\varphi(0)}{\phi(0)} = \frac{2}{\sqrt{2\pi}} < 1$ thus $\frac{\varphi(\beta)}{\phi(\beta)} < 1$. Therefore $\mu_{d_0,\sigma_B}^c = d_0 - \sigma_B \frac{\varphi(\beta)}{\phi(\beta)} > d_0 - \sigma_B > \delta$. Thus $m \geq \mu_{d_0,\sigma_B}^c - \delta > 0$ with probability $P > 1 - \epsilon$.

Case 2b ($d_0 > \sigma_B$ and $c < d_0$): Let $\delta := \frac{c - \sigma_B}{2} > 0$. For $N \geq N_0$, the mean m estimated on blocks of $\hat{d} < c$ satisfies $m \geq \mu_{d_0,\sigma_B}^c - \delta$ with probability $P > 1 - \epsilon$. Define a correction term $\gamma(\beta) := \frac{\varphi(\beta)}{\phi(\beta)} + \beta$ measuring the error incurred by the approximation $\frac{\varphi(\beta)}{\phi(\beta)} \approx -\beta$. Note that $\gamma(\beta)$ is monotonically increasing in β (Rmk. D.37) and $\gamma(0) = \frac{\varphi(\beta)}{\phi(\beta)} < 1$ (see above) and $\beta \leq 0$

---

[21]This is a well-known principle from extreme-value theory, but for our purposes a very simple approximation will suffice.

in the present case, so $\gamma(\beta) < 1$. Therefore $\mu^c_{d_0,\sigma_B} = d_0 - \sigma_B \frac{\varphi(\beta)}{\phi(\beta)} = c - \sigma_B \gamma(\beta) > c - \sigma_B > \delta$. Thus $m \geq \mu^c_{d_0,\sigma_B} - \delta > 0$ with probability $P > 1 - \epsilon$.

In any case, we found N_0 such that for $N \geq N_0$, $p_1 > 1 - \epsilon$. The claim follows since $\epsilon > 0$ was arbitrary.

$\square$

D.4.5 Beyond Acceptance Intervals

The main point of a direct test for weak-regime dependence is the generation of a suitable data-set to access d_0 without the necessity to identify individual blocks as belonging to any regime. There are of course many ways to generate such a data-set, such that false-positive control becomes valid under suitable assumptions. By Prop. 5.12, no general error-control (without assumptions), is possible however. The design of a test should thus include careful consideration of its associated assumptions, as they contribute to the interpretation of test-results.

In this section we detail two basic considerations behind our approach. First, we discuss the relation to other, potentially simpler, approaches. This also elucidates the applicability assumption 5.14. Then, we discuss the plausibility, relevance and extension beyond cases with exactly two regimes (Ass. D.15).

Simpler Methods and Applicability: We start by giving the limits in which an "uncorrected" testing approach on a cut-off data-set should work, then explore a simple but insightful baseline method. By an uncorrected test, we mean:

Definition D.38 (Uncorrected Test). Choose a cutoff c, independence-test $\hat{T}_{\text{indep}}$ on samples from blocks of dependence d less than $d < c$ (we assumed signs are flipped, such that $d_1 > 0$, see above) or compute the mean of such blocks.

Recomputing $\hat{T}_{\text{indep}}$ by merging all relevant blocks into a single data-set can have statistical advantages if regimes are sufficiently homogeneous internally; this choice does not change the overall understanding. The uncorrected test is applicable if none of the problems (i-iii) listed in §5.2.3 are relevant:

Assumption D.39 (Uncorrected Applicability). Require a large cutoff $c \gg \sigma_B$, few impurities $d_1 \gg c$ and few invalid blocks $\chi \approx 0$ (or more intuitive: $L \gg B$). Since $\sigma_B \approx 1/\sqrt{B}$ these can be summarized as (with L and d_1 "fixed by nature"):

$$L \gg B \gg 1/\sqrt{c} \gg 1/\sqrt{d_1}$$

We first inspect the condition $c \gg \sigma_B$. Assuming $\hat{T}$ to be normal, one could compute the mean of a truncated at c normal distribution, which is known, this is what eventually leads to the acceptance-interval approach described above. There is, however, a very simple procedure that may be more robust against violations of the assumption of exactly two regimes and illustrates some interesting aspects of our setup:

Definition D.40 (Two-Sided Cutoff). Choose a cutoff c, test $\hat{T}$ on samples from blocks of dependence d with $d \in [-c, c]$ or compute the mean of such blocks.

One could of course have chosen the absolute value of d as score in the first place, but there is an interesting feature to the distinction of the two formulations as given: The first one ("uncorrected") splits the data into two regimes, then tests on one of these. The second one ("baseline") splits the data into three parts, and even though for blocks with $d < -c$ we should be rather convinced that they are likely in the low-dependence regime (they are far from $d_1 > 0$), we may still "sacrifice" quality of the regime-estimates (and data points) if that serves our understanding of the final result which we are actually interested in. This freedom was gained by asking *directly* (in the sense of §1) for the final result, rather than insisting on a time-resolved estimate of indicators first.
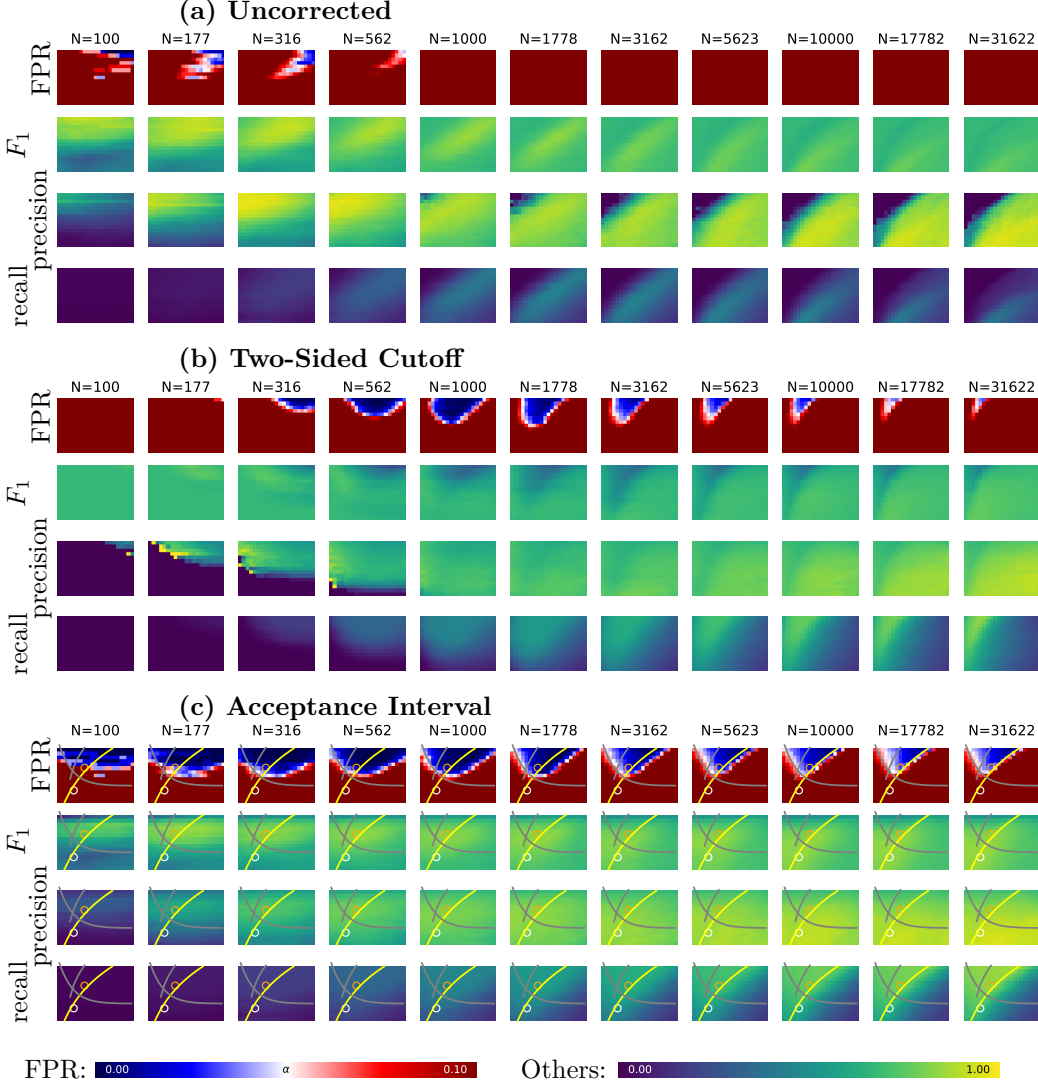
(a) Uncorrected

(b) Two-Sided Cutoff

(c) Acceptance Interval

Figure D.8: *Method Comparison for Weak-Regime:* Different metrics (see left-hand side labels) for the method variations described in §D.4.5. Image coordinates correspond to hyperparameters, x-axis: cutoff $c = 0.1 \ldots 0.6$ (linear, left-to-right) and y-axis: block-size $B = 5 \ldots 50$ (logarithmic, top-to-bottom). The different images per row are for different sample-sizes $N = 10^2 \ldots 10^{4.5}$ (logarithmic, see labels). In panel (c), hyperparameter choices are indicated orange (generic regimes) and white (large regimes). Additional markers and curves shown in (c) are discussed in §D.4.6.

Assumption D.41 (Two-Sided Cutoff Applicability)**.** Require few impurities $d_1/c \gg \sigma_B$ and few invalid blocks $\chi \approx 0$.

$$L \gg B \quad \text{and} \quad c\sqrt{B} \gg d_1$$

Note, that this cost us some data points however, and while we do not rely on $c \gg \sigma_B$ anymore, larger c will still lead to larger sample counts.

In figure D.8, some numerical results on these different approaches (for pairwise tests, $Z = \emptyset$) are shown. Due to the prior distribution of ground-truth parameters in the data-set, the validity of error-control (generally depending on ground-truth and hyperparameters point-wise) translates at least in part into valid regions in hyperparameter space for the "corrected" approaches. Generally, the acceptance-interval method is from a practical perspective easier

to apply, because the precision is rather homogeneous, making hyperparameter choices easier. At least within the range of our numerical experiments, also the overlap of hyperparameters with good precision *and* good recall is substantially larger than for the simpler approaches.

Finally, in terms of interpretability, the acceptance-interval method having the simplest applicability assumption is easiest to interpret, providing yet another advantage over simpler approaches.

Unified Description: These three approaches are all special cases of using two (possibly different) cutoffs at the left and right hand side. Indeed, the theoretical analysis of the acceptance-interval approach given above also applies to this more general description (the modification of the interval by a bias $\mu_{m,\sigma}^c$ on one side and σ_χ on the other side then turns into different biases $\mu_{m,\sigma}^{c\pm}$ on both sides plus possibly different choices of σ_χ for both sides).

The uncorrected approach then uses $c_\pm = \infty$, the two-sided cutoff $c_+ = c_-$ and the acceptance-interval $c_- = \infty$.

Beyond Exactly Two Regimes: The relevance and plausibility of the assumption of exactly two regimes was already discussed in §D.2.2, where one remaining and challenging case was that of multiple dependent regimes with different signs of their dependencies. In this case, separation Δd needs to be sufficiently large to the lowest absolute value of d_1 on either side, and a cutoff c needs to be chosen accordingly. For smoothly varying dependence, a suitable interpretation for example of time spent near zero needs to be adapted. A method in the sense of the "unified" description (see previous paragraph) can in principle improve robustness against these problems. We leave a more detailed study of more sophisticated regime-structure and a suitable interpretation of results in such cases to future work.

D.4.6 Semi-Heuristic Hyperparameter Choices

As before (see §D.3.4 for general principles), we provide semi-heuristic choices for the simplified prior knowledge of generic vs. large regimes (cf. Convention D.25).
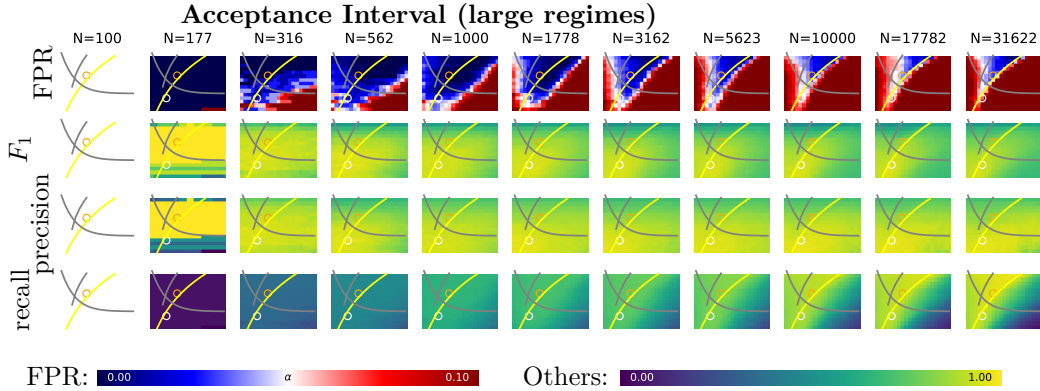

Figure D.9: *Pairwise Tests of Weak-Regime (large regimes):* Same as Fig. D.8c, but for large ground-truth regimes. The first column has 0 data points, the second only ≈ 20, per pixel, which is why they look unsmooth (or blank) and should not be over-interpreted.

Pairwise tests: In Fig. D.8c (generic regimes) and D.9 (large regimes), we show results for pairwise tests using the acceptance interval method. The larger grid (containing smaller images) is organized by sample-count (left to right) and different scores (rows). Within each smaller image, the axes correspond to hyperparameters: The x-axis corresponds to

different values of the cutoff $c = 0.1 \ldots 0.6$ (linear) and the y-axis to block-size $B = 5 \ldots 50$ (logarithmic, from top to bottom).

We first focus on the first row of images, showing FPR. Especially for larger $N \geq 1000$, there is surprisingly little dependence on N, primarily the image gets sharpened. This is initially surprising. We belief it is explained best, by this primarily visible structure being related to applicability of Lemma D.31 (given the model-prior / benchmark dataset) and thus FPR-control rather than finite-sample behavior in applicable cases. Indeed the structure does seem to be interpretable in this sense. To this end, we focus on D.9 (large regimes) and high N, where the structure visible best.

The first evident feature is the break-down of FPR-control near the left edge of the images. The reason for this is in the convention[22] of accepting only for $n_c \geq n_0^{\min}$. This makes sense from the perspective of detecting regimes conservatively (in doubt, return a global hypothesis and avoid clutter; see also Rmk. 5.13 and the discussion there, relating this choice to "validity assessment").

Remark D.42. It is of course possible to output a special token for rejection based on $n_c < n_0^{\min}$ for downstream processing to express potential invalidity of the test.

A more detailed analysis turns out to be more difficult. We make the following ansatz:

$$n_c = a \left(\phi(\frac{c}{\sigma_B}) - \frac{B}{N}s \right), \qquad (*)$$

where s is the total number of regime-switches; further we approximate $\sigma_B \approx B^{-\frac{1}{2}}$. This equation is motivated by a being the true regime-fraction, $\phi(\frac{c}{\sigma_B})$ being the probability of a valid d_0 block having $\hat{d} \leq c$ (thus contributing to the count n_c) and $\frac{B}{N}s \approx \chi$ (if there is at most one switch per block, then there are $\frac{B}{N}s$ data points in invalid blocks). Now, a is a random variable on the data-set, so really there is some value of $\phi(\frac{c}{\sigma_B}) - \frac{B}{N}s = \nu$ where we pass a level-line (e. g. 5% error rate) and we make a (fixed) guess for $\xi = \frac{s}{N} \approx \frac{1}{\ell}$, the typical ratio of switches to total data points (for the large-regime case, we know $\xi < 0.005$). Shown in the images as gray curves are (numerical) solutions to this equation for c and B for values $\xi = 0.02$, $\nu = 0.5$ (a guess for ν obtained by based on typical values of a and refinement after fixing ξ by comparison to the numerical results), corresponding to the gray downward curve (henceforth referred to as generic regime guess), and for $\xi = 0.004$, $\nu = 0.7$ corresponding to the gray upward curve (henceforth referred to as large regime guess). It is not trivial to see why, but solutions to the above equation at some point transition from a downward to an upward slope (compare the qualitatively different behavior of the two gray lines shown in the figures). Intriguingly a similar behavior is observed for the boundary of the valid region of the acceptance interval test for generic and large regimes respectively. Indeed the generic regime guess fits the left-hand side boundary in Fig. D.8c surprisingly well, while the large regime guess does not seem to make any sense here. In Fig. D.9 on the other hand, the large regime guess is an ok fit to the data (for large N), while the generic regime guess seems completely off.

In summary, we find both in numerical solution of an analytic approximation and in numerical experiments a kind of phase-transition in the form of the left boundary of valid (on average on the uninformative prior) for FPR-control hyperparameters. Thus in this case, the choice of hyperparameters for large as opposed to generic regimes should reflect this qualitative change. As a consequence, the large-regime hyperparameter set may have low regime recall (from high weak-regime-independence FPR) on small regimes, but perform substantially better on large regimes.

On the right hand side of the images, there is (again especially clearly visible in Fig. D.9 for large N), an apparent concave valid region at the top. When assessing the different validity requirements Ass. 5.14 (see also statement of Lemma D.31), one routinely obtains

---

[22]Changing this convention in the test, changes this feature in results, not shown.

terms of the form $\frac{c}{\sigma_B} \approx c\sqrt{B}$. This happens for example also for the equation $(*)$ above, in the limit where $\chi \approx 0$ (which is different from the challenge studied above) for n_c, and then for σ_χ (by plugging into $A_c = \frac{n_c}{\Theta}$ and then into $(1 - \frac{A}{A_c})c \le \sigma_\chi$ in Lemma D.31). Since we use $\sigma_\chi = 0 = $ const in our numerical experiments (see Rmk. D.33), manifolds of fraction of constant rate of invalid models thus correspond to lines of $c\sqrt{B} = $ const. In the images of Fig. D.8c and Fig. D.9 one such level line (for $c\sqrt{B} = 1$, which to our best understanding only co-incidentally matches the data, there is no obvious reason for this constant to be equal to 1) has been indicated in yellow. It matches the right-hand side border of the valid region astonishingly well for large N.

We can thus explain the observed structure qualitatively reasonably well from (semi-)analytic ideas that depend only on rather generic validity ideas without detailed prior knowledge about regime-structure. So our semi-heuristic hyperparameter choices should not deviate substantially from this FPR-validity region. However, in practice, we are also interested in precision and recall of the implied regime-detection. The dependence on N does not seem strong or clear enough, to mandate N-dependent hyperparameters. We pick one (c, B) pair for generic regimes (orange circle; $c = 0.275$, $B = 11$, these are pixel coordinates hence the odd numbers) and one pair for large regimes (white circle; $c = 0.2$, $B = 31$) based on the idea of respecting FPR-validity, maintaining precision and then assessing for good recall on the uninformative prior benchmark.

Conditional Tests: Figures D.10 and D.11 show (for generic and for large regimes respectively), in three large columns: FPR, precision and recall; within each large column a grid of images, where within this grid, the x-direction is sample-size N, and the y-direction is conditioning-set size $|Z|$. Each individual image is a hyperparameter scan (x-direction: c, y-direction: B, increasing top to bottom). The most immediate feature is a region of trivial (constant) results in the top of the images that grows with increasing $|Z|$ (moving down in the grid). This region of trivial decisions occurs, because there are no longer enough data points within a single block of size B (small B are at the top of individual images). Partial correlation has an effective number of degrees of freedom (per block) of $B - 3 - |Z|$. So for the lowest row of images ($|Z| = 20$), B needs to be at least 24 for the test to apply. With B being shown on a logarithmic scale the middle-point of the y-axis for $B = 5 \ldots 80$ is at $B = 20$ (because $\frac{20}{5} = 4 = \frac{80}{20}$). Thus this trivial region extends beyond the middle of the images in the lower part of the grid.

Besides this apparent, but easily explicable feature, the behavior seems to be similar to the unconditional case. The trivial region at the top does not simply overlay the previous picture, but rather "compresses" it downward. This makes sense, as the trade-offs of the unconditional case (B vs. χ) really are trade-offs σ_B vs. χ of effective degrees of freedom, so this behavior is expected. Again (as in the unconditional case) there does not seem to be a strong N-dependence, and we choose hyperparameters independent of N.

In terms of actual hyperparameter choices, we start with c. For the *large* regime case Fig. D.11, there is not much visible change, so we keep the previous value of c unchanged (and independent of $|Z|$). For the generic regime case, Fig. D.11, best visible for the FPR-plots, the best values of c start at larger values than for the large-regime case, but than seem to become progressively smaller. This could be, because for larger $|Z|$ the required large (effective) size of B moves the trade-off with χ to regions of the behavior of χ more similar to the large regime case. The trend is rather small, and a simple linear (in $|Z|$) choice of c seems to account reasonably well for it. For a concrete choice, see below.

The choice of B mostly has to adapt for the downward-shift due to the trivial region. this shift is linear in $|Z|$, so again a linear ansatz seems reasonable.

For concrete numerical choices (both for c and for B), we pick an "optimal" pixel in the image in the top row and in the bottom row of the grid and interpolate linearly. This leads to somewhat odd numbers, but should otherwise be acceptable. This leads to, for large regimes: $c = 0.2$ (as before) and $B = 31 + |Z|\frac{59-31}{20} \approx 31 + 1.4|Z|$ and for generic regimes: $c = 0.275 + |Z| * \frac{0.25-0.275}{20} \approx 0.275 - 0.00125|Z|$ and $B = 11 + |Z| * \frac{43-11}{20} \approx 1.6|Z|$. The
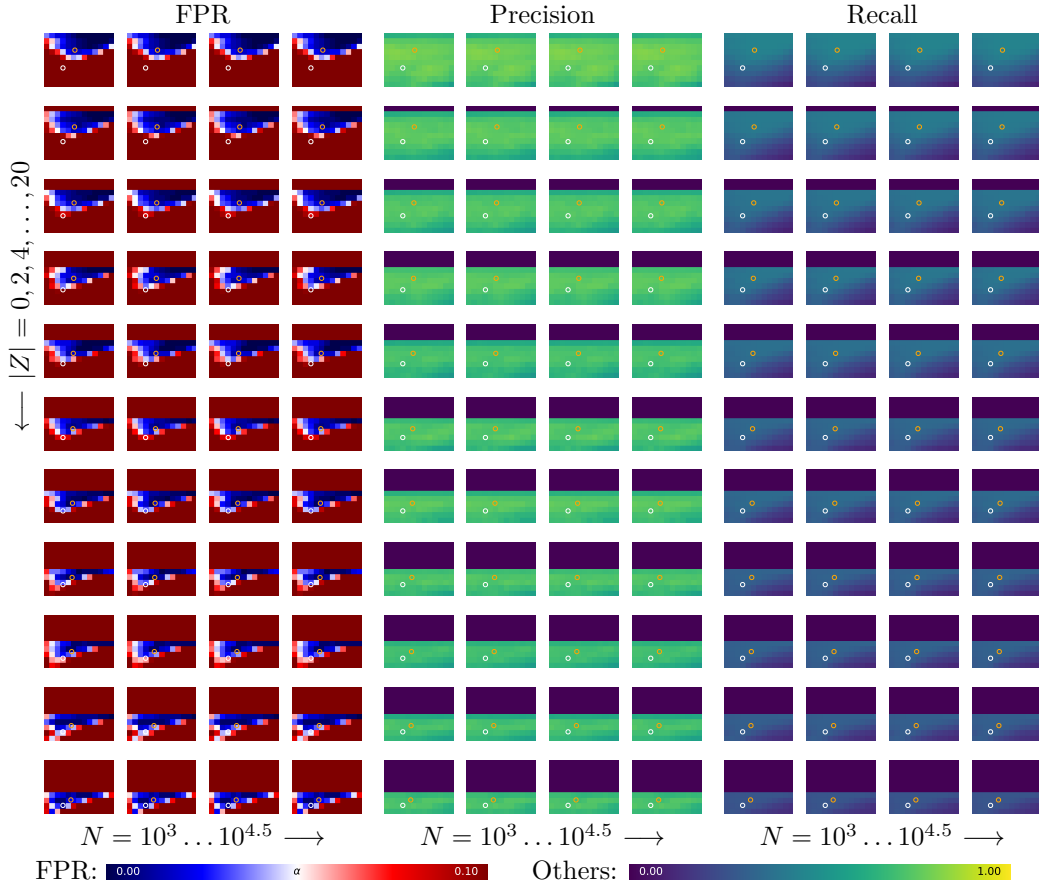
Figure D.10: *Conditional Weak-Regime Test:* FPR, precision and recall for the acceptance-interval test. Shown are for four different $N = 10^3 \ldots 10^{4.5}$ sample-sizes (columns) and conditioning-set sizes $|Z| = 0, 2, 4, \ldots, 20$ (rows) images resolving hyperparameters $c = 0.1 \ldots 0.5$ in x-direction (linear, left-to-right) and $B = 5 \ldots 80$ in y-direction (logarithmic, top-to-bottom). Circles are again proposed hyperparameter choices.

most relevant part is scaling of B with $|Z|$ using a coefficient greater 1 to stay outside the trivial part of the hyperparameter range.
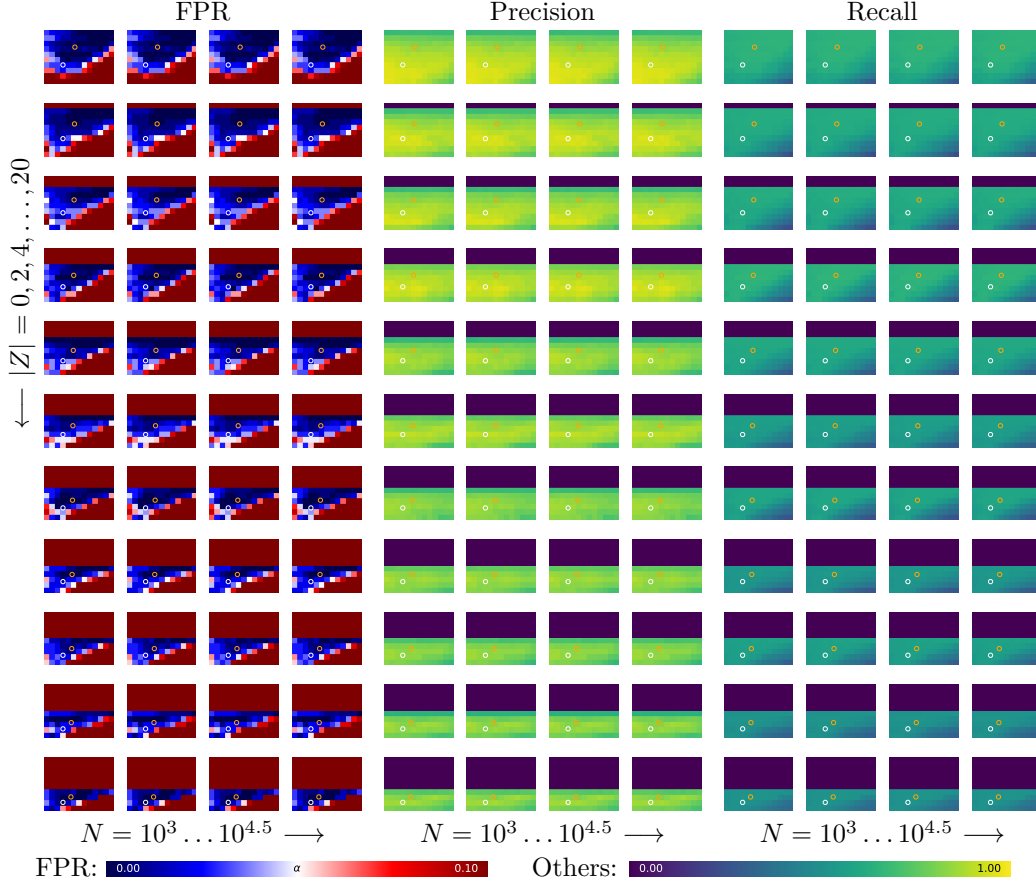
Figure D.11: *Conditional Weak-Regime Test (large):* Same as Fig. D.10, but for large true regimes.

D.4.7 Indicator Relation Tests

For the material in §6 will need a test for indicator implications in the sense of Def. F.12. This problem can essentially be reduced to the question of controlling weak regimes discussed in section §D.4 up to this point as follows: We first focus on the simplest case $K = 1$, i.e. given the marked independencies $X_1 \perp\!\!\!\perp_{R_1} Y_1 | Z_1$ with associated indicator R_1 (Def. 4.4), $X_2 \perp\!\!\!\perp_{R_2} Y_2 | Z_2$ with associated indicator R_2 we want to know if

$$R_1(t) = 0 \quad \Rightarrow \quad R_2(t) = 0.$$

Previously, in this section §D.4, the task of weak-regime testing was approached by assigning blocks to a low-dependence data-set (by a cutoff), and then test on this selected data for independence in an consistent and interpretable way respecting the selection-bias (mean-value shift) in the truncated low-dependence results and impurities included from the other regime. Here, we assign blocks to a proxy data-set based on low dependence in the first independence $X_1 \perp\!\!\!\perp Y_1 | Z_1$ (see "data-set selection" below), and then test on this selected data for the second independence $X_2 \perp\!\!\!\perp_{R_2} Y_2 | Z_2$.

The previous case (weak-regime testing), then corresponds to the case where $X_1 = X_2$, $Y_1 = Y_2$, and $Z_1 = Z_2$, i.e. when both tests (and block-scores d_1, d_2) are deterministically / maximally dependent. Now, depending on the graphical structure, both tests may be anywhere between independent and strongly dependent. Since the dependent case works as before, we first focus on what changes in the independent case (or if tests / scores become more independent).

The independent case is in part simpler, for example, there would be no selection bias on

the independent regime (mean-value shift by truncation). However, this also means that "lost" data points no longer cancel out "impurities" (for small enough cutoffs) in the sense of Lemma D.30. We account for this by a simple approximation of: The true regime-fraction as a^{est}, the number of blocks below the cutoff relative to the total number of blocks (under Ass. 5.14 this is an upper bound), with the constraint that $a^{\text{est}} \in [a_{\min}, 1 - a_{\min}]$; The dependence of the dependent regime by the heuristic $d_1^{\text{est}} \approx \frac{d^{\text{est}} - a^{\text{est}} d_0^{\text{est}}}{1 - a^{\text{est}}}$, where d^{est} is the mean over $\hat{d}$ of all blocks and d_0^{est} the mean over blocks below the cutoff. Then we shift the upper bound of the acceptance interval by $d_1^{\text{est}}(1 - \phi(\frac{c}{\sigma_B}))$, where the survival-function $(1 - \phi(\frac{c}{\sigma_B}))$ (for σ_B the standard-deviation of $\hat{d}$ on blocks of size B and c the cutoff) estimates the number of "lost" data points, thus $d_1^{\text{est}}(1 - \phi(\frac{c}{\sigma_B}))$ mimics the term that in Lemma D.30 cancels the contribution from impurities.

In practice, these tests / scores are not independent: These tests will typically be used to resolve induced indicator problems as in example 4.8. So in practice the problem can be very similar to what we had before (especially given the considerations in §F.10.1). Indeed using the acceptance interval method proposed above we find in numerical experiments similar behavior as for the weak-regime case. Results tend to be worse on finite-sample experiments, which is not surprising, considering the higher complexity of this problem.

If the left-hand-side of the implication contains more than one indicator $K > 1$ (see Def. F.12), we assign the blocks to the candidate data-set if they are in the low-dependence regime for all of the indicators on the left-hand-side. This can lead to low sample-counts and may make it hard to reject an implication with many terms on the left; in §6, we show that at least in the acyclic case, only few implication-tests and mostly a small number of entries on the left-hand-side are required.
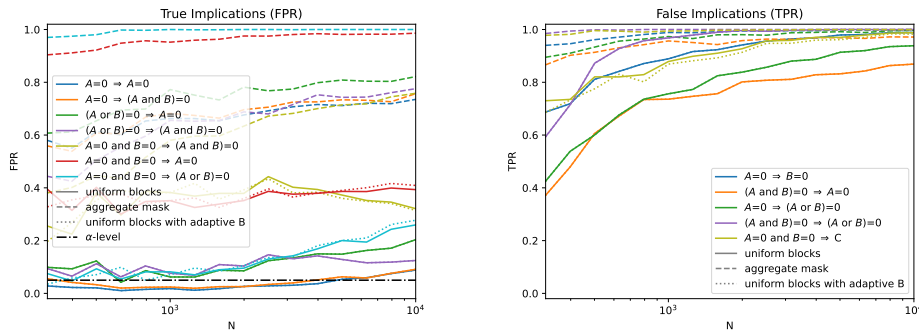

Figure D.12: *Implication Testing (methods):* Here segment-lengths of underlying indicators are chosen comparatively large ≥ 100, as boolean combinations may produce substantially smaller effective segments. The present version of this test is preliminary, see text.

Data-Set Selection: As indicated above, we want to select a low-dependence candidate data-set for the right-hand side test from the left-hand side tests. If hyperparameters, in particular B, are selected test-specific (for example dynamically from data, or because the conditioning-sets are of different size), we might have $B_1 \neq B_2$. The simplest solution is to use the same, for example the largest of the B_i, value for the block-size B for all computations of $\hat{d}$ (referred to as "uniform blocks" below). Another possible approach is, to aggregate assignments of blocks on the left hand side (potentially at different B_i) into a mask *per-sample*. Then compute the score for the right-hand-side test on all masked data (without blocks). We refer to this approach as "aggregate mask". For partial correlation the change in effective sample count from computing $\hat{d}$ as a mean over blocks to computing it on all data can be used to heuristically relate the result to previous considerations, nevertheless

getting good results on numerical experiments is difficult. A comparison of these data-set selection methods is shown in Fig. D.12.
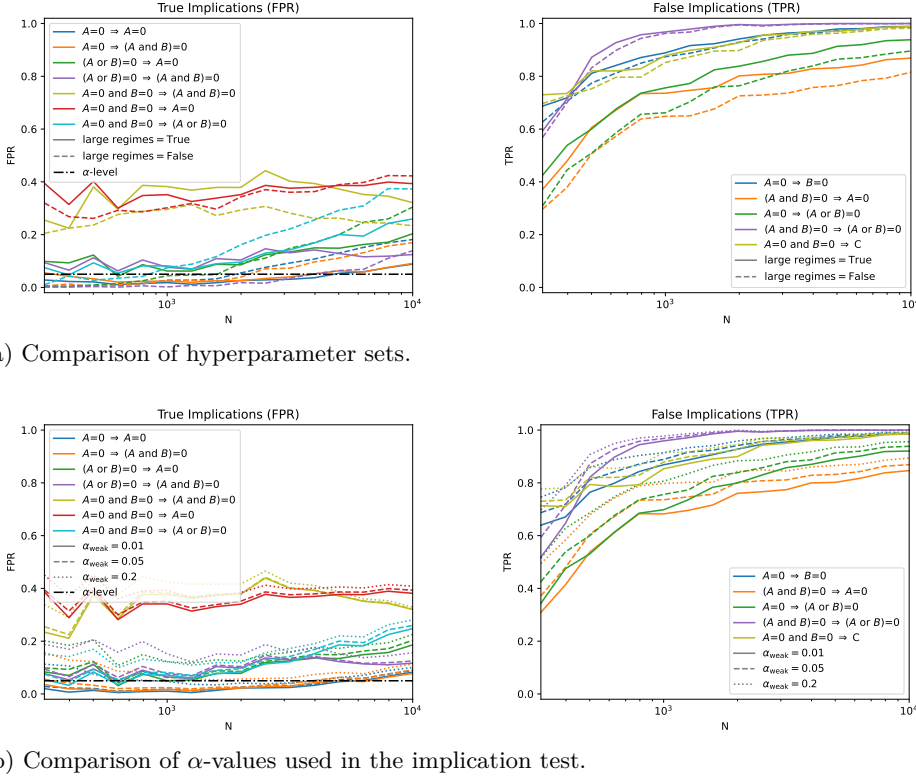

(a) Comparison of hyperparameter sets.

(b) Comparison of α-values used in the implication test.

Figure D.13: *Implication Testing (behavior):* Here segment-lengths of underlying indicators are chosen comparatively large ≥ 100, as boolean combinations may produce substantially smaller effective segments. The present version of this test is preliminary, see text.

Empirical Behavior   In Fig. D.13, we show results for different test-scenarios and different hyperparameter choices. In terms of FPR-control, the tests need further work, but for the present application, these tests are much less relevant than the mCITs discussed at length before. The primary goal of the implementation here is to demonstrate feasibility on a conceptual level, and given that our basic implementation already performs substantially better than random shows that this kind of indicator–indicator comparison is a solvable problem. Nevertheless, it is also a fundamentally hard problem, thus as already pointed out in §6, avoiding this type of test where possible is likely a more important next step.

D.5   Marked Independence

In view of the impossibility results Prop. 5.3 and Prop. 5.12, "strong" correctness in the naïve sense is not possible for an mCIT. However, there are still at least two types of meaningful results: A "weak Bayesian convergence" (see §C.2) shown below, or assessment of validity, by assumptions as Ass. 5.14 or by inspecting the data see future work §D.7.2.

By combining independence-testing, homogeneity-testing and weak-regime testing, we get the following convergence result for the induced mCIT as specified by Def. 5.9 (i. e. relative to $d = 0$, disregarding general CI-testing problems [57], cf. Rmk. 5.8):

Theorem 2. *We assume Ass. 5.7/D.7 (there is an underlying $\hat{d}$ with known or estimated null-distribution, for its variance on block-size B write σ_B^2) additionally satisfying Ass. D.10 and Ass. D.12 (estimates by $\hat{d}$ are stochastically ordered, and on invalid blocks are stochastically ordered relative to valid blocks), Ass. D.13 ($\hat{d}$ is approximately normal, see Rmk. D.14) and Ass. D.15 (there are exactly one or exactly two regimes).*

Let $\Lambda : \mathbb{N} \to \mathbb{R}$ be a scale (see Def. C.22) with $\Lambda \to \infty$, and assume we are given a pattern Patt *(Def. 5.4) which is asymptotically-Λ compatible (Def. C.29) with the indicator meta-model $\mathcal{R}$ (see intro to §C) generating our data.*

Construct an mCIT by first testing homogeneity, if the result is

(a) homogeneity is accepted, then test dependence (on basis of Ass. 5.7)

    (i) if independence is accepted, the result is global independence,

    (ii) if independence is rejected, the result is global dependence.

(b) homogeneity is rejected, then test for a weak regime,

    (i) if $d_0 = 0$ is accepted, the result is a true regime,

    (ii) if $d_0 = 0$ is rejected, the result is global dependence.

Then there exist hyperparameters (cf. statements of Lemma D.22 and Lemma D.34) for the binomial homogeneity-test and the acceptance-interval weak-regime test, such that the result is weakly asymptotically correct (Def. C.11) as specified by Def. 5.9 (cf. Rmk. 5.8).

Proof. This follows from the weak asymptotic correctness of the constituting tests, shown in Lemma D.22 (quantile estimates can be bootstrapped, example D.20, or CIT-specific analytical estimates, see example D.18 for partial correlation) and Lemma D.34. The existence of hyperparameters is shown in examples D.23, D.35. The subcases of (a), global dependence and independence, are formally trivial by our specification of results Def. 5.9 and Ass. D.7 (consistency of $\hat{d}$); in practice this means, they are distinguished correctly if the underlying CIT based on $\hat{d}$ is applicable (see Rmk. 5.8). $\square$

Remark D.43. It is important to note that hyperparameters can be chosen uniformly (without inspecting the model or data). For adaptive (to data) hyperparameters, see §D.7.1.

This includes the "uninformative" temporal cases:

Corollary D.44. *Given an uninformative temporal prior (Def. C.17), using a persistent-in-time pattern (Def. 5.4) then given $B(N)$ with $B(N) \to \infty$ and $\frac{B(N)}{\log(N)} \to 0$, there are hyperparameters such that the mCIT described in Thm. 2 is weakly asymptotically correct.*

Proof. See example C.30: A persistent-in-time pattern is asymptotically weakly Λ-compatible with the uninformative prior of Def. C.17, if $\frac{\Lambda(N)}{\log(N)} \to 0$. This follows from Lemma C.28 via Lemma C.26.

The claim then follows via the Theorem 2, and the fact that suitable hyperparameter choices exist after fixing B first (see examples D.23, D.35). $\square$

It also includes all "trivial" scaling cases except for the infinite duration ($\Lambda = \text{const}$) case, which is not possible (Prop. 5.12):

Corollary D.45. *Let $\mathcal{R}_N(t) := \bar{\mathcal{R}}(t/\Lambda(N))$ for $\bar{\mathcal{R}} : \mathbb{R} \to \{0,1\}$ with lower bound Δt_{min} on smallest structures (Rmk. C.6). If $\Lambda(N) \to \infty$, given $B(N)$ with $B(N) \to \infty$ and $\frac{B(N)}{\Lambda(N)} \to 0$, then using a persistent-in-time pattern (Def. 5.4) there are hyperparameters such that the mCIT described in Thm. 2 is weakly asymptotically correct.*

Proof. By example C.23, the regimes grow at least Λ-uniformly, thus by Lemma C.26, $\mathcal{R}_N$ is Λ-compatible with the persistent-in-time pattern, so the claim follows via Theorem 2, and the fact that suitable hyperparameter choices exist after fixing B first (see examples D.23, D.35). $\square$

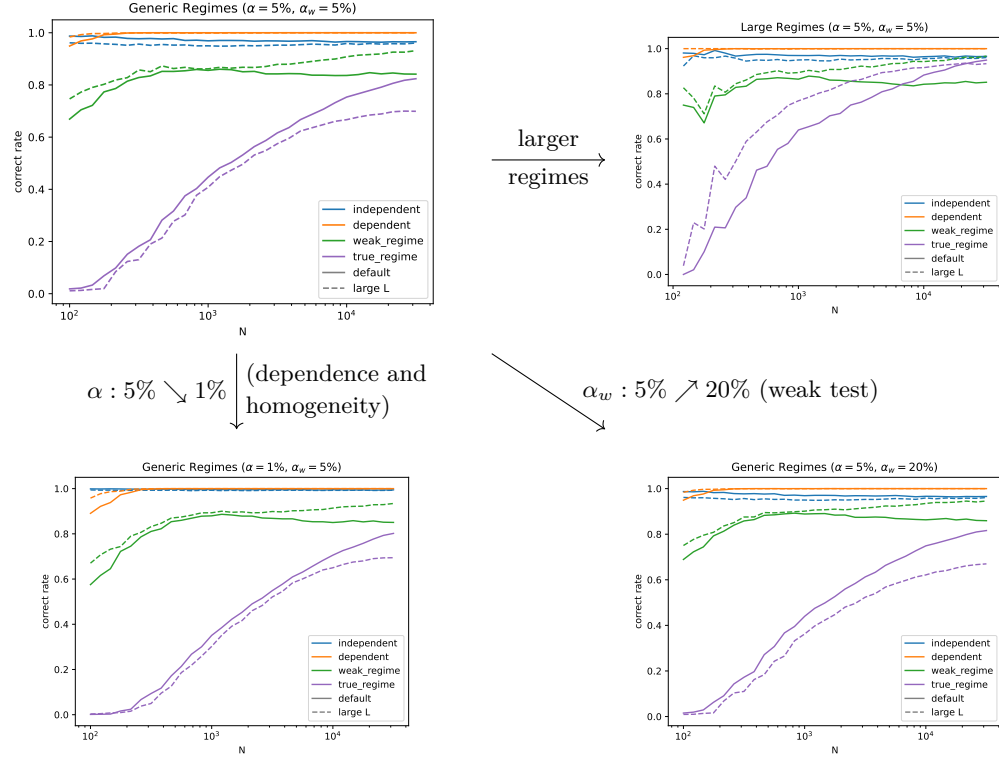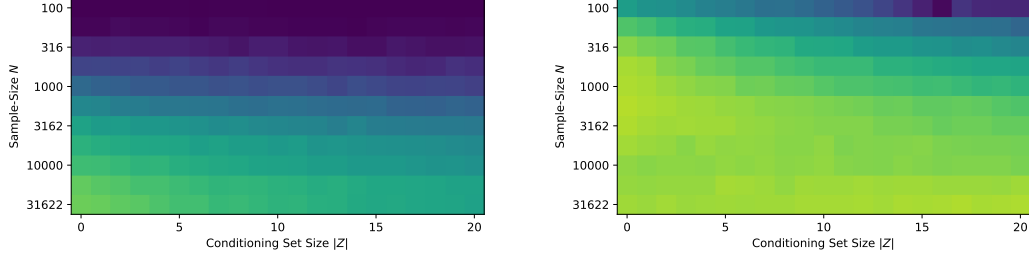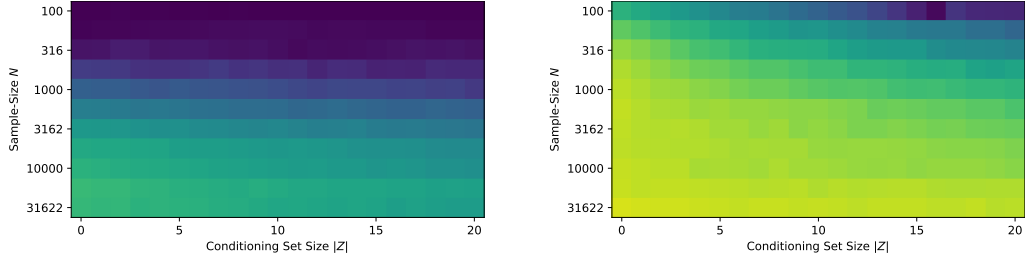### D.5.1 Numerical Experiments and Validation

Figure D.14: *Validation of pairwise mCIT:* Shown is the correct rate of classification of different scenarios by the mCIT. The outputs of "weak regime" will be merged into "dependent".

For the sake of completeness, we also included some results from numerical experiments for the assembled full mCIT. Figure D.14 shows the rates of correct assignment of different ground-truths (distinguishing between week regime and globally dependent scenarios, which is not required for the finial test-output, but informative). As is expected from the previous discussions, there is a clear an systematic hierarchy visible: On the standard global hypotheses the test converges very fast and reaches 1 or $1 - \alpha$ already for small N. Next the weak regime-case increases also rather quickly, but then (especially for the generic regimes hyperparameters) plateaus at a finite value, likely this is related to test-validity (Ass. 5.14) being violated at a finite rate. Finally the ratio of correct results for the true-regime case grows slowest, which is also consistent with our previous findings of having difficulty in achieving high recall on true regimes.

Conditional Tests: Figures D.15 and D.16 show results for conditional mCITs. Shown is again the rate of correct results, this time only for the more interesting cases of weak and true regimes (we do have plots for the global hypotheses, they do not show anything new). The main observation is that especially for the generic regime hyperparameter set, large N are required to achieve reasonable recall on true regimes.
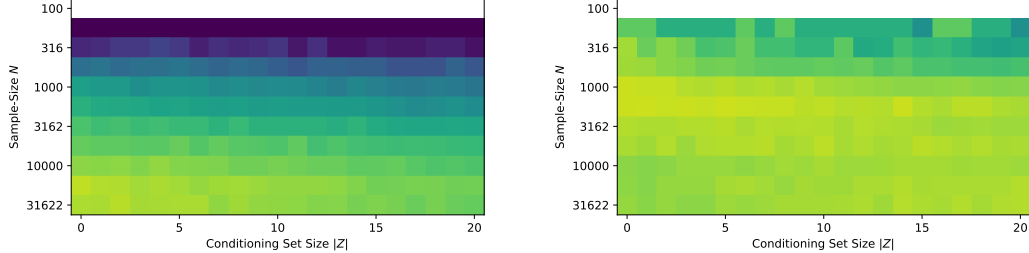
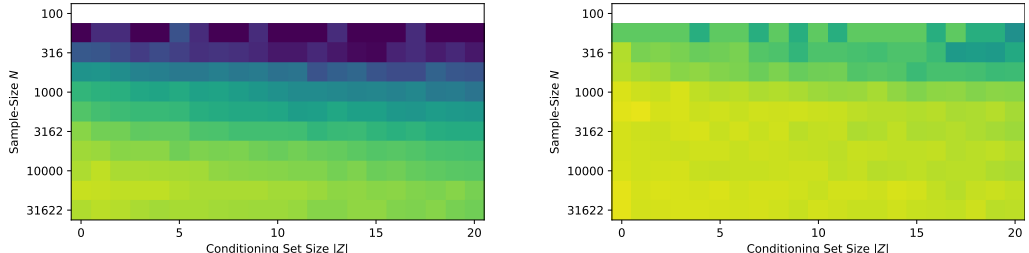(a) hyperparameter set for generic regimes, true regime (lhs) and weak regime (rhs).

(b) hyperparameter set for large regimes, true regime (lhs) and weak regime (rhs).

Figure D.15: *Validation of conditional mCIT (generic regimes):* Shown is the correct rate of classification of different scenarios (true regime and weak regime) by the mCIT. Image coordinates are conditioning-set size $|Z| = 1 \ldots 20$ on the (linear) x-axis and sample-size $N = 10^2 \ldots 10^{4.5}$ on the (logarithmic) y-axis.

(a) hyperparameter set for generic regimes, true regime (lhs) and weak regime (rhs).

(b) hyperparameter set for large regimes, true regime (lhs) and weak regime (rhs).

Figure D.16: *Validation of conditional mCIT (large regimes):* Same as Fig. D.15, but for ground truth regimes of larger length.

D.6   Conditional Tests

Conditional tests have been already discussed with hyperparameter choices (§D.3.4, §D.4.6), and explicitly in the main text at §5.3. An interesting observation that we have not yet discussed is that a block-wise (or at least partially local in the pattern) approach to regressing out for CIT-testing (in this case via partial correlation, thus linear regressors), technically uses samples less efficiently in the IID case, but provides additional robustness against non-IID
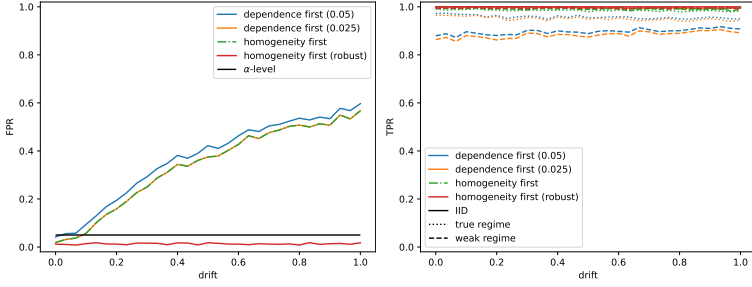
Figure D.17: Conditional testing with and without robust configuration, that is, using block-wise (local in the pattern) regressing out. Sample-size is $N = 1000$, block size is $B = 25$.

(or non-stationary) behavior in the mechanisms underlying the effect of the conditioning set Z on the pair X, Y.

For example consider a simple confounder-model $X \leftarrow Z \rightarrow Y$ with linear effects $X = \alpha Z + \eta_X$, $Y = \beta Z + \eta_Y$. In the IID case the independence $X \perp\!\!\!\perp Y|Z$ is easily found. But what if the coefficients α and β become even slightly time-dependent? Many coefficients in real world models *are* really time dependent, think for example of electrical resistance as coefficient between voltage and current, which is really temperature dependent, thus often de facto also time-dependent, albeit slowly varying. In practice we then effectively test if $\alpha(t)$ and $\beta(t)$ are sufficiently independent – however, even if they are, given that they vary on a much larger time-scale, they have a much lower effective number of degrees of freedom, so analytical estimates of the null-distribution are bound to fail if not carefully adapted; estimates for example by bootstrap / shuffle approaches will likely not correctly respect this structure either.

Fig. D.17 shows the behavior of simple drifts: α and β start / end at $1 + \gamma$ times the value they end / start with, drifting linearly (in time) in between. The x-axis in Fig. D.17 encodes this γ factor describing drift-strength ($\gamma = 0$ means no drift, thus IID data). Already at low drifts $\gamma = 0.1 \ldots 0.2$ FPR-control starts to fail visibly, a trend that becomes even much worse for stronger drifts.

We expect, already from potential non-trivial model-indicators, the presence of some non-stationarities in mechanisms, thus we use the more robust block-wise regressing out in the numerical results of this paper. The reasons for this choice are similar to those given at the end of §5.2.1.

D.7   Future Work

We briefly summarize some relevant topics that could be subject to future work.

D.7.1   Adaptive hyperparameters

In principle, hyperparameters for the mCIT can be chosen locally, i. e. for each test $X \perp\!\!\!\perp Y|Z$ individually. Doing so by hand is typically not a plausible approach, however, it means that our approach could benefit particularly strongly from automated hyperparameter choices.

To some small degree, the dependence of our simplified hyperparameter sets on the size $|Z|$ of the conditioning set already chooses parameters per test. More general a procedure for inspecting data and adapting hyperparameters correspondingly seems plausible. One observation that could be leveraged to this end is the trade-off shown in Fig. 5.6:

On the collection of values obtained by applying $\hat{d}$ to blocks, larger blocks lead to better separated peaks at d_0 and d_1, but they also eventually lead to more invalid blocks, thus to worse separation of peaks (see black dash–dot line in Fig. 5.6 illustrating the combined / full data-set distribution). In particular by trying different block-sizes B, there should be an "optimal separation" for some B_0. This B_0 might not yet be the optimal choice for B itself, but it can probably be related to a good choice for B or leveraged to estimate the true typical regime-length ℓ; numerical experiments with kernel-smoothing density estimation support this idea.

Similarly, if finite-data results are good enough to obtain a two-peak structure, the relative size of peaks and / or location of minimum in between could be used to assess a or directly q_a to inform the choice of c in order to maintain validity of the weak-regime test (Ass. 5.14).

D.7.2 Assessing Validity

An assessment of data as in §D.7.1 could further be employed to validate applicability-assumptions of the weak-regime test (Ass. 5.14). For example, given estimates (and approximations of their uncertainty) for the terms appearing in Ass. 5.14 could in principle allow for $\frac{\alpha}{2}$ confidence applicable hyperparameters plus $\frac{\alpha}{2}$ error-control under applicability leading to an overall error-control at α. As a concrete example, consider that for partial correlation the value σ_B and thus the width of peaks induced by valid blocks can be analytically estimated, hence $\chi \approx 0$ can in principle be falsified by finding strong deviations from this expected peak-width.

It will in practice (except for huge data-sets) likely be difficult to always find $\frac{\alpha}{2}$ confidence applicable hyperparameters, that also provide reasonable power; indeed by Prop. 5.12 this may not even be possible. A potentially practicable compromise could be to only assess the plausibility of used hyperparameters being valid, to inform the user (or the further processing pipeline) about the potential issue.

D.7.3 Leverage CPD and Clustering Techniques

Global CPD and clustering techniques as alternatives to our framework are discussed in §B.4. Here we focus instead on how to leverage CPD and clustering within our framework as approaches to exploit persistence and to solve the univariate problem (Fig. 5.3). In §D.1.5 we already summarized, why we currently do *not* use CPD, but instead aggregate data into a priori fixed blocks.

In principle the persistence assumption can be employed in ways different from the approach via blocks of data used in this paper. A standard approach would be change-point-detection (CPD) and an application of the dependence-score on segments rather than blocks. In our framework CPD – when used as a drop-in for the block-based approach – can be applied locally for example to gradients of scores or changes in the target (often, albeit not always, a changing link will change the variance and entropy of its target) or on dependence-scores on (smaller) blocks or sliding windows of data, avoiding the much more difficult global / multivariate problem. Indeed for comparatively small data-sets and *non-parametric independence-tests* this may be a very practical and useful approach.

Further, the univariate problem §5.2, in particular the weak-regime test §5.2.3, might substantially benefit from the use of clustering approaches applied to (for example per block) dependence-scores. Indeed, as Fig. 5.3 illustrates, the univariate problem really *is* a clustering problem with some interesting constraints. However, it seems in practice to be difficult to obtain reliable confidence intervals for cluster-locations – this is the reason why we formulate the weak-regime test as a modified independence-test rather than a modified clustering method.

D.7.4 Combining Block-Sizes

We always only use a single block-size to assess each test. In practice it is often better to combine multiple sizes (see for example [44], using random block-sizes to solve a different but in technical aspects related problem). The use of different block-sizes could also be employed to gain insights about the reliability of a result.

Block-sizes (and even the whole aggregation approach) need not necessarily be the same for all variables involved in a test. E. g. for conditional tests, regressing out of conditions (or conditional shuffle-testing) could reasonably be done on a larger time-scale than a dependence-scoring on the residuals, see §5.3.

E   Details on the Core Algorithm

Here, a formal analysis of the core algorithm is given. The main result is a proof of its oracle-consistency (Thm. 1).

E.1   Finding States On-The-Fly

During each iteration in the core algorithm (Algo. 2), the set J of marked (regime-dependent) independencies contains only those marked independencies already found in previous iterations. Even in the oracle case, the typical underlying CD-algorithm will *not* check all possible independence-statements, only those in its lookup-region (see §B.8; depending on which results the checked independencies provide). This means the set J found in the core-algorithm is incomplete: generally $J \subsetneq \mathrm{IM_{oracle}}^{-1}(\{R\})$. We have to verify that the set J (at termination of the algorithm) is yet always large enough to find all identifiable states, and we need our state-space construction algorithm to consistently (in a suitable sense to be specified) operate on incomplete J in initial rounds. In particular, we have to specify "J-specific" state-spaces that *should* be recovered.

This subsection provides suitable J-specific state-space definitions from the model-perspective and relates them to representations via mappings $J \to \{0, 1\}$. Then it is shown that J can be discovered on-the-fly in the sense that there is always at least one marked independence result of type "true regime" if J is not large enough for J-states to capture all CD-identifiable states. The core algorithm 2 only terminates once no such new marked results are found (once $J' = \emptyset$), thus termination of the algorithm implies that J *was* indeed large enough for J-states to capture all CD-identifiable states. Finally, we fix a formal specification that `construct_state_space` has to satisfy to be applicable with our proofs. This specification is satisfied by the results of §6 (see Thm. 3).

Notation E.1. In Def. 3.9, we defined states $s \in S$ which have an associated oracle independence-structure $\mathrm{IS_{oracle}}(M_s)$ by example 3.13. This is itself a mapping $I^{2+*} \to \{0, 1\}$, but it can also be understood as a mapping in s. We denote these as follows:

$$\mathrm{IS_{oracle}}(M_*) : S_T \to \mathcal{I}, s \mapsto \mathrm{IS_{oracle}}(M_s)$$
$$s : I^{2+*} \to \{0, 1\}, \vec{i} \mapsto \mathrm{IS_{oracle}}(M_s)(\vec{i})$$

We will keep the notation of replacing a open (input) variable by a $*$ also in other places throughout this section.

Given only partial knowledge (from the previous iteration) of marked independencies $J \subset \mathcal{I}$, we have to

(a) represent reached states in a practically accessible way,

(b) give a criterion when J is large enough to find all identifiable states and

(c) ensure this criterion is satisfied before the algorithm terminates.

We start by working towards a representation.

Definition E.2 (Model J-States)**.** Let $J \subset I^{2+*}$ be a fixed set independence-test indices. We will call J the marked independencies due to its usage in the core algorithm. On reached states S_T (Def. 3.21), define an equivalence-relation $\sim_J$ as follows (using notation E.1):

$$s \sim_J s' :\Leftrightarrow \forall \vec{j} \in J : s(\vec{j}) = s'(\vec{j}).$$

We then define S_T^J as the set of equivalence-classes and call it the set of J-states.

Example E.3. If $J = \emptyset$, then $S_T^J = \{s_\emptyset\}$ contains a single element, as any two states agree on $J = \emptyset$ (and $S_T \neq \emptyset$). This also shows that evidently two states of the same equivalence class $s \sim_J s'$ can have different (ground-truth) graphs $g_s \neq g_{s'}$ if J is chosen too small.

As the example shows, J can be too small to capture all state-dependence, thus motivating the following definition.

Definition E.4 (Marked Completeness)**.** We call a set $J \subset \mathcal{I}$ of marked independencies (CD-)complete, iff $\forall s, s' \in S_T$: $s \sim_J s' \Rightarrow s \sim_{\text{CD}} s'$.

Completeness of J ensures that all state-descriptions fit together nicely.

Lemma E.5 (Complete J-States Factor Identifiable States)**.** *If J is complete, then the quotient map $S_T \twoheadrightarrow S_T^{\text{CD}}$ factors as $S_T \twoheadrightarrow S_T^J \twoheadrightarrow S_T^{\text{CD}}$.*

Proof. Immediate from the definition of completeness of J. □

J-states further have a simple representation in terms of mappings:

Lemma / Notation E.6 (Map-Represented J-States)**.** There is an injective mapping (again using notation E.1),

$$S_T^J \hookrightarrow \text{Map}(J, \{0,1\}) \ , \quad s_J \mapsto s_J|_J := \big(\vec{j} \mapsto \tilde{s}(\vec{j})\big),$$

where $\tilde{s}$ is any representative of s_J (for well-definedness, see proof). We denote the image of S_T^J in $\text{Map}(J, \{0,1\})$ also as S_T^J. That is, we regard J-states S_T^J as a subset of $\text{Map}(J, \{0,1\})$.

Proof. The mapping is well-defined: Let $s_J \in S_T^J$ and representatives $\tilde{s}, \tilde{s}' \in s_J$ be arbitrary. By construction of $s \sim_J s'$, thus for $\vec{j} \in J$: $s(\vec{j}) = s'(\vec{j})$.

Injectivity: Let s_J, s'_J with $s_J|_J \equiv s'_J|_J$ be arbitrary. Equivalence of mappings on J precisely means $\forall \vec{j} \in J : s_J(\vec{j}) = s_J(\vec{j})$, which by definition E.2 is equivalent to $s_J \sim_J s'_J$. Thus $s_J = s'_J$ in the set of $\sim_J$ equivalence-classes S_T^J. □

Remark E.7. This mapping is *not* necessarily well-defined for the quotient S_T^{CD} (if J is not complete). For example on finite data test-results may not be consistent with any single graph, and many algorithms use some kind of conflict resolution [46]. Additionally CD will typically not even inspect every statement in $\mathcal{I}$. On the other hand, the mapping $\text{IS}_{\text{oracle}}(M_*) : S_T \to \mathcal{I}$ (before taking any quotients) is generally not injective as states could be different with the same independence-structure, for example two nodes and states $X \to Y$ and $X \leftarrow Y$.

We need a formal object corresponding to the "pseudo cit" used in Algo. 1, which helps to represent a given J-state:

Definition E.8 (J-Resolved Pseudo Independence-Atoms)**.** The J-resolved marked independence oracle $\text{IS}_{\text{pseudo}}^{M, s_J}$ for M associated to $s_J \in S_T^J$ is an extension (as a mapping) of $s_J|_J$ from $J \subset I^{2+*}$ to all of I^{2+*} by the marked independence oracle $\text{IM}_{\text{oracle}}(M)$ of example 4.6 as a marked independence structure (Def. 4.3), i.e. :

$$\text{IS}_{\text{pseudo}}^{M, s_J} : I^{2+*} \to \{0,1,R\} \ , \quad \vec{i} \mapsto \begin{cases} s(\vec{i}) & \text{if } \vec{i} \in J \\ \text{IM}_{\text{oracle}}(M)(\vec{i}) & \text{otherwise.} \end{cases}$$

Further, define the trivial choice[23] map c as

$$c : \{0,1,R\} \to \{0,1\}, \quad \begin{cases} 0 \mapsto 0 \\ 1 \mapsto 1 \\ R \mapsto 1 \end{cases} .$$

The core-algorithm will not converge before J is complete:

Lemma E.9 (Incomplete J Will Grow). *If J is not complete, then $\exists \vec{j} \in \mathrm{L}_{\mathrm{CD}}(c \circ \mathrm{IS}^{M,s_J}_{\mathrm{pseudo}})$, i.e. in the lookup-region (Def. B.5), with $\vec{j} \notin J$ and $\mathrm{IS}^{M,s_J}_{\mathrm{pseudo}}(\vec{j}) = R$.*

Proof. If J is not complete, then by definition $\exists s, s' \in S_T$ with $s \sim_J s'$ but $s \nsim_{\mathrm{CD}} s'$. By definition of $\sim_{\mathrm{CD}}$, thus $\mathrm{CD}(\mathrm{IS}_{\mathrm{oracle}}(M_s)) \neq \mathrm{CD}(\mathrm{IS}_{\mathrm{oracle}}(M_{s'}))$. We denote the image of s in S_T^J by s_J, then by $s \sim_J s'$ we have $s_J = s'_J$, thus $\mathrm{IS}^{M,s_J}_{\mathrm{pseudo}} = \mathrm{IS}^{M,s'_J}_{\mathrm{pseudo}}$. Thus without loss of generality we may assume

$$G_s := \mathrm{CD}(\mathrm{IS}_{\mathrm{oracle}}(M_s)) \neq \mathrm{CD}(c \circ \mathrm{IS}^{M,s_J}_{\mathrm{pseudo}}) =: G^{\mathrm{pseudo}}_{s_J}, \qquad (*)$$

because if $\mathrm{CD}(c \circ \mathrm{IS}^{M,s_J}_{\mathrm{pseudo}}) = \mathrm{CD}(\mathrm{IS}_{\mathrm{oracle}}(M_s))$ then $\mathrm{CD}(c \circ \mathrm{IS}^{M,s'_J}_{\mathrm{pseudo}}) = \mathrm{CD}(c \circ \mathrm{IS}^{M,s_J}_{\mathrm{pseudo}}) = \mathrm{CD}(\mathrm{IS}_{\mathrm{oracle}}(M_s)) \neq \mathrm{CD}(\mathrm{IS}_{\mathrm{oracle}}(M_{s'}))$ (by the above results), thus switching the roles of s, s' ensures $(*)$ in this case.

By contraposition of the defining property of lookup-regions in Def. B.5, equation $(*)$ implies $\exists \vec{j} \in \mathrm{L}_{\mathrm{pseudo}} := \mathrm{L}_{\mathrm{CD}}(c \circ \mathrm{IS}^{M,s_J}_{\mathrm{pseudo}})$ with

$$c \circ \mathrm{IS}^{M,s_J}_{\mathrm{pseudo}}(\vec{j}) \neq \mathrm{IS}_{\mathrm{oracle}}(M_s)(\vec{j}). \qquad (**)$$

By definition of $\mathrm{IM}_{\mathrm{oracle}}(M)$ in example 4.6 (cf. Rmk. 4.10), the marked oracle $\mathrm{IM}_{\mathrm{oracle}}(M)(\vec{j})$ takes the value 0 (or 1) if and only if all states share this value 0 (or 1), in which case in particular the state s has the oracle-value $\mathrm{IS}_{\mathrm{oracle}}(M_s)(\vec{j}) = 0$ (or 1); thus the above in-equality $(**)$ can only be satisfied for $\mathrm{IM}_{\mathrm{oracle}}(M)(\vec{j}) = \mathrm{IS}^{M,s_J}_{\mathrm{pseudo}}(\vec{j}) = R$ finishing the proof. Note that in this case, $c \circ \mathrm{IS}^{M,s_J}_{\mathrm{pseudo}}(\vec{j}) = 1$ hence s was a representative such that $\mathrm{IS}_{\mathrm{oracle}}(M_s)(\vec{j}) = 0$. $\qquad\square$

Convergence of the algorithm ensures that on the last iteration's run no results $= R$ were reported. That means, no pseudo-test, on its lookup-region, encountered a value R. In particular the choice of c (and $R \mapsto 1$) was irrelevant for the final result.

Lemma E.10 (Complete Pseudo-Atoms are Oracles). *If, using $L^s_{\mathrm{pseudo}} := L_{\mathrm{CD}}(c \circ \mathrm{IS}^{M,s_J}_{\mathrm{pseudo}})$, $\forall s_J \in S_T^J$: $R \notin \mathrm{IS}^{M,s_J}_{\mathrm{pseudo}}(L^s_{\mathrm{pseudo}})$ then*

$$\forall s \in S_T: \quad \mathrm{CD} \circ \mathrm{IS}^{M,s_J}_{\mathrm{pseudo}} = \mathrm{CD} \circ \mathrm{IS}_{\mathrm{oracle}}(M_s)$$

In other words, the following diagram commutes:

$$
\begin{array}{ccc}
S_T & \xrightarrow{\quad \mathrm{CD} \circ \mathrm{IS}_{\mathrm{oracle}}(M_*) \quad} & \\
{\scriptstyle s \mapsto s_J} \Big\downarrow & \mathrm{CD} \circ \mathrm{IS}^{M,*}_{\mathrm{pseudo}} \searrow & \mathcal{G}_{\mathrm{CD}} \\
S_T^J & \nearrow &
\end{array}
$$

Proof. By $R \notin \mathrm{IS}^{M,s_J}_{\mathrm{pseudo}}(L_{\mathrm{CD}}(L^s_{\mathrm{pseudo}}))$, we have for $\vec{j} \in L^s_{\mathrm{pseudo}} - J$ that $\mathrm{IS}^{M,s_J}_{\mathrm{pseudo}}(\vec{j}) = \mathrm{IM}_{\mathrm{oracle}}(M)(\vec{j}) = \mathrm{IS}_{\mathrm{oracle}}(M_s)(\vec{j}) = s(\vec{j})$. Further on J, we have by definition $\mathrm{IM}_{\mathrm{oracle}}(M)(\vec{j}) = s_J(\vec{j}) = s(\vec{j})$. Thus $c \circ \mathrm{IS}^{M,s_J}_{\mathrm{pseudo}}|_{L^s_{\mathrm{pseudo}}} = \mathrm{IS}^{M,s_J}_{\mathrm{pseudo}}|_{L^s_{\mathrm{pseudo}}} = \mathrm{IS}_{\mathrm{oracle}}(M_s)|_{L^s_{\mathrm{pseudo}}}$. By definition B.5 of lookup regions, thus $\mathrm{CD}(c \circ \mathrm{IS}^{M,s_J}_{\mathrm{pseudo}}) = \mathrm{CD}(\mathrm{IS}_{\mathrm{oracle}}(M_s))$. $\qquad\square$

Finally, we have to employ correctness of the CD-algorithm. This is formally required, because S_T^{CD} was defined via $s \sim_{\mathrm{CD}} s' :\Leftrightarrow g_s \sim_{\mathrm{CD}} g_{s'}$ in Def. 3.23, i.e. while the equivalence relation on graphs is CD-specific, the graphs are the true graphs.

Lemma E.11 (Reformulate Consistency). *If CD is consistent (Def. 3.18), then $\forall s \in S_T$: $G_s = \mathrm{CD}(\mathrm{IS}_{\mathrm{oracle}}(M_s))$, where G_s is the equivalence-class in $\mathcal{G}_{\mathrm{CD}}$ of the ground truth graph $g_s \in \mathcal{G}_{\mathrm{gt}}$. The mapping G_* factors through S_T^{CD}. In other words, the following diagram*

commutes:

$$
\begin{array}{ccc}
S_T & \xrightarrow{\;\text{CD} \circ \text{IS}_{\text{oracle}}(M_*)\;} & \\
\downarrow & & \mathcal{G}_{\text{CD}} \\
S_T^{\text{CD}} & \xrightarrow{\quad G_* \quad} &
\end{array}
$$

Proof. This is immediate from the definition of consistency, which specified precisely $g_s \in$ $\text{CD}(\text{IS}_{\text{oracle}}(M_s))$. The factorization of G_* is by definition of S_T^{CD} as the quotient of $s \sim_{\text{CD}}$ $s' \Leftrightarrow G_s = G_{s'}$. $\qquad\square$

Now we can assemble these observations into our main technical result:

Lemma E.12 (Complete Recovery is Oracle-Consistent)**.** *If* CD *is consistent, J is complete and using $L_{\text{pseudo}}^s := L_{\text{CD}}(c \circ \text{IS}_{\text{pseudo}}^{M,s_J})$, then $\forall s_J \in S_T^J$ with $R \notin \text{IS}_{\text{pseudo}}^{M,s_J}(L_{\text{pseudo}}^s)$:*

(a) $\forall s_J \in S_T^J : G_s = \text{CD}(c \circ \text{IS}_{\text{pseudo}}^{M,s_J})$, where G_s is the equivalence-class in $\mathcal{G}_{\text{CD}}$ of the ground truth graph $g_s \in \mathcal{G}_{\text{gt}}$ for any representative $s \in s_J$.

(b) The images agree $\text{img}\big(\text{CD} \circ c \circ \text{IS}_{\text{pseudo}}^{M,*}\big) = \text{img}\big(G_*\big)$, *thus*

$$
\Big\{ \text{CD}(c \circ \text{IS}_{\text{pseudo}}^{M,s_J}) | s_J \in S_T^J \Big\} = \Big\{ G_s | s \in S_T^{\text{CD}} \Big\}.
$$

Indeed, the following diagram commutes (we already know from Lemma E.5 that the left-hand side factors like this, from Lemma E.11 that the outer triangle commutes and from Lemma E.10 that the upper triangle commutes; the claim above states that the lower triangle also commutes):

$$
\begin{array}{ccc}
S_T & \xrightarrow{\quad\text{CD} \circ \text{IS}_{\text{oracle}}(M_*)\quad} & \\
\downarrow {\scriptstyle \text{CD} \circ c \circ \text{IS}_{\text{pseudo}}^{M,*}} & & \mathcal{G}_{\text{CD}} \\
S_T^J & \nearrow {\scriptstyle G_*} & \\
\downarrow & & \\
S_T^{\text{CD}} & &
\end{array}
$$

Proof. Let $s_J \in S_T^J$ and a representative $s \in S_T$ of s_J be arbitrary. By Lemma E.11, $G_s = \text{CD}(\text{IS}_{\text{oracle}}(M_s))$. By Lemma E.10, $\text{CD}(\text{IS}_{\text{oracle}}(M_s)) = \text{CD}(c \circ \text{IS}_{\text{pseudo}}^{M,s_J})$. This shows (a).

Here well-definedness (applying G_s to any representative s) follows indirectly, but it is also evident from Lemma E.5. By this Lemma it is also clear that this choice of s can be replaced by applying the surjective quotient-mapping $q' : S_T^J \twoheadrightarrow S_T^{\text{CD}}$ to s_J. The previous result then reads $G_{q'(s_J)} = \text{CD}(c \circ \text{IS}_{\text{pseudo}}^{M,s_J})$. In particular, the images agree $\text{img}(G_* \circ q') = \text{img}(\text{CD} \circ c \circ \text{IS}_{\text{pseudo}}^{M,*})$ because the mappings agree. With q' being surjective, also the claim (b) follows. $\qquad\square$

The marked independence oracle (and thus the pseudo tests) are recovered from data by the mCIT (see §5), so partial state-space construction needs to provide guarantees only about finding the correct $S_T^J \subset \text{Map}(J, \{0, 1\})$.

Definition E.13 (State-Space Construction)**.** Fix a non-stationary model M. A state-space construction is a mapping S^* that assigns to each set $J \subset I^{2+*}$ of marked independencies

$(\forall \vec{j} \in J : \mathrm{IM}_{\mathrm{oracle}}(M)(\vec{j}) = R)$ a subset $S^J \subset \mathrm{Map}(J, \{0, 1\})$ by using a suitable indicator-relation structure (e. g. IR from Def. F.9 in the case of the implementation for acyclic models in §F.8).

$$S^* : \mathrm{Subsets}\left(\mathrm{IM}^{-1}(\{R\})\right) \times \mathcal{I}_R \to \mathrm{Subsets}\left(\mathrm{Map}(J, \{0, 1\})\right) , \quad (J, \mathrm{IR}) \mapsto S^J(\mathrm{IR}).$$

Given a M-oracle for this indicator-relation structure (e. g. $\mathrm{IR}_{\mathrm{oracle}}(M)$ of example F.13) we call $S^* := S^*(\mathrm{IR}_{\mathrm{oracle}}(M))$ M-sound if $\forall J : S^J \subset S_T^J$, and M-complete if $\forall J : S^J \supset S_T^J$.

Fix a class of non-stationary models $\mathcal{M}$. We call S^* $\mathcal{M}$-sound / $\mathcal{M}$-complete if it is M-sound / M-complete $\forall M \in \mathcal{M}$.

If $J = \emptyset$, then the result is trivial $S^J = \mathrm{Map}(\emptyset, \{0, 1\})$, otherwise the state-space construction may assume (in the oracle case) $J \supset \mathrm{L}_{\mathrm{CD}}(c \circ \mathrm{IM}_{\mathrm{oracle}}(M)) \cap \mathrm{IM}_{\mathrm{oracle}}(M)^{-1}(\{R\})$ (see proof of Thm. 1 in §E.2 below; the inclusion of this restriction on the form of J into the definition will be further discussed in Rmk. F.31).

E.2 The Actual Algorithm

The results in §E.1 already provide the core technical requirements. It remains to relate these results to the algorithmic implementation and assemble the formal claims of the theorem.

Thm 1. *Given a non-stationary model M (Def. 3.4 / 3.7), a marked independence oracle* $\mathrm{IM}_{\mathrm{oracle}}(M)$ *(Def. 4.6; invoked as* `marked_independence` *in algorithm 1), an abstract CD-algorithm* CD *(Def. 3.16; invoked as* `CD` *in algorithm 1), which is consistent (Def. 3.18) on a set of models $\mathcal{M}$ including all reached states (Def. 3.21) $\forall s \in S_T : M_s \in \mathcal{M}$ and a sound and complete on a model-class containing M, state-space construction (Def. E.13; invoked as* `construct_state_space` *in algorithm 2).*

Then algorithm 2 terminates after a finite number of iterations and its output is a set (i. e. no ordering or characterization of states by model properties is implied) which consists of precisely one graph (a CD equivalence class, Def. 3.14) per CD-identifiable state $s \in S_T^{\mathrm{CD}}$

$$\left\{G_s \big| s \in S_T^{\mathrm{CD}}\right\} \quad \text{such that} \quad \forall \tilde{s} \in s : g_{\tilde{s}} \in G_s,$$

where $g_{\tilde{s}}$ is the ground-truth graph in state $\tilde{s}$ (which is a representative of the CD-identifiable state s).

Proof. **The algorithm terminates after a finite number of iterations** (see also Rmk. E.14): Let J_r denote the set J in run r (starting with $r = 0$). Then $J_{r+1} = J_r \cup J'_r$, and if $J_{r+1} = J_r$ the algorithm terminates at step r. Further $J_r \subset J_r \cup J'_r = J_{r+1}$, i. e. as long as the algorithm does not terminate the size of the set J_r strictly increases with r, thus $|J_r| \geq r$ (because $|J_0| = 0$). Since $J_r \subset I^{2+*}$ and I^{2+*} is finite, the algorithm terminates after a finite number of iterations.

Relation of algorithmic to formal description: In the marked independence oracle case (see hypothesis), the function `pseudo_cit` in the sub-algorithm `run_cd` (given s_J as input) computes $c \circ \mathrm{IS}_{\mathrm{pseudo}}^{M, s_J}$. Thus `run_cd` returns (besides J') the graph output $\mathrm{CD}(c \circ \mathrm{IS}_{\mathrm{pseudo}}^{M, s_J})$.

Concerning J'_s, we note that J'_s contains precisely those indices $\vec{j'} \in I^{2+*}$ that

(i) were not already contained in J, i. e. $J'_s \cap J = \emptyset$,

(ii) are encountered by running CD, which by definition are those in $L_{\mathrm{pseudo}}^s := L_{\mathrm{CD}}(c \circ \mathrm{IS}_{\mathrm{pseudo}}^{M, s_J})$, i. e. $J'_s \subset L_{\mathrm{pseudo}}^s$ and

(iii) on which the mCIT (in the oracle case the marked oracle $\mathrm{IM}_{\mathrm{oracle}}$) returned the result R, i. e. $J'_s \subset \mathrm{IM}_{\mathrm{oracle}}^{-1}(\{R\})$.

Finally, by soundness and completeness of the state-space construction (by hypothesis), $S_r = S_T^{J_r}$. For applicability of the state-space construction, see "restricted form of J for state-space construction" near the end of this proof.

Thus the $R \notin \mathrm{IS}_{\mathrm{pseudo}}^{M,s_J}(L_{\mathrm{pseudo}}^s)$ part of the hypothesis of Lemma E.12 is satisfied. But additionally it also shows, if $J' = \emptyset$ (thus if the algorithm terminates), the contra-position of Lemma E.9 applies hence J is complete. So in this case (if $J' = \emptyset$) Lemma E.12 applies (for this s_J, but the core-algorithm unifies all J' returned by invocations of `run_cd` for all s_J, so J' in the core-algorithm is only empty, if this is satisfied for all $s_J \in S^J = S_T^J$, see below).

Correctness of output: We inspect the last round executed before termination (whose results are returned). In particular $J' = \emptyset$, thus $\forall s \in S_r : J_s' = \emptyset$ because $J' = \cup_{s \in S_r} J_s'$.

We first show, by contradiction, that J is complete. Assume J were not complete. By Lemma E.9 (and comparison to the formal description via points (i-iii) of J_s' given above), there $\exists \vec{j}' \in \mathrm{L}_{\mathrm{CD}}(c \circ \mathrm{IS}_{\mathrm{pseudo}}^{M,s_J}) = L_{\mathrm{pseudo}}^s$ (ii), with $\vec{j}' \notin J$ (i) and $\mathrm{IS}_{\mathrm{pseudo}}^{M,s_J}(\vec{j}') = R$ (iii), thus $\vec{j}' \in J_s'$. This contradicts $J_s' = \emptyset$ (see above), and J must be complete.

Next, we show that Lemma E.12 applies. Consistency of CD is given by hypothesis and completeness was shown above so it remains to show $\forall s_J \in S_T^J = S_r$: $R \notin \mathrm{IS}_{\mathrm{pseudo}}^{M,s_J}(L_{\mathrm{pseudo}}^s)$ (the equality $S_T^J = S_r$ is by soundness and completeness of the state-space construction, see above). We again show this by contradiction. Assume there were $s_J \in S_r$ with $R \in \mathrm{IS}_{\mathrm{pseudo}}^{M,s_J}(L_{\mathrm{pseudo}}^s)$, i.e. assume there were a s_J and $\vec{j}' \in L_{\mathrm{pseudo}}^s$ (ii) with $\mathrm{IS}_{\mathrm{pseudo}}^{M,s_J}(\vec{j}') = R$ (iii). Note that $\mathrm{IS}_{\mathrm{pseudo}}^{M,s_J}(\vec{j}') = R$, by definition (Def. E.8), implies $\vec{j}' \notin J$ (i). Thus by the above translation of algorithmic terms to formal terms all conditions (i-iii) are satisfied and $\vec{j}' \in J_s'$. This contradicts $J_s' = \emptyset$ (see above), and the hypothesis of Lemma E.12 must be satisfied.

By Lemma E.12b,

$$\left\{ \mathrm{CD}(c \circ \mathrm{IS}_{\mathrm{pseudo}}^{M,s_J}) | s_J \in S_T^J \right\} = \left\{ G_s | s \in S_T^{\mathrm{CD}} \right\}.$$

The left-hand side is (by the relation of algorithms to formal descriptions above) the set of (graph) outputs produced by `run_cd` on $S_r = S_T^J$. The core-algorithm applies `run_cd` precisely to $S_r = S_T^J$, thus the set of (graph) outputs produced is indeed the set on the left-hand-side. Thus the algorithm outputs the set $\{G_s | s \in S_T^{\mathrm{CD}}\}$ as claimed.

Restricted form of J for state-space construction: Our specification of state-space construction (Def. E.13), allows the state-space construction to assume

$$J \supset \mathrm{L}_{\mathrm{CD}}(c \circ \mathrm{IM}_{\mathrm{oracle}}(M)) \cap \mathrm{IM}_{\mathrm{oracle}}(M)^{-1}(\{R\})$$

in non-trivial ($J \neq \emptyset$) cases. We show that this property of J is always ensured by the core-algorithm. In the initial round $J_0 = \emptyset$. By our convention that c maps R to 1, and the definition of lookup-regions (Def. B.5), the initial round will execute the pseudo-cit (in the oracle case) on the elements of $\vec{j} \in \mathrm{L}_{\mathrm{CD}}(c \circ \mathrm{IM}_{\mathrm{oracle}}(M))$. In the oracle case, those $\vec{j}$ with additionally $\mathrm{IM}_{\mathrm{oracle}}(M)(\vec{j}) = R$, are collected into $J_1 = \mathrm{L}_{\mathrm{CD}}(c \circ \mathrm{IM}_{\mathrm{oracle}}(M)) \cap \mathrm{IM}_{\mathrm{oracle}}(M)^{-1}(\{R\})$. In subsequent iterations, J can only grow, thus for $r \geq 1$, $J_r \supset J_1$. Therefore, the state-space construction is only invoked from the core-algorithm with J satisfying this restriction / assumption on J as stated in Def. E.13. $\square$

Remark E.14. In practice the convergence is very fast (the number of outer iterations in the core-algorithm is low). As the reader may convince themselves, the first iteration (by specification of the pseudo-cit) produces the union-graph, see Lemma F.18 (or its acyclification in the cyclic case). In the acyclic case (see §6), all states can be found on tests performed on the union-graph, if no finite-sample errors occur. Thus the algorithm terminates after $r = 1$ in this case.

F Details on State-Space Construction

The main purpose of this section is to approach – and under suitable assumptions to resolve – the question of representation of states and detected indicators, with the eventual goal of implementing `construct_state_space` (Def. E.13) for use in the core algorithm. We first recall the basic problem of induced indicators from §4.2, which was illustrated by:

Example 4.8 (Induced Indicators)**.** Consider $X \leftarrow Y \rightarrow Z$ with only R_{XY}^{model} non-trivial. This will, besides $R_{XY|\emptyset}$ non-trivial, also lead to $R_{XZ|\emptyset}$ non-trivial, even though R_{XZ}^{model} is trivial. Further, while both are non-trivial, $R_{XZ|\emptyset} \equiv R_{XY|\emptyset}$; the underlying model only has two states (as opposed to the four potential values the pair $(R_{XY|\emptyset}, R_{XZ|\emptyset})$ could take): One with the link $X \leftarrow Y$ active, one with the link $X \leftarrow Y$ not active.

We will approach this problem by first finding and representing states, then expressing detected indicators relative to these states. For the above example, there are two states corresponding to presence / absence of the link $X \leftarrow Y$. They can be "represented" by (the value of) the independence $X \perp\!\!\!\perp Y$. Finally, the detected indicators can be expressed as functions of the (binary) state, thus relative to the representing test $X \perp\!\!\!\perp Y$ (in the example, all non-stationary independencies, agree with this representing one) rather than as a time-resolved function.

We will start by discussing assumptions that allow for a systematic resolution of this problem. Next, there is an additional, so far neglected, step: Formulating a hypothesis test, that can be tested directly (without requiring time-resolution of any indicators) and is simple enough to be accessible in practice, yet general enough that its (oracle-)results suffice to recover from a marked independence structure the full multi-valued independence-structure. From there, we can follow the program laid out above to produce an algorithm `construct_state_space` that satisfies the requirements of the core algorithm (Algo. 2). Finally, we give a simple approach to transfer edge-orientations between states, which allows for simple output-representation by a labeled union-graph, and lay out relevant topics for future work.

F.1 Assumptions

For simplicity, we focus on the acyclic case. This will simplify the representation of model-indicators, the required hypothesis-testing and many other arguments.

Assumption F.1 (Acyclicity)**.** The (true) union graph is ancestral (an AG), i.e. it contains no directed or almost directed cycles. Per-state graphs are additionally maximal (MAGs; see Rmk. F.2). We use definitions of these terms as given for example in [70].

Remark F.2. The necessity of state-graphs to be MAGs is not immediately evident. It arises due to the following problem: Assume there are precisely two states, with the denser (graph's) one not being a MAG. Than this denser graph contains one or multiple inducing paths. In the sparser (graph's) state some of these inducing paths may vanish additional to the true model indicator's link. In this case *multiple* links can change at once, even for modular changes (see Ass. F.6 below). It is possible to remedy these issues by suitable post-processing (see §F.10.4), but this would require a more complex (in terms of implementation and number of tests required) approach.

We mostly ignored the details of *how* causal discovery algorithms discover graphs. Here we *do* require that the CD-algorithm is of a particular (albeit very general) form (see Rmk. F.4 and example F.5 below)

Assumption F.3 (Conventional Skeleton Discovery)**.** The CD-algorithm CD (on the given model class) is such that

  (a) Resolved Skeleton: If g and g' (which can occur as state-graphs in our model class) have different skeleta, then $g \not\sim_{\mathrm{CD}} g'$.

(b) Exploitation of Sparsity (in skeleton phase): if $\text{IS} \leq \text{IS}'$, then $\text{L}_{\text{CD}}(\text{IS}) \subset \text{L}_{\text{CD}}(\text{IS}')$.

(c) Local Edge Removal: if $\text{CD}(\text{IS})$ contains no edge between X and Y, then $\exists Z$ such that $(i_x, i_y, \vec{i}_z) \in \text{L}_{\text{CD}}(\text{IS})$ and $X \perp\!\!\!\perp_{\text{IS}} Y|Z$.

Remark F.4. The authors are not aware of any commonly used constraint-based algorithm that would actually violate this assumption. At least the ones used in the numerical experiments in this paper abide by it, simply by virtue of how skeleta are discovered. Parts (a) and (b) are assumed for simplicity, essentially avoiding the discussion of partial (incomplete J) discovery in §F.8; they are very likely not necessary for our method, just convenient for the proofs. There are plausible scenarios where one might want to consider CD-algorithms violating (a), for example when aiming for the estimation of a particular effect, it may not be necessary to recover the correct skeleton everywhere. Note, that in the presence of hidden confounders, (a) can be violated because the representatives of the same MAG can have different skeleta at inducing paths (see Rmk. F.2 and §F.6); Ass. F.1 excludes this. Part (b) could be plausibly violated if for denser graphs more work has to be done to find edge-orientations by additional tests. In practice, part (b) could be weakened (given appropriate definitions) for example to a statement about lookup-regions of the skeleton phase (see its application in the proof of Lemma F.22).

The condition (c) is required for the way model-indicators are currently represented, see Lemma F.22. It is even for MAGs *possible* (at least in principle) to violate this assumption (c), by creative construction of a CD-algorithm, see example F.5. The practical usefulness of algorithms violating (c) seems to very strongly hinge on prior knowledge about certain independencies being much more difficult to assess than others. For example, if we knew that the link X to Y in example F.5, if it exists, might have a very complicated functional form, while other parts of the model are linear, the logic of the example below could be favorable.

Example F.5 (Unconventional CD-Logic)**.** Consider an acyclic, causally sufficient model with the following causal graph:

$$
\begin{array}{ccc}
Z' & & W' \\
\downarrow & & \downarrow \\
Z \longrightarrow X \dashrightarrow Y \longrightarrow W
\end{array}
$$

Any paths from the left sub-graph (X, Z, Z') to the right sub-graph (Y, W, W') can be blocked by either X or Y, and the colliders are both unshielded, thus we can find the two subgraphs and the absence of any edge (ignoring X–Y for now) connecting them indirectly (other than through $X \to Y$). Further, by $Z' \perp\!\!\!\perp Y|X$, there cannot be an edge $X \leftarrow Y$. Hence the presence or absence of the edge $X \to Y$ can be determined non-locally, by testing $Z \perp\!\!\!\perp Y$. Thus we need not test any independence of the form $X \perp\!\!\!\perp Y|S$ for any S to consistently distinguish the two graphs with / without $X \to Y$. In particular, there exists a constraint based algorithm (for example, try the above trick, if it does not work apply PC) that is consistent on causally sufficient acyclic models, yet does *not* satisfy Ass. F.3c.

Further, we assume changes are modular (see §F.10.4).

Assumption F.6 (Modular and Reached)**.** Changes are modular (Def. C.3), that is links change independently of each other, thus the reachable states are all combinations (presence / absence) of changing links (non-trivial indicators). Further we assume all reachable states are reached in the given data.

F.2   Notations

From §E, we use:

Notation F.7. To interpret marked independence structures we occasionally use the choice

map c from Def. E.8:

$$c : \{0, 1, R\} \to \{0, 1\}, \quad \begin{cases} 0 \mapsto 0 \\ 1 \mapsto 1 \\ R \mapsto 1 \end{cases} .$$

Acyclicity allows to simplify the notation for model-indicators:

Notation F.8. Given assumption Ass. F.1 (acyclicity), there is a total order of nodes (extending the partial order $X \leq Y :\Leftrightarrow X \in \mathrm{Anc}(Y)$) called a causal order. By acyclicity, if $X_i = X \leq Y = X_j$, then $Y \notin \mathrm{Pa}(X)$, thus $R_{ji} \equiv 0$. So all information about this link is in R_{ij}. Thus we will only consider

$$R_{XY}^{\mathrm{model}}(t) := R_{ij}^{\mathrm{model}}(t) + R_{ji}^{\mathrm{model}}(t) = \max(R_{ij}^{\mathrm{model}}(t), R_{ji}^{\mathrm{model}}(t)) \quad \text{for } X = X_i, \, Y = X_j.$$

By definition of states S (Def. 3.9), all model-indicators can be written as functions of S (instead of T). Since by definition (Def. 3.4 / 3.7) all qualitative changes in the model come from the changes in state (see Lemma 3.10), also all detected indicators an be written as a function of S. We will still denote these by R_{XY}^{model} and $R_{XY|Z}$ etc., but explicitly write the argument as s, i.e. $R_{XY}^{\mathrm{model}}(s)$, $R_{XY|Z}(s)$ and so on.

It will turn out that many of the subsequent results have elegant expressions relative to the following simple ordering-relations:

Definition F.9. On the set of indicators we consider the following partial order:

(a) $$R_1 \leq R_2 \quad :\Leftrightarrow \quad \forall t : R_1(t) \leq R_2(t)$$

For fixed X, Y this induces a preorder on $Z \subset V - \{X, Y\}$:

(b) $$Z_1 \leq_{XY} Z_2 \quad :\Leftrightarrow \quad R_{XY|Z_1} \leq R_{XY|Z_2}$$

States can be partially ordered by density of (active) model-indicators:

(c) $$s_1 \leq s_2 \quad :\Leftrightarrow \quad \left(\forall R^{\mathrm{model}} : R^{\mathrm{model}}(s_1) \leq R^{\mathrm{model}}(s_2) \right)$$

And finally graphs can be partially[24] ordered by d-connectivity (the reader may note a certain similarity to the ordering relation used by [11]):

(d) $$g_1 \leq g_2 \quad :\Leftrightarrow \quad \left(X \not\perp_{g_1} Y | Z \Rightarrow X \not\perp_{g_2} Y | Z \right)$$

Notation F.10. For binary indicators, part (a) is equivalent to an implication (of independencies)

$$R_1 \leq R_2 \quad \Leftrightarrow \quad \left(R_2(t) = 0 \Rightarrow R_1(t) = 0 \right)$$

motivating the notation $(R_2 \Rightarrow R_1) :\Leftrightarrow (R_1 \leq R_2)$.

F.3 Required Hypothesis Tests

Assume we knew the regime-marked independence structure IM. Then any detected state (element of IX) is given by some combination of truth-values for the true regimes in IM. There is only a finite (and N independent) number of such combinations, thus it suffices to exclude finitely many *not* appearing in IX. However, there can still be many possible combinations of truth-values. In practice, under the assumptions of this section, it will suffice to test implications with the following simplified[25] form:

---

[24]They can certainly be preordered, those identified by constraint-based algorithms can also be partially ordered. This distinction will not matter here.

[25]In principle, there could be arbitrary boolean relations required on both sides. Instead it suffices to test with a boolean and on the left and a single indicator / representing independence on the right.

Notation F.11. A multi-index $\vec{i} = (i_X, i_Y, (i_{Z_1}, \ldots, i_{Z_k}))$ identifies an independence-relation $X \perp\!\!\!\perp Y|Z$. We call this test marked if $X \perp\!\!\!\perp_R Y|Z$ with respect to some fixed marked independence structure (Def. 4.3), usually we will use the marked oracle (example 4.6). If the test at $\vec{i}$ is marked, there is an associated detected indicator (example 4.8) $R_{\vec{i}}$.

Definition F.12 (Indicator Implication-Relations)**.** Given the marked independencies $\vec{i}_1$, $\vec{i}_2$, $\ldots$, $\vec{i}_{K+1} \in J \subset I^{2+*}$ we call the statement

$$R_{\vec{i}_1}(t) = R_{\vec{i}_2}(t) = \ldots = R_{\vec{i}_K}(t) = 0 \quad \Rightarrow \quad R_{\vec{i}_{K+1}}(t) = 0$$

an indicator implication. This is equivalent to

$$R_{\vec{i}_{K+1}} \leq \sum_{j=1}^{K} R_{\vec{i}_j}.$$

To keep everything binary, the sum on the right-hand side in the last equation can be replaced by a boolean 'or'. The implication-relation structure IR is then formally a mapping

$$\mathrm{IR} : \left(I^{2+*}\right)^{*+1} \to \{0, 1\},$$

i.e. we assign truth-values (true or false) to statements of the form $R_1(t) = R_2(t) = \ldots = R_K(t) = 0 \Rightarrow R_{K+1}(t) = 0$ (cf. example F.13).

Recall that we had defined a marked independence structure (Def. 4.3) and associated oracle (example 4.6), similarly here:

Example F.13 (Implication-Relation Oracle)**.** The implication-relation oracle $\mathrm{IR}_{\mathrm{oracle}}$ of a non-stationary SCM M (Def. 3.4 / 3.7) is the implication-relation structure, which assigns to each implication statement $R_{\vec{i}_1}(t) = R_{\vec{i}_2}(t) = \ldots = R_{\vec{i}_K}(t) = 0 \Rightarrow R_{\vec{i}_{K+1}}(t) = 0$ the truth value of the corresponding expression of the true (taking values determined by the induced observable distribution of M) indicators R (see Rmk. F.14, which gives an alternative definition from $\mathrm{IX}_{\mathrm{oracle}}$).

Remark F.14. The multi-valued independence-structure oracle $\mathrm{IX}_{\mathrm{oracle}}$, implies a implication-relation oracle: The relation $R_{\vec{i}_{K+1}} \leq \sum_{j=1}^{K} R_{\vec{i}_j}$ is true in the implication-relation oracle, i.e. $\mathrm{IR}_{\mathrm{oracle}}((\vec{i}_1, \ldots, \vec{i}_K), \vec{i}_{K+1}) = 1$, if and only if

$$\forall \mathrm{IS} \in \mathrm{IX}_{\mathrm{oracle}} : \quad \mathrm{IS}(\vec{i}_{K+1}) \leq \sum_{j=1}^{K} \mathrm{IS}(\vec{i}_j).$$

Thus knowledge of this relation-structure is necessary for the reconstruction of $\mathrm{IX}_{\mathrm{oracle}}$ (which in turn is necessary to solve the MCD problem by Lemma 4.13). Here we show that, at least under the assumptions of the present section, knowledge of marked independencies plus these relations is also sufficient to reconstruct $\mathrm{IX}_{\mathrm{oracle}}$.

While formulated via indicators, this is again a statement whose complexity does *not* grow with the sample-size N, and can be tested "directly" similar to the marked independencies (§4.1). In practice, we can use constraints from causal modeling to further simplify what form the left-hand-side in this definition may take, the number of summands on the left-hand-side and the total number of tests (see also §F.10.1). The implementation of these tests is discussed in §D.4.7.

Cyclic models seem to additionally require a type of "union test" (a boolean 'or' on the left hand side of the implications), see example F.23 and §F.10.2.
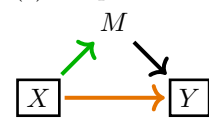
(a) basic example:

$X \leftarrow Z \rightarrow Y$

(b) "in sequence":

$X \leftarrow Z \rightarrow Y$

(c) "in parallel":

Figure F.1: Different layouts of independently changing (differently colored) links. Main point of interest is $R_{XY|\emptyset}$.

F.4 Helpful Observations

In cases where multiple links might change independently, the situation can quickly become quite complex as the following example shows:

Example F.15 (Requirement For Boolean Combinations)**.** In Fig. F.1, different types of combinations of multiple indicators are shown. While (a) is the previous, rather basic example, (b) and (c) illustrate how different boolean combinations arise. First, focus on the empty conditioning set: In case (b), there is no path from X to Y iff either the green *or* the orange link vanish. In case (c), there is no path from X to Y iff both the green *and* the orange link vanish. We return to these cases in example F.26.

While the previous example shows that in general detected indicators can arise from model-indicators as complicated boolean combinations, we can always reorder such combinations to first consider all boolean 'and' (and only have to test these), and afterwards all boolean 'or' (cf. §F.7) by the following observation: Taking away a link can disconnect an open path, but it cannot unblock a closed path.

Lemma F.16 (Monotonicity of State to d-Separation Assignment)**.** *Under Ass. F.1 (union acyclicity), the assignment of states to state-graphs is monotonically increasing with respect to the orders in Def. F.9c, d:*

$$s_1 \leq s_2 \quad \Rightarrow \quad g_{s_1} \leq g_{s_2} \quad \overset{\text{def}}{\Leftrightarrow} \quad \left(X \not\perp\!\!\!\perp_{g_{s_1}} Y | Z \Rightarrow X \not\perp\!\!\!\perp_{g_{s_2}} Y | Z \right)$$

Proof. Given $s \leq s'$. We have to show $X \not\perp\!\!\!\perp_{g_s} Y | Z \Rightarrow X \not\perp\!\!\!\perp_{g_{s'}} Y | Z$.

Let X, Y, Z be arbitrary. Assume $X \not\perp\!\!\!\perp_{g_s} Y | Z$, otherwise there is nothing to show. By definition, there is an open path γ in g_s between X and Y with Z blocked. By $s \leq s'$, all edges contained in g_s are also edges in $g_{s'}$ in particular all edges along γ (a path in g_s) are edges in $g_{s'}$, thus γ is a well-defined path in $g_{s'}$. A path γ is open by definition, if (i) all non-colliders on γ are not in Z and (ii) all colliders on γ have a descendant in Z (where we formally define descendants to include Z itself: $Z \in \text{Desc}(Z)$). With γ being open in g_s, both criteria are satisfied in g_s, we have to check them in $g_{s'}$. By acyclicity, the distinction collider vs. non-collider is the same in g_s and $g_{s'}$.

(i) Since Z is unchanged, all non-colliders are still not in Z. This condition is still satisfied in $g_{s'}$.

(ii) Let W be an arbitrary collider on γ. Because γ is open (given Z) in g_s, $\exists W' \in \text{Desc}_{g_s}(W) : W' \in Z$, where $\text{Desc}_{g_s}(W)$ are the descendants of W in g_s. It suffices to show $\text{Desc}_{g_s}(W) \subset \text{Desc}_{g_{s'}}(W)$, then $W' \in \text{Desc}_{g_{s'}}(W)$ and the condition is still satisfied in $g_{s'}$. By definition, $\text{Desc}_g(W) := \{ \tilde{W} \mid \exists$ directed path γ' in g from W to $\tilde{W} \}$. Any directed path γ in g_s is a directed path in $g_{s'}$ from $s' \leq s$ (see above) and acyclicity. Thus $\text{Desc}_{g_s}(W) \subset \text{Desc}_{g_{s'}}(W)$.

Thus we have seen γ is an open path in $g_{s'}$. Therefore $X \not\perp\!\!\!\perp_{g_{s'}} Y | Z$, concluding the proof. □

Under suitable Markov and faithfulness properties, this result also applies to independence oracles.

Lemma F.17 (Monotonicity of Detected-Indicators)**.** *Under Ass. F.1 (union acyclicity) and Ass. 3.24 (faithfulness), if $s \leq s'$, then $\text{IS}_{\text{oracle}}(M_s) \leq \text{IS}_{\text{oracle}}(M_{s'})$. In particular $s \leq s'$ $\Rightarrow R_{XY|Z}(s) \leq R_{XY|Z}(s')$.*

Proof. Let $\vec{j} \in I^{2+*}$ be arbitrary. If $\mathrm{IS}_{\mathrm{oracle}}(M_s)(\vec{j}) = 1$, then $\vec{j}$ is d-connected[26] in g_s by the Markov-property 3.25. By $s \leq s'$ and the previous Lemma F.16, $\vec{j}$ is also d-connected in $g_{s'}$. By faithfulness, thus $\mathrm{IS}_{\mathrm{oracle}}(M_{s'})(\vec{j}) = 1$. Finally, the value $R_{XY|Z}(s)$ is 0 iff $X \perp\!\!\!\perp_{\mathrm{IS}_{\mathrm{oracle}}(M_s)} Y|Z$ (by definition of detected indicators Def. 4.4), i.e. $R_{XY|Z}(s) = \mathrm{IS}_{\mathrm{oracle}}(M_s)(i_x, i_y, i_{\vec{z}})$, so the claim $R_{XY|Z}(s) \leq R_{XY|Z}(s')$ also follows. $\qquad\square$

This also characterizes the union-graph and the pseudo-cit:

Lemma F.18 (Union States and Graphs). *Under Ass. F.1 (union acyclicity) and Ass. 3.24 (faithfulness), $c \circ \mathrm{IM}_{\mathrm{oracle}}(M) = \mathrm{IS}_{\mathrm{oracle}}(M; s_{\mathrm{union}})$, where s_{union} is the state where all model-indicators are active ($= 1$). If additionally CD is consistent then $G_{\mathrm{union}} = \mathrm{CD}(\mathrm{IS}_{\mathrm{oracle}}(M; s_{\mathrm{union}}))$ is the equivalence-class of the union-graph.*

Proof. Note, that $\forall s \in S : s_{\mathrm{union}} \geq s$ by construction. Let $\vec{j} \in I^{2+*}$ be arbitrary. If $\mathrm{IM}_{\mathrm{oracle}}(M)(\vec{j}) \in \{0, 1\}$, then $c \circ \mathrm{IM}_{\mathrm{oracle}}(M)(\vec{j}) = \mathrm{IM}_{\mathrm{oracle}}(M)(\vec{j}) = \mathrm{IS}_{\mathrm{oracle}}(M; s_{\mathrm{union}})(\vec{j})$ by definition of the marked oracle (example 4.6). If $\mathrm{IM}_{\mathrm{oracle}}(M)(\vec{j}) = R$, then $\exists s', s''$ such that $\mathrm{IS}_{\mathrm{oracle}}(M_{s'})(\vec{j}) = 0$, $\mathrm{IS}_{\mathrm{oracle}}(M_{s''})(\vec{j}) = 1$, again by definition of the marked oracle (example 4.6). By maximality $s_{\mathrm{union}} \geq s''$ and the previous Lemma F.17, we therefore have $c \circ \mathrm{IM}_{\mathrm{oracle}}(M)(\vec{j}) = c(R) = 1 = \mathrm{IS}_{\mathrm{oracle}}(M_{s_{\mathrm{union}}})(\vec{j})$ also in this case.

The second claim about the union-graph follows by definition of the union graph. $\quad\square$

Another simple, but very helpful, observation is that under Ass. F.6 (modularity, reachedness), the reached state-space is spanned (as a $\mathbb{Z}/2\mathbb{Z}$ vector-space) by the model indicators (see Def. 3.9). Here the assumption is reachedness as opposed to reachability (Lemma C.4).

Lemma F.19 (Modular Reachedness). *Given Ass. F.6 (modularity, reachedness) the reached states $S_T = S$ are given by all combination of model indicators (see Def. 3.9).*

Proof. By modularity (independence of changes), the reachable states are given by the tuples of values taken by the non-trivial model-indicators, thus are the elements of the product of (binary) value-spaces of those indicators. By Ass. F.6, reachable states are reached. $\quad\square$

F.5   Model Indicators

Under the acyclicity assumptions of the present section, the model-indicator is contained by all detected indicators in the following sense:

Lemma F.20 (Model Indicators are Lower Bound). *Assuming Ass. 3.24 (faithfulness), and Ass. F.1 (acyclicity), fix an arbitrary pair X, Y, then R_{XY}^{model} is a lower bound for detected indicators w.r.t. the ordering from Def. F.9a. That is, for all Z the detected indicator $R_{XY|Z}$ is comparable to and greater than R_{XY}^{model}:*

$$\forall Z : R_{XY|Z} \geq R_{XY}^{\mathrm{model}}$$

Proof. Let Z, t be arbitrary. We can equivalently show $R_{XY}^{\mathrm{model}}(t) \neq 0 \Rightarrow R_{XY|Z}(t) \neq 0$. If $R_{XY}^{\mathrm{model}}(t) \neq 0$, the direct path $X \to Y$ is open, thus there is no Z blocking it and therefore $X \not\perp\!\!\!\perp_{g_t} Y|Z$. By faithfulness, d-separation implies independence, thus $R_{XY|Z}(t) \neq 0$. $\quad\square$

Corollary F.21. *In particular, under the assumptions of the lemma, if there is a Z with $X \perp\!\!\!\perp Y|Z$, and thus $R_{XY|Z} \equiv 0$, then $R_{XY}^{\mathrm{model}} \equiv 0$ is also trivial.*

So the model-indicator is a lower bound (w.r.t. our ordering relation), further this lower bound is attained, i.e. the model-indicator is realized as the minimum in the following sense (conventional skeleton discovery is here obviously required to ensure the completeness of the discovered state-space in part b):

---

[26]Since $\vec{j} = (i_x, i_y, i_{\vec{z}})$ corresponds to a test $X_{i_x} \perp\!\!\!\perp X_{i_y}|X_{i_{\vec{z}}}$, it makes sense to say "$\vec{j}$ is d-connected in g" if $X_{i_x} \not\perp\!\!\!\perp_g X_{i_y}|X_{i_{\vec{z}}}$.

Lemma F.22 (Representation of Model Indicators)**.** *Assume Ass. F.3 (conventional skeleton discovery), Ass. F.1 (acyclicity) and Ass. 3.24 (faithfulness). Given X, Y, and a consistent (Def. 3.18) CD, then there is a set Z, such that*
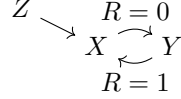
(a) *$R_{XY|Z} \equiv R_{XY}^{\mathrm{model}}$ and*

(b) *The test $X \perp\!\!\!\perp Y | Z$ is in the lookup-region of the union graph: $\vec{j} = (i_x, i_y, i_{\vec{z}}) \in \mathrm{L}_{\mathrm{CD}}(c \circ \mathrm{IM}_{\mathrm{oracle}}(M))$.*

Proof. By Lemma F.18, $c \circ \mathrm{IM}_{\mathrm{oracle}}(M) = \mathrm{IS}_{\mathrm{oracle}}(M_{s_{\mathrm{union}}})$, where s_{union} is the state with all non-trivial model-indicators equal to one. Let s_{XY} be the state where $R_{XY}^{\mathrm{model}}(s_{XY}) = 0$, while all other model-indicators are 1 (see Lemma F.19). By Ass. F.3a, $\mathrm{CD}(\mathrm{IS}_{\mathrm{oracle}}(M_{s_{\mathrm{union}}})) \neq \mathrm{CD}(\mathrm{IS}_{\mathrm{oracle}}(M_{s_{XY}}))$. By Ass. F.3c, this implies the existence of a test of the form $\vec{j} = (i_x, i_y, i_{\vec{z}}) \in \mathrm{L}_{\mathrm{CD}}(\mathrm{IS}_{\mathrm{oracle}}(M_{s_{XY}}))$, with $R_{\vec{j}}(s_{XY}) = 0$. By Ass. F.3b (and $s_{XY} \leq s_{\mathrm{union}}$ and Lemma F.17) $\mathrm{L}_{\mathrm{CD}}(\mathrm{IS}_{\mathrm{oracle}}(M_{s_{XY}})) \subset \mathrm{L}_{\mathrm{CD}}(\mathrm{IS}_{\mathrm{oracle}}(M_{s_{\mathrm{union}}}))$. Since (by Lemma F.18, see start of this proof), $c \circ \mathrm{IM}_{\mathrm{oracle}}(M) = \mathrm{IS}_{\mathrm{oracle}}(M_{s_{\mathrm{union}}})$, this shows that the test $\vec{j}$ satisfies requirement (b).

With Lemma F.20, it suffices to show $R_{XY|Z} \leq R_{XY}^{\mathrm{model}}$ for part (a). Let s' be an arbitrary state. If $R_{XY}^{\mathrm{model}}(s') = 1$, then $R_{XY|Z} \leq R_{XY}^{\mathrm{model}}$. If $R_{XY}^{\mathrm{model}}(s') = 0$, we have $s' \leq s_{XY}$ (by construction of s_{XY}). By Lemma F.17 thus $\mathrm{IS}_{\mathrm{oracle}}(M_{s'}) \leq \mathrm{IS}_{\mathrm{oracle}}(M_{s_{XY}})$. In particular $R_{XY|Z}(s') \leq R_{XY|Z}(s_{XY}) = 0 \leq R_{XY}^{\mathrm{model}}(s')$. Since s' was arbitrary, we thus have shown $R_{XY|Z} \leq R_{XY}^{\mathrm{model}}$, completing the proof. $\qquad\square$

In the presence of cycles, a more complex representation-logic, including representation by "union-tests" would be required:

Example F.23. Consider a cyclic model with the following union graph,

$$
\begin{array}{c}
Z \searrow \quad R = 0 \\
X \overset{\longrightarrow}{\underset{\longleftarrow}{}} Y \\
R = 1
\end{array}
$$

with two regimes, where in one the edge $X \to Y$ is present, while in the other one $X \leftarrow Y$. Then

$$\text{Regime } R = 0: \ Z \not\perp\!\!\!\perp Y \text{ and } Z \perp\!\!\!\perp Y | X$$
$$\text{Regime } R = 1: \ Z \perp\!\!\!\perp Y \text{ and } Z \not\perp\!\!\!\perp Y | X,$$

i.e. the independence-statements are complementary (one always holds). More generally, if there was an independently changing link $Z \to Y$, then the model-indicator R_{ZX}^{model} would be represented by the union (or product) $R_{ZX}^{\mathrm{model}} = R_{ZY|\emptyset} R_{ZY|X}$.

For acyclic models, we already find one possible (albeit unlikely optimal in the finite sample case) procedure to obtain a model indicator:

Corollary F.24. *Assume CD is consistent (Def. 3.18), Ass. F.3 (conventional skeleton discovery), Ass. F.1 (acyclicity) and Ass. 3.24 (faithfulness). Knowing all detected indicators $R_{XY|Z}$, the model indicator on XY is the product of all detected indicators on this link: $R_{XY}^{\mathrm{model}} = \prod_Z R_{XY|Z}$.*

In practice, it may be more efficient to find a representor whose existence is guaranteed by lemma F.22:

Corollary F.25. *Assume CD is consistent (Def. 3.18), Ass. F.3 (conventional skeleton discovery), Ass. F.1 (acyclicity) and Ass. 3.24 (faithfulness). Fix X, Y. Then $\exists \min_{XY}\{Z \subset V - \{X,Y\}\}$ with respect to the order-relation defined in Def. F.9b and the detected indicator associated to this minimum coincides with the model indicator:*

$$R_{XY}^{\mathrm{model}} \equiv R_{XY|\min_{XY}\{Z \subset V - \{X,Y\}\}}$$

Further, at least one Z realizing this minimum is such that $X \perp\!\!\!\perp Y|Z$ is in the lookup-region $\mathrm{L_{CD}}(c \circ \mathrm{IM_{oracle}}(M))$.

The search for this (in general non-unique) minimum $\min_{XY}\{Z \subset V - \{X,Y\}\}$ can be easily and efficiently implemented (see Algo. 3): Initialize all model-indicators as trivial $\equiv 1$ (as CD starts from a fully connected graph). Whenever $X \perp\!\!\!\perp Y|Z$ for some Z, update $R_{XY}^{\mathrm{model}} \equiv 0$, whenever we find $X \perp\!\!\!\perp_R Y|Z$ thus a non-trivial $R_{XY|Z}$, update $R_{XY}^{\mathrm{model}} = R_{XY|Z}$ if $R_{XY|Z} \leq R_{XY}^{\mathrm{model}}$. This last comparison is either trivial[27] (if the previous value for R_{XY}^{model} was trivial), or a comparison with $R_{XY}^{\mathrm{model}} = R_{XY|Z'}$ (i. e. a previously found representation by a detected indicator), so it requires only testing of implications of the form Def. F.12 between detected indicators (in fact, here always $K = 1$ in Def. F.12).

Algorithm 3 Model Indicator Discovery (union-acyclic case, g_s are MAGs)

1: **Input:** A set I of all independencies tested, a set $J \subset I$ of marked independencies.
2: **Output:** A set $\mathcal{R}$ containing exactly one representative $R_{\vec{j}} = R_{XY|Z}$ for each non-trivial model-indicator R_{XY}^{model}, such that $R_{XY}^{\mathrm{model}} \equiv R_{XY|Z}$. Enumerating $R_{\vec{j}}$ by $\vec{j}$, we can consider $\mathcal{R} \subset J$.
3: Initialize $\mathcal{R} = \emptyset$.
4: Define $I_{XY} := \{\vec{i} = (i_X, i_Y, \vec{i}_Z) \in I | i_X \text{ is index of } X, i_Y \text{ is index of } Y\}$.
5: Define $J_{XY} := I_{XY} \cap J$.
6: **for** each pair / link (X,Y) with $J_{XY} \neq \emptyset$ **do**
7:     **if** $\exists \vec{i}_z$ with $(i_X, i_Y, \vec{i}_Z) \in I_{XY}$ and $X \perp\!\!\!\perp Y|Z$ **then**
8:         **continue** with next link.
9:     **end if**
10:     Initialize $R_{XY}^{\mathrm{model}} :\equiv 1$.
11:     **for** $\vec{j} \in J_{XY}$ with associated $R_{\vec{j}} = R_{XY|Z}$ **do**
12:         **if** $R_{XY|Z} \leq R_{XY}^{\mathrm{model}}$ **then**   ▷ If $R_{XY}^{\mathrm{model}} \equiv 1$ this is always true.
13:             Replace $R_{XY}^{\mathrm{model}} :\equiv R_{XY|Z}$.   ▷ Rmk: By $\vec{j} \in J$, $R_{XY|Z}$ is non-trivial.
14:         **end if**
15:     **end for**
16:     Add R_{XY}^{model} to $\mathcal{R}$.   ▷ Rmk: By $J_{XY} \neq \emptyset$, the added indicator is non-trivial.
17: **end for**
18: **return** $\mathcal{R}$

Finally, if changes are independent (Ass. F.6), then the non-trivial model-indicators span the state-space, see Lemma F.19. I. e. knowledge of all model indicators allows in this case to enumerate all states. Before we continue with characterizing these states by properties of the model in §F.6, we briefly apply the above ideas to an example.

Example F.26 (Continuing Example F.15)**.** We apply the previous section to example F.15 (see Fig. F.1). In case (b), $X \perp\!\!\!\perp Y|Z$, so the model-indicator $R_{XY}^{\mathrm{model}} \equiv 0$ is correctly concluded to be trivially zero. In case (c), $X \perp\!\!\!\perp_R Y|M$ with $R_{XY|M} \leq R_{XY|\emptyset}$ thus $\{M\} \leq_{XY} \emptyset$, so while $R_{XY|\emptyset}$ depends on both model-indicators, we correctly represent $R_{XY}^{\mathrm{model}} \equiv R_{XY|M}$.

F.6   Interpretation of Discovered States

When defining model properties in §3 we in particular defined states of models (§3.3). While the elements of a multi-valued independence-structure also correspond to "states" of the independence-structure (see example 4.11), it is not clear in general, how the elements of the multi-valued independence-structure can be associated to states on the model. We will refer to this task as indicator translation.

---

[27]If $R_{XY}^{\mathrm{model}} \equiv 1$, then $R_{XY|Z} \leq R_{XY}^{\mathrm{model}}$ is always true, if $R_{XY}^{\mathrm{model}} \equiv 0$, then $R_{XY|Z} \leq R_{XY}^{\mathrm{model}}$ is always false.

Definition F.27 (Indicator Translation)**.** Given a non-stationary SCM M with state-space $S(M)$ (Def. 3.9) and extended independence-structure $\mathrm{IX}_{\mathrm{oracle}}(M)$, then the indicator translation is the mapping

$$\psi : S(M) \twoheadrightarrow \mathrm{IX}_{\mathrm{oracle}}(M), \quad s \mapsto \mathrm{IS}_{\mathrm{oracle}}(M_s).$$

Remark F.28. By definition, $\mathrm{IX}_{\mathrm{oracle}}(M)$ consists precisely of the elements of the form $\mathrm{IS}_{\mathrm{oracle}}(M_s)$, so ψ always exists and is surjective. Given only data produced by an SCM M, we will typically not have prior knowledge of either $S(M)$ or the mapping ψ. Discovering an indicator translation thus means giving the discovered elements of $\mathrm{IX} = \mathrm{IX}_{\mathrm{oracle}}(M)$ an interpretation in terms of model properties (see §6). Generally ψ may not be injective, if some model-states lead to the same independence structure (for example if the are in the same Markov equivalence-class); thus the inverse is not generally well-defined and such an interpretation in terms of model properties may not be uniquely identifiable.

In the presence of hidden latent confounders (and inducing paths) or cycles, this is a rather non-trivial question. However, under the present assumptions, the evident interpretation applies:

Example F.29 (Acyclic Model-Interpretation)**.** Assume Ass. F.1 (acyclicity), Ass. 3.24 (faithfulness) and Ass. F.6 (modularity and reachedness), then the state-translation in this sense is given by the bijection $S \xrightarrow{1:1} \langle R^{\mathrm{model}} \rangle$ (by Lemma F.19). In cases where all model-indicators can be discovered (see §F.5), we can thus interpret states in model-terms: Since we describe states by the values taken by model indicators, a state can be interpreted in model-terms, by saying the mechanisms at the non-trivial indicators are active iff the value of the corresponding model-indicator is one in this state.

F.7 Representation of Detected Indicators

The next step is to represent detected indicators as functions of the state. Since states under the present modularity assumptions (Ass. F.6) are described by the values of the model-indicators (Lemma F.19), this can be reduced to relations to model-indicators. Indeed, by using previous observations (in particular Lemma F.16), and given representing tests of model-indicators (cf. Lemma F.22), this can be accomplished by using *only* implication-tests of the form described in Def. F.12.

We know, that $R_{\vec{j}}$ can be written as a function of the state only (see Lemma 3.10). Further the state $s = (s_1, \ldots, s_k)$ is described by the values s_i of the model-indicators. While both domain (state-space) and target ($\{0,1\}$) of $R_{\vec{j}}$ have natural structures as $\mathbb{Z}/2\mathbb{Z}$ vector spaces, the map $R_{\vec{j}}$ is of course not linear (Example F.15). In particular, given k model indicators, there are not k, but 2^{2^k} choices (for each of the 2^k states, $R_{\vec{j}}$ can take 2 possible values). Fortunately, by Lemma F.17, $s \leq s' \Rightarrow R_{XY|Z}(s) \leq R_{XY|Z}(s')$ (for all detected indicators $R_{XY|Z}$), thus we know $R_{\vec{j}}$ is monotonic, which will help us to reduce the search-space. This is what ultimately makes Algo. 4 work.

Lemma F.30 (State-Resolution of Detected Indicators)**.** *Given a marked independence $\vec{j} \in J$, the set $\mathcal{R} \subset J$ of model-indicators represented by marked independencies (cf. §F.5), and an oracle $\mathrm{IR}_{\mathrm{oracle}}$ (see example F.13) for implication-tests of the form Def. F.12 (used for the test in line 16 of the algorithm). Then the output of Algo. 4 yields the detected indicator $R_{\vec{j}}(s)$ as a function of state.*

Proof. The result corresponds to a function of s: The algorithm returns either an element of $\mathcal{R}$ (line 6), or a subset of (the initial) C (line 21). In both cases, the result is a set of monomials of elements of $\mathcal{R} \subset J$. Elements of $\mathcal{R}$ represent the model-indicators, thus $\bar{R}$ (see line 2) is a boolean combination of of model-indicators. Model-indicators, by definition of our state-space, take a known value $s_i = \pi_i(s)$ on state s. Thus $\bar{R}(s)$ is given by s as the specified boolean combination of known values s_i.

Correctness: Let s be arbitrary. Case 1 ($R_{\vec{j}}(s) = 1$): Note that either the return-statement in line 6 was executed or line 16 is tested true at least once, but never both or none.

Case 1a (line 16 is tested true at least once): In this subcase $N \neq \emptyset$ and If $R_{\vec{j}}(s) = 1$, then by line 16 (rather: by contraposition of the if-statement's condition), $\forall r \in N: r(s) = 1$, thus $\bar{R}(s) = 1$.

Case 1b (the return-statement in line 6 was triggered): The state s_0 with all entries 0 (equivalently: all model indicators evaluate to 0 on s_0) satisfies $\forall s' : s' \geq s_0$ by construction, in particular by Lemma F.17, $\forall s' : R_{\vec{j}}(s') \geq R_{\vec{j}}(s_0)$. If it were $R_{\vec{j}}(s_0) = 1$, then this would imply $R_{\vec{j}} \equiv 1$ is non-trivial, which contradicts $\vec{j} \in J$. Thus $R_{\vec{j}}(s_0) = 0$ and $s \neq s_0$. Let $R' := \text{or}_{R^{\text{model}} \in \mathcal{R}} R^{\text{model}}$, by construction $R'(s'') = 0 \Leftrightarrow s'' = s_0$. Therefore the implication $R'(t) = 0 \Rightarrow R_{\vec{j}}(t) = 0$ in line 16 would produce a true result and we would be in case (a) if it had been tested, thus $R' \in C$ still remains in C when we encounter the return statement in line 6. Therefore case $\bar{R}(s) = R'(s) = 1$. Note that R' was not removed from C by line 17, if this line had been triggered, we would be in case (a).

Case 2 ($R_{\vec{j}}(s) = 0$): If $R_{\vec{j}}(s) = 0$, define $S_0 := \{R^{\text{model}} \in \mathcal{R} | R^{\text{model}}(s) = 0\}$. Further let $R'(\tilde{s}) := \text{or}_{R^{\text{model}} \in S_0} R^{\text{model}}(\tilde{s})$. Note, that $R' \in C_{\text{init}}$ is an element of C (as initialized in line 3) and that $R'(s) = 0$ (by construction of S_0). Indeed given *any* state s' with the $R'(s') = 0$, then $s' \leq s$: otherwise there would have to be $r \in \mathcal{R}$ with $r(s') = 1$ and $r(s) = 0$, thus $r \in S_0$. Then $R'(s') = \text{or}_{R^{\text{model}} \in S_0} R^{\text{model}}(s') \geq r(s') = 1$ contradicting $R'(s') = 0$.

Thus for an arbitrary s', we have $R'(s') = 0 \Rightarrow s' \leq s \Rightarrow R_{\vec{j}}(s') \leq R_{\vec{j}}(s) = 0$, where the last step finally and crucially uses the monotonicity property. Since this holds for arbitrary s' it holds for all times $t \in T = \sigma^{-1}(S)$, i.e. $R'(t) = 0 \Rightarrow R_{\vec{j}}(t) = 0$. With $R' \in C_{\text{init}}$ there are two cases:

Case 2a ($R' \in C_{\text{init}}$ is reached by the for-loop): In this case the test (oracle evaluation) of $R'(t) = 0 \Rightarrow R_{\vec{j}}(t) = 0$ in line 16 produces the result `true` (this implication is correct, as was shown above). In particular R' gets added to N and is contained in the final result. Thus $\bar{R}(s) \leq R'(s) = 0$.

Case 2b (R' was removed from C by line 17): The removal in line 17 is only triggered if there is r with R' containing all factors of r, i.e. $r(\tilde{s}) = \text{or}_{R^{\text{model}} \in S_0'} R^{\text{model}}(\tilde{s})$ for some $S_0' \subset S_0$ which was added to N, in particular this r is in the final result. Clearly by $S_0' \subset S_0$ we have $\forall \tilde{s}: r(\tilde{s}) = \text{or}_{R^{\text{model}} \in S_0'} R^{\text{model}}(\tilde{s}) \leq \text{or}_{R^{\text{model}} \in S_0} R^{\text{model}}(\tilde{s}) = R'(\tilde{s})$. In particular $\bar{R}(s) \leq r(s) \leq R'(s) = 0$.

Case 2c (the return-statement in line 6 was triggered): Since $R' \in C_{\text{init}}$ and neither case (a) or (b) apply, $R' \in C$ is still in C and is thus returned. In this case actually $\bar{R}(s) = R'(s) = 0$.

Thus in all sub-cases, $\bar{R}(s) = 0 = R_{\vec{j}}(s)$ (the last equality is by case-hypothesis of case 2). $\qquad\square$

F.8 State-Space-Construction Result

We formalize the results of this section as a two phase algorithm, which is applicable with the core algorithm in §E. This means, we formally show that the previous results can be combined to satisfy the formal specification of state-space construction (Def. E.13) used by the core algorithm:

Theorem 3F (State-Space Construction)**.** *Assume* CD *is consistent (Def. 3.18), Ass. F.3 (conventional skeleton discovery), Ass. F.1 (acyclicity) and Ass. 3.24 (faithfulness) and Ass. F.6 (modularity). Given are further oracles for marked independencies* $\text{IM}_{\text{oracle}}$ *(example 4.6) and for indicator-implications* $\text{IR}_{\text{oracle}}$ *(example F.13).*

---

[28]C contains, by definition, boolean combinations of at least $n \geq 1$ different (thus $n \leq |\mathcal{R}|$) model-indicators. Here, "ordered by increasing monomial degree" means we start with all entries with $n = 1$, then all entries with $n = 2$ etc. until we reached all elements of C. This is a heuristic choice to keep the left-hand-side in implication-tests simple; a specific ordering is not required by the proof / for correctness.

Algorithm 4 Indicator Representation (union-acyclic case, g_s are MAGs)

1: **Input:** A set $\mathcal{R} \subset J$ of model-indicators represented by (marked) test-indices, a marked test-index $\vec{j} = (i_x, i_y, i_z) \in J$

2: **Output:** A set N of monomials of the form $R_k = (R_{i_1} \text{ or } \ldots \text{ or } R_{i_n})$ of model-indicators, such that the boolean combination $\bar{R}_N = \text{and}_{k \in N} R_k$ satisfies $\bar{R} = R_{\vec{j}}$

3: Initialize the candidate-set $C := \{R_{i_1} \text{ or } \ldots \text{ or } R_{i_n} | i_j \neq i_{j'} \text{ if } j \neq j'; R_{i_j} \in \mathcal{R}; n \geq 1\}$

4: Initialize the necessary set $N := \emptyset$

5: **if** $\vec{j} \in \mathcal{R}$ (as a representor) **then**

6:      **return** $\{R_{\vec{j}}\}$

7: **end if**

8: **if** $\exists \vec{j}' = (i'_x, i'_y, i'_z) \in \mathcal{R}$ with $i'_x = i_x$ and $i'_y = i_y$ **then**

9:      Remove all combinations *not* involving $\vec{j}'$ as a factor from C

10: **end if**

11: **for** element $r \in C$ ordered by increasing monomial degree[28] **do**

12:      **if** $|C| = 1$ and $N = \emptyset$ **then**

13:          **return** C ▷ for finite-sample stability, not needed with oracle

14:      **end if**

15:      Remove r from C

16:      **if** test: $r(t) = 0 \Rightarrow R_{\vec{j}}(t) = 0$ **then**   ▷ $r = 1$ is necessary for $R_{\vec{j}} = 1$

17:          remove all combinations involving (containing all factors of) r from C

18:          replace $N := N \cup \{r\}$

19:      **end if**

20: **end for**

21: **return** N

If $J = \emptyset$, then $S^J = \text{Map}(\emptyset, \{0,1\})$. Otherwise, apply first Algo. 3 to find model-indicators $\mathcal{R}$, and their product-space S_M. Then Algo. 4 applied with this $\mathcal{R}$ as argument yields representations $R_{\vec{j}}(s)$ for each $\vec{j} \in J$. The mapping

$$S_M \hookrightarrow \text{Map}(J, \{0,1\}), s \mapsto (\vec{j} \mapsto R_{\vec{j}}(s))$$

is injective, in particular we can identify S_M with its image $S^J := \{\vec{j} \mapsto R_{\vec{j}}(s) | s \in S_M\}$.

Then, the described assignment $J \mapsto S^J \subset \text{Map}(J, \{0,1\})$ is a sound and complete state-space construction (Def. E.13) for any model satisfying the assumptions listed in the hypothesis.

Proof. **Phase I: Model Indicators.** Let R_{XY} be an arbitrary model indicator.

Case 1 (R_{XY} is non-trivial): By Lemma F.22, there is a representing test for each model indicator (part (a)) $R_{XY}^{\text{model}} \equiv R_{\vec{j}}$ and by part (b), this test is in $\vec{j} \in \text{L}_{\text{CD}}(c \circ \text{IM}_{\text{oracle}}(M))$. By non-triviality of R_{XY}^{model} (and $R_{XY}^{\text{model}} \equiv R_{\vec{j}}$), also $R_{\vec{j}}$ is non-trivial, thus $\text{IM}_{\text{oracle}}(M)(\vec{j}) = R$ (by definition, see example 4.6). According to Def. E.13, we may assume $J \supset \text{L}_{\text{CD}}(c \circ \text{IM}_{\text{oracle}}(M)) \cap \text{IM}_{\text{oracle}}(M)^{-1}(\{R\})$. Therefore $\vec{j} \in J$ and the result $\vec{j}'$ of Algo. 3 satisfies $R_{\vec{j}'} \leq R_{\vec{j}}$ if both are comparable (the algorithm finds a minimum). By Lemma F.20 the model-indicator is minimal and comparable to all detected indicators on the link X–Y, in particular $R_{\vec{j}} \leq R_{\vec{j}'}$ and both are comparable (thus by the above also $R_{\vec{j}'} \leq R_{\vec{j}}$). Thus $R_{\vec{j}'} \equiv R_{\vec{j}} =\equiv R_{XY}^{\text{model}}$. Note, that while the partial order induces a preorder on J, this preorder will typically not be anti-symmetric, i.e. we cannot conclude $\vec{j} = \vec{j}'$. This is not a problem as we only require *a* test $\vec{j}$ to represent R_{XY}^{model}.

Case 2a ($R_{XY}^{\text{model}} \equiv 0$): By Ass. F.3 (conventional skeleton discovery), there is a test $X \perp\!\!\!\perp Y | Z$ in the lookup-region of the union-graph $\text{L}_{\text{CD}}(c \circ \text{IM}_{\text{oracle}}(M))$. In particular Algo. 3 will discard this link and not include it into its output.

Case 2b ($R_{XY}^{\text{model}} \equiv 1$): By Lemma F.20, the model-indicator is minimal, that is for all Z:

$R_{XY|Z} \geq R_{XY}^{\text{model}} \equiv 1$, and the marked-independence oracle always returns 1 on this link. In particular Algo. 3 will never consider this link and not include it into its output.

Thus we obtain the correct state-space S_M (Lemma F.19) with valid representatives of all non-trivial model-indicators.

Phase II: Resolution of Detected Indicators. By Lemma F.30, Algo. 4 given a marked test $\vec{j} \in J$ produces a representation $\bar{R}_{\vec{j}}(s)$ such that $\bar{R}_{\vec{j}} \equiv R_{\vec{j}}$. In particular for any state $s \in S_M$, we have $\text{IS}_{\text{oracle}}(M_s)(\vec{j}) = \bar{R}_{\vec{j}}(s)$. This is (see Notation E.1) denoted as $s(\vec{j})$ in Lemma / Notation E.6 where the interpretation of S_T^J as a subset of $\text{Map}(J, \{0, 1\})$ is then specified precisely as $\vec{j} \mapsto s(\vec{j})$. Therefore the image of the mapping

$$S_M \hookrightarrow \text{Map}(J, \{0, 1\}), s \mapsto (\vec{j} \mapsto R_{\vec{j}}(s))$$

which is called S^J in the statement of the proposition, satisfies indeed $S^J = S_T^J$ as required. (If we identify S_M and the true S_T in a suitable way – see §F.6 – then this mapping is the same as the mapping in Lemma / Notation E.6). $\qquad\square$

Remark F.31. The inclusion of the constraint $J \supset \text{L}_{\text{CD}}(c \circ \text{IM}_{\text{oracle}}(M)) \cap \text{IM}_{\text{oracle}}(M)^{-1}(\{R\})$ into Def. E.13 is a particular example of the requirement for coordination between the core-algorithm (and also the choice of c), the state-space construction and the used CD-algorithm CD. Some degree of fine-tuning concerning these interfacing-requirements in future work is likely not avoidable. The main point of our presentation is not the strict low-level enforcement of a particular interface between modules, but rather the clear specification of logically separate modules: mCIT testing, state-space construction, core-algorithm and underlying CD-algorithm solve different problems and can be largely *understood* individually. They have to be fit together in practice, but this is primarily a lower level (implementation type) question, as opposed to the higher lever (design type) solution of the respective main tasks.

F.9 Edge-Orientation Transfer

By Ass. F.1 (acyclicity), orientations cannot change between states. Additionally, under our assumptions, the model indicators are found and attributed correctly (example F.29); all changes manifest in *edge-removals* only (on the true graphs). Thus, when in practice only partial graphs (with some edges unoriented) are recovered for the G_s, we can transfer orientations between states in a straight-forward manner:

Lemma F.32 (Orientation Transfer). *Given Ass. F.1, if $X \circ\!\!-\!\!* Y$ in G_s with a definitive edge mark $*$ at Y (arrow-head or tail) and any edge mark $\circ$ at X, and X, Y are adjacent in $G_{s'}$, then $X \circ\!\!-\!\!* Y$ in $G_{s'}$, i. e. edge marks are preserved.*

Proof. By union-acyclicity, edge-marks cannot change: An edge-flip would immediately lead to a union-cycle, a change $\leftrightarrow$ to $\rightarrow$ would imply the existence of an almost directed cycle in the union graph. With the union graph being a AG (Ass. F.1), neither are possible. Thus, if the edge is present in s', then it has the same edge marks as in s. $\qquad\square$

Note, that JCI [37] arguments may allow for orientations of edges in the union-graph. By our assumptions, the union-graph does correspond to a reached space (see Lemma F.18) so the lemma above applies. Indeed, the same arguments of the last proof work just as well on the union-graph, thus leading to an alternative (more direct) proof of:

Lemma F.33 (Orientation Transfer from Union-Graph). *If $X \circ\!\!-\!\!* Y$ in G^{union}, and X, Y are adjacent in G_s, then $X \circ\!\!-\!\!* Y$ in G_s.*

Proof. Apply Lemma F.18 to obtain a representing state s_{union}. Then apply Lemma F.32 with s_{union} and s. $\qquad\square$

Finally, note that orientations transferred to a state G_s in one of these ways may make new orientation-rules applicable in that state. Thus it may be necessary to iterate orientation-phases and transfer-phases till convergence (until none of the graphs changes anymore; since we only get *more* orientations [monotonicity] and there is a finite number of edges to orient in the graph [boundedness], this iteration is guaranteed to converge after a finite number of rounds). The uniformity of edge marks across states and union-graph, means the causal system can be summarized (under the assumptions of the present section) by a single graph with edges with non-trivial model-indicator marked as varying:

Notation F.34. Our final output (under the assumptions of the present section) is represented by a union-graph, with edges corresponding to non-trivial model-indicators marked (e. g. in color), see Fig. 1.1.

Under the assumption of modular / independent changes (Ass. F.6), all links vary independently and there is (in principle) no reason to distinguish them (use different colors). In practice there are at least two important reasons to use individual markings (different colors): One is the potential post-processing for relations between states (§F.10.4), the other is the potential post-processing for (time-)resolutions (§B.9).

F.10 Future Work

Our state-space construction requires many assumptions, in particular acyclicity, and may require many complicated tests for large numbers of model-indicators. The presented approach provides a proof of concept and shows that a systematic formal treatment is possible. Yet, many interesting questions remain open. We summarize some of them in this section.

F.10.1 Locality of Translation

Model indicators are local in the model, in the sense of only affecting a single link. Detected indicators are "semi-local" in that they only depend on the collection of paths between two nodes X, Y. So how local is semi-local? I. e. do detected indicators for tests $X \perp\!\!\!\perp Y | Z$ really depend on model-indicators "far away" in the graph from both X and Y? There are multiple different reasons that make us belief that indeed semi-local here means more local than global:

(a) A test becomes independent only if *all* paths from X to Y vanish, if X and Y are far apart in the graph, this either requires the graph to be very sparse (compared to model-indicator density) or to be separated by a bottleneck. Both should be visible from the (union) graph skeleton.

(b) A regime is only detected in practice, if the remaining (after possibly many 'hops') signal-to-noise ratio remains high. This limits the plausible distance between X, Y to be considered. This observation is known for CD more generally to be relevant, future progress on this problem for the general case may be useful to the present problem.

(c) Causal discovery aims at leveraging local separating-sets, for example PC searches for subsets of parents. The remaining independencies do not have to be tested, as they follow from the local properties of the graph. Similarly, a suitable analysis of the causal (union-)graph – which in the acyclic case is known already at the point where indicator-translation is performed – should allow to reduce the search for model indicators and relations of model-indicators to their neighborhood in the graph.

(d) Sufficient knowledge about the causal graph can imply knowledge of the form of detected indicators, as in example F.15. It may thus be possible to extract representations of detected indicators or at least restrict possible explanations (representations via model indicators).

(e) So far, our regime detection happens on-the-fly on tests that are executed by the CD-algorithm anyway. It is of course possible, to inject between model-indicator discovery and representation of detected indicators, an additional testing phase to block overlapping influences of multiple indicators.

Points (a) and (b) could be approached in practice by testing for dependence on model-indicators, for example in a JCI-sense, which one might want to do anyway. Points (c-e) could offer a very general approach, but require the systematic incorporation of d-separation rules into indicator-translation. We leave these to future work.

F.10.2 Cyclic Models
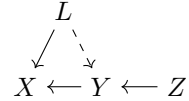
As was demonstrated in example F.23, cyclic models require novel "union tests" besides implication tests. Somewhat surprisingly, these may be easier to realize on data: The null hypothesis can be the existence of a split of the data, such that in each subset (at least) one of two independencies holds. Other than the weak regime (and implication) testing problems, this does *not* require the combination of a rejection (of homogeneity) with acceptance of independence (in the weak regime), instead this single null hypothesis can be accepted or rejected.

F.10.3 Inducing Paths (and Almost Cycles)

We excluded the almost cyclic case (in presence of latent variables) together with the cyclic case, because similar problems occur:

Example F.35. Inducing paths on non-AG union graphs:

On the right-hand side, assume L to be a hidden latent (i.e. unobserved), and the dashed arrow to be active only in regime A but not in B.

$$L$$
$$X \leftarrow Y \leftarrow Z$$
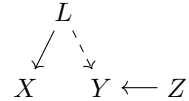
In this case in regime B, $X \perp\!\!\!\perp Z | Y$, but in regime A, $X \not\perp\!\!\!\perp Z | Y$ as the path through L is now open. $X \not\perp\!\!\!\perp Z$ in both cases. The non-deletable link $Z \to X$ in regime A is called an "inducing path" (see e.g. [61; 70]).

There are also some encouraging observations, however. For example, a JCI-argument unveils Y as the only child of the indicator R. If the link $Z \to X$ were real and would change, then either X or Z would have to be a child of R. Thus, in this particular example, we actually *know* that we found an inducing path. Conversely one may also be able to draw the conclusion that a some link cannot be an inducing path if there is no candidate for a confounder inducing it:

Example F.36. No inducing path possible:

Compared to the previous example, the arrow $Y \to X$ was removed, there is no almost cycle.

$$L$$
$$X \qquad Y \leftarrow Z$$
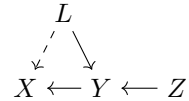
In this case $X \perp\!\!\!\perp Z$, and $X \perp\!\!\!\perp Y | R = B$. For the edge $X \to Y$ to come from an inducing path, there would have to be a candidate for an inducing path.

There are, however, also examples, where no such decision seems to be possible from independence-structure alone:

Example F.37. Ambiguous Case:

Compared to the first example, only the changing (dashed) arrow has been change to be $L \to X$ instead of $L \to Y$.

$$L$$
$$X \leftarrow Y \leftarrow Z$$

In this case, the JCI-observations of X being the only child of R no longer excludes the path $Z \to X$ being real.

Actually the model on the right leads to the same extended independence-structure.

$$X \overset{\leftarrow}{\longleftarrow} Y \longleftarrow Z$$

As the last example F.37 shows, there is no remedy to the problem of inducing paths in general. This is of course not surprising: Even in the stationary (or IID) case, inducing paths cannot be identified as such from independence-structure alone [65]. From this perspective it is quite intriguing that sometimes (see examples F.35, F.36 and their discussions) one *can* confirm or exclude the possibility of an inducing path and thereby narrow down the location of the actual change in the model.

Both the theoretical problem and the practical execution of such a decision-logic in a stable and reliable way seem quite complex, so we leave the details of an exhaustive treatment to future work.

F.10.4 Non-Modular Changes

We can of course use our implication tests to compare model-indicators – or their representors – as well (see also §B.7). This lead to subset-relations between regimes, thus allow for an analysis of the state-space beyond the assumption of modularity. Indeed our approach is not incompatible with non-modular changes; rather it approximates models around their modular limits, thus it is only *optimized* for modular changes (the extraction of any non-modular knowledge requires additional tests). This is an important difference to "global" approaches that start their approximation in a sense from the opposite limit.

G   Table of Contents

Contents

G   Table of Contents